LONG TERM CHANGES IN IRRIGATION WATER REQUIREMENT

Ph.D. THESIS

by

SHIULEE CHAKRABORTY

DEPARTMENT OF WATER RESOURCES DEVELOPMENT & MANAGEMENT
INDIAN INSTITUTE OF TECHNOLOGY ROORKEE
ROORKEE- 247667 (INDIA)
JUNE, 2014

LONG TERM CHANGES IN IRRIGATION WATER REQUIREMENT

A THESIS

Submitted in partial fulfilment of the requirements for the award of the degree

of

DOCTOR OF PHILOSOPHY

in

WATER RESOURCES DEVELOPMENT AND MANAGEMENT

by

SHIULEE CHAKRABORTY

DEPARTMENT OF WATER RESOURCES DEVELOPMENT & MANAGEMENT
INDIAN INSTITUTE OF TECHNOLOGY ROORKEE
ROORKEE- 247667 (INDIA)
JUNE, 2014

INDIAN INSTITUTE OF TECHNOLOGY ROORKEE
ROORKEE

CANDIDATE'S DECLARATION

I hereby certify that the work which is being presented in the thesis entitled "**LONG TERM CHANGES IN IRRIGATION WATER REQUIREMENT"** in partial fulfilment of the requirement for the award of the Degree of Doctor of Philosophy and submitted in the Department of Water Resources Development and Management of the Indian Institute of Technology Roorkee, Roorkee is an authentic record of my own work carried out during a period from December, 2010 to June, 2014 under the supervision of Dr. S. K. Mishra, Professor, Dr. U.C. Chaube, Emeritus Fellow, Department of Water Resources Development and Management, Indian Institute of Technology Roorkee, Roorkee and Dr. R.P. Pandey, Scientist 'F', National Institute of Hydrology, Roorkee.

The matter presented in this thesis has not been submitted by me for the award of any other degree of this or any other Institute.

(SHIULEE CHAKRABORTY)

This is to certify that the above statement made by the candidate is correct to the best of our knowledge.

(R.P. Pandey)	(U.C. Chaube)	(S.K. Mishra)
Supervisor	Supervisor	Supervisor

Date:

The Ph.D. Viva-Voce examination of **Ms**. **Shiulee Chakraborty,** Research Scholar, has been held on…….

Supervisors Chairman, SRC External Examiner

Head of the Department/Chairman, ODC

ABSTRACT

It is widely believed that the impact of climate change on agriculture has become one of the important issues in water resource management. The available water resource would be altered by change in rainfall pattern and rate of evaporation. Further, higher evapotranspiration (ET) would result in greater amount of irrigation water requirement (IWR). Despite availability of a number of ET estimation methods in literature, the accurate assessment of ET/IWR is a complicated task due to the limitations and assumptions associated with different methods. It is understood that the climate change may alter the demand for irrigation water in future on regional and the global scale. Hence, there is a need to study long term change in the key climatic variables (rainfall, minimum and maximum temperature, relative humidity, wind speed) which affect the ETo/CWR/IWR. Very few studies have been carried out in India on long term changes in irrigation water requirement. Present study is taken up to enhance the understanding of region specific changes in IWR on long term basis. Earlier studies have focused on assessment of climatic variables and crop water requirement based on perturbation method for scenario generation with GCM. With the development of statistical downscaling model (LS-SVM), the regional climate change assessment studies are becoming more accepted. Therefore, this study proposes to use LS-SVM model to study the impact of climate change on IWR. This study has focus on quantification of future irrigation requirements on long term basis, which is necessary for sustainable management of basin water resources.

This study has been carried out in the Seonath river basin (area = 30,860 sq. km), falling in Chhattisgarh State (India), is the longest (380 km) tributary of Mahanadi Basin, comprising 25% of the basin area. Agriculture is the main occupation of the people in the sub-basin. There are two cropping seasons viz, kharif (mid June to October) and rabi (November to mid April). The mean annual rainfall in the basin varies from 1005 mm to 1255 mm. The major part of rainfall occurs only within 3 monsoon months (July-September). It is also reported that the study area faces adverse effects of frequent droughts and thus crop production is adversely affected in drought years.

The trends in annual and seasonal rainfall time series from 1960-2010 have been analyzed using Mann–Kendall test and the Sen's Slope estimator for 24 stations in the Seonath river basin. The analysis has revealed that there is a significant decreasing trend in

annual rainfall (-2.4 mm/yr) at 75% of the stations (northern part of basin) and non-significant decreasing trend in annual rainfall at 17% of the stations (southern part of basin). Moreover, the decreasing trends in seasonal rainfall are found significant for most of the stations. Decrease in monsoon rainfall at the rate of 2.79 mm/yr is likely to have significant adverse impact on rainfed agriculture in future. The conventional approach of planning for Rabi crop irrigation needs to be critically examined. Also, there is a need to examine supplemental irrigation requirements for Kharif (monsoon) season crops in the region.

Rising trend has been observed in mean maximum temperature for monsoon and winter whereas there is decreasing trend in mean maximum temperature for summer season. The mean minimum temperature in monsoon, winter and summer seasons shows rising trend all over the basin. Few stations located in Northern part of the basin show non-significant rising trend in mean seasonal temperature. The minimum temperature has increased more as compared to maximum temperature over 51 years period of analysis. The percentage change in minimum temperature is highest for the month of November followed by December and January. The variability is observed to be more pronounced in minimum temperature ranging from 1.69% to 2.78%. For annual maximum and minimum temperature, the upper half of the basin shows more variability. The results of study indicate that the mean annual temperature is likely to increase by 1.98°C in next 100 years. Further, winter temperature may increase by 2.06°C, monsoon temperature may increase by 4.73°C and summer temperature may decrease by -0.528°C over the study area.

The temperature changes may have significant impacts on rainfed crop cultivation due to increase in evapotranspiration. In the study area, the monsoon temperature is expected to increase by 4.73°C over 100 years. This rise in temperature may cause significant increase in the irrigation water requirements and may cause water shortages. Therefore conventional irrigation planning procedures for Rabi as well as Kharif crops need to be revised.

Monthly trend analysis of Relative Humidity (RH) shows significant decreasing trend for months of July, September, October and November. Whereas, from March to June insignificant increasing trends are observed. The highest change in magnitude of RH is observed for July, September, October and November months. The inter-annual variability in RH of the basin ranges from 0.9 to 2.2%.

The monthly and seasonal assessment of trend in wind speed (WS) and its variability is significant in order to quantify its effect on ET. On seasonal basis, significant increasing trend is obtained for WS in monsoon and winter season all over the basin. On monthly time scale, the highest rate of change is seen in August followed by July, June and September. The percentage change is highest for the entire basin ranging from 38% to 61%. The inter-annual variability (23%) is observed in monthly WS in northern part of the basin. Overall, there is increasing trend in monthly and seasonal WS for the entire basin.

To measure the consistency and accuracy of ETo methods, the estimates obtained from six different methods (Hargreaves, Thornthwaite, Blaney-Criddle Method, Priestley-Taylor Method, Penman-Monteith Method and Turc Method) have been compared with pan evaporation data (Ep). According to statistical performance evaluation Penman-Monteith, Hargreaves and Thornthwaite methods have performed well. The radiation-based Priestley-Taylor and temperature based Blaney-Criddle method indicate lowest correlation values.

The pan coefficient (Kp) has been estimated for the study region. The study illustrates that the Kp varies significantly from month to month (0.56 to 0.89) for the study area. The highest and lowest Kp value have been obtained for the month of July and November, respectively. Thus, if the standard average value of Kp (0.70) is used for assessment of ETo, it will provide erroneously large variation in ETo ranging from 11.8% to 56.3%.

According to sensitivity analysis temperature is the most important driving parameter which effects ETo and next to that is relative humidity. Bilaspur station shows highest sensitivity coefficient of 1.77 in relation to temperature. It means ETo would increase by 17.7% in response to the 10% rise in maximum temperature if other meteorological variables remain constant. However Rajnandgaon station shows the highest value of sensitivity coefficient in relation to RH (-1.28) which means 10% decrease in RH causes increase in ETo by 12.8%. Hargreaves and Thornthwaite methods are therefore not recommended for this study area as these methods donot take into consideration the RH parameter.

In this study, the Kc values recommended by FAO paper No. 56 have been adjusted according to climatic conditions of the study area. The average Kc values for major crops (kharif paddy, rabi wheat and summer paddy) for four crop growth stages viz, initial,

development, mid and late season have been computed. For Kharif paddy, percentage change in adjusted Kc value with respect to FAO recommended Kc values during different crop growth stages varies from -1% to -15% whereas for rabi crops (Wheat and Summer paddy) it range from -2% to -16% and -9% to -23% respectively. The CWR computed using FAO-56 Kc values gives significantly different (higher) values due to sub-humid climate of the basin. It is therefore, decided to use the adjusted Kc values for precise estimation of CWR and subsequently IWR.

Trend and variability of annual and monthly ETo time series have been analyzed for 8 stations for which data are available. The increase in ETo is estimated as 13.4 mm/yr on annual time scale. On the seasonal scale, summer ETo trend is decreasing by -10.4 mm/yr. The winter and monsoon ETo show increase at the rate of 21 mm/yr and 22 mm/yr, respectively. The estimates of ETo for the months of December, January, February, July and August show non-significant increasing trend. However significant increasing ETo trend have emerged for the months of September October and November. The highest (3.4-3.6%) variability in annual ETo is seen in the stations located at southern part of the basin while rest of the stations exhibits inter-annual variability ranging from 1.0%-1.8%. The results of this study will be useful for the reliable estimation of supplemental irrigation water requirements.

In order to detect trends in IWR, the MK-test and Sen's slope have been used for the 51-year period. For Kharif season increasing trend is detected at 88% of the stations, and remaining 12% of the stations show non-significant increasing trend. Further, significant positive slopes are dominant for wheat crop, (with 63% of the stations). For summer paddy, 50% of the stations show significant increasing trend and rest 50% shows non-significant increasing trend. The IWR for Kharif and Rabi seasons are increasing at the rate of 3.627 mm/yr and 1.264 mm/yr respectively. These changes are characterized by a relative increase in Kharif IWR by 47%, while Rabi IWR by 23%.

Overall, the results of the study show an increase in IWR for agricultural crops it may be due to high variability of rainfall pattern, rise in temperature, wind speed and decrease in RH. These findings shall be helpful in more realistic planning and efficacious utilization of basin water resources.

In a recent study by Mishra et al., (2014), developed a relationship between Soil Conservation Service Curve Number (SCS-CN) and ETo. Since ETo is a important parameter in estimation of IWR, therefore an attempt has been made to develop a relationship between IWR and CN. In this study, the CN derived from rainfall-runoff data on seasonal scale (Kharif and Rabi season) has been related to IWR of same scale and high R^2 values of 0.970 and 0.926 for Kharif and Rabi seasons are found for calibration period. The results are validated with R^2 values of 0.957 and 0.954 for Kharif and Rabi seasons, respectively; indicating the existence of a strong IWR-CN relationship.

The supportive results of the proposed model assume to be a good substitute for complex IWR assessment, particularly in the area where meteorological parameters are not easily obtainable.

The four statistical downscaling models viz., Artificial Neural Network (RBF), Multilayer Perception (MLP), Multiple Linear Regression (MLR), Model Tree (MT), Least Square Support Vector Machine (LS-SVM) are used for comparative study. The results of analysis indicate that for each climatic variable, LS-SVM model is performing best followed by MT and ANN (MLP).

The annual rainfall is projected for the period of 2011-2100 and it is expected to increase from year 2020s upto 2090 in range varying from 2.74 mm/decade to 18 mm/decade. The annual rainfall is predicted to decrease for the period of 2091-2100. However for maximum temperature the increasing trend is predicted for the entire projected period and the highest temperature change is predicted for two decades i.e, 2021-2030 and 2031-2040. The rate of change may vary from 0.1°C/decade to 0.5°C/decade for monsoon and 0.01°C/decade to 0.3°C/decade for post monsoon season. For the minimum and mean temperature the overall increasing trend is observed but for Tmin the highest temperature rise is expected in the period of 2061-2070. The change in magnitude for minimum temperature for monsoon season is varies from 0.2°C/decade to 0.7°C/decade, whereas for post-monsoon season the minimum temperature may vary from 0.02°C/decade to 0.5°C/decade. It can be inferred that warming is expected to be more pronounced during the night than day. The relative humidity forecasts represent a significant decreasing trend for Kharif season and non-significant decreasing trend for rabi season for two decades i.e., 2020s and 2090s period. The projected wind speed shows non-significant increasing trend

for the entire basin. Wind speed projections are highly uncertain with extremes in 2090s during Kharif season whereas for rabi season the uncertainty is for 2020s and 2050s period.

The ETo have been predicted to increase in future for all months. Particularly, the change in ETo is more in the months of May to August due to the large projected changes in Tmax and Tmin variables. The peak is observed for the month of June 25 mm over 100 years.

The monthly IWR in future have been estimated using the projections of rainfall (downscaled from LS-SVM model) and CWR projections. The IWR for Kharif paddy crop is projected to increase by 84%, 71% and 32% in the 2020s, 2050s and 2090s respectively whereas, for Rabi wheat crop IWR is predicted to increase by 201%, 163%, and 91%, for the three decades (2020s, 2050s, and 2090s). However for summer paddy the IWR may increase by 184%, 215% and 90% for 2020s, 2050s and 2090s periods respectively.

Keywords: SCS Curve Number method, Reference Evapotranspiration, Irrigation Water Requirement, Crop Water Requirement, Trend Analysis.

ACKNOWLEDGEMENT

God has been exceptionally kind to me without his blessings, this thesis would not have been completed.

This thesis is part of a most remarkable journey of my life. I could keep this thesis on the correct path only with the support and encouragement of numerous people, including my supervisors, my family members, my friends, associates and various institutes. It is challenging to recollect every person who has contributed to this thesis, but I would like to acknowledge everyone who has touched my life in any way.

First and foremost, I would like to express my sincere appreciation towards my supervisors Prof. U.C Chaube, Emeritus fellow, Dr. S. K Mishra, Professor, Department of Water Resources Development and Mangement, Indian Institute of Technology, Roorkee and Dr. R.P Pandey, Scientist-"F", National Institute of Hydrology, Roorkee for providing constant support and encouragement during the tenure of my research work. I gratefully acknowledge Prof. U.C Chaube for the continued belief, invaluable contribution, advice and constructive criticism which particularly challenged my ideas and contributed to my thesis work to a great extent. My gratitude to Dr. S.K Mishra for his scientific discussions and insightful suggestions which became the threads and I could finally weave those threads into the finished product in the form of my thesis. I am also extremely indebted to Dr. R.P Pandey for being my mentor, resolving methodological issues and carefully analyzing my thesis which led to many meaningful insights.

I take this opportunity to thank Prof. Deepak Khare, Head, Department of Water Resources Development and Management, Indian Institute of Technology Roorkee, for providing the necessary resources during my research period. I owe a great deal of gratitude to Prof. Nayan Sharma, Chairman, SRC and the committee members Dr. C.S.P Ojha, Professor, Department of Civil Engineering and Dr. Ashish Pandey, Associate Professor, Department of Water Resources Development and Management, IIT Roorkee for their valuable suggestions and moral support.

A special thanks to Dr. Arpan Sherring, Professor, Sam Higginbottom Institute of Agriculture, Technology and Sciences, Allahabad, U.P and Dr. Anupama Nayak, Assistant

Executive Engineer, Water Resource Deparment, Odisha for their constant help and encouragement.

I am also immensely indebted to Department of Science and Technology (DST), INSPIRE Fellowship for providing the financial assistance during my research work.

I would like to thank and appreciate my friends Sananda Kundu, Arun Mondal, Prabhash Mishra, Surendra Chandhania, Rituraj Shukla, Pratibha Warwade, Pranuthi, Sarita Gajbhiye, Dheeraj Kumar and other fellow friends for providing support, love, contribution and encouragement during my thesis work.

Finally, I would like to thank my family, my parents, Debal Chakraborty and Soma Chakraborty; sister, Er. Shaonlee Goswami; my fiance, Pavan KR Murthy; my brother-in-law, Sourabh Goswami and Pankaj KR M; my mother-in-law, Aruna Devi M. My family always encouraged me, lifted my spirits, supported me during the crunch time. My family's unconditional love and support are the base of my thesis work.

(SHIULEE CHAKRABORTY)

TABLE OF CONTENTS

Chapter No.	TITLE	Page No.
	CANDIDATE'S DECLARATION	
	ABSTRACT	i
	ACKNOWLEDGEMENT	viii
	TABLE OF CONTENTS	x
	LIST OF TABLES	xvi
	LIST OF FIGURES	xviii
	LIST OF SYMBOLS AND ABBREVIATIONS	xxii
1.	**INTRODUCTION**	**1**
	1.1 GENERAL	1
	1.2 BACKGROUND OF THE STUDY	1
	1.3 RESEARCH OBJECTIVES	4
	1.4 ORGANIZATION OF THESIS	5
2.	**REVIEW OF LITERATURE**	**7**
	2.1 GENERAL	7
	2.2 STUDIES ON CLIMATIC TREND AND VARIABILITY IN INDIA	9
	2.2.1 Temperature Trend	9
	2.2.2 Rainfall Trend	11
	2.2.3 Relative Humidity Trend	12
	2.2.4 Reference Evapotranspiration Trend	12
	2.2.5 Remarks	13
	2.3 EVAPOTRANSPIRATION (ET)	15
	2.3.1 Impact of meteorological variables on Evapotranspiration	18
	2.3.2 Remarks	21
	2.4 SCS-CN METHOD	21
	2.4.1 Application of SCS-CN Method in Hydrology	24
	2.4.2 Remarks	25
	2.5 CLIMATE CHANGE AND ITS IMPACT ON IRRIGATION WATER REQUIREMENT	27
	2.5.1 Climate Change Models	27

2.5.2 Importance of bias correction in climate change scenario generation 30
2.5.3 Impact of climate change on irrigation water requirement 31
2.5.4 Remarks 32
3. STUDY AREA AND DATA 34
3.1 STUDY AREA 34
3.1.1 Location and Extent of the Basin 34
3.1.2 Water Scarcity in the Basin 34
3.1.3 Climate 36
3.1.4 Agriculture and Land use 36
3.1.5 Soil Type 37
3.1.6 Socio-economic Aspects 38
3.2 DATA USED AND PROCESSING 39
3.2.1 Hydro-meteorological data 39
3.2.2 Ancillary data 40
3.2.3 Remote Sensing Data 41
3.2.4 Characteristics of Meteorological Stations 42
4. ASSESSMENT OF TRENDS IN CLIMATIC VARIABLES 45
4.1 INTRODUCTION 45
4.2 DATA 47
4.3 METHODOLOGY 47
4.3.1 Homogeneity Test 47
4.3.2 Dependency Test (Autocorrelation coefficient) 47
4.3.3 Statistical Test for Trend and Variability Analysis 48
4.3.3.1 Mann–Kendall Test (Non-parametric) 48
4.3.3.2 Modified Mann Kendall Test 49
4.3.3.3 Theil-Sen's Slope Estimator 50
4.3.3.4 Percentage Change 50
4.3.4 Statistical Procedure for Rainfall Variability Analysis (Coefficient of Variation) 51
4.3.5 Spatial Analysis 51

4.4 RESULTS AND DISCUSSION 52
4.4.1 Trend Analysis of Rainfall 52
4.4.1.1 Trend Analysis 52
4.4.1.2 Analysis of Annual Rainfall Variability Pattern (Coefficient of Variation) 57
4.4.2 Trend Analysis of Temperature (Tmax, Tmin, Tmean) 58
4.4.3 Trend Analysis of Relative Humidity 66
4.4.4 Trend Analysis of Wind Speed 71
4.5 SUMMARY 75
5. INTER-COMPARISON OF REFERENCE EVAPOTRANSPIRATION ASSESSMENT METHODS 76
5.1 INTRODUCTION 76
5.2 DATA 78
5.3 METHODOLOGY 78
5.3.1 Estimation of Pan Coefficient (Kp) and Evapotranspiration (ETp) 78
5.3.2 Penman-Monteith equation 79
5.3.3 Priestley-Taylor method 79
5.3.4 Turc Method 79
5.3.5 Hargreaves Method 80
5.3.6 Thornthwaite Method 80
5.3.7 Blaney-Criddle Method 81
5.3.8 Model Evaluation Statistics 81
5.3.8.1 Mean absolute error 81
5.3.8.2 Root mean square error 81
5.3.8.3 Sum of squares of errors 81
5.3.8.4 Coefficient of determination 81
5.3.9 Sensitivity Analysis 82
5.4 RESULTS 83
5.4.1 Estimation of Pan Coefficient (Kp) 83
5.4.2 Comparison of ETo methods 85
5.4.3 Sensitivity to Climatic Parameters 87

5.5 SUMMARY 90

6. LONG TERM TREND ANALYSIS TO DETECT CHANGE IN IRRIGATION WATER REQUIREMENT (IWR) 91

6.1 INTRODUCTION 91

6.2 METHODOLOGY 92

6.2.1. Estimation of ETo 92

6.2.2. Determination of CWR/IWR 92

6.2.3. Statistical Test for Trend and Variability Analysis 94

6.3 RESULTS 95

6.3.1 Computation of ETo, CWR, IWR 95

6.3.2 Implication for Irrigation Planning 97

6.3.3 Effect of Climate Change on Kc values 97

6.3.4 Reference Evapotranspiration Trend 105

6.3.5 Analysis of Annual ETo Variability Pattern 110

6.3.6 Trends in Irrigation Water Requirement 111

6.3.7 Changes in IWR over the period 1960–2010 113

6.4 SUMMARY 116

7. RELATIONSHIP BETWEEN IRRIGATION WATER REQUIREMENT AND SCS-CURVE NUMBER 117

7.1 INTRODUCTION 117

7.2 METHODOLOGY 119

7.2.1 Determination of Curve Number (CN) 119

7.2.2 Relationship between CN and IWR 120

7.2.3 Performance Evaluation 123

7.2.3.1 Nash-Sutcliffe efficiency (NSE) 123

7.2.3.2 Coefficient of determination (R^2) 123

7.2.3.3 Index of agreement (d) 124

7.2.3.4 Percent bias (PBIAS) 124

7.2.3.5 Root Mean Square Error (RMSE) 124

7.3 RESULTS 125

7.3.1Determination of CN 126

7.3.2 Relationship between CN and IWR 126
7.3.3 Validation of the proposed relationship 133
7.3.4 Advantages and Limitations of Proposed Model 138
7.4 SUMMARY 138
8. STATISTICAL DOWNSCALING OF CLIMATIC VARIABLES, THEIR FUTURE PREDICTION AND IMPACT ON IRRIGATION WATER REQUIREMENT 139
8.1 INTRODUCTION 139
8.2 MATERIAL AND METHODS 141
8.2.1 Dataset 141
8.2.2 Methodology 142
8.2.2.1 Least Square Support Vector Machine (LS-SVM) 142
8.2.2.2 Artificial Neural Network Model 144
8.2.2.3 Multiple Linear Regressions 144
8.2.2.4 Model Tree model 145
8.2.2.5 Bias Correction 146
8.2.2.6 Model Evaluation Statistics 147
8.3 RESULTS AND DISCUSSION 149
8.3.1 Inter-comparison of Statistical Downscaling Models 149
8.3.2 Selection of Predictor Variables 151
8.3.3 Impact of Climate Change on Meteorological Variables 154
8.3.4 Impact of Climate Change on Reference Evapotranspiration (ETo) 158
8.3.5 Impact of Climate Change on Irrigation Water Requirement (IWR) 161
8.3.5.1 Kharif Irrigation Water Requirement (Paddy) 163
8.3.5.2 Rabi Irrigation Water Requirement (Wheat) 163
8.3.5.3 Rabi Irrigation Water Requirement (summer paddy) 163
8.4 SUMMARY 166
9. SUMMARY AND CONCLUSIONS 168
9.1 SPATIAL AND TEMPORAL TRENDS IN CLIMATIC VARIABLES 169
9.1.1 Rainfall Trend 169

9.1.2 Temperature Trend 169
9.1.3 Relative Humidity (RH) Trend 170
9.1.4 Wind Speed (WS) Trend 170
9.2 INTER-COMPARISON OF ETo ASSESSMENT METHODS 171
9.3 ASSESSMENT OF CROP COEFFICIENT, CWR, IWR AND THERE LONG TERM TREND 172
9.3.1 Assessment of Crop Coefficient (Kc) 172
9.3.2 Trend Analysis of Reference Evapotranspiration (ETo) 172
9.3.3 Trend Analysis of Irrigation Water Requirement (IWR) 173
9.4 IWR-CN RELATIONSHIP 173
9.5 PREDICTION OF CLIMATE CHANGE IN FUTURE 174
9.6 CONCLUSIONS 175
9.7 MAJOR RESEARCH CONTRIBUTIONS 176
9.8 SCOPE FOR FUTURE RESEARCH 177
BIBLIOGRAPHY **178**
ANNEXURES **214**

LIST OF TABLES

Table No.	Description	Page No.
2.1	Studies on Climatic Variability in India	14
2.2	Various methods of ETo estimation and their sensitivity to climatic variables	20
2.3	Application of SCS-CN methodology in different hydrological studies	26
2.4	Impact of climate change on irrigation water requirement	32
3.1	Characteristics of Meteorological Stations located in Seonath river basin	43
4.1	Results of regional average annual and seasonal rainfall for entire Seonath River Basin	55
4.2	Rate of change in annual and seasonal rainfall for Seonath river basin over 100years	55
4.3	Sen Slope estimator (°C/100 years) for maximum, minimum, mean temperature for different months	66
5.1	Climatic variables involved in selected methods for ETo estimation	77
5.2	Errors and correlation between Pan ET and other ET models for Seonath basin	87
5.3	Correlation Analysis of ETo with Meteorological Variables (Temperature, Rainfall, Relative Humidity and Wind Speed) in Seonath River Basin	88
6.1	Statistic of (seasonal) meteorological variables used for the computation of ETo, CWR, IWR	98
6.2	Average monthly values of rainfall, Pe and ETo for the computation of CWR/IWR	99
6.3	Percentage change in computed Average crop coefficient (Kc) values with FAO recommended Kc values at different growth stages of major crops in Seonath River Basin.	99
6.4	Monthly ETo trends by Mann–Kendall test (Bold value indicates significant level)	108
6.5	Results of regional average annual and seasonal ETo for entire Seonath Basin	110

6.6	Sen's Slope of Monsoon and Post Monsoon IWR over the period of 1960-2010	115
7.1	Computation of CWR for Kharif Paddy (P), Rabi Wheat (W) and Summer Paddy (SP) for each stages of crop growth period (1960-1989, calibration period)	127
7.2(a)	Computation of ETo, CWR, IWR, CN for derivation of CN-IWR relation for monsoon season	129
7.2(b)	Computation of ETo, CWR, IWR, CN for derivation of CN-IWR relation for post monsoon season	130
7.3	Range of IWR and CN for Seonath River Basin	132
7.4	Performance Evaluation of Developed Model	137
7.5	Rainfall deviation for monsoon and post-monsoon season	137
8.1	Selected Predictor Variables for downscaling of predictands	153
8.2	Abbreviation of selected predictor variables	154
8.3	Seasonal trends in climatic variables for future (2011-2100)	158

LIST OF FIGURES

Figure No.	Description	Page No.
2.1	Flowchart describing methods and climatic variables involved in the assessment of IWR	8
2.2	Proportionality concept of the existing SCS-CN method	23
3.1	Index map of Seonath River Basin (study area)	35
3.2	Crops and cropping pattern of Seonath river basin (Source: Directorate of Economics and Statistics, Chhattisgarh)	36
3.3	Land use of Seonath river basin	37
3.4	Soil map of Seonath River Basin	38
3.5	Field photographs showing landuse/cover types in the Seonath basin and basin runoff outlet	39
3.6	Location of Meteorological stations in Seonath basin	40
3.7	Digital Elevation Model of Seonath River Basin	42
3.8	Physical characteristics at locations of meteorological stations in Seonath basin	44
4.1	Percentage of Stations correlated for different climatic parameters (Annual and Seasonal)	48
4.2	Flowchart presenting methodology for trend and variability analysis of meteorological variables	52
4.3	Trend in annual and seasonal rainfall in Seonath river basin over the period of 1960-2010 (a) Annual (b) Monsoon (c) Summer (d) Winter	54
4.4	Temporal Trends of Annual and Seasonal Rainfall	57
4.5	Inter-annual Variability of Rainfall Variable	58
4.6	Spatial distribution of annual and seasonal trends in maximum temperature	60
4.7	Percentage of station with significant trend for Seonath River Basin	61
4.8	Spatial map of minimum temperature trend in Seonath river basin over 51 years (a) Annual (b) Summer (c) Winter (d) Monsoon	61
4.9	Percentage of stations with trend exist in the entire basin	62

4.10	Spatial trend analysis of average temperature on annual and seasonal timescales	63
4.11	Temporal trend in average temperature at annual and seasonal scale	64
4.12	Percentage change in maximum and minimum temperature over 51 years	64
4.13	Inter-annual variability of maximum and minimum temperature	65
4.14	Temporal Monthly Relative Humidity Trend at Seonath River Basin over 51 years	67
4.15	Percentage of Stations with significant Trend at Annual and Seasonal Scale	68
4.16	Spatial distribution of Annual and Seasonal Relative Humidity Trend	68
4.17	Monthly Rate of Change in Relative Humidity over 51 years (1960-2010)	69
4.18	Spatial Distribution of Percentage Change in annual relative humidity	70
4.19	Spatial Distribution of Inter-annual Variability in Annual Relative Humidity	70
4.20	Temporal Trend of Wind Speed over 51 years in Seonath river basin	71
4.21	Spatial trend distribution of wind speed for (a) Monsoon (b) Summer (c) Winter over entire Seonath river basin	72
4.22	Percentage of Stations shows trends in seasonal wind speed	73
4.23	Monthly Wind Speed Trend Magnitudes over 51 years	73
4.24	Percentage change in Wind Speed over 51 years	74
4.25	Spatial Variability of wind speed in Seonath river basin	74
5.1	Flowchart describing methodology for the present study	83
5.2	Monthly variation of pan coefficients	84
5.3	Monthly variation of ETo using recommended and estimated Kp values	84
5.4	Monthly average reference evapotranspiration (ETo) for the study area	86
5.5	Mean and Annual Reference Evapotranspiration for Seonath basin	86

5.6	Mean monthly sensitivity coefficients for each climate variable in Seonath Basin	89
5.7	Average yearly sensitivity (a) Spatial pattern of % change in ETo with 10% rise in climatic variables (b) Sensitivity coefficient for each climatic variable in Seonath River Basin	89
6.1	Flowchart represent methodology of the study	95
6.2(a)	Crop coefficient (Kc) curve for Rice using growth stage lengths of 31, 32, 52, and 25 days	100
6.2(b)	Crop coefficient (Kc) curve for wheat using growth stage lengths of 30, 30, 40, and 30 days	100
6.2(c)	Crop coefficient (Kc) curve for summer paddy using growth stage lengths of 20, 30, 40, and 30 days	101
6.3	Monthly variation of CWR estimated using FAO recommended and region specific Kc values. The hatched area shows the amount of crop water requirement (a) Kharif season (b) Rabi season	101
6.4	Kc values under climate change scenario (a) Kharif Rice (b) Rabi Wheat (c) Summer Paddy	102
6.5	Monthly variation of future CWR estimated using FAO recommended and region specific Kc values. The hatched area shows the amount of crop water requirement (a) Kharif season (b) Rabi season	104
6.6	Monthly Variations of ET and Rainfall	105
6.7	Plots of Kendall Z statistic for the annual and seasonal ETo trend during 1960-2010 (a) Annual; (b) Monsoon; (c) Winter; (d) Summer	107
6.8	Percentage of stations showing increasing and decreasing trend for the Seonath river basin	108
6.9	Percentage change in annual (ETo) for the Seonath river basin	109
6.10	Monthly ETo trend slope values over 51 years (1960–2010) for the Seonath river basin	109
6.11	Spatial distribution of inter-annual variability of annual ETo (CV)	111
6.12	Trends in Irrigation Water Requirement for Seonath river basin	112

6.13	Total IWR. The hatched area shows the amount of Irrigation requirements	112
6.14	Trend in Irrigation Water Requirements (a) Kharif Crop (Paddy) (b) Rabi Crop (Wheat) (c) Rabi Crop (Summer Paddy)	114
6.15	Percentage of station with increasing/decreasing trend	115
7.1	Flowchart describing methodology to establish IWR-CN relationship	125
7.2	Development of a relationship between IWR and S for (a) Monsoon (b) Post-monsoon seasons	133
7.3	Validation of IWR-S relationship for (a) monsoon and (b) non-monsoon seasons	135
7.4	Validation of proposed model for 4 datasets (1990-94, 1995-99, 2000-04, 2005-10) for (a) Monsoon (b) Post-Monsoon seasons	136
8.1	Statistical downscaling framework	148
8.2	NSE and R^2 calibration values for four downscaling methods	149
8.3	NSE and R^2 validation values for four downscaling methods	150
8.4	Downscaling results of meteorological variables for the entire basin	155
8.5	Future projections of meteorological variables from HadCM3 GCM output with A2 scenario for entire basin	157
8.6	Monthly reference evapotranspiration for Seonath River Basin estimated from HadCM3 GCM output for A2 scenario	159
8.7	Rate of Change in Reference Evapotranspiration over 100 years	159
8.8	Reference Evapotranspiration trend on annual and seasonal scales for two decades	160
8.9	Percentage Change in IWR of Kharif Paddy, Wheat and Summer Paddy	162
8.10	Irrigation Water Requirement of Kharif Paddy	164
8.11	Spatial distribution of Future Irrigation Water Requirement for (a) Kharif (Paddy) (b) Rabi (Wheat) (c) Rabi (Summer Paddy)	164
8.12	Irrigation Water Requirement of Rabi Wheat	165
8.13	Irrigation Water Requirement of Rabi Summer Paddy	166

LIST OF ABBREVIATIONS AND SYMBOLS

ABBREVIATIONS

AMC	Antecedent Moisture Condition
ANN	Artificial Neural Network
CC	Correlation Coefficient
CCCSN	Canadian Climate Change Scenarios Network
CCIS	Canadian Climate Impacts Scenarios
CN	Curve Number
CUSUM	Cumulative Sum
CV	Coefficient of Variation
CWR	Crop Water Requirement
d	Index of agreement
D	Pan evaporation
DEM	Digital Elevation Model
ERDAS	Earth Resource Data Analyzing System
ET	Evapotranspiration
ETc	Crop evapotranspiration
ETo	Reference Evapotranspiration
ETp	Pan evapotranspiration
ETp	Pan Evapotranspiration
FAO	Food and Agriculture Organization
GCM	Global Climate Model
GCP	Ground control points
GIS	Geographical Information System
GLCF	Global Land Cover Facility
HadCM3	Hadley Centre Coupled Model, version 3
hrs	Hours
IDW	Inverse Distance Weight
IMD	Indian Metrological Department
IPCC	Intergovernmental Panel on Climate Change
IWD	Irrigation Water Demand
IWR	Irrigation Water Requirement

Kc	Crop Coefficient
Km/day	Kilometer per day
Kp	Pan coefficient
kPa	Kilo Pascal
L	Length of the year
LANDSAT	Land Satellite
LS-SVM	Least Square Support Vector Machine
m	Meters
MAE	Mean absolute error
MJ	Mega Joules
MK	Mann Kendall
MLP	Multiple Linear Perception
MLR	Multiple linear Regression
mm	Millimeters
MMK	Modified Mann Kendall
MT	Model Tree
MTPS	Model Tree With Pruning And With Smoothing
MUSLE	Modified Universal Soil Loss Equation
n	Sunshine hours
NBSS&LUP	National Bureau of Soil Survey and Land Use Planning
NCAR	National Center for Atmospheric Research
NCEP	National Centers for Environmental Prediction
NSE	Nash-Sutcliffe efficiency
P	Atmospheric Pressure
PBIAS	Percent bias
P_c	Percentage Change
PCA	Principal Component Analysis
PCC	Partial Correlation Coefficient
Pe	Effective Rainfall
PET	Potential Evapotranspiration
PM	Penman-Monteith
R^2	Coefficient of determination
RBF	Radial Basis Function
RCM	Regional Climate Model

RH	Relative Humidity
RMSE	Root mean square error
Rs	Solar Radiation
S	Sensitivity Coefficient
SCS-CN	Soil Conservation Service Curve Number
SDC	State Data Centre
SMC	Soil moisture condition
SOI	Survey of India
sq. km	Square Kilometers
SRTM	Shuttle Radar Topography Mission
SSE	Sum of squares of errors
SWAT	Soil and Water Assessment Tool
T	Temperature
USDA	United States Department of Agriculture
WMO	World Meteorological Organization
WS	Wind Speed

SYMBOLS

%	Percentage
°C	Degree Centigrade
CO_2	Carbon-di-oxide
E_I	Interception Loss
E_S	Soil Evaporation
E_T	Daily transpiration
F	Actual Infiltration
G	Soil Heat Flux Density
Ia	Initial Abstraction
Kc	Crop Coefficient
Kcb	Basal Crop Coefficient
P	Rainfall
Q	Direct Surface Runoff
RH	Relative Humidity
Rn	Net Radiation
S	Potential Maximum Retention
Tmax	Maximum Temperature

Tmean	Mean Temperature
Tmin	Minimum Temperature
U2	Wind Speed at 2m height
W	Root-Zone Moisture
W*	Root-Zone Storage Capacity
α and β	Coefficient and exponent of IWR-CN relation
β	Slope Magnitude
$\beta_{T,S}$	Coefficient of transpiration plus soil evaporation
Δ	Slope Vapour Curve
λ	Initial Abstraction Coefficient
μ	Mean
ρ_k	Autocorrelation coefficient
ρk	Autocorrelation function
σ	Sigma

CHAPTER 1

INTRODUCTION

1.1 GENERAL

It is generally believed that climate change would have adverse impact on rainfed as well as irrigated agriculture. Presently, about 90% of the global water utilization is for irrigation purpose, and over 40% of the crops are produced under irrigated conditions (Doll and Siebert, 2002). Further climate change may alter the spatial and temporal pattern of sectoral water demand (irrigation, industrial, domestic, environmental etc.) on global and regional scale. With the world's growing population, it is expected that irrigated agriculture would have to be extended in future on large scale. However, it is not yet known whether there will be sufficient water available for the necessary extension. Thus, it is important to reliably quantify the future changes in irrigation water requirement (IWR) especially for those areas where agriculture is the primary activity in various river basins in India.

Surface irrigation schemes comprise of i) surface storage and/or diversion structures, ii) irrigation water distribution, iii) drainage network, iv) on farm development works etc. These schemes involve huge investment of capital and other resources. Irrigation schemes are planned to serve the purpose of providing adequate, timely and reliable water supply for the crops to meet their irrigation water requirement (IWR) over the life of project (usually 50 to 100 years). Irrigation water requirements of crops are based on average fortnightly or monthly climatic data. Over the year variability is not considered in the irrigation schemes and also, it is assumed that irrigation water requirements shall be same over the years.

Planning horizon of irrigation schemes typically range from 50 years to 100 years. During this length of period, changes may occur in climatic variables of a given region and therefore irrigation water requirements may also change significantly. On supply side, water availability for irrigation may also get adversely affected.

1.2 BACKGROUND OF THE STUDY

Water resources management is of major concern in India, where agriculture is the key and most important activity playing a key role in sustainable development. Climate change affects agriculture due to higher temperature and rainfall variability. The available water resource may be altered due to change in rainfall pattern and increase in rate of

evaporation. It is of common knowledge that, higher evapotranspiration (ET) due to temperature rise demands greater amount of water for irrigation and, at the same time, a higher temperature causes change in crop physiology and shortens the crop growing period, which in turn reduces the irrigation days. These contradictory phenomena may, however, change the total irrigation water demand. Since water utilization in agriculture sector far exceeds water requirement in any other sectors, the knowledge of rain water and irrigation water utilization for agriculture becomes the key component in managing the water resources efficiently. Number of research studies have been carried out to investigate the impact of climate change in terms of trend and variability analysis of climatic factors such as temperature, rainfall, reference evapotranspiration (ETo) and pan evapotranspiration (ETp) (Schwartz and Randall, 2003; Garbrecht et al., 2004; Hegerl et al., 2007; Fu et al., 2009; Saghravani et al., 2009; Hakan et al., 2010; Tekwa and Bwade, 2011). Scrutiny of literature indicates that there have been large number of studies to investigate possible changes in climatic variables like temperature and rainfall. Therefore, the studies analyzing climate change impacts on agriculture water demand are very important and need comprehensive investigations (Doll, 2002).

Most of the current hydrologic models, water-management model, and crop growth models require an accurate estimation of reference evapotranspiration (ETo) for reliable assessment of crop water requirement (CWR) and irrigation water requirement (IWR). The accurate assessment of ETo is a key component for the quantification of supplemental irrigation water requirement of different crops during their critical growth periods. A large number of methods ranging from simple empirical to complex physical methods are available in literature to estimate ETo. The important and widely used methods are Penman, (1948); FAO-24 Penman, (1977); Priestley-Taylor, (1972); Hargreaves-Samani (1982); Turc, (1961); Jensen-Haise (1963); FAO-56 Penman-Monteith, (1965) etc. The above methods have been developed and tested for varying geographic and climatic conditions. Since empirical and semi-empirical methods have been developed for particular sets of conditions, their use is restricted to specific conditions only (Beven, 2001). Physical methods are based on physical processes between plant and atmosphere, and therefore, represent only point estimation of ETo, therefore, all such methods must be calibrated and validated with field data (lysimeter data) before use (Vorosmarty et al., 1998). The International Commission for Irrigation and Drainage (Allen et al., 1994) and the Food and Agricultural Organization (FAO-56) (Allen et al., 1998) have recommended the use of

physically based Penman-Monteith (PM) method for computation of reference/potential evapotranspiration using climatic data, specifically when sufficient meteorological data are available to ensure reliable estimates.

Soil moisture condition (SMC) generally represents the moisture contained in the root zone depth of a soil profile (normally 1-2 m top layer) which can potentially evaporate and/or take active part in transpiration. Therefore, evapotranspiration (ET) is directly influenced by SMC. ET as such affects the land surface energy dynamics, climatology, hydrology, and ecology (Vinnikov et al., 1999; Moran et al., 2004). SMC depends on the water holding capacity that depends on the soil type. Furthermore, it is closely related with the potential maximum retention (or curve number), only parameter of the popular Soil Conservation Service Curve Number (SCS-CN) method, for a watershed can be characterized by a particular set of curve numbers with three distinct antecedent moisture conditions (AMC). Since these curve numbers are derived from the real rainfall-runoff data of a watershed (Mishra et al., 2008), they represent both watershed and its hydro-meteorological characteristics. The CN parameter of SCS-CN method and ET has been investigated by Mishra et al., (2014). The linking of these two different concepts supported by the argument that the watershed characteristics (land use/treatment, soil type, climate etc.) which affect CN also influence the ET mechanism, albeit differently. Despite availability of number of models in literature, the accurate assessment of ET is a complicated task as it involves spatial and temporal heterogeneity in meteorological and climatic parameters, soil moisture status, surface cover type, soil classes and plant water availability etc. (Makkeasorn et al., 2006). As per the knowledge ET is a major component in estimation of IWR and it is function of ET. Therefore, SCS-CN method and IWR relationship has to be investigated for simpler, yet reliable assessment of IWR at seasonal and watershed scales if rainfall runoff data of the basin is available.

On a global scale, numbers of studies have been carried out to study the impact of climate change on irrigation water requirement (Elgaali et al., 2007; Rodriguez Diaz et al., 2007; Yano et al., 2007; Sahid, 2011; Rehana and Majumdar, 2012). The aforesaid studies have focused on the estimation of projected irrigation water requirement using either of the following approaches (i) use of perturbation method for the generation of climate change scenario by GCM outputs, (ii) applying available downscale data for the generation of climate change scenario, (iii) employing modeling software for future prediction of IWR. Further some studies may provide erroneous estimation of future IWR (CWR-effective

rainfall) as this account for total rainfall instead of using effective rainfall. IWR is extremely sensitive to change in some of the climatic variables. Thus, more accurate climate change scenario for predictions of meteorological parameters (evapotranspiration, temperature, wind speed, relative humidity and rainfall) would be needed. It is necessary to consider all those climatic variables which affect the ETo/CWR/IWR in order to understand the changes in the future irrigation water demand. The downscaling model (LS-SVM) is well accepted in the climate change impact assessment studies in the recent years by the research community (Tripathi et al., 2006)

The study has been carried out for Seonath river basin which is part of the Mahandi river system in Chhattisgarh State, India. The study area falls in dry sub-humid climatic regions of India. The average annual rainfall in Seonath river basin varies from 1000 mm to 1255 mm. Nearly 85% of the mean annual rainfall occur in monsoon period (June to September). Rainfall in remaining part of the year is very little and therefore, most of the tributaries of Seonath River get dried by mid-winter season (i.e., end of December month). The pattern of water utilization for agriculture has also changed over the years. Therefore, assessment of irrigation water requirement (IWR) at the micro-regional level and its impact on agriculture is necessary for developing strategies for mitigation of water stress in the basin. In the light of literature review and emerging facts in the respect of irrigation water supply and demand imbalance, present study has been taken up to assess long-term changes in IWR

1.3 RESEARCH OBJECTIVES

Based on the above discussion, specific objectives for the present research work are stated below:

1. Assessment of temporal trends and spatial variability of key meteorological variables in the study area.

2. Estimation of region specific pan coefficient (Kp) on monthly basis to compute reference evapotranspiration (ETo). Inter-comparison of available models for estimation of ETo and conducting sensitivity analysis of ETo with respect to key climatic variables.

3. Assessment of region specific crop coefficient for different crop growth stages, crop water requirement (CWR) and irrigation water requirement (IWR) for major crops and long term trend analysis in ETo and IWR.

4. Development of relationship between Soil Conservation Service Curve number (SCS-CN) and IWR.

5. Application of different statistical downscaling models, their inter-comparison for future prediction of climatic variables and its impact on irrigation water requirement (IWR).

1.4 ORGANIZATION OF THESIS

The thesis is organized in nine chapters as follows:

Chapter One: The first chapter briefly describes the importance and problems related to IWR, the present state-of-the-art knowledge, and outline the research objectives.

Chapter Two: The second chapter describes the review of relevant literature on different components of study such as i) long term trends in climatic variables, ii) ET estimation methods, their relative merits and impact of climatic variables, iii) application of SCS-CN methodology in hydrological studies and iv) impact of climate change on irrigation water requirement.

Chapter Three: This chapter presents description of the study area and data used to carry out the study.

Chapter Four: This chapter presents the details of study, methodology and result of long term trends in hydro-meteorological variables in the Seonath river basin.

Chapter Five: This chapter deals with comparative study of various methods for estimation of reference evapotranspiration (ETo), seasonal variability of pan coefficient, and sensitivity analysis of ETo with different climatic variables.

Chapter Six: Chapter six presents the detailed procedure used for estimation of crop coefficient, CWR and subsequently IWR of major crops in the basin. Further the monthly ETo is corrected with crop coefficients for each crop to compute CWR which in turn are used to compute the IWR of the crop. Furthermore, detailed procedure to estimate trend and abrupt changes in ETo and IWR is discussed.

Chapter Seven: This chapter presents the mathematical rationale developed to propose the relationship between irrigation water requirement and curve number (IWR-CN). Furthermore, the chapter also discusses the results of developed model, its validation and criteria for model evaluation.

Chapter Eight: This chapter deals with downscaling of National Centers for Environmental Prediction (NCEP) data and prediction of future hydro meteorological data using Hadley Centre Coupled Model, version 3 (HadCM3) data by different downscaling methods and identification of best prediction model for the study area. The results obtained have been used to determine the long term trend and variability in climatic variables and its effect on IWR for future years.

Chapter Nine: Important results of the research work are synthesized in this chapter. Certain conclusions are drawn and scope for future research work is also mentioned in this chapter.

CHAPTER 2

REVIEW OF LITERATURE

This chapter deals with the review of literature on important aspects of the present study. In the light of major objectives of the present research work, the literature review is covered in four sections. The first section presents the review of literature on studies of trends in climatic variables in India. Second section includes commonly employed reference evapotranspiration (ETo) estimation methods, their limitations and impact of climatic variables in ETo computation. The third section deals with the concept of popular SCS-CN method and its numerous applications in different areas of hydrology. Last section incorporates climate change and its impact on irrigation water requirement.

2.1 GENERAL

Studies on Irrigation Water Requirement (IWR) are one of the most important components for regional water budget for planning and management of water resources. IWR refers to the depth of irrigation water, excluding rainfall, stored as soil moisture or ground water that is required consumptively for crop production (USDA, 1970). It is the amount of water required during the cropping period for successful crop cultivation and it is estimated by subtracting the amount of water available to the crop through natural precipitation, i.e., rainfed irrigation, and available soil moisture from the crop evapotranspiration. Therefore, IWR includes estimation of reference evapotranspiration (ETo), crop water requirement (CWR), soil moisture and effective precipitation. Complete methodology for estimation of IWR has been summarized in the flowchart presented in Figure 2.1.

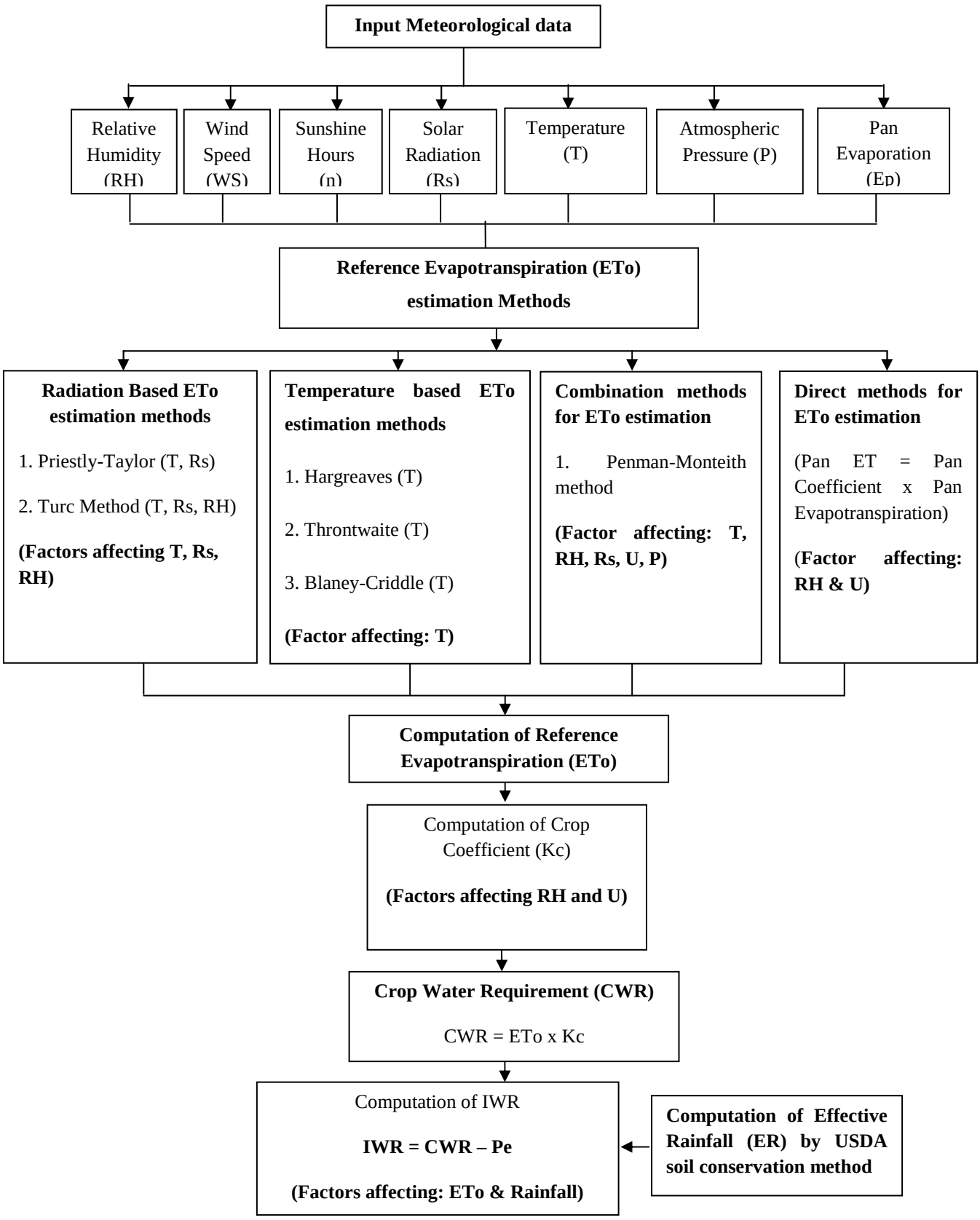

Figure 2.1 Flowchart describing methods and climatic variables involved in the assessment of IWR

The first important parameter in IWR assessment is ETo, which can be calculated by numerous methods available in literature. The next important parameter in IWR estimation is crop water requirement. It is an empirical estimate of the total amount of water required for a crop growing in a given area under known climatic conditions so that crop production is not limited by lack of water. The CWR is computed using ETo and a crop coefficient (Kc). The third and one of the most significant parameters in IWR assessment is effective rainfall (ER). It is defined as a part of actual rainfall that is available to meet the potential transpiration of cropped area. The amount of effective rainfall depends and varies just as total rainfall varies (FAO, 1975). Several methods are reported in literature for the estimation of ER, such as i) nomograph suggested by Hershfield (1964); ii) Renfro Equation method by Chow (1964); iii) U.S. Bureau of Reclamation method (USBR) given by Stamm (1967); iv) empirical table given by Brouwer and Heibloem, 1986; and v) a soil–water balance model (Patwardhan et al. 1990). Yet another method of ER estimation is USDA-SCS method recommended by the United States Department of Agriculture (USDA, 1967). It is one of the widely used and accepted methods for ER estimation (Cuenca 1989; Jensen et al. 1990; Kuo et al. 2006).

Global warming due to emission of green house gases such as CO_2 causes changes and variability in meteorological factors such as air temperature, relative humidity, solar radiation and rainfall (IPCC 2007). Due to these changes in meteorological variables the evapotranspiration is potentially affected and thus causes the changes in irrigation water requirement of crops in different regions (Elgaali et al., 2007; Rodriguez Diaz et al., 2007; Yano et al., 2007; Sahid, 2011; Rehana and Majumdar, 2012).

2.2 STUDIES ON CLIMATIC TREND AND VARIABILITY IN INDIA

2.2.1 Temperature Trend

In India, numerous studies have been carried out to detect and quantify long term changes in temperature. The temperature trend and variability have been better estimated using long-term data series. A study conducted by Hingane et al. (1985) has shown increasing trend in mean annual temperature. During 20th century, an analysis of long term temperature data for 73 stations (1901-1982) has shown increasing trend in mean annual surface air temperatures over India. It has been observed that about 0.4 °C increase in temperature has taken place on country scale during the period of 8 decades. The study carried out by Sinha Ray et al. (1997) has shown that the changes in mean annual

temperature are partly due to rise in the minimum temperature related to enhanced extent of urbanization. Examination of long-term variation in the annual mean temperature of highly industrial and densely populated cities such as Mumbai and Kolkata have shown increasing trend in annual mean temperature with change of 0.84°C and 1.39°C over 100 years, respectively (Hingane, 1995). These warming rates are much higher than the values reported for the country as a whole. Rupa Kumar et al. (1994) have shown that the countrywide mean maximum temperature had risen by 0.6°C and mean minimum temperature had decreased by 0.1°C. Pant and Kumar (1997) analyzed trends in annual and seasonal air temperatures from 1881 to 1997 and reported that there has been increasing trend in mean annual temperature with increase of 0.57°C over 100 years. However, as the trend of mean minimum temperature is not statistically significant, they concluded that most of the increase in mean surface air temperature over India is due to the increase in daytime temperature. The trend and change in magnitude of temperatures over India/Indian sub-continent for last century has been noticed to be mostly consistent with the global trend and magnitude. In India, increasing trend in temperature is mainly found in winter and post-monsoon seasons. The non-significant trend is found in monsoon temperatures in many part of country except for Northwest India which shows significant decreasing trend. Bhutiyani et al. (2007) concluded that North West Himalayas (NWH) of India has shown rise in air temperature due to increases in maximum and minimum air temperatures, and warming is more pronounced in maximum temperature. They have accomplished that there were inter-connection between the precipitation and temperature variation in the NWH till late 1960s. However, after 1970s, these connections appear to become weaker. It may be due to presence of other factors like increase in greenhouse gases in the atmosphere. Mall et al. (2007) concluded that all India mean annual temperature showed significant warming trend of 0.05°C/10 year during the period 1901-2003. The recent period from 1971 to 2003 has seen a relatively accelerated warming of 0.22°C/10 year, which is largely due to unprecedented warming during the last decade. Dhorde et al. (2009) reported air temperature trends of densely populated cities of India (Delhi, Kolkata, Mumbai and Chennai). They reported a significant increasing trend in maximum temperature during winter and monsoon at Mumbai city whereas remaining cities recorded significant increase in minimum temperature during winter. They reported that the negative change in air temperature is due to increase in population.

2.2.2 Rainfall Trend

Several studies have been conducted to detect the trend and variability in rainfall over India. These studies do not show clear rising or falling trend in mean annual rainfall over India (Sarkar and Thapliyal, 1988; Thapliyal and Kulshrestha, 1991). The trend analysis of mean annual rainfall has shown that five year running mean has deviated from normal rainfall within ±1 standard deviation (Thapliyal and Kulshreshtha, 1991). However the monsoon rainfall shows no significant trend on a long term basis, mostly for overall India (Mooley and Parthasarathy, 1984), but few parts of India shows significant long term trends in rainfall observed by different researchers (Raghavendra, 1974; Chaudhary and Abhyankar, 1979). A study has been carried out by Rupa Kumar et al. (1992) to show trends in monthly rainfall records of 306 stations falling in India. They found that area of north-east India, north-west peninsula and north-east peninsula show falling trend in summer and monsoon rainfall over India. However, they also reported a rising trend in monsoon rainfall for north-west, west coast and central peninsular India. The decreasing percentage change varies between -6 to -8% over 100 years whereas the increasing percentage change ranges from 10 to 12% over 100 years. Though these trends are statistically significant, but they account for a relatively small part of the total variance in the rainfall. Srivastava et al. (1998) reported the existence of a definite trend in rainfall over smaller spatial scale. Mirza et al., (1998) carried out trend and persistence analysis for Ganges, Brahmaputra and Meghna river basins. They found that precipitation in Ganges basin is by and large stable. Precipitation in one sub division in the Brahmaputra basin shows a decreasing trend and another shows an increasing trend. One of three subdivision of the Brahmaputra basin shows a decreasing trend while another shows an increasing trend. Sinha Ray and De (2003) summarized the existing information on climate change and trends in the occurrence of extreme events with special reference to India. They concluded that all India rainfall and surface pressure show no significant trend except some periodic behaviour. The frequency of heavy rain events during the south-west monsoon has shown an increasing trend over certain parts of the country. On the other hand, decreasing trend has been observed during winter, pre-monsoon and post-monsoon seasons. Lal (2001) and MOEF (2004) reported a large random variation in rainfall over India, with no regular trend is noticeable on annual and seasonal scales. However, rising trend in the seasonal rainfall have been found in North Andhra Pradesh, West Coast, and Northwest India and decreasing trend has been found for Orissa, East Madhya Pradesh and Northeast India during recent years. Kumar et al. (2010) also studied a rainfall trend on monthly, annual and seasonal scales for the period of 135 years (1871-

2005) for 30 sub-regions of India. They found a rising trend in annual rainfall for half of the sub-divisions, but only Coastal Karnataka, Punjab and Haryana shows statistically significant trend. Likewise, only one sub-region viz., Chhattisgarh shows a significant falling trend. Overall, on an Indian scale no significant trend has been detected for annual, seasonal and monthly rainfall.

2.2.3 Relative Humidity Trend

Very few studies have been reported on relative humidity (RH) trend over India. A study has been carried out by Singh et.al, 2008 to detect long term trend in rainfall and relative humidity for nine river basins located in northwest and central India (viz., Lower Indus, Ganga, Brahamani and Subarnarekha, Mahanadi, Tapi, Narmada, Mahi, Sabarmati, Luni) over 90-100 years. They found an increasing trend in rainfall and relative humidity for almost all the river basins. The maximum increase in rainfall is observed for lower Indus followed by Tapi river basin. Further, an increasing trend in relative humidity has been reported on seasonal and annual scale for majority of river basins. An increase in annual mean relative humidity for six river basins (Western river basins) has been found in the range of 1–18% of mean per 100 years, while a decrease for two river basins (Brahamani and Subaranrekha river basin) 1-13% of mean per 100 years has been observed. The net increase in RH is by 2.4% of mean per 100 years.

2.2.4 Reference Evapotranspiration Trend

Bandyopadhyay et al. (2009) has analyzed the temporal trend of evapotranspiration (ET) along with its region wise spatial variation for 32 years (1971–2002) for 133 selected stations over different agro-ecological regions of India. Reference evapotranspiration (ETo) has been estimated by the globally accepted FAO Penman Monteith method. These ETo values have been then analyzed by a nonparametric Mann–Kendall test with modified effective sample size approach for serially correlated data and Sen's slope to determine the existence and magnitude of any statistically significant trend over the time period considered in the study. They found a significant decreasing trend in ETo for all over India during the study period, which may be mainly caused by a significant increase in the relative humidity and a consistent significant decrease in the wind speed throughout the country. Duhan et al., 2012 also analysed a trend in ETo for Tons river basin, Madhya Pradesh over the period of 34 years (1969-2003). They found a decreasing trend in ETo on annual and

seasonal scales over the years. This is mainly due to increase in air temperature and net solar radiation. The annual ETo is decreased at the rate of -1.75 to -8.98 mm/year.

Mishra et al. (2009) examined the affect of climate change on rainfall in the Kansabati basin, West Bengal, India. They studied trends in future rainfall based on annual, wet and dry periods using global climate model (GCM) and scenario uncertainty. They found that there is probable increase in annual and monsoon rainfall trend during 2051–2100 for A2 scenario and a decreasing trend in dry period rainfall for B2 scenario. The persistence in dry period rainfall has been observed to be highest for north-west part of the basin. Patra et al. (2012) studied temporal variation in monthly, seasonal and annual rainfall for Orissa state, India during 1871 to 2006. Long term changes in rainfall characteristics have been determined by both parametric and non-parametric tests. The analysis revealed non-significant decreasing trend in annual as well as monsoon rainfall, whereas increasing trend in post-monsoon rainfall over the state of Orissa. Rainfall during winter and summer seasons showed a rising trend. Based on departure from mean, rainfall analysis also showed an increased number of dry years compared to wet years after 1950. They found that changing rainfall trend during monsoon months is a major concern for the rainfed agriculture and also this will affect hydro power generation and reservoir operation in the region. The studies relevant to the study area of present research are summarized and presented in Table 2.1.

2.2.5 Remarks

The studies reviewed above pertain to different basins and regions of India including climate change studies of Mahanadi river basin. The several studies on Mahanadi basin dealt with trend analysis of rainfall and relative humidity only. Number of studies have been carried out to detect trend in rainfall and temperature in India, however studies on trend analysis of other meteorological variables (relative humidity and wind speed) are limited. Therefore, trend and variability analysis of relative humidity and wind speed also need to be analysed. As long term changes in climatic variables viz., rainfall, temperature, relative humidity and wind speed may lead to changes in evapotranspiration and in turn irrigation water requirement on long term basis. Therefore, it is important to carry out detailed analysis of changes in climatic variables and their impact on regional irrigation water requirement.

Table 2.1 Studies on Climatic Variability in India

Authors	Study Area and period	Climatic Variable	Major Findings/Remarks
Kumar et al., (2010)	36 meteorological sub-divisions of India, (1871-2005)	Rainfall	Coastal Karnataka, Punjab and Haryana show statistically significant trend and Chhattisgarh shows a significant falling trend. Overall for India, no significant trend has been observed for annual, seasonal and monthly rainfall.
Singh et al., (2008)	Nine river basin located in north west and central part of India (Lower Indus, Ganga, Brahamani and Subarnarekha, Mahanadi, Tapi, Narmada, Mahi, Sabarmati, Luni)	Rainfall and Relative Humidity	Increasing trend in rainfall and relative humidity for almost all the river basins. The maximum increase in rainfall is observed in lower Indus basin followed by Tapi river basin. Increasing trend in relative humidity has been reported on seasonal and annual scale for majority of river basins.
Mall et.al, (2007)	India, (1901-2003)	Temperature	Significant increasing trend in mean annual temperature at the rate of 0.05°C/10 year during the period 1901-2003. The recent period from 1971 to 2003 has seen a relatively accelerated warming of 0.22°C/10 year, which is largely due to unprecedented warming during the last decade.
Bandyopadhyay et al. (2009)	Agro-ecological regions of India, (1971-2002)	Reference evapotranspiration	Significant decreasing trend in ETo for all over India during the study period, mainly caused by a significant increase in the relative humidity and a constant significant decrease in the wind speed.

2.3 EVAPOTRANSPIRATION (ET)

Evapotranspiration (ET), the major component of the hydrologic cycle, is important for planning and operation of irrigation systems. ET depends on several climatological factors, such as temperature, humidity, wind speed, radiation, and type and growth stage of the crop. ET can be either directly measured using lysimeter, catchment water balance, and Pan evaporation approaches or indirectly by using climatological data. Lysimeter, a popular instrument for measuring ET, is often expensive in terms of its construction, and its operation requires skill. It is, however, most accurate if surface cover condition of the catchment perfectly matches the inside cover conditions of the lysimeter. However, exact simulation of prototype field condition in lysimeter is practically not possible and hence the results obtained may not be very accurate. Furthermore, the lysimeter experiment needed extensive care, longer time and high cost for its operation which is normally not practicable.

Nevertheless, the water balance method yields the best estimates of mean long-term evaporation from large (plain) river basin (Gidrometeoizdat, 1967). However, the estimation of ET using water balance method is often limited due to inconvenience and inaccuracy in measurement of ground water inflow and outflow especially at shorter time span. Furthermore, pan evaporation method is one of the simplest and least time consuming method of irrigation scheduling and has been used successfully in most parts of the world (Prestt, 1986). However, the common problem is the selection of accurate pan factor which depends on the surrounding of the pan. Further, crop coefficients, which depend on the crop characteristics and local conditions, are used to convert evapotranspiration (ET) to crop ET. Evapotranspiration (ET) is defined as “the rate of evapotranspiration from a hypothetical crop with an assumed crop height (0.12 m) and a fixed canopy resistance (70 s/m) and albedo (0.23) which would closely resemble to evapotranspiration from an extensive surface of green grass cover of uniform height, actively growing, totally shading the ground and under unlimited water condition” (Allen et al., 1998).

A large number of methods varying from simple empirical to complex physically based have been developed for different parts of the world. These methods utilize the climatological data and can be grouped into three broad categories i.e. temperature based, radiation based, and combination theory based methods. Since solar radiation provides the energy required for the phase change of water, several methods (Makkink, 1957; Turc, 1961; Priestley and Taylor, 1972; Doorenbos and Pruitt, 1977) have been developed for ET

estimation. The radiation based methods show good results in humid climates where the aerodynamic term is relatively small, but the performance in arid condition are erratic and normally underestimate evapotranspiration. Turc (1960) developed a formula based on solar radiation and mean air temperature for 10 days period which was later modified by Turc (1961). Turc radiation method is the best method for ET estimation for humid locations. Priestley-Taylor (1972) method is the approximation of Penman method based on the fact that for very large areas the second term of the Penman equation is approximately thirty percent that of the first. Jensen-Haise (1963) method is often classified as a solar radiation method, however air temperature is also used and the coefficients used in the model are based on other inputs such as elevation and long term mean temperature (Burman et al., 1983).

In temperature based ET method, a relationship has been developed between air temperature and ET. Hargreaves, Thornthwaite, and Blaney-Criddle etc. are the few examples of temperature-based ET estimation methods. However, temperature-based methods are empirical and require local calibration in order to achieve satisfactory results. Thornthwaite (1948) correlated mean monthly temperature with ET for the east-central US and developed an equation which is widely used throughout the world. Thornthwaite method usually underestimates ET. However, simplicity in generating the seasonal distribution of ET is one of the strengths of the method (Jensen et al., 1990). A formula developed by Makkink (1957) for estimation of ET based on solar radiation and air temperature is still employed in Western Europe. Makkink formula used the energy term of the Penman equation, solar radiation, and a constant (negative and small in magnitude). The Blaney and Criddle (1950) procedure for estimating ET is well known in the western USA and has been used extensively elsewhere (Singh, 1989). The method uses temperature as well as daily sunshine duration, minimum daily relative humidity, and the day-time wind speed at 2 m height. The model is quite sensitive to the wind speed variable and somewhat insensitive to the estimate of relative humidity. Christiansen (1968) and Christiansen and Hargreaves (1969) reduced weather data requirements up to only estimated extraterrestrial radiation, air temperature and calculated the difference between maximum and minimum air temperatures to predict the effects of relative humidity and cloudiness. These efforts resulted in a very simple and accurate Hargreaves and Samani (1985) method for ET estimation. This method is most suitable for both arid and humid locations, if only maximum and minimum temperatures are available. The combination methods have been developed by

combining the energy balance and mass transfer approaches. These methods combine fundamental physical principles and empirical concepts based on standard meteorological observations and have been widely used for estimation of ET from climatic data. Penman (1948) first derived the combination equation by combining components of energy balance and aerodynamics. Later, many scientists modified the Penman equation by incorporating stomatal resistance, modifying the wind function and vapor pressure deficits (Penman, 1963; Monteith, 1965; Wright and Jensen, 1972; Doorenbos and Pruitt, 1977; Wright, 1982). Penman-Monteith, FAO-24 Penman, 1982 Kimberly-Penman, and FAO-24 corrected Penman are the few examples of combination methods. An ASCE Committee (Jensen et al., 1990) evaluated the performance of 20 different methods against the measured ET for 11 stations around the world under different climatic conditions. The Penman-Monteith method has ranked as the best method for all climatic conditions. However, the subsequent ranking of other methods varied with climatic condition. A user friendly Decision Support System (DSS) was developed for ET estimation by George et al. (2002) which helps the user to decide the best ET method following ASCE ranking based on the data availability and the prevailing climatic condition.

As discussed above, several empirical, semi-empirical, and physically based methods are available and these differ from each other based on input data availability, accuracy and use over the last 50 years in different parts of the world. The applicability of ET estimation methods are well documented in the text books related to hydrology and meteorology. The following text discusses some major uncertainties in ET methods. The available ET methods have been shown to produce inconsistent results, as much high as 500 mm/yr (Amatya et al., 1995; Federer et al., 1996; Lu et al., 2005). In ET estimation by using remote sensing, an uncertainty of 20-30% in western riparian corridors of cottonwood has been reported (Nagler et al., 2005). Study of Cleugh et al. (2007) revealed that most sophisticated Penman-Monteith method using MODIS remote sensing data and surface meteorology as input also encountered an error between 20 and 25%. However, this uncertainty is due to inaccuracy in measurement of input parameters. It is worth noting here that the methods like Penman-Monteith are high data demanding and are also sensitive to data. Furthermore, the simple methods like Blaney-Criddle (1950), Thornthwaite (1948) and Hargreaves (1982), employing only temperature data, are not very accurate especially under extreme climatic conditions. These methods underestimated (up to 60%) ET in windy, dry, and sunny areas, while in calm, humid, and cloudy areas, the ET is overestimated (up to

40%). Brutsaert (1982) reported that in the case of evaporation besides sampling; there is also the problem of determining it at a point location. However, in many situations, a single meteorological station data represents the climate of a large catchment, a poor spatial representation. This problem is frequently encountered in ET calculation using formulae requiring large data input. Xu and Singh (2002) compared the performance of the five best ET estimation methods from each category, viz., Hargreaves and Blaney-Criddle (temperature-based category), Makkink and Priestley-Taylor (radiation-based category), and Rohwer (mass-transfer-based category) with respect to Penman-Monteith (Allen et al., 1998), and found their acceptable performance when the parameters are locally determined. They also concluded that the differences of performance between these best methods selected from each category are smaller than the differences between the different methods within each category as reported in earlier studies (for example, Xu and Singh, 2000, 2001). Though the Penman-Monteith method is usually considered as a standard method, it performs well on saturated surfaces, and specifically, when its assumptions are met and reliable input data are available. However, several researchers raise an important question: Is the Penman model the most relevant ET model for catchment modelling? (Qudin et al., 2005). Morton (1994) critically states on Penman's approach as follows: "The use of the Penman-Monteith equation to estimate evaporation from hydrologically significant areas has no real future, being merely an attempt to force reality to conform to preconceived concept derived from small wet regions". Therefore the above mentioned studies give the performance of different ET estimation methods in extreme situations.

2.3.1 Impact of meteorological variables on Evapotranspiration

Evapotranspiration (ET) estimates from cropped field are essential in studies related to climate, hydrology and agricultural water management. The accurate assessment of reference evapotranspiration (ETo) is essential where water resources are limited. There are numbers of climatic variables which effect ET estimates viz., temperature, relative humidity, sunshine duration, solar radiation and wind speed. When the required set of climatological data is available for a location, ETo is often calculated using combination method. This method might be used to assess the validity of the coefficients in other ETo models, but the calibration and validation of the coefficients requires that the sensitivity of ETo to climate variables are determined (Doorenbos and Pruitt, 1975; Jensen et al., 1990; Steiner et al., 1991). To understand the relative role of each climate variable in calculation of ETo, sensitivity analysis is required (Saxton, 1975). By definition, sensitivity analysis is the study

of how the variation in the model input parameters affects the output of a model (Saltelli et al., 2004). A sensitivity analysis shows the effect of change of one factor on another (McCuen, 1973). If the change of the dependent variable of an equation is studied with respect to change in each of several independent variables, the sensitivity coefficients will show the relative importance of each of the variables to the model solution. Saxton (1975) derived sensitivity coefficients by differentiating the combination terms for the Penman (1948) method with respect to each variable. Results showed that the equation is most sensitive to net radiation. Smajstrla et al. (1987) defined the sensitivity coefficient as the slope of the curve of ETo versus the climatic variable being studied. Piper (1989) reported that the faulty measurement of wet bulb temperature, sunshine hours and wind speed causes the similar relative effect on ETo estimates. In the same context, Ley et al. (1994) performed sensitivity analysis for Penman-Wright ETo model (Penman-Kimberly) to found inaccuracy in parameters and climatic data by a factor perturbation simulation approach for Washington State. This model is mainly sensitive to maximum and minimum temperatures. Rana and Katerji (1998) analyzed the sensitivity of the Penman-Monteith method for semi-arid climate for a reference grass surface, grain sorghum, and sweet sorghum in Italy. They found reference grass surface is sensitive to available energy and aerodynamic resistance whereas sweet sorghum, model is sensitive to vapour pressure deficit and for grain sorghum under water stress condition, model is mostly responsive to canopy resistance. Recently, Irmak et al. (2006) found sensitivity coefficient of the standardized daily ASCE-Penman-Monteith equation for different climates of the United States. However, various researchers reported the significant climatic variables which effects ETo are solar radiation in Russia and United States (Peterson et al., 1995), in China (Gao et al., 2006; Liu et al., 2004; Thomas, 2000) and in Israel (Cohen et al., 2002) while others factor effects the ETo estimates is wind speed in Australia (Rayner, 2007; Roderick et al., 2007), in Tibetan Plateau (Chen et al., 2006; Zhang et al., 2007), in Canadian Prairies (Burn and Hesch, 2007), in Iran (Dinpashoh et al., 2011) and North East India (Jhajharia et al., 2011), and relative humidity is most sensitive to ETo in India (Chattopadhyay and Hulme, 1997), as well as to maximum temperature in China (Cong and Yang, 2009) and in western half of Iran (Tabari et al., 2011a). The investigation by Yu et al. (2002) concluded that solar radiation and wind speed are the most sensitive and the least sensitive variables of the modified Penman formula, respectively and the relative humidity has the property that increasing their values will decrease the evapotranspiration estimates. A sensitivity analysis of Penman–Monteith method has been performed by Bois et al. (2005) showed that wind

speed and solar radiation temporal variability have a great impact on potential evapotranspiration computation. Therefore, wind speed omission in empirical formulae can thus be an important source of uncertainties for ET estimation (possible maximum evapotranspiration or potential ET), especially under Mediterranean conditions. Radiation based methods, using remotely sensed solar radiation from satellites images, are more accurate than temperature based methods in Oceanic and Mediterranean climates. Gong et al., 2006 calculated the spatial variations of long-term mean monthly and yearly sensitivity coefficients. They found relative humidity to be most sensitive climatic variable, followed by solar radiation, temperature and wind speed. They also reported that the middle and lower regions of the basin shows large spatial variability of the sensitivity coefficients for all the climatic variables. The above literature review is summarized in Table 2.2.

Table 2.2 Various methods of ETo estimation and their sensitivity to climatic variables

Author	Study Area and period	Major Findings
Inter-comparison of ET estimation methods		
Tabari et al. (2011a)	Rasht station in northern Iran.	Radiation-based Irmak and Ritchie methods, the temperature-based Blaney–Criddle method, Hargreaves-M4 method and the Snyder's pan evapotranspiration method are best suitable methods for humid climate of Iran.
Praveen et al. (2011)	Ponnampet, South Kodagu, India (2009)	The Penman-Monteith, Blaney-Criddle and Pan evapotranspiration methods are the best methods to estimate evapotranspiration in the study area. The Penman method can be used to get somewhat reasonable estimates though it overestimates the evapotranspiration a little.
Lu et al. (2005)	39 forested watersheds in the southeastern United States (1961-1990)	Based on the availability of input data and correlations with AET values, the Priestley-Taylor, Turc, and Hamon methods have been recommended for regional applications in the southeastern United States.
Sensitivity of ET with climatic variables		
Cleugh et al. (2007)	Virginia Park, northern Queensland and Tumbarumba, south east New South Wales	ETo estimated using Penman-Monteith method gives an error between 20 and 25% if MODIS remote sensing data and surface meteorology data are used as input. The uncertainty is due to inaccuracy in measurement of input parameters.
Gong et al. (2006)	Changjiang (Yangtze River) basin, China, (1960-2000)	They found relative humidity to be most sensitive climatic variable, followed by solar radiation, temperature and wind speed. Also the middle and lower regions of the basin are highly sensitive to climatic variables.

2.3.2 Remarks

Over the last 50 years, several empirical, semi-empirical, and physically based methods have been developed for the estimation of ETo in different parts of the world considering availability of meteorological data. According to past studies Penman-Monteith method is usually recommended as standard method for ETo estimation. The Penman-Monteith method is a combination of energy balance and mass transfer approach for estimation of ETo. This method is high data demanding and accuracy of this method is dependent on the accuracy of recorded meteorological variables which forms the major drawback of this method. Accurate observations of all the meteorological variables may not be available on long term basis in many regions of the world; particularly in India. Thus, the application of temporally varying ET (estimated from complex methods) is nothing but to increase the complexity in calculation of irrigation water requirement. Choice of a method for ETo estimation depends on the following factors: availability of reliable long term climatic data, the intended use, and the regional climatic condition.

2.4 SCS-CN METHOD

The SCS-CN method is a well accepted and widely practiced technique in applied hydrology because it is simple, easy to understand and applicable to watersheds with minimum of hydrologic information requirements. Beside the task for which method was originally intended, various advanced applications of the methodology have also been reported, and the existence of potential to extend the method in other areas advocated.

The SCS-CN method is based on the water balance equation along with two basic assumptions. The first assumption associates the ratio of actual direct surface runoff (Q) to the total rainfall (P) (or maximum potential surface runoff) to the ratio of actual infiltration (F) to the amount of the potential maximum retention (S). The second assumption relates the initial abstraction (Ia) to S and also described as potential post initial abstraction retention (McCuen, 2002). Expressed mathematically:

(a) Water balance equation

$$P = Ia + F + Q \qquad (2.1)$$

(b) Proportional equality (First hypothesis)

$$\frac{Q}{P-Ia} = \frac{F}{S} \quad (2.2)$$

(c) Ia-S relationship (Second hypothesis)

$$Ia = \lambda S \quad (2.3)$$

The values of P, Q, and S are in depth dimensions, while the initial abstraction coefficient (λ) is dimensionless. Though the original method was developed in U.S. customary units (inch), an appropriate conversion to SI units (cm) is possible (Ponce, 1989). In a typical case, a certain amount of rainfall is initially abstracted as interception, infiltration, and surface storage before runoff begins. A sum of these three at initiation of surface runoff is usually termed as "initial abstraction".

The first hypothesis (Eq. 2.2) is primarily a proportionality theory (Figure 2.2). This proportionality concept incorporated three major envelopes of interpretation, viz., (i) reconciles the popular concept of partial area contributing with the curve number (Hawkins, 1979); (ii) undermines the source area concept (Steenhuis et al., 1995), allowing runoff generation only from saturated or wetted fractions of the watersheds; and (iii) ignores the statistical theory (Moore and Clarke, 1981; Moore, 1983; 1985), based on the runoff production from only saturated (independent or interacting) storage element. The parameter S of the SCS-CN method depends on soil type, land use, hydrologic condition, and antecedent moisture condition (AMC). Similarly, the initial abstraction coefficient λ is frequently recognized as a regional parameter depending on geologic and climatic factors (Boszany, 1989; Ramasastry and Seth, 1985). The existing SCS-CN method assumes λ to be equal to 0.2 for practical applications which has been frequently questioned for its validity and applicability (Hawkins et al., 2001), invoking many researchers for a critical examination of the Ia–S relationship for pragmatic applications. More recently, Zhi-Hua Shi (2009) examined Ia-S relationship using six years of rainfall and runoff event data from three gorges area of China. They reported that the Ia/S values computed with rainfall-runoff event data ranges from 0.010 to 0.154, with a median value of 0.048. The second hypothesis (Eq. 2.3) is a linear relationship between initial abstraction Ia and potential maximum retention S. Coupling Eqs. (2.1) and (2.2), the expression for Q can be written as:

$$Q = \frac{(P - I_a)^2}{P - I_a + S} \quad (2.4)$$

Eq. (2.4) is the general form of the popular SCS-CN method and is valid for P ≥ Ia; Q = 0otherwise. For λ = 0.2, the coupling of Eqs. (2.3) and (2.4) results into

$$Q = \frac{(P-0.2S)^2}{P+0.8S} \quad (2.5)$$

Eq. (2.5) is well recognized as popular form of the existing SCS-CN method. Thus, the existing SCS-CN method with λ = 0.2 is a one-parameter model for computing surface runoff from daily storm rainfall, having versatile importance, utility and vast untapped potential. The potential maximum retention (S) ranges from 0 ≤ S ≤ ∞, and dimensionless curve number (CN) varies from 0 ≤ CN ≤ 100, as:

$$S = \frac{25400}{CN} - 254 \quad (2.6)$$

Where, S is in mm. The difference between S and CN is that the former is a dimensional quantity (L) whereas the latter is non-dimensional. In an ideal situation, the value of CN =100 represents a condition of zero potential maximum retention (S= 0), that is, an impermeable watershed. Conversely, CN = 0 depicts a theoretical upper bound to potential maximum retention (S = ∞) that is an infinitely abstracting watershed.

Many researchers attempted towards the practical design values validated by experience lying in realistic range (40, 98) (Van-Mullem, 1989). It is proper and appropriate to

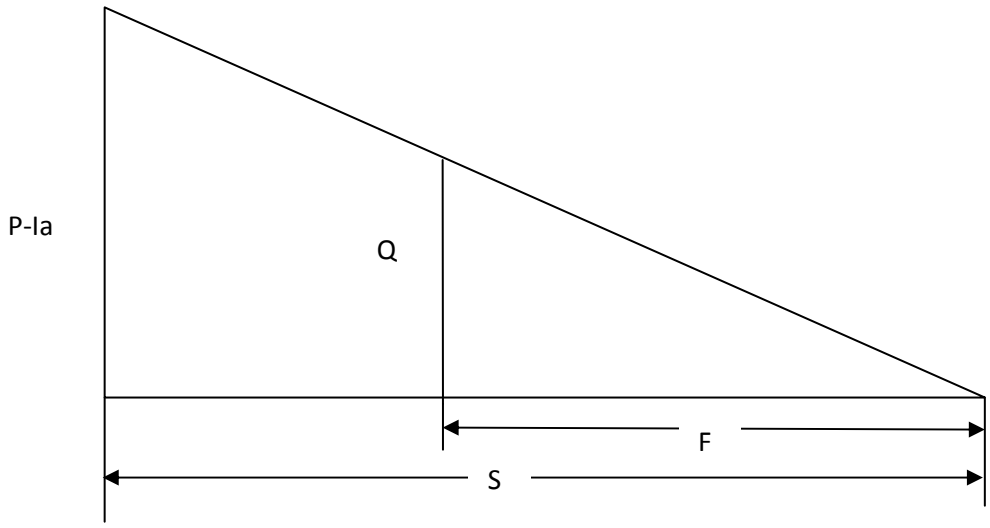

Fig. 2.2 Proportionality concept of the existing SCS-CN method (after Mishra and Singh, 2003a)

explicitly mention here that CN has no intrinsic meaning; it is only a convenient transformation of S to establish a 0-100 scale (Hawkins, 1978).

2.4.1 Application of SCS-CN Method in Hydrology

Since its development, the SCS-CN method has witnessed myriad applications all over the world (Mishra and Singh, 2003a). Rallison (1980) provided detailed information about the origin and evaluation of the methodology and highlighted major concerns to its application to hydrology and water resources problems it was designed to solve and suggested future research areas. A significant amount of literature has been published on the SCS-CN method in the recent past and several recent articles have reviewed the method at length. For example, McCuen (1982) provided guidelines for practical application of the method to hydrologic analysis. Ponce and Hawkins (1996) critically examined this method; discussed its empirical basis; delineated its capabilities, limitation and uses; and identified the areas of research in SCS-CN methodology. Hjelmfelt (1991), Hawkins (1993), Bonta (1997), McCuen (2002), Bhunya et al (2003), and Schneider and McCuen (2005) suggested procedures for determining curve numbers for a watershed using field data. Yu (1998) derived the SCS-CN method analytically assuming the exponential distribution for the spatial and temporal variation of the infiltration capacity and rainfall rate, respectively. Mishra and Singh (1999a, 2002a) derived the method from the Mockus (1949) method and from linear and non-linear concepts, respectively. Mishra and Singh (2003b) presented a state-of-the-art account and mathematical treatment of the SCS-CN methodology, and its application to several areas. Originally, the method has been intended for event based rainfall-runoff modeling but the method has been extended for long-term hydrologic simulation (Williams and LaSeur, 1976; Hawkins, 1978; Knisel, 1980; Pandit and Gopalakrishnan, 1996; Mishra and Singh, 2004a; and Geetha et al., 2007). SCS-CN method is also constructed as an infiltration model (Aron et al., 1977; Mishra and Singh, 2002, 2004b). Hielmefelt (1980) proposed an SCS-CN based infiltration equation comparable with Holtan and Overton infiltration equations to compute infiltration rate from uniform rainfall intensity. Mishra (1998) and Mishra and Singh (2002) introduced a term for steady state infiltration rate and proposed an infiltration equation by expressing the SCS-CN method in the form of Horton method assuming constant rainfall intensity. Jain et al. (2006) applied existing SCS-CN method, its variant, and the modified Mishra and Singh (2002) model to a large set of rainfall-runoff data from small to large watersheds and concluded that the existing SCS-CN method is more suitable for high runoff producing agricultural watersheds

than to watersheds showing pasture/range land use and sandy soil. Gaur and Mathur (2003) suggested synthetic SCS unit pulse hydrographs for generating overland roughness predictive equations for facilitating their application to kinematic wave modeling in ungauged situations. It indicated SCS-CN potential for hydrological evaluation of ungauged catchments. Yuan et al. (2001) modified the SCS-CN method to estimate subsurface drainage for five drainage monitoring stations. The method has also been successfully applied to distributed watershed modeling (White, 1988; Moglen, 2000; and Mishra and Singh, 2003a).

Mishra et al. (2006) coupled the SCS-CN method with the universal soil loss equation (USLE) to develop a new model for assessment of the rainstorm-generated lumped sediment yield from a watershed. The proposed model is based on three assumptions: (1) the potential maximum retention (S) is presented in terms of the USLE parameters, (2) the runoff coefficient (C) is equal to the degree of saturation, and (3) the sediment delivery ratio is equal to the runoff coefficient. Furthermore, Tyagi et al. (2008) extended the sediment yield model to estimate the temporal rates of sediment yield from rainfall events for a watershed. The proposed model uses SCS-CN based infiltration model for calculation of rainfall-excess rate and the SCS-CN based proportionality concept for assessment of sediment-excess. Besides above application, the SCS-CN method has also been used, in association with erosion models for computation of sediment yield. Modified Universal Soil Loss Equation (MUSLE) (Williams, 1975), Agricultural Non-Point Source model (AGNPS) (Young, et al., 1989), Soil and Water Assessment Tool, SWAT (Arnold et al., 1993), Erosion-Productivity Impact Calculator, EPIC (Williams et al., 1983) are but a few examples. Also in a recent study Mishra et al. (2014) developed a linkage between PET and CN using SCS-CN methodology. The various application of SCS-CN methodology in hydrology is listed in Table 2.3.

2.4.2 Remarks

The SCS-CN method is a widely accepted technique applied in hydrology because it is simple, easy to understand and applicable to watersheds with minimum hydrologic information requirements. Beside the task for which method has been originally proposed, various advanced applications of the methodology have also been reported. Now with the modified SCS-CN methodology long term hydrologic simulations can be made with reasonable accuracy. There is a scope to extend the SCS-CN methodology to relate Curve Number (CN) with irrigation water requirement (IWR) to evolve a simple approach for field applications.

Table 2.3 Application of SCS-CN methodology in different hydrological studies

Authors	Broad category	Study area and period	Major Findings
Mishra et al. (2014)	SCS-CN based Potential evapotrans-piration estimation	Eight river basins viz., Hemavati, Manot, Haridaynagar, Mohegaon, Kalu, Ghodahado, Ramganga and Seonath of India	The proposed PET-CN relationship based on SCS-CN concept performs well for eight different agro-climatic river basins in India. The high correlation values support the usefulness of the relationship
Tyagi et al. (2008)	SCS-CN based Sediment yield model	Seven watersheds viz., Karso, Bihar; Banha, Bihar; Mansara, U.P; W2 Treynor, USA; W6 Goodwin Creek, USA; W7 Goodwin Creek, USA; W14 Goodwin Creek, USA;	The proposed model uses SCS-CN based infiltration model for calculation of rainfall-excess rate and the SCS-CN based on proportionality concept for assessment of sediment-excess.
Mishra et al. (2006)	SCS-CN based Sediment yield model	Twelve watersheds viz., Nagwa, Bihar; Karso, Bihar; Mansara, U.P; W2 Treynor, USA; W6 Goodwin Creek, USA; W7 Goodwin Creek, USA; W14 Goodwin Creek, USA; Cincinnati Asphalt pavement at milestone, USA; 123 NAEW, USA; 129 NAEW, USA; Coshocton, USA; 182 NAEW, USA	The proposed model has been coupled the SCS-CN methodology with the universal soil loss equation (USLE) to develop a new model for assessment of the rainstorm-generated lumped sediment yield from a watershed.
Jain et al. (2006)		US. Department of Agriculture-Agricultural Research Service (USDA-ARS) Water Database	The reported SCS-CN methodology is applicable to a large set of rainfall-runoff data from small to large watersheds and it is concluded that the existing SCS-CN method has been more suitable for high runoff producing agricultural watersheds than to watersheds showing pasture/range land
Mishra and Singh (2004a)	SCS-CN based infiltration model	Waco and Amicalola Creek watersheds	The results of the study are found relevant when the total rainfall is equal to or greater than half of the potential maximum retention (S). The extended SCS-CN methodology is tested, the simulated and observed infiltration and rainfall excess rates are found to be in good agreement.

2.5 CLIMATE CHANGE AND ITS IMPACT ON IRRIGATION WATER REQUIREMENT

2.5.1 Climate Change Models

It is well known that GCMs, is a significant tool for the assessment of climate change. GCMs represent several earth systems comprising of atmosphere, oceans, sea ice and land surface and have substantial potential for assessment of climate change. At large scales, GCMs which have been increasingly evolving over several decades are able to predict reliably the most crucial features of global climate. On the other hand, these same models perform poorly at smaller spatial and temporal scales related to regional impact analyses (Grotch and MacCracken, 1991; Wilby and Wigley, 1997). The major cause is that the spatial resolution of GCM grids is too coarse to resolve many vital sub-grid scale processes and GCM outputs are then often unreliable at individual grid and sub-grid box scales (Wilby et al., 1999; Xu, 1999). To solve this problem two downscaling techniques viz., dynamic downscaling and statistical downscaling have been proposed. In the dynamic downscaling approach a Regional Climate Model (RCM) is embedded into GCM. The RCM is essentially a numerical model in which GCMs are used to fix boundary conditions (Fowler et al., 2007). The major disadvantage of RCM model is its complex design and high computational cost, which limits its application in climate change impact assessment studies. Moreover, RCM is rigid in terms of expanding the region or moving to a somewhat different region needs rebuilding of complete test (Crane and Hewitson, 1998). Statistical downscaling processes seek to represent empirical relationships that transform large-scale features of GCM (predictors) to regional-scale climatic variables (predictands), such as rainfall and temperature etc. (Tripathi et al., 2006). The three implicit hypotheses incorporated in statistical downscaling (Hewitson and Crane, 1996) are the predictors are variables of significance and are rationally modeled by the horde GCM. Secondly, the empirical correlation is valid also under changed climatic conditions. And thirdly, the predictors used totally signify the climate change signal. The statistical downscaling methods are commonly categorised into three groups: weather model system (Conway et al., 1996; Fowler et al., 2000; Bardossy et al., 2005), weather generators (WGs) (Kilsby et al., 2007) and regression models (Wilby et al., 1999; Zorita and Storch, 1999; Tripathi et al., 2006; Ghosh and Mujumdar, 2007). Among the statistical downscaling methods, regression models, are perhaps the most popular methods, which are employed to directly estimate a relationship between the predictor and predictand. The examples of regression model comprises of artificial neural networks (ANNs) (e.g., Cavazos, 1997; Crane and Hewitson,

1998; Zorita and Storch, 1999; Schoof and Pryor, 2001; Cannon and Whitfield, 2002; Olsson et al., 2004; Coulibaly et al., 2005), multiple regression models (MRMs) (Wilby et al., 1999), canonical correlation analysis (CCA) (von Storch et al., 1993) and singular value decomposition (SVD) (Huth, 1999). MRMs and ANNs have been applied widely due to strong capability in regression analysis and forecasting. It has been extensively used in a variety of physical science applications, including hydrology (Govindaraju and Rao, 2000; Raghuwanshi, 2006). Despite a number of advantages, the traditional neural network models have several disadvantages including possibility of getting trapped in local minima and subjectivity in the choice of model architecture (Suykens, 2001). Vapnik (1998) developed the Support Vector Machine (SVM) a novel machine learning algorithm and provided remedy to the aforementioned problems. Recently, SVM has been broadly employed in the fields of classification and regression analysis (Tripathi et al., 2006; Ghosh and Mujumdar, 2007). Tripathi et al. (2006) developed a SVM approach for statistical downscaling of monthly rainfall and the result gives a good substitute to ANNs. Also, SVM has been widely used in several fields (Yu and Liong, 2007; Geol Arun, 2012). Beside numerous advantages the SVM model has some limitations such as low implementation efficiency, inflexibility to noise and outliers, slow simulation speed, problem in handling large samples set. To overcome this problem of handling large data samples improved algorithms have been developed (Joachims, 1999; Mangasarian and Musicant, 1999; Platt, 1998; Lee et al., 2005). Lee et al. (2005) developed a new model for solving the regression of large-scale training data called the Smooth Support Vector Machine (SSVM). Chen et al., 2012 reported results obtained using SSVM have been compared with those from an artificial neural network (ANN). The comparisons showed that SSVM is appropriate for performing climate change impact assessment studies as a statistical downscaling tool in the region. The temporal trends for future rainfall is decrease during the period of 2011–2040 in the upper half of the basin and increasing trend in rainfall after 2071 in the whole of Hanjiang Basin. The projected rainfall is estimated using SSVM model for A2 scenario for two GCM outputs viz., CGCM2 and HadCM3. More recently, downscaling has found wide application in hydro-climatology for scenario construction and simulation/ prediction of (i) regional precipitation (Kim et al., 2004); (ii) low-frequency rainfall events (Wilby et al, 1998) (iii) mean, minimum and maximum air temperature (Kettle and Thompson, 2004); (iv) soil moisture (Georgakakos and Smith, 2001; Jasper et al., 2004); (v) runoff (Arnell et al., 2003) and streamflows (Cannon and Whitfield, 2002); (vi) wind speed (Faucher et al., 1999) and potential evaporation rates (Weisse and Oestreicher, 2001); (vii) soil erosion and crop yield

(Zhang et al., 2004); (viii) landslide occurrence (Buma and Dehn, 2000; Schmidt and Glade, 2003) and (ix) water quality (Hassan et al., 1998).

It is now widely believed that climate change will have impacts on water resources availability and management throughout the world. The urban sectors, irrigated agriculture and hydropower production are the major sectors which are affected by climate change (IPCC, 2007). The global warming leads to changes in seasonality of river flows with prior spring peak flows, rising winter and falling summer flows in eastern North America (Barnett et al., 2005; Dibike and Coulibaly, 2005). Recently, number of hydrological impact studies has been carried out to study the impact of climate change on water quality variation in river basin (Deng and Patil, 2011). According to Wilby (2008), the uncertainty is related to downscaling method, global climate model (GCM) structure and climate change scenario (which is associated with future civilization). To this end, very few recent studies have been attempted to address the above mentioned uncertainties. McAlpine et al. (2007) reported impact of regional climate change on vegetative cover. They found major changes in regional climate, with a shift from humid and cooler condition to warmer and drier conditions, particularly in southeast Australia. These changes in Australia's regional climate advocated that land cover change is probably a contributing factor to the observed trends in temperature and rainfall at the regional scale. Kay et al. (2009) studied the impact of climate change impact on flood frequency for two river basins in England. In this study, four scenarios viz., SRES A1F1, B2, B1 and A2 (IPCC, 2000) have been considered also five GCMs outputs have been used along with the delta change approach to estimate GCM uncertainty. A single GCM has been used with both the RCM and a delta change approach to examine uncertainty in downscaling method. They reported that the majority of the uncertainty is due to climate modelling, i.e. selected GCM and RCM structures. Other research studies have also investigated the different arrangements of the above stated sources of uncertainty, the work by Wilby and Harris (2006); Minville (2008); Jiang et al. (2007) and Wilby (2005). Ludwig et al. (2009) examine the climate change based on the comparison of two physically based models and one conceptual model. They reported that the differences in model structure complexities can play an important role in the assessment of model outcome. Finally, Poulin et al. 2011 presented the consequences of model structure and parameter equifinality associated to hydrological modeling in climate change impact studies. This study reveals that the impact of hydrological model structure uncertainty is more important than the effect of parameter uncertainty, under past and recent climate as well as future climate change scenario.

2.5.2 Importance of Bias Correction in Climate Change Scenario Generation

The climate change impact assessment study is of increasing interest due to its adverse impact on various fields. The GCMs is used for the projections of future climate change caused by natural variability or anthropogenic activities (Intergovernmental Panel on Climate Change (IPCC), 2007). Despite continuous efforts to improve GCM's capability of simulating historical climates, the use of bias correction methods is essential for the impact assessment studies of climate change for more improved projections. The significance of bias correction methods has been described in the special report of the IPCC (Seneviratne et al., 2012). In estimating probable hydrologic impacts of climate change (e.g., Arnell, 2004; Oki and Kanae, 2006), a suitable bias correction has been applied to projected temperature (T) and precipitation (P) for error free estimation of projections. Dettinger et al. (2004) carried out the climate change impact assessment study in the Sierra Nevada of California to study the climate change impact on river flow by using bias-corrected on GCM projected temperature and precipitation data. Lehner et al. (2006) also predict the risk of flood and drought due to climate change by applying a hydrologic model embedded with the bias-corrected atmospheric data. In addition, bias correction has also been applied to the Regional Climate Model (RCM) simulations such as the studies conducted in four basins of the United States (Hay et al., 2002) and Ireland (Steele-Dunne et al., 2008). Number of bias correction methods has been used to improve the regional climate downscaling simulation. Wu and Lynch (2000) examined the impact of climate change on seasonal carbon cycle in Alaska through a dynamical downscaling approach in which they constructed the linear bias correction (LBC) of an RCM by adding projected changes of temperature and specific humidity in a GCM simulation to reanalysis climate. A similar technique has been applied by Sato et al. (2007) to examine the affect of global warming on regional rainfall over Mongolia. The bias correction has also been applied to correct the projected wind speed, temperature, geo potential height, specific humidity, and sea surface temperature. The result of the study reveals that the rainfall intensity predicted with the new method has been closer to observations than the traditional method. Patricola and Cook (2010) also employed a similar method as applied by Sato et al. (2007). The climatological LBCs in the above mentioned studies maintain deviations on the seasonal time scale but eliminate the diurnal and synoptic effects. Holland et al. (2010) proposed a complex bias correction method for hurricane simulation. The bias correction developed by Holland et al. (2010) maintained the diurnal, synoptic effects and the inter-annual variations in the LBC by correcting GCM

climatological mean bias with 6-hourly National Centers for Environmental Prediction (NCEP)–National Center for Atmospheric Research (NCAR) reanalysis data and GCM outputs. They recommended that the dynamical downscaling prediction with GCM bias correction can generate realistic tropical cyclone frequency because the bias correction reduced the impracticable high vertical wind shear over the tropical North Atlantic. Jin et al. (2011) proposed a statistical regression model between GCM and reanalysis data to reduce the GCM climatological bias, and then the bias-corrected GCM output data have been used to force an RCM to predict winter precipitation over the western United States.

2.5.3 Impact of Climate Change on Irrigation Water Requirement

There are various studies having focus on assessment of changes in crop productivity due to climate change (e.g. Easterling et al., 1993; Rosenzweig and Parry, 1994; Singh et al., 1998; Brown and Rosenberg, 1999; Parry et al., 2004; Harmsen et al., 2009; Liu et al., 2010). The studies focusing on the impacts of climate change on irrigation demands using general circulation model (GCM) outputs are becoming more accepted in recent years. Yano et al. (2007) analysed the impact of climate change on crop growth and irrigation water requirement for a wheat–maize cropping pattern in Mediterranean environment of Turkey. The projected temperature and precipitation have been obtained by superimposing projected anomalies of GCMs on observed climate variables of the baseline period. Elgaali et al. (2007) studied the regional impact of climate change on irrigation water requirement by taking rainfall and evapotranspiration into consideration for Arkansas River Basin in southeastern Colorado. In this study assumption is made that there is no alteration in crop phenology and they found an overall increasing water demand for crops due to climate change. Similar study by Rodriguez Diaz et al. (2007) reported the increase in irrigation water demand ranging from 15% and 20% by 2050 in the Guadalquivir river basin in Spain with disturbed climate change scenarios of temperature, solar radiation, rainfall, wind speed (U2) and relative humidity (RH). Shahid (2011) estimated the changes of irrigation water requirement for dry-season Boro rice in northwest Bangladesh with respect to climate change, with projected changes in rainfall and temperatures predicted using the weather generator software named SCENario GENerator (SCENGEN). De Silva et al. (2007) reported an increase in irrigation water requirement of 13% to 23% depending on climate change scenarios. The projected temperature, radiation, wind speed and relative humidity have been estimated by applying the percentage changes of GCM to the baseline dataset. Rehana and Majumdar (2012) reported that the monthly rainfall is increased in the Bhadra

reservoir command area. From the study RH, Tmax and Tmin are projected to increase with small changes in wind speed. Consequently, the reference evapotranspiration estimated by the Penman–Monteith equation, has been predicted to increase. The irrigation requirements have been projected to increase due to projected increase/change in other meteorological variables (viz., Tmax and Tmin, solar radiation, RH and U2) but not effected by increase in projected rainfall. The Table 2.4 summarises the various impact assessment studies related to irrigation water demand.

Table 2.4 Impact of climate change on irrigation water requirement

Author	Study Area and period	Broad Category	Findings
Rodriguez Diaz et al. (2007)	Guadalquivir river basin, Spain	Irrigation water requirement	Increase of irrigation demand between 15% and 20% in seasonal irrigation by 2050
Elgaali et al, (2007)	Arkansas River Basin, Southeastern Colorado, 1960–1990	Irrigation water requirement	Increase in irrigation water demand in HAD and CCC climate change scenarios
Shamsuddin Shahid (2011)	Bangaldesh, 1998–2002	Irrigation water requirement	Increase in daily use of water for irrigation due to increase in temperature
Rehana and Majumdar (2012)	Bhadra command area, Karnataka, India	Irrigation water requirement	The annual IWR for paddy, sugarcane, permanent garden and semidry crops are predicted to increase
Yano et al. (2007)	Mediterranean environment of Turkey	Crop growth and Irrigation water demand	The irrigation water demand for wheat is increased due to projected decrease in rainfall and for maize crop irrigation water requirement is decreased by 15% for future period.
De Silva et al. (2007)	Sri Lanka	Climate change impact study on paddy irrigation water requirement	Increase in irrigation water requirement for paddy by 13% to 23% depending on climate change scenarios. The climatic variables have been estimated by applying the percentage changes of GCM to the baseline dataset.

2.5.4 Remarks

The above mentioned studies have focused on the estimation of projected irrigation water requirement using following methods/approach:

i) Use of perturbation method for the construction of climate change scenario generated with GCM outputs. In this method average change in GCM outputs is applied to baseline period (observed climatic data) for projection of climatic variables. The major drawbacks of this method are: it is based on the assumption that the change in climate is relatively stable over space, the results are sensitive to the selected baseline period, and the method produces transient climate change scenarios. The aforesaid limitations of the method may often lead to incorrect assessment of IWR.

ii) Using globally available downscale data for the generation of climate change scenario may provide erroneous assessment of projected climatic data.

iii) Use of climate change modeling software viz., SCENGEN for future prediction of IWR. The SCENGEN model only gives temperature and rainfall projections. Other climatic variables are ignored in the impact assessment study of future irrigation water demand.

iv) In some of the studies, estimation of future IWR is erroneous as total rainfall is considered instead of using effective rainfall to find IWR. The effective rainfall computation incorporates the percolation and soil water retention. It is one of the key components in the assessment of projected IWR.

The review of literature reveals that the IWR is extremely sensitive to variability and changes in climatic factors. Thus more accurate climate change scenario for predictions of meteorological factors (evapotranspiration, temperature, wind speed, relative humidity and rainfall) would be needed. The LS-SVM downscaling model appears to be widely used and accepted in the climate change impact assessment studies in the recent years by the research community.

Based on the literature review, background and objectives for the present research work have been formulated as given in chapter 1. The next chapter analyses the characteristics of the study area and availability of long term temporal data used in the analysis.

CHAPTER 3

STUDY AREA AND DATA

This chapter is divided into two sections viz., study area and data. The first section gives a concise geographic description about Seonath River Basin. It includes location and extent of the basin, hydrological issues faced by the population. A brief depiction of climate, physiography, soils, agriculture and land use is also included. The later section (data) deals with the description of various datasets used in the study and elaborates the step by step methodology of the data processing and map making.

3.1 STUDY AREA

3.1.1 Location and Extent of the Basin

The Seonath river basin (area = 30,860 sq. km) (Figure 3.1), in Chhattisgarh State (India), is the longest tributary sub basin of River Mahanadi, comprising 25% of the Mahanadi basin area. The river traverses a length of 380 km. It originates near village Panabaras in the Rajnandgaon district and drains area of three districts of Chhattisgarh state namely Durg, Rajandgaon, and Bilaspur. The basin is located between latitudes 20°16' N to 22°41' N and Longitudes 80°25' E to 82°35' E. Its main tributaries are Tandula, Arpa, Kharun, Agar, Hamp, and Maniyari streams. The average elevation of the basin is 329 m above mean sea level with minimum and maximum elevation of 204 m and 1058 m respectively.

3.1.2 Water Scarcity in the Basin

The study area (Seonath river basin) falling in Chhattisgarh State faces frequent droughts. Most of the tributaries of Seonath River get dried by mid-winter season and both rural and urban areas are subjected to severe water crisis during the summer season due to erratic and skewed nature of rainfall. Multipurpose water demand has increased with growth in population and the pattern of water availability and utilization has also changed with time. Sustainability has become a challenging issue in water resources development and management.

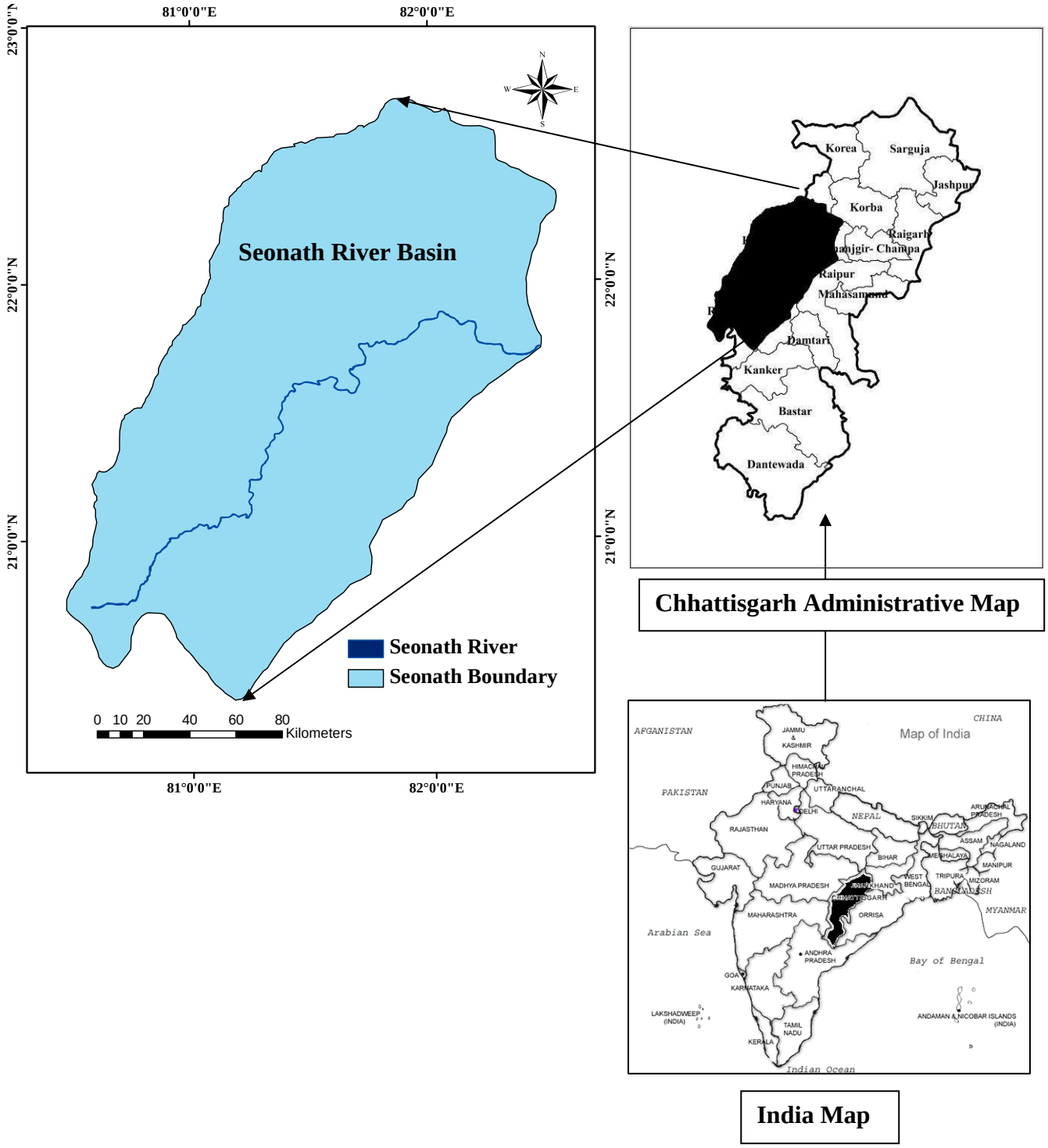

Figure 3.1 Index map of Seonath River Basin (study area)

3.1.3 Climate

The river basin experiences a sub-humid type of climate. The geographical factors such as distance from the sea and altitude have influenced the basin climate. The mean annual rainfall in the basin varies from 1005 mm to 1255 mm. The major part of rainfall occurs only within three monsoon months (July-September). It experiences higher humidity levels during monsoon season. The summer season prevails from April to middle of June. The climatic condition during summer is hot and gusts of dry wind blow; the temperature varies from 40°C to 45.5°C. The mean daily maximum temperature varies from 42°C to 45.5°C for the hottest month of May. During winter the temperature varies between 10°C and 25 °C.

3.1.4 Agriculture and Land use

Agriculture is the main occupation of people in this sub-basin. About 76% of the basin area is under cultivation. There are two cropping seasons namely, monsoon (kharif) season from mid-June to October and post-monsoon (rabi) season from November to middle of April. Rice is the major crop of monsoon season covering 94% of the cultivated basin area (Figure 3.2 a). During rabi season, wheat, summer paddy, pulses and oilseed are grown. The kharif rice, wheat and summer paddy are the main crops covering an area of about 22679 sq. km i.e., 98% of the basin cultivated area (Figure 3.2 b).

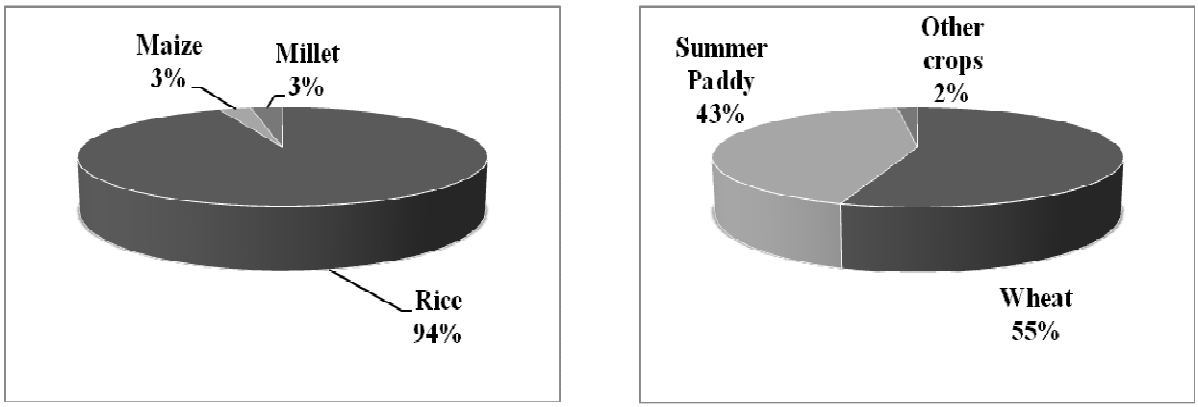

(a) Kharif Season Crops **(b) Rabi Season Crops**

Figure 3.2 Crops and cropping pattern of Seonath river basin (Source: Directorate of Economics and Statistics, Chhattisgarh)

The land use map of the basin is shown in Figure 3.3. The land use map of the basin is prepared by using LANDSAT images downloaded from GLCF site. Detailed procedure is described in section 3.2.3.

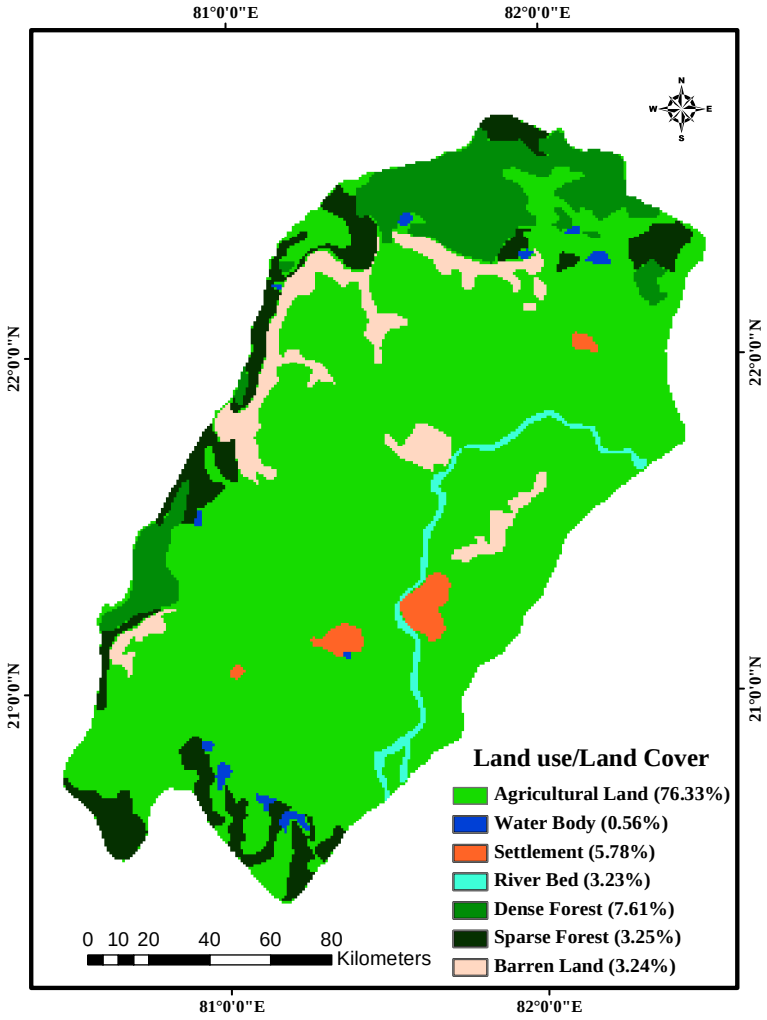

Figure 3.3 Land use of Seonath river basin

3.1.5 Soil Type

The main soil types found in the basin are sandy clay covering 72.28% of the basin area followed by silt loam 17.29% of the basin area (Figure 3.4). Sandy clay predominates in the middle whereas loam and silt loam are found in lower reaches of the drainage channels and in the upstream channel sandy loam are also found.

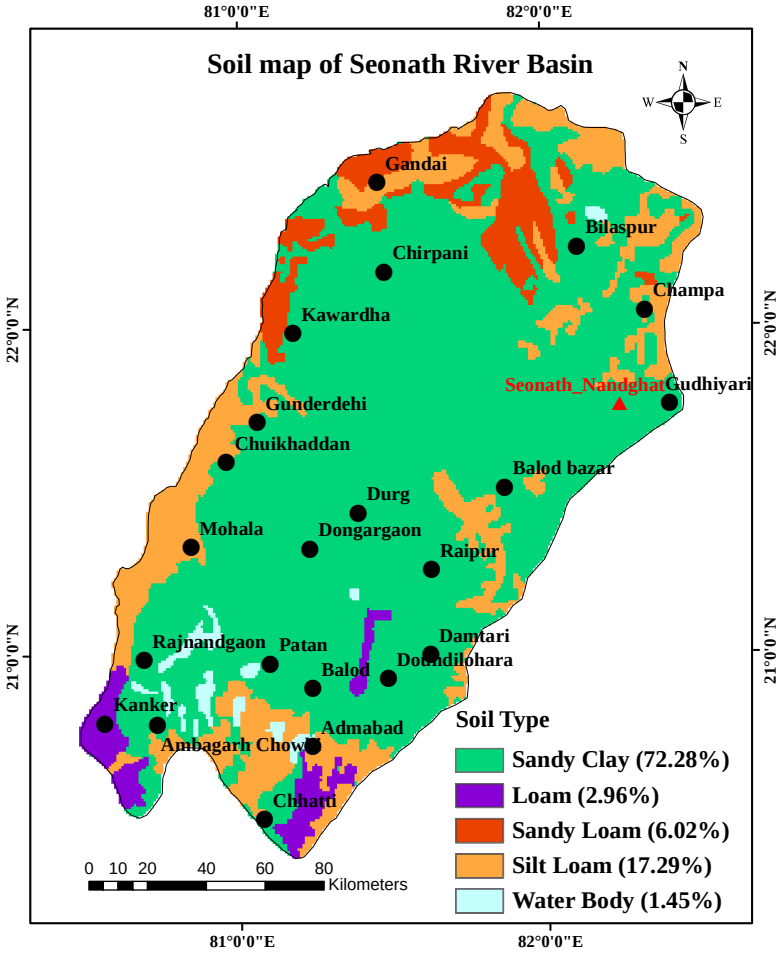

Figure 3.4 Soil map of Seonath River Basin

3.1.6 Socio-Economic Aspects

The indigenous tribal population constitutes the major portion of the population in the state. All the developmental activities which have taken place have more or less bypassed them and they remain marginalized and outside the mainstream. This is a significant developmental challenge each in terms of economic progress and, additionally from socio-cultural point of view. The major urban centres in the basin are Raipur and Durg. Seonath basin, because of its rich mineral reserve and adequate power resource has a favorable industrialized ambiance. The important industries currently accessible in the basin are iron & steel plant at Bhilai which produces 20% of the country's steel output. Mining of iron, coal, and manganese are other industrial activities.

Following photographs depicting land use land cover of the study area have been taken during the field visit (Figure 3.5).

Paddy Fields at different locations in the Seonath basin

Barren land **Industrial Area (BSP)**

Forest Land **Outlet of the basin: Nandghat**

Figure 3.5 Field photographs showing landuse/cover types in the Seonath basin and basin runoff outlet

3.2 DATA USED AND PROCESSING

Hydro-meteorological data have been collected from India Meteorological Department (IMD), Pune, and State Data Centre (SDC) Raipur, as detailed below:

3.2.1 Hydro-Meteorological Data

The daily meteorological data [Rainfall, Temperature (maximum, minimum and mean)] of 24 stations have been collected from IMD, Pune for 51 years (1960-2010). Observed data on wind speed and relative humidity is available only for eight stations. The pan evaporation data is available only for one station viz., Raipur. The location of the

stations is shown in Figure 3.6. Also, the discharge data for the same period at the single outlet namely Nandghat, has been obtained from State Data Centre, Department of Water Resources, Raipur (Chhattisgarh).

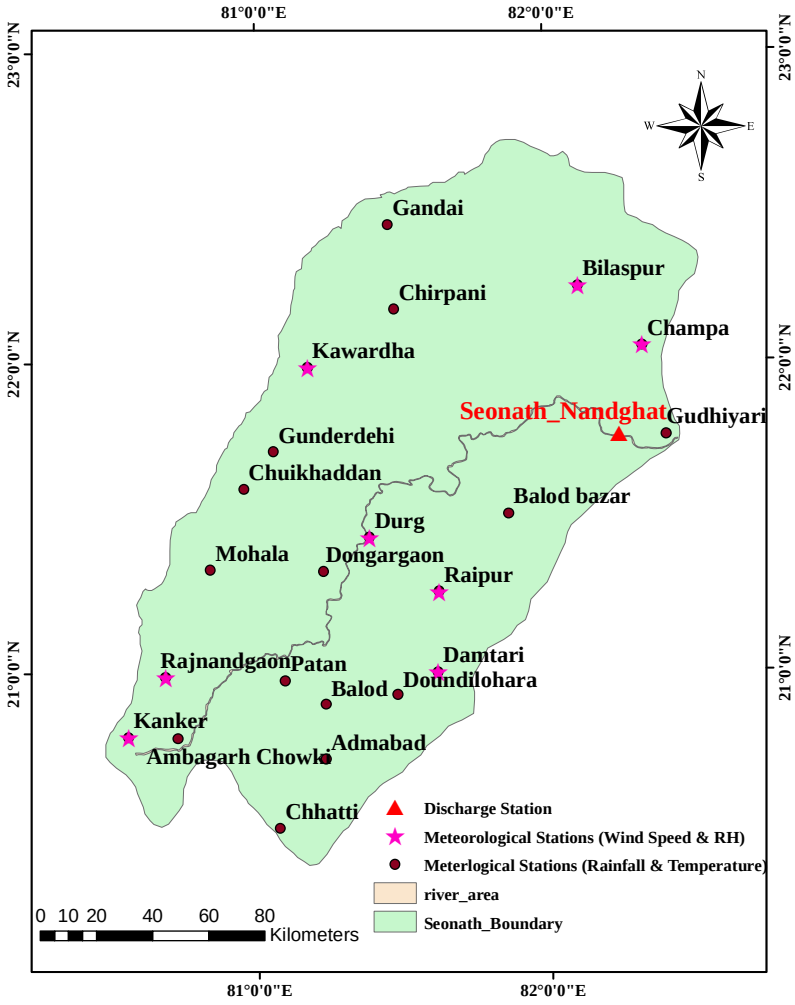

Figure 3.6 Location of Meteorological stations in Seonath basin

3.2.2 Ancillary Data

NBSSLUP Soil Map

The soil map of the basin at 1:50,000 scale has been obtained from NBSSLUP (National Bureau of Soil Survey and Land Use Planning), Nagpur. It has been carefully scanned and exported to ArcGIS. Different soils have been carefully traced and the polygons representing various soils are filled with different colours for proper identification. The areas under different soils have been identified.

Toposheets

The study area is covered in Survey of India topographical maps (Toposheets numbered 64C, 64D, 64F, 64G, 64H at 1:50,000 scale). These maps have been acquired from Survey of India (SOI) for boundary digitisation of the basin. The maps have been scanned and saved in tiff format and imported in ERDAS 9.2 for further processing. The latitude and longitude of the ground control points are converted to actual ground co-ordinate. The boundary of the Seonath Basin is then carefully digitised.

3.2.3 Remote Sensing Data

LANDSAT data

The IRS-P6 AWiFs (56 resolution) images which cover the study area have been used to prepare the land cover maps for the year 2003. The images are pre processed and mosaiced to create a seemless image of the whole basin. The images have been classified using unsupervised classification (Isodata clustering) technique into several classes (200) and they are merged based on their spectral signatures into seven land cover types. The preliminary classified layer is then improved with Visual Interpretation Technique and Ground control points (GCP). Thus, landuse/cover map has been prepared by using an integrated digital and visual classification method.

Digital Elevation Model (DEM)

The Shuttle Radar Topography Mission (SRTM) data are digital elevation data on a horizontal grid spacing of 1 arc seconds (approximately 30m resolution). Further the downloaded images have been used for the preparation of digital elevation model (DEM) and drainage network using Arc GIS software version 9.3. The data is acquired from the URL: (http://glcfapp.glcf.umd.edu:8080/esdi/) for basin delineation and drainage network extraction. The DEM of the basin is illustrated in Figure 3.7.

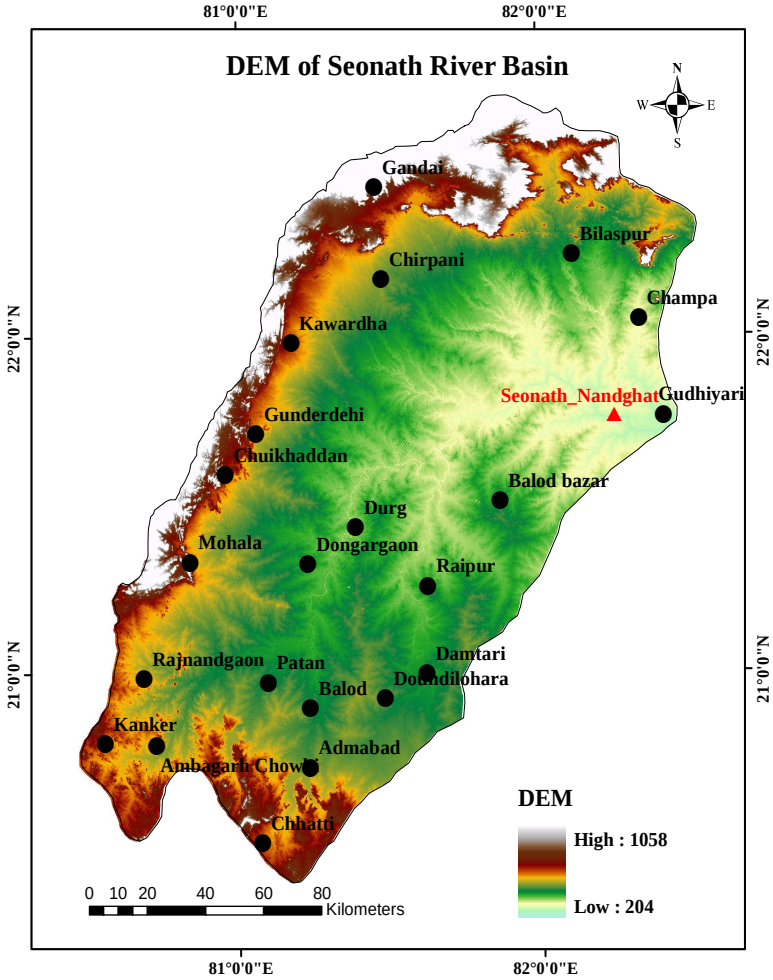

Figure 3.7 Digital Elevation Model of Seonath River Basin

3.2.4 Characteristics of Meteorological Stations

The composite map (Figure 3.8 and Table 3.1) has been prepared to illustrate the attributes of different meteorological stations located within Seonath River Basin. Figure 3.8a and Table 3.1 col.6 shows the elevation of different stations. The Gandai station (in kawardha district) is located at highest elevation (525 m) whereas Gudhiyari station (in Durg district) is located at lowest elevation (226 m). The major land use of the basin is for agriculture except in Raipur district which shows major settlement; therefore the basin is described as an agriculture basin (Figure 3.8c, Table 3.1 col.4). The soil type is almost same at all the locations i.e, sandy clay except few locations viz, Mohala, Gandai and Admabad which have silty loam type soil (Figure 3.8b, Table 3.1 col.5).

Table 3.1 Characteristics of Meteorological Stations located in Seonath river basin

Station	District	Area (Sq.km)	Land Use	Soil Type	Elevation	
Column 1	***Column 2***	***Column 3***	***Column 4***	***Column 5***	***Column 6***	
Ambagarh Chowki	Rajnandgaon	5688.63	Agricultural Land	Sandy Clay	337	
Chuikhaddan				Sandy Clay	337	
Dongargaon				Sandy Clay	255	
Mohala				***Silt Loam***	330	
Rajnandgaon				Sandy Clay	316	
Balod Bazar	Raipur	3877.25	Settlement and Barren land	Sandy Clay	254	
Raipur				Sandy Clay	287	
Simga				Sandy Clay	285	
Chhatti	Dhamtari	533.15	Agricultural Land	Sandy Clay	430	
Damtari				Sandy Clay	326	
Chirapani	Kawardha	3525.13	Agricultural Land and Dense Forest	Sandy Clay	353	
Kawardha				Sandy Clay	357	
Gandai				***Silt Loam***	525	
Doundi Lohara	Durg	8474.67	Agricultural Land and Barren Land	Sandy Clay	317	
Durg				Sandy Clay	288	
Patan				Sandy Clay	332	
Admabad				***Silt Loam***	314	
Balod				Sandy Clay	324	
Gudhiyari					226	
Gondly				Sandy Clay	312	
Dongaragaon				Sandy Clay	324	
Gunderdehi				Sandy Clay	313	
Bilaspur	Bilaspur	6916.18	Agricultural Land	Sandy Clay	272	
Champa	Jhanjgir-Champa	553.2	Agricultural Land	Sandy Clay	232	

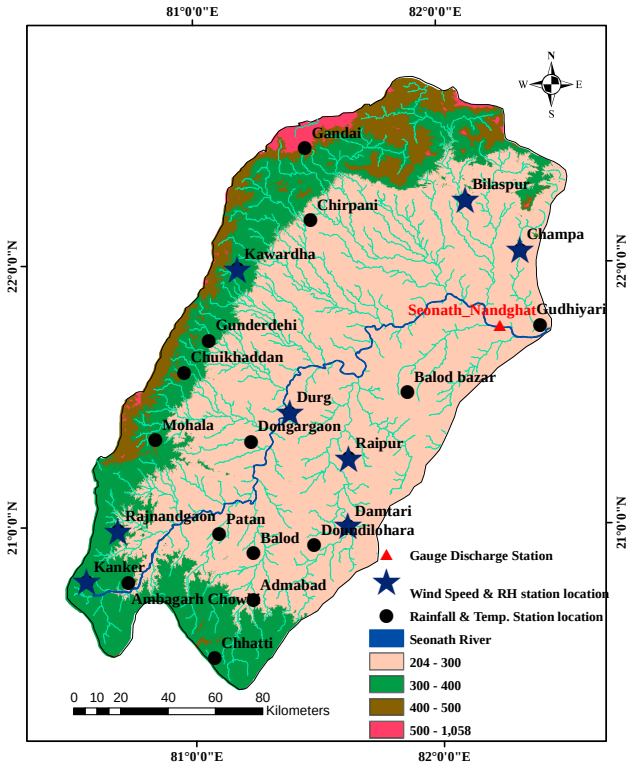

(a) DEM and Drainage network

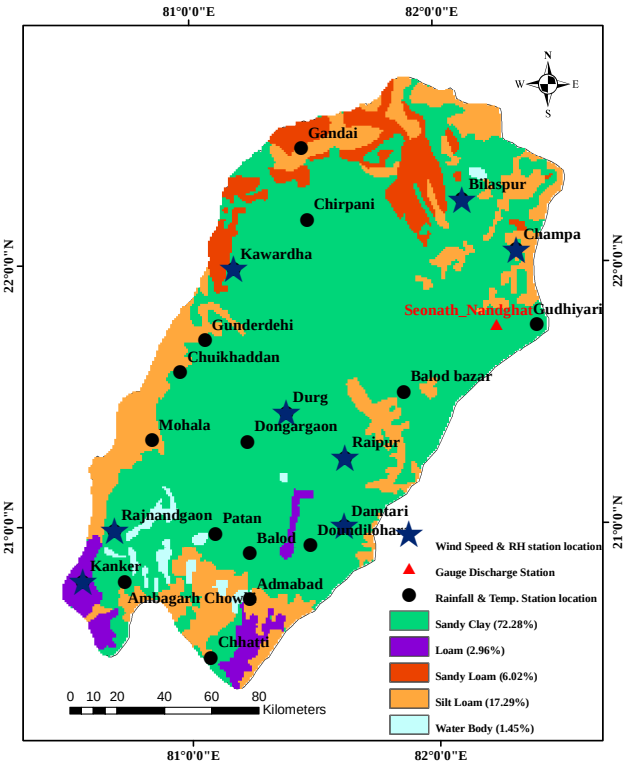

(b) Soil Type

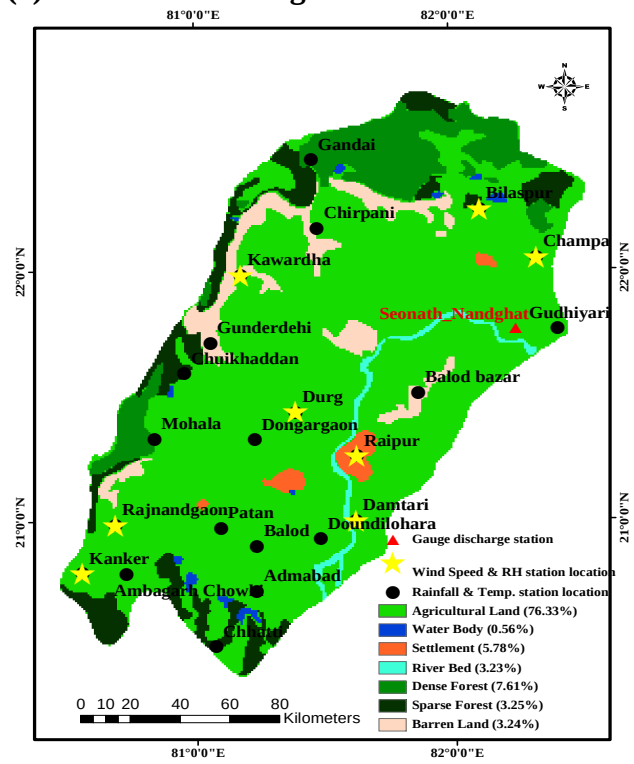

(c) Land Use/Cover Map

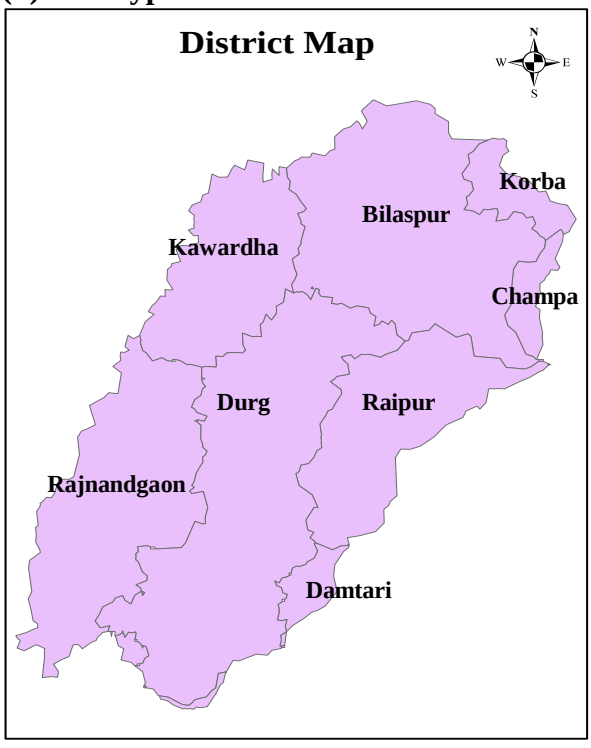

(d) District Map

Figure 3.8 Physical characteristics at locations of meteorological stations in Seonath basin

CHAPTER 4

ASSESSMENT OF TRENDS IN CLIMATIC VARIABLES

Global warming and intensified human activities, coupled with the harsh natural conditions and a fragile ecosystem, have caused great changes in the eco environment in various parts of the world.

This Chapter deals with the investigation of long term trend and variability in climatic variables in the Seonath River basin. Statistical tests for trend of major climatic variables have been made in this study.

4.1 INTRODUCTION

Indian agriculture primarily depends on monsoon (June-October) rainfall. Rainfed agriculture has a distinct place in Indian agriculture, occupying 68 per cent of the total cultivated area and supporting 40 percent of human and 60 percent of livestock population (Sharma and Soni, 2006). Study of significant climatic changes especially changes in occurrence and distribution of rainfall is necessary in the sustainable management of irrigation schemes and planning of irrigated agriculture. The random and/or systematic variation of annual rainfall has great consequences in the planning of irrigation schemes (Gadgil, 1986) and therefore, identification and quantification of climatic change need to be factored in sustainable development of irrigated agriculture in India.

A study has shown a decline in intensity distribution of spring and summer rainfall in one part of United Kingdom whereas the reverse changes have been observed in other zones of United Kingdom (Osborn et al. 2000). Downward rainfall trends with 20% decrease in rainy days have been observed in Bologna agro-meteorological station, Italy (Ventura et al. 2002). Similarly, Karpouzos et al. (2010) found an overall non significant decreasing trend in annual rainfall for the period from 1974 to 2007 in Pieira Region of Greece. Several researchers (Byun et al., 1992a, b; Byun and Han, 1994; Byun, 1996; Byun and Lee, 2002) have found that there is a period of increased rainfall in spring season for Korea. In India, Kumar et al. (2010) has reported large spatial and temporal variations in rainfall trend. Out of 30 sub-divisions in the country, half of the regions have shown rising trend in mean annual rainfall with significant increasing trends in Haryana, Punjab, and Coastal Karnataka. Also, a significant rising trend in mean annual rainfall in most of the

districts of Chhattisgarh region is reported (Kumar et al., 2010). Based on the long term average of monthly and annual rainfall of Coimbatore district, Rathod and Aruchamy (2010) found that the central and northern parts of the district have the highest annual rainfall variability. On the other hand, the eastern and south western parts of the district have evidence of declining variability. Nearly similar trends in precipitation time series for 96 stations in Turkey have been reported by Partal and Kahya (2006). Vennila (2007) reported declining trends in monthly and seasonal rainfall including its intensity and frequency for Vattamalaikarai river basin in Tamil Nadu.

Thus, the changing pattern of rainfall and its impact on water resource availability is an important climatic problem for the water resource and irrigation planners today. In relation to global warming, strong evidence indicates that rainfall changes are already taking place on both the global (Bradley et al., 1987; Hulme et al., 1998) and regional scales (Maheras, 1988; Yu and Neil, 1993; Rodriguez-Puebla et al., 1998). Future climate changes may involve modifications in climatic variability as well as changes in average occurrences of annual and seasonal rainfall (Rind et al., 1989; Katz and Brown, 1992; Mearns et al., 1997).

Inter-annual variability is a better (than mean value) and one of the most important indicators of the reliability of rainfall (Semenov and Porter, 1994; Corte-Real et al., 1998). Ayanlade et al. (2009) evaluated the variation in climatic parameters using Kriging interpolation and concluded that the rainfall varies with time and space in Guinea Savanna of Nigeria. Recently, Dash et al. (2009) applied the IMD criteria of rainy day (i.e. rainfall $\geq$ 2.5 mm per day) to identify variability of wet and dry events across India. Thus, understanding of rainfall trend from past data at the regional level is important for agriculture. Success or failure of rainfed crops is closely linked with rainfall pattern. Therefore, assessing rainfall variability has been an integral part of water resources planning and management.

Temperature also plays an important role in detecting climatic change brought about by urbanization and industrialization. According to IPCC (2007) report, the warming has been increased by 0.74°C during the period 1901-2005. According to the recent approximation by IPCC (2007) the temperature has increased by 0.74°C during the period 1901-2005. Dhorde et al. (2009) has reported a rising trend in annual and seasonal temperature for four major cities of India (Kolkata, Mumbai, Delhi, Chennai). One of the

effects of urbanization is rise in minimum temperature of the cities. However for Meghalaya similar results of rising trend for temperature have been obtained with increase in maximum temperature by +0.086 °C/year while minimum temperature decreasing by -0.011°C/year (Choudhury et al., 2012). In addition trends in Relative Humidity were investigated for India. Singh et.al, 2008a have found an increase in annual mean relative humidity (1-18% of mean per 100 years) for six river basins (Lower Indus, Ganga, Tapi, Narmada, Mahi, Sabarmati and Luni). While a decrease in trend has been observed for three river basins (Brahamani, Mahanadi and Subarnarekha) from 1 to 13% of mean per 100 years.

In the light of above the trend and variability analysis of rainfall, temperature, relative humidity and wind speed has been carried out using the methodology presented below.

4.2 DATA

The daily data of rainfall, maximum and minimum temperature, relative humidity and wind speed have been collected from India Meteorological Department (IMD), Pune, and State Data Centre, Department of Water Resources, Raipur (Chhattisgarh) from 1960-2010 (51 years). For rainfall, maximum temperature and minimum temperature data is available for 24 stations whereas for wind speed and relative humidity, data is only available for eight stations. The detail information about the stations has been presented in Chapter 3. These data has been used to check the trend and variability on annual and seasonal time scale viz. summer (March-May), winter (November to January) and monsoon (late June to October) for Seonath River Basin falls in Chhattisgarh State.

4.3 METHODOLOGY

4.3.1 Homogeneity Test

Double Mass Curve analysis has been carried out to check the homogeneity in the annual and monthly data series.

4.3.2 Dependency Test (Autocorrelation coefficient)

The dependency of different meteorological parameters has been computed using lag-1 serial correlation coefficient. Presence of positive or negative autocorrelation affects the detection of trend in a series (Hamed and Rao, 1998; Yue et al., 2002, 2003; Cunderlik and Burn, 2004; Novotny and Stefan, 2007). With a positively auto-correlated series, there

are more chances of a series being detected as having trend while there may be actually none. If the r_1 value fall within the confidence interval, the data are assumed to be serially independent otherwise the sample data are considered to be significant serially correlated. Lag-1 autocorrelation coefficient is used to detect the presence of serially correlation in data series. In this study, almost all the series are found to be non-correlated except few of the series are correlated (Figure 4.1).

$$\rho_k = \frac{\sum_{t=1}^{n-k}(x_t-\bar{x}_t)(x_{t+k}-\bar{x}_{t+k})}{[\sum_{t=1}^{n-k}(x_t-\bar{x}_t)^2 * \sum_{t=1}^{n-k}(x_{t+k}-\bar{x}_{t+k})^2]^{1/2}} \quad (4.1)$$

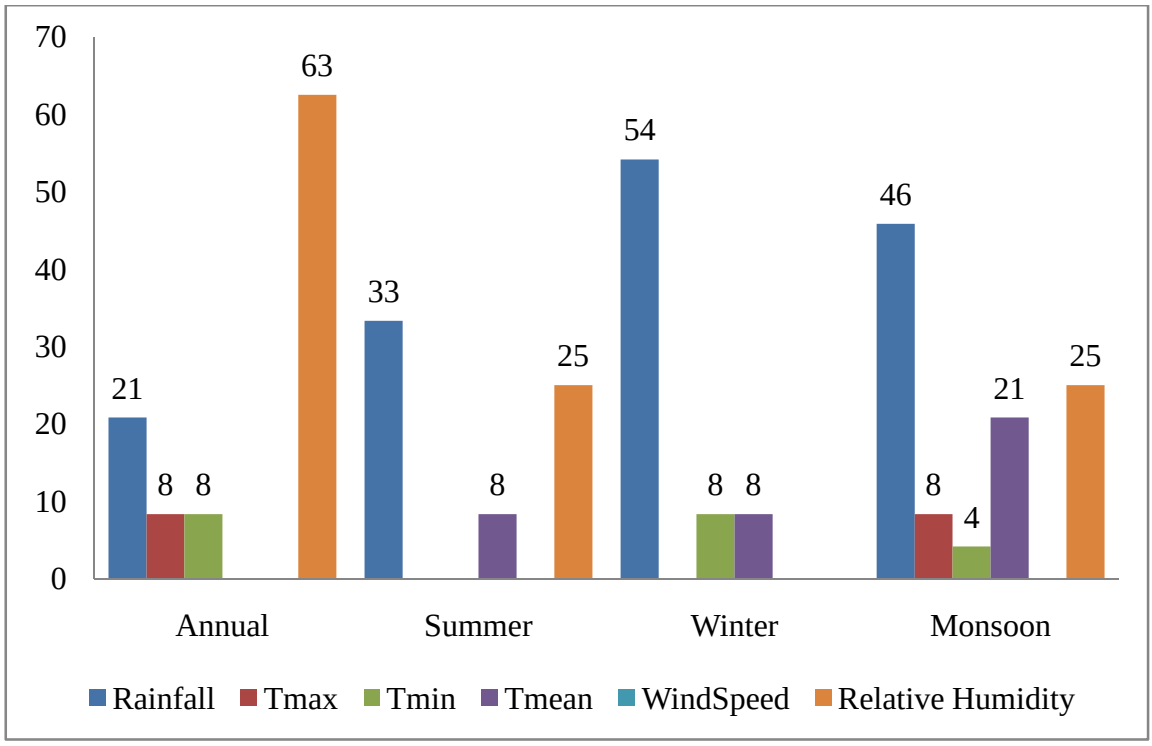

Figure 4.1 Percentage of Stations correlated for different climatic parameters (Annual and Seasonal)

4.3.3 Statistical Test for Trend and Variability Analysis

4.3.3.1 Mann–Kendall Test (Non-parametric)

The Mann-Kendall test (Yu and Neil, 1993; Douglas et al., 2000; Yue et al., 2003; Burn et al., 2004, Singh et al., 2008a, b) is used to detect monotonic (increasing or decreasing) trends and is widely used for detecting trends in time series because it is simple, robust, accommodates missing values, and the data need not conform to any statistical distribution (Libiseller and Grimvall, 2002; Gilbert, 1987). Since there are chances of outliers to be present in the dataset, the non-parametric Mann–Kendall test is useful because

its statistic is based on the (+ or -) signs, rather than the values of the random variable, and therefore, the trends determined are less affected by the outliers (Helsel and Hirsch, 1992; Birsan et al., 2005). The Mann-Kendall test is based on the statistic S. Each pair of observed values yi, yj (i >j) of the random variable is inspected to find out whether yi > yj or yi < yj. Let the past category of pairs be P, and the later type of pairs be M. Then S is described as the difference between former and later pairs.

$$S = P - M \tag{4.2}$$

For n > 10, the sampling distribution of S is as follows. Z follows the standard normal distribution

where;

$$Z = \begin{cases} \dfrac{S-1}{\sqrt{Var(S)}} & if \quad S > 0 \\ 0 & if \quad S = 0 \\ \dfrac{S+1}{\sqrt{Var(S)}} & if \quad S < 0 \end{cases} \tag{4.3}$$

$$Var(S) = \frac{N(N-1)(2N+5) - \sum_{k=1}^{n} t_k (t_k - 1)(2t_k + 5)}{18} \tag{4.4}$$

The trend is said to be decreasing if Z is negative and the computed probability is greater than the significance level. The trend is supposed to be rising if the Z value is positive and the computed probability is greater than the significance level. If the estimated probability is smaller than the significance level, there is no trend.

4.3.3.2 Modified Mann Kendall Test

Pre-whitening has been used to detect a trend in a time series in presence of autocorrelation (Cunderlik and Burn, 2004). However, pre-whitening is reported to reduce the detection rate of significant trend in the MK test (Yue et al., 2003). Therefore, the MMK test (Hamed and Rao, 1998; Rao et al., 2003; Basistha et al., 2009) has been employed for trend detection of an autocorrelated series. In this, the autocorrelation between ranks of the observations ρ_k are evaluated after subtracting a non-parametric trend estimate such as Theil

and Sen's median slope from the data. Only significant values of ρ_k are used to calculate the variance correction factor n/n^*_s, as the variance of S is underestimated when the data are positively autocorrelated.

$$\frac{n}{n*_s} = 1 + \frac{2}{n(n-1)(n-2)} * \sum_{k=1}^{n-1}(n-k)(n-k-1)(n-k-2)\rho_k \qquad (4.5)$$

where n is the actual number of observations, n^*_s is considered as an 'effective' number of observations to account for autocorrelation in the data and ρk is the autocorrelation function of the ranks of the observations. To account only for significant autocorrelation in data, number of lags can be limited to 3 (Rao et al., 2003). The corrected variance is then computed as

$$V^*(S) = V(S)(\frac{n}{n*_s}) \qquad (4.6)$$

Where; V (S) is from Equation (4.4). The rest is as in the MK test.

4.3.3.3 Theil-Sen's Slope Estimator

In addition to recognize whether a trend exists, the trend magnitude has been assessed by Sen's Slope Estimator (β), and expanded by Hirsch et al. (1982). To estimate trend magnitude Theils-Sen's slope (β) approach is used in this study. In other words, the slope estimator β is the median over all possible combinations of pairs for the whole data set (Hirsch et al., 1982). A positive value of β indicates an 'upward trend' (increasing values with time), while a negative value of β indicates a 'downward trend' (Xu et al. 2007, Karpouzos et al. 2010). The slope estimates of N pairs of data are first computed by

$$\beta = \frac{(x_j - x_k)}{(j - k)} \qquad (4.7)$$

for i = 1, . . . N, where, x_j and x_k are data values at times j and k (j > k), respectively. The median of these N values of β is Sen's estimator of slope.

4.3.3.4 Percentage Change

Some trends may not be evaluated to be statistically significant while they might be of practical interest and vice versa. For the present study, change percentage has been computed by approximating it with a linear trend. That is change percentage equals median slope multiplied by the period length divided by the corresponding mean, expressed as

percentage (P_c) followed by Yue and Hashino (2003). The percentage change is estimated by following formula.

$$P_c = \frac{\beta * L}{\mu} \quad (4.8)$$

Where, P_c = Percentage Change, β = Slope Magnitude, L = Length of the year and μ = Corresponding mean

4.3.4 Statistical Procedure for Rainfall Variability Analysis (Coefficient of Variation)

The coefficient of variation (CV) is a statistical measure of how the individual data points vary about the mean value. A greater value of CV is the indicator of larger spatial variability, and vice versa. In this study, annual variability of the time series of rainfall, temperature, relative humidity and wind speed have been analyzed for Seonath River basin using CV (Landsea and Gray, 1992).

4.3.5 Spatial Analysis

The Spatial interpolation technique (Singh and Chowdhury, 1986; Lebel et al., 1987) is employed to determine the spatial pattern of meteorological variables using Arc GIS 9.3. The geographic information systems (GIS) tool is widely used in the processing of spatially distributed hydrological modeling (Maidment, 1991; Eldho et al., 2006; Jat et al., 2009; Pandey et al., 2011). In recent times, GIS interpolation method has been widely used to show the spatial distribution of evapotranspiration, temperature and rainfall (Haberlandt 2007; Cheng et al., 2007) and it provides the layout and drawing tools essential to present the outcomes visually. GIS technique assist researchers to understand the natural environment (Jang et al., 2007). The application of interpolation technique in evapotranspiration have been reported by several researchers (Dinpashoh, 2006, Iran; Zhao et al,. 2004, Zuli River Basin in China; and Bai et al., 2006, Shanxi Province, China) with inverse distance weight (IDW) technique. Thus, it is significant to identify spatial and temporal variations as it will affect crop water requirement. The overall methodology for the analysis used in this Chapter is presented in the form of flowchart in Figure 4.2.

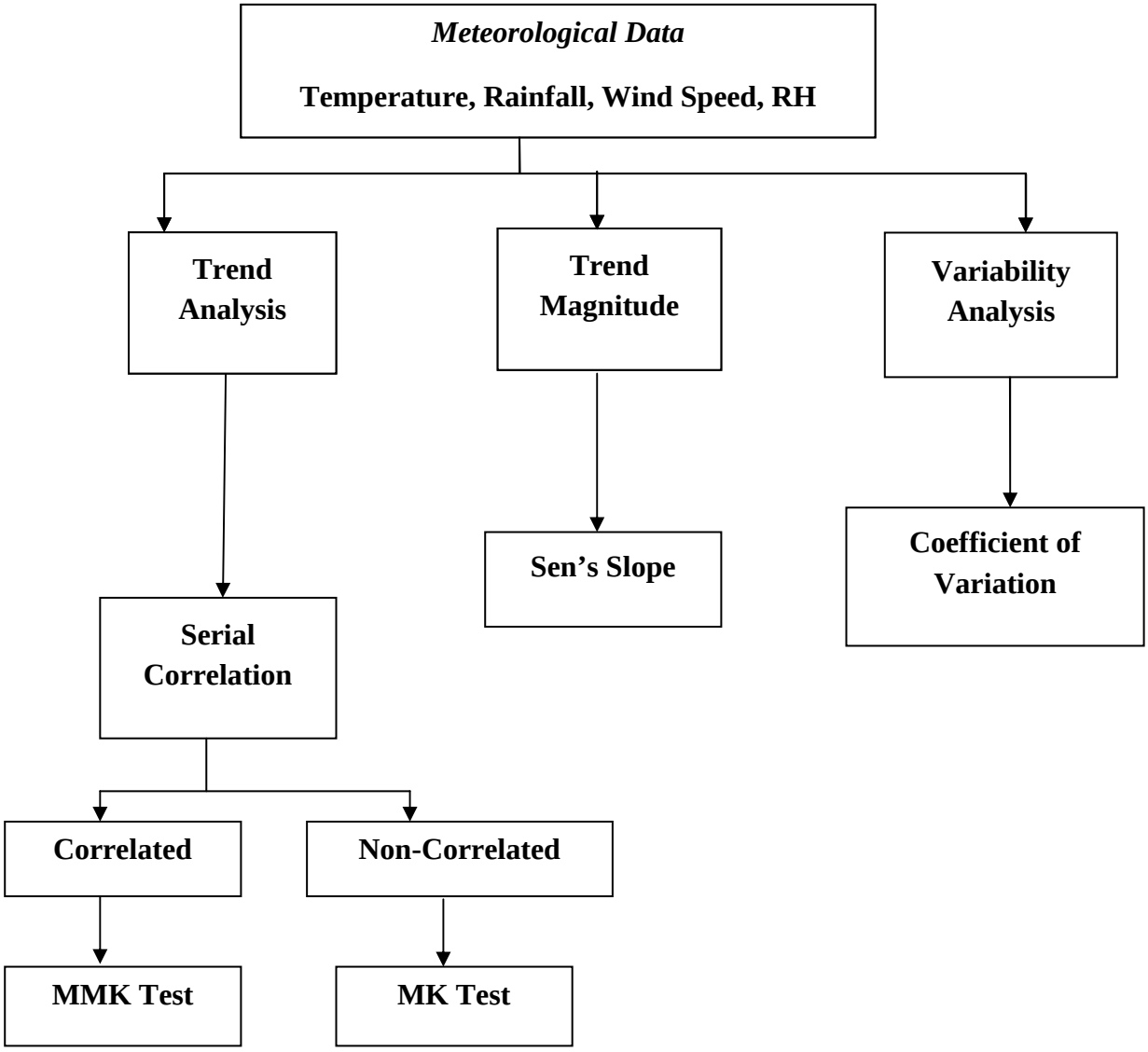

Figure 4.2 Flowchart presenting methodology for trend and variability analysis of meteorological variables

4.4 RESULTS AND DISCUSSION

4.4.1 Trend Analysis of Rainfall

4.4.1.1 Trend Analysis

To analyze the causal mechanism behind the rainfall trends, the trend analysis is performed. The results of the spatial distribution of the annual and seasonal trends at 95% significance level in Seonath River basin are shown in Figure 4.3. All four seasons have been characterized by decreasing rainfall at most stations except few stations falling in the districts of Rajnandgaon, Durg, Raipur and Damtari which shows non-significant decreasing

trend. (Fig. 4.3 b, c and d). Decreasing trends for the annual rainfall are mainly observed in the overall study area of Seonath River basin. The majority of the rainfall time series of different stations shows negative values whereas few stations in southern Seonath river basin shows non-significant decreasing trend (Figure 4.3). Additionally, Table 4.1 presents Sen's slopes for annual and seasonal rainfall for the study basin. However the weighted rainfall time series for Seonath basin as a whole shows insignificant decreasing trend for all the seasons (Table 4.1, Column 1). However rate of decrease in rainfall was estimated as -2.79 mm/year for monsoon season followed by -2.4 mm/year for annual series. The rate of change for summer season is negligible (i.e. -0.5 mm/year) and it is zero for winter season (Pl. see Table 4.1, Column 2). The percentage variability was highest for monsoon season 43.95% followed by annual rainfall variability of 30.78% (Table 4.1, Column 4). Table 4.2 presents the rate of change for annual and seasonal rainfall in different stations of Seonath basin over 100 years. It is evident from Table 4.2 that the winter season shows negligible or no change whereas monsoon season shows the highest rate of change of rainfall over 100 years followed by summer season. Significant decreasing rate of change has been found in annual rainfall too. The annual and monsoon seasons shows highest rate of change for the stations falling in Rajnandgaon and Durg district. Figure 4.4 shows the percentage of stations with increasing/decreasing trends for different seasons. The winter season has the greatest percentage of stations showing a decreasing trend (87%), followed by monsoon and summer with 83%. On average, the annual rainfall time series shows that the 83% of stations in the basin have decreasing trend (Figure 4.4). Overall decreasing trends in rainfall were observed for the entire river basin for all the seasons. The above results are found in conformity with the results of past studies for rainfall in Mahanadi river Basin (Singh et al., 2008a; Jain and Kumar, 2012).

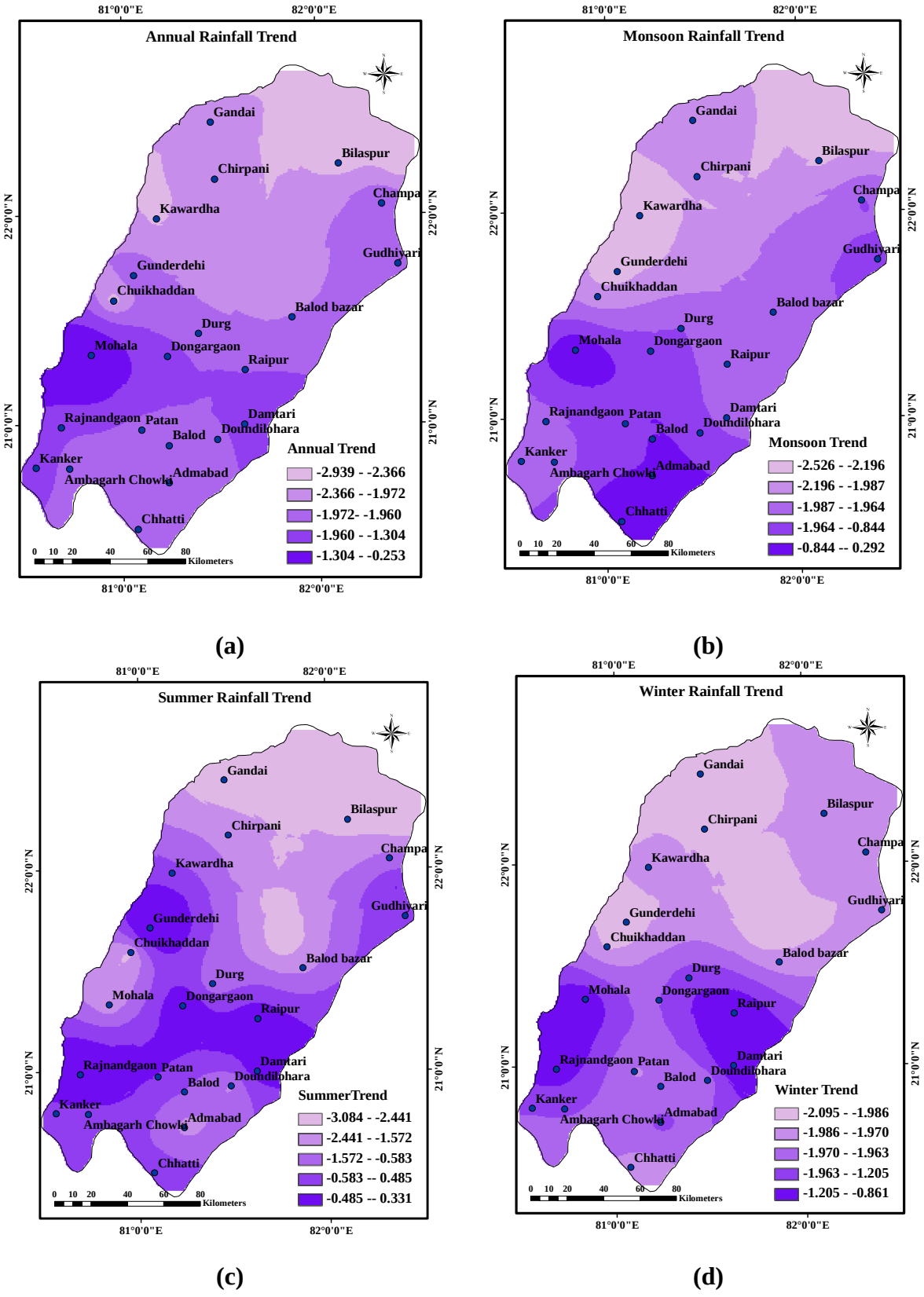

Figure 4.3 Trend in annual and seasonal rainfall in Seonath river basin over the period of 1960-2010 (a) Annual (b) Monsoon (c) Summer (d) Winter

Table 4.1 Results of regional average annual and seasonal rainfall for entire Seonath River Basin.

Entire Seonath River Basin	Rainfall			
	Z-values MK	**Sen's Slope (β)**	**% Change over 51 year**	**% Variability over 51 year**
	(Col.1)	**(Col.2)**	**(Col.3)**	**(Col.4)**
Annual	-0.529	-2.4	-12.33	30.78
Summer	-0.472	-0.5	-9.0	6.95
Winter	-0.444	0.0	-1.7	17.19
Monsoon	-0.994	-2.79	-21.64	43.95

Table 4.2 Rate of change in annual and seasonal rainfall for Seonath river basin over 100years

Station	District	Annual	Summer	Winter	Monsoon
Ambagarh Chowki	Rajnandgaon	-56.081	-52.37479	No Change	-56.3299
Chuikhaddan		-95.9808	-56.6814	-2.2957	-61.5019
Dongargaon		-58.3605	-41.2496	No Change	-61.803
Mohala		-62.2027	-46.128	No Change	-87.5889
Rajnandgaon		-54.9545	-79.587	3.65294	-72.2979
Balod Bazar	Raipur	-5.3532	-18.2782	No Change	-30.9181
Raipur		-6.76718	13.3452	1.95	-34.5968
Simga		-1.18462	-15.1031	No Change	-32.1889

Chhatti	Dhamtari	-31.7827	-30.8291	-0.93006	-17.6468
Dhamtari		-25.9212	-33.702	-2.1509	-15.0018
Chirapani	Kawardha	-26.5177	-2.5292	-0.88248	-15.9326
Kawardha		-29.6049	-3.18103	-1.4399	-17.6366
Gandai		-23.7458	-2.7566	-1.38889	-29.0365
Doundi Lohara	Durg	-61.7549	-44.099	-0.33559	-70.645
Durg		-63.5321	-40.2784	No Change	-62.771
Doundi		-64.26535	-44.9623	No Change	-74.7478
Admabad		-72.6222	-16.000	No Change	-71.5982
Balod		-68.98445	-36.38131	No Change	-74.5104
Gudhiyari		-73.6222	-37.70391	No Change	-74.656
Gondly		-72.1357	-42.45	No Change	-75.382
Gurur		74.22222	No Change	No Change	-73.651
Gunderdehi		-78.69531	60.6955	-3.59688	-73.071
Bilaspur	Bilaspur	-37.137	-32.098	No Change	-45.683
Champa	Jhanjgir-Champa	-27.2342	-23.332	-1.2241	-32.2432

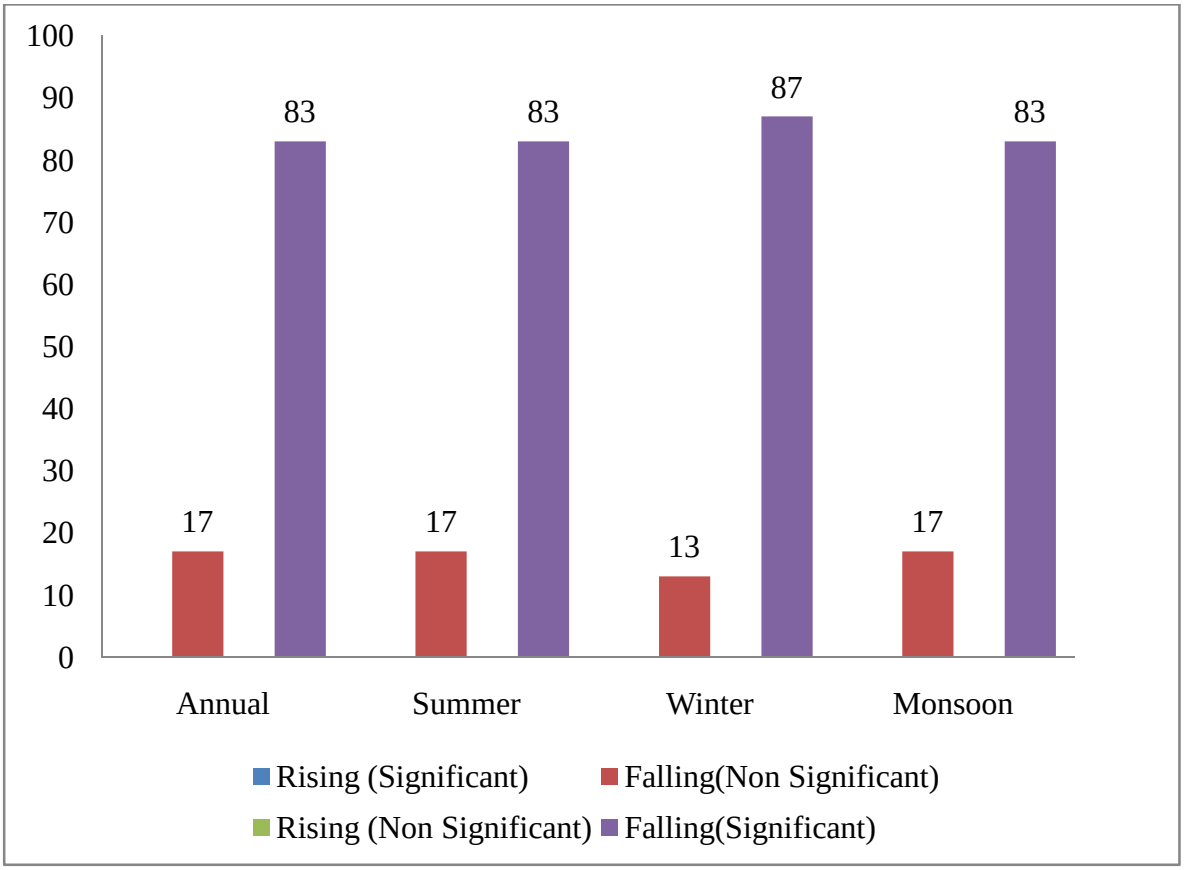

Figure 4.4 Temporal Trends of Annual and Seasonal Rainfall

4.4.1.2 Analysis of Annual Rainfall Variability Pattern (Coefficient of Variation)

The rainfall variability was determined using Coefficient of Variation (CV). A decrease in rainfall trend and increase in its variability is seen in Northern parts of the basin (Figure 4.5). The highest variability is experiences in Bilaspur and Korba, and it is lowest in Durg and Rajnadgaon districts.

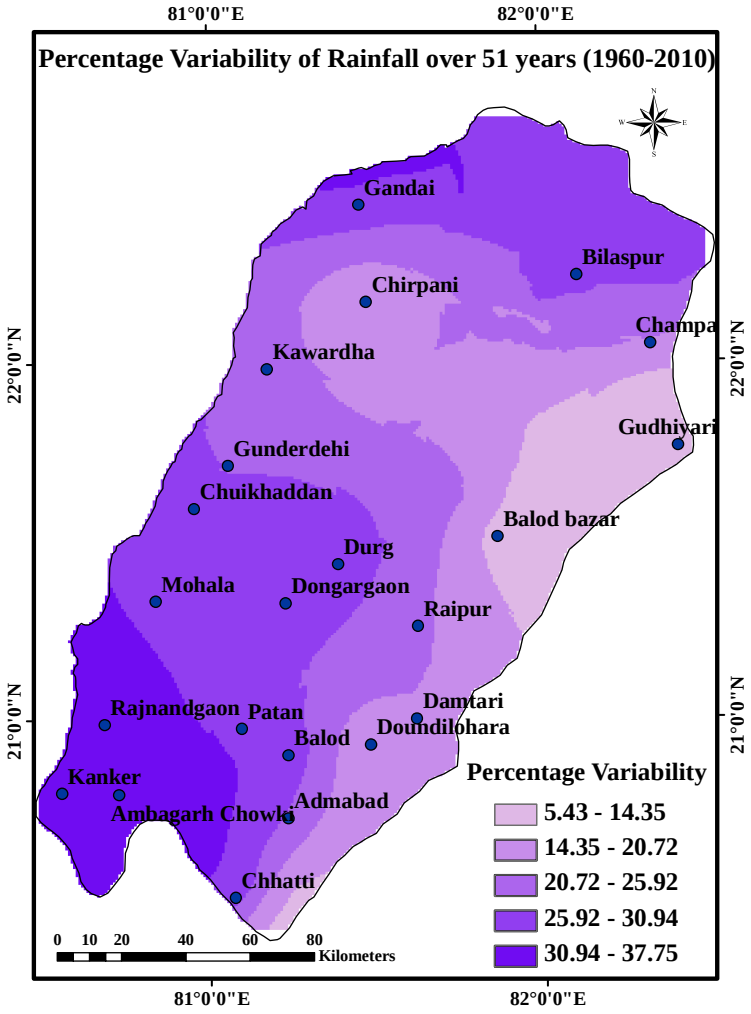

Figure 4.5 Inter-annual Variability of Rainfall Variable

4.4.2 Trend Analysis of Temperatures (Maximum, Mean and Minimum)

The Mann-Kendall statistics is used to estimate the trends of maximum temperature (Tmax), minimum temperature (Tmin) and mean temperature (Tmean) at 95% significant level. The rising trend was observed in Tmax for all the seasons except for summer which shows decreasing trend for all the stations (Figure 4.6). The monsoon season shows significant increasing trend for all the stations (Figure 4.7). On the contrary, Tmax for summer season at all the stations showed non-significant decreasing trend. However, annual Tmax in 80% of the stations showed insignificant increasing trend (Figure 4.7). However minimum and average temperature reveals rising trend in annual and seasonal scale for the entire basin. The annual Tmin shows significant increasing trend for all the stations except Bilaspur and Champa districts which fall in the Northern part of the basin (Figure 4.8 a). Again the Champa and Bilaspur districts have non-significant increasing trend (Figure 4.8

a). Tmax for summer season reveals non-significant increasing trend for all the stations (Figure 4.8 b). It can be seen from Figure 4.8 c and Figure 4.8 d that all the stations have significant increasing trend for winter and monsoon season. Figure 4.9 presents the percentage of stations with rising/falling trend of annual and seasonal Tmin.

For Tmean rising trend was obtained for entire basin except few stations located in the Northern region of the basin for all the seasons (Figure 4.10). The Monsoon season exhibits significant rising trend followed by winter and annual average temperature (Figure 4.10). The summer average temperature reveals that the 33% of stations have decreasing trend (Figure 4.11). The Sen's slope is used to estimate percentage change in Tmax, Tmin and Tmean. The Tmin has increased more as compared to Tmax. The percentage change was increasing for all months except for March to June (Figure 4.12). The percentage change of rise in Tmin was highest for the month of November followed by December and January (Figure 4.12). The inter-annual variability for Tmax and Tmin is depicted in (Figure 4.13). The variability was observed to be more pronounced in Tmin ranges from 1.69% to 2.78% (Figure 4.13 b). The analysis of maximum and minimum temperature has indicated that the northern parts have faced relatively more variability than the southern part of the basin. Similarly variability in Tmax has been found more in the northern parts with highest variability of 1.93% (Figure 4.13 a). Interestingly, increasing trends of maximum temperature occurred for all months except March, April, May and June i.e., for summer season (Table 4.3). The Tmax and Tmin during November month have higher significant increase in the order of 2.75 °C/100 years and 4.31 °C/100 years, respectively. From Table 4.3 it can be seen that the magnitude of increasing trend of Tmin has been higher compared to the Tmax. It reveals that the evaporation in day time could have been more and consequently, it could lead to higher water requirement for crops (Table 4.3). Overall highly significant increasing trend in mean, maximum and minimum temperature for Seonath river basin was observed. The above results are well supported by the findings of studies conducted by Rao et al. (1993) for Mahanadi river basin and by Subash and Sikka (2013) for Chhattisgarh state.

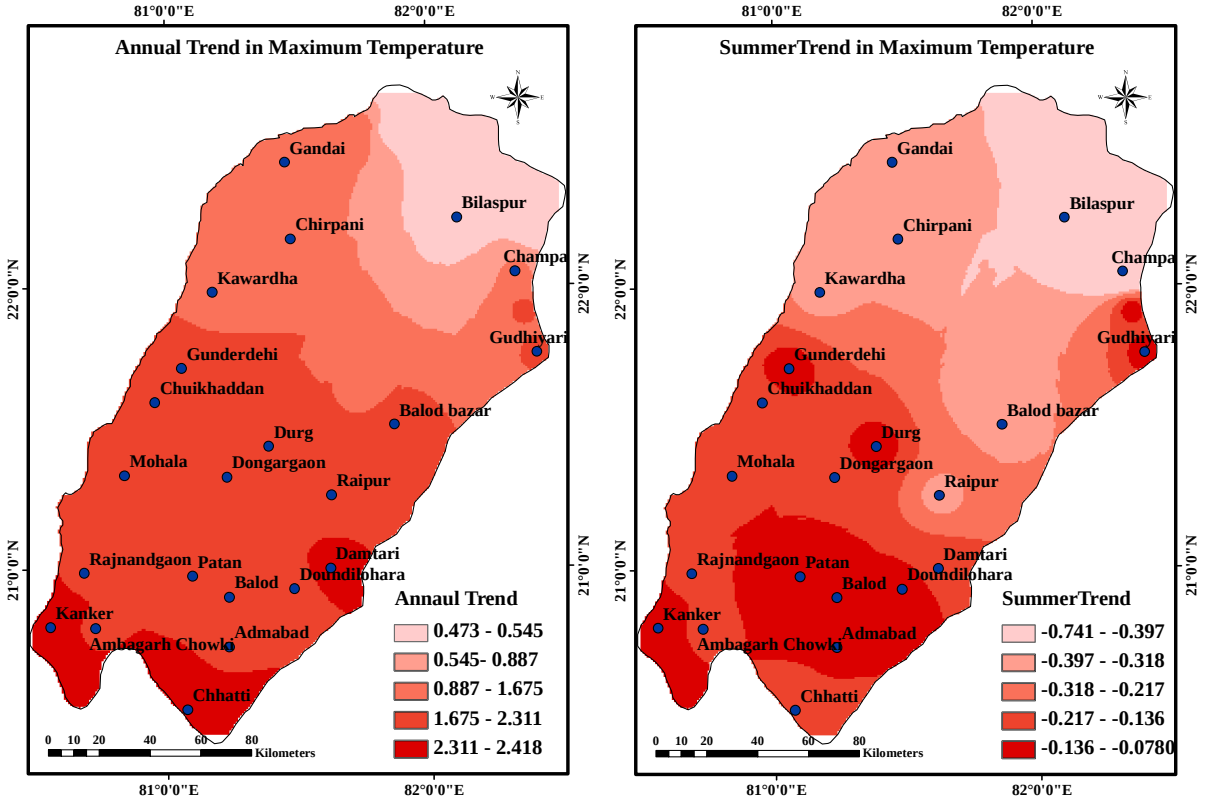

(a) Annual (b) Summer

(c) Monsoon (d) Winter

Figure 4.6 Spatial distribution of annual and seasonal trends in maximum temperature

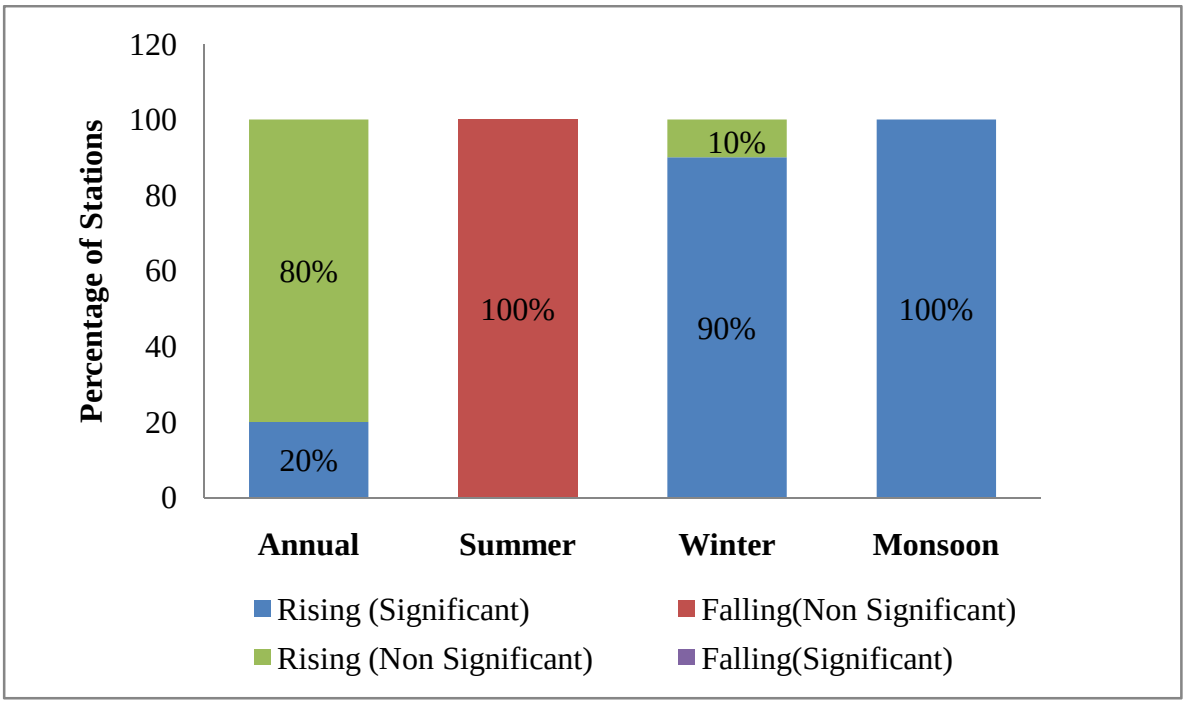

Figure 4.7 Percentage of station with significant trend for Seonath River Basin

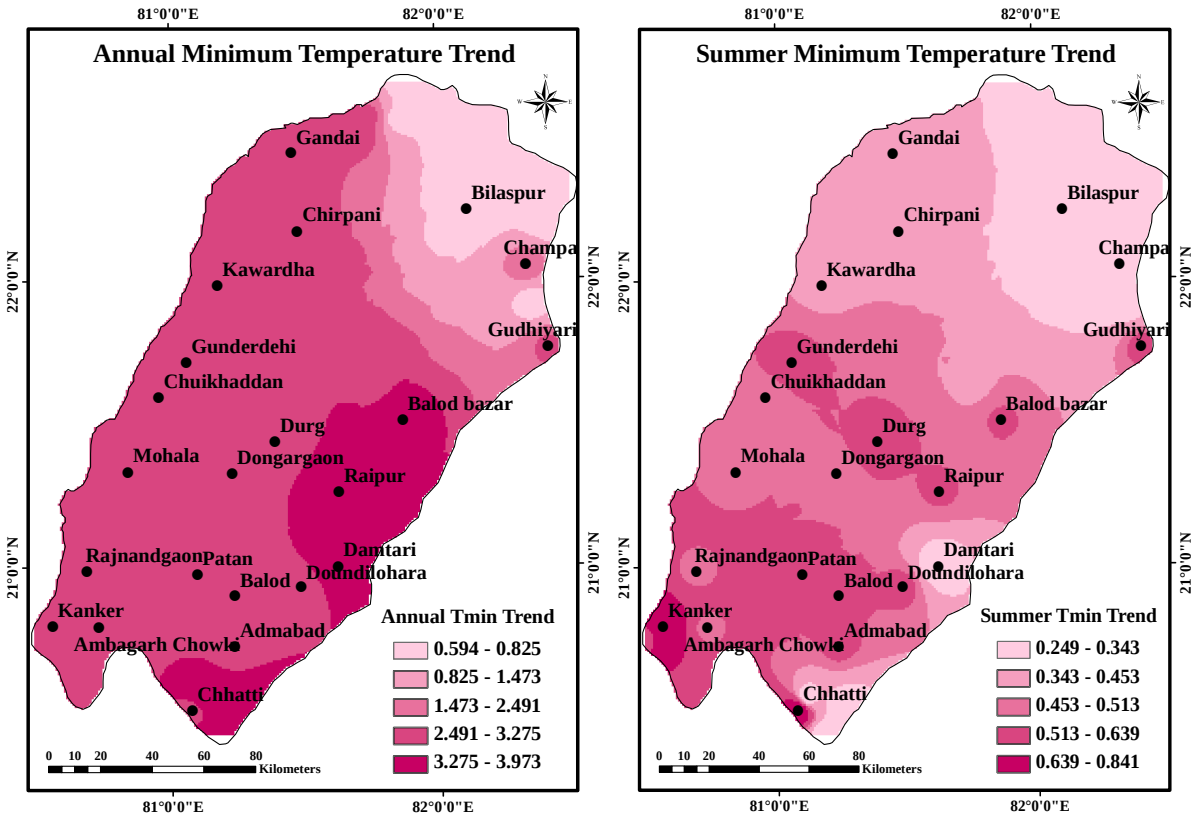

(a) **(b)**

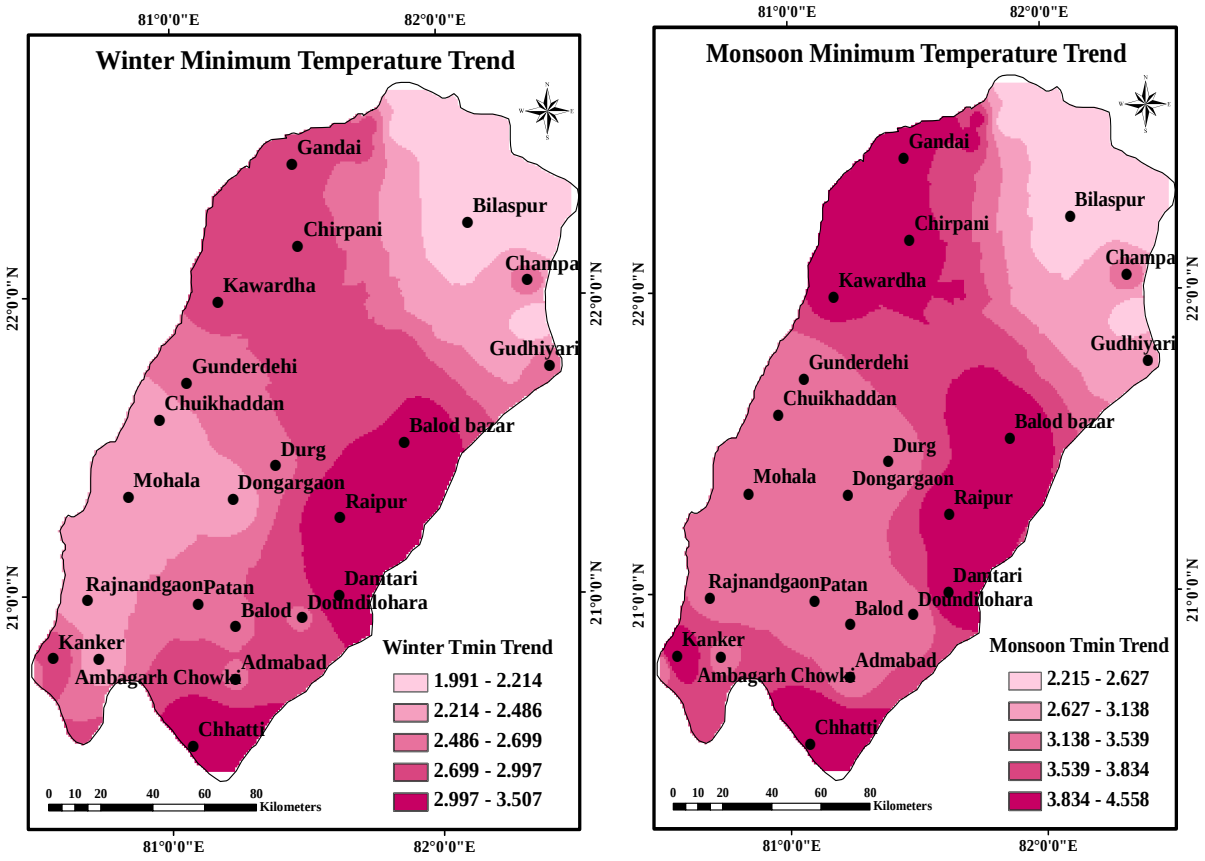

(c) **(d)**

Figure 4.8 Spatial map of minimum temperature trend in Seonath river basin over 51 years (a) Annual (b) Summer (c) Winter (d) Monsoon

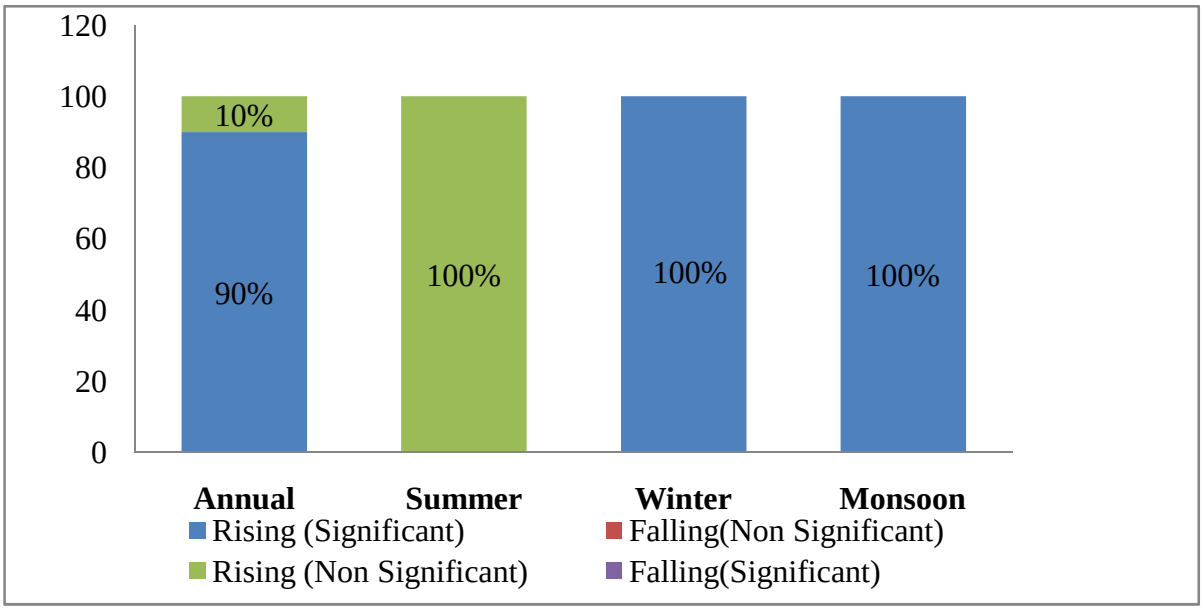

Figure 4.9 Percentage of stations with trend exist in the entire basin

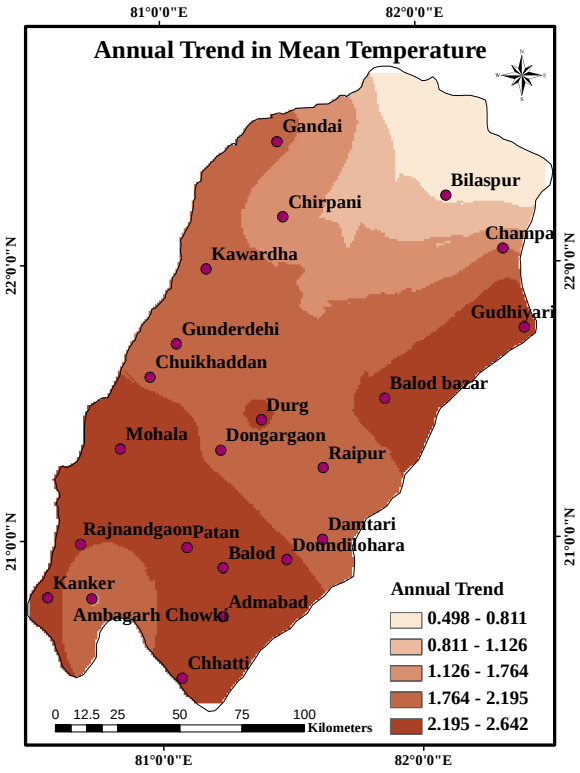

(a) Annual

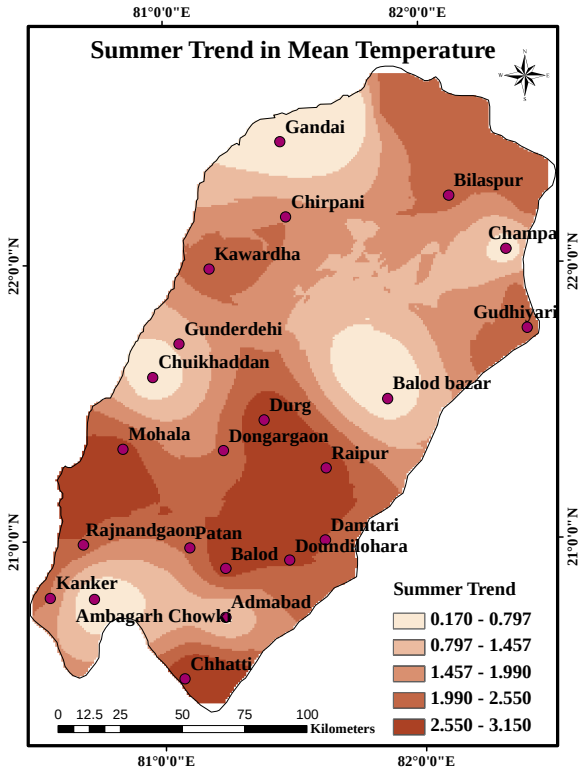

(b) Summer

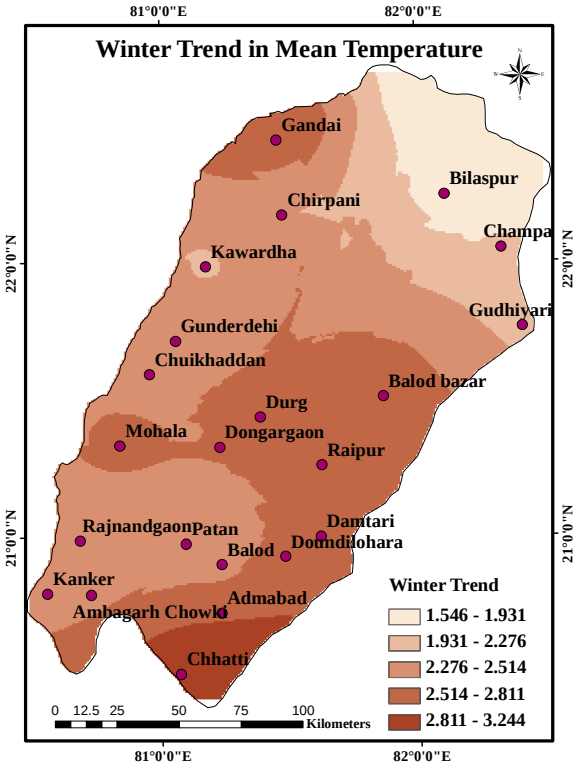

(c) Winter

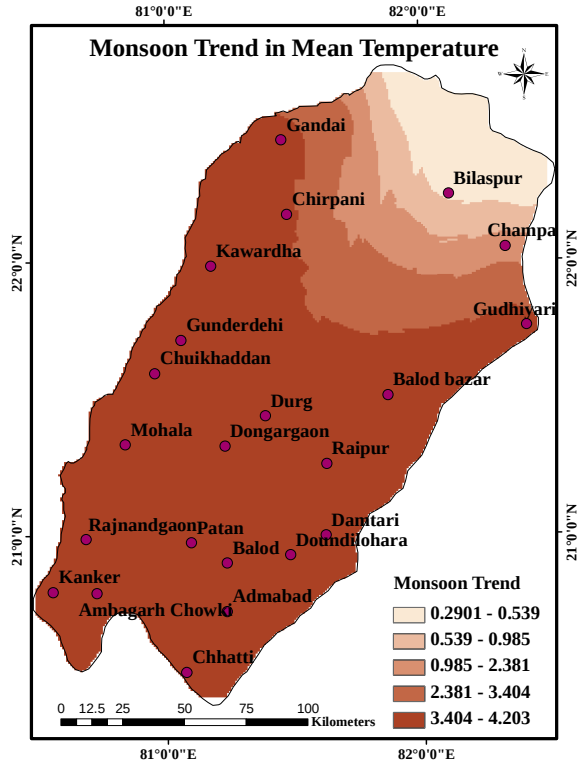

(d) Monsoon

Figure 4.10 Spatial trend analysis of average temperature on annual and seasonal timescales

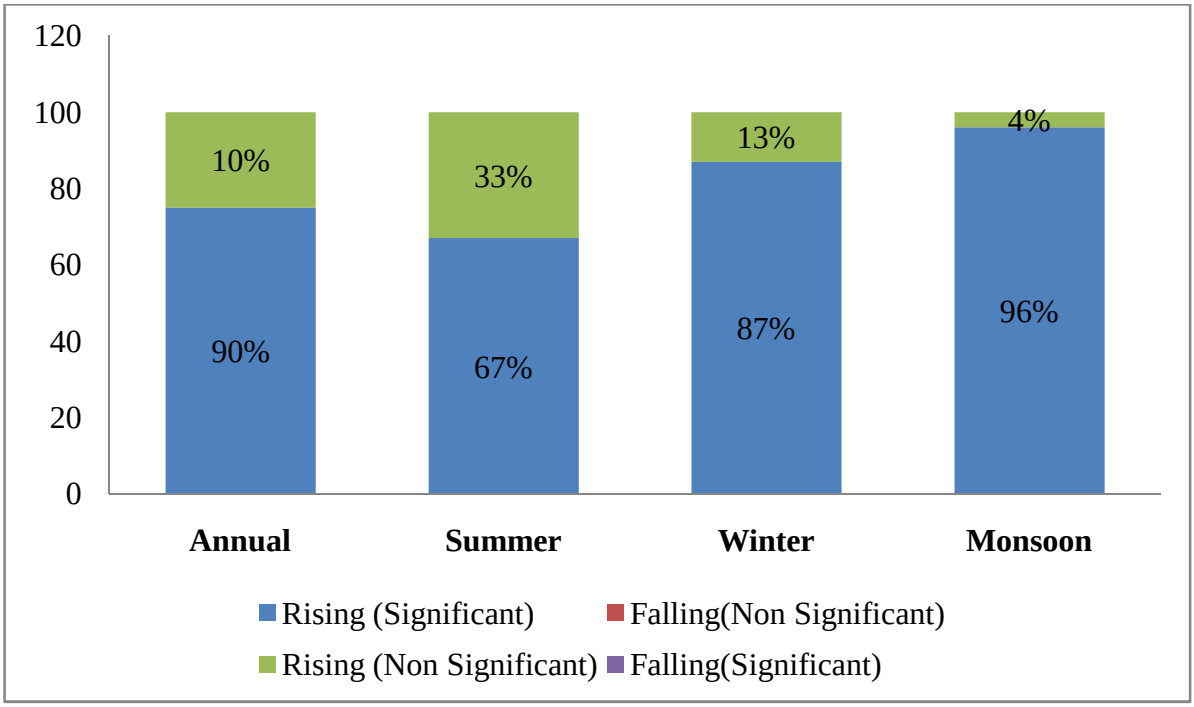

Figure 4.11 Temporal trend in average temperature at annual and seasonal scale

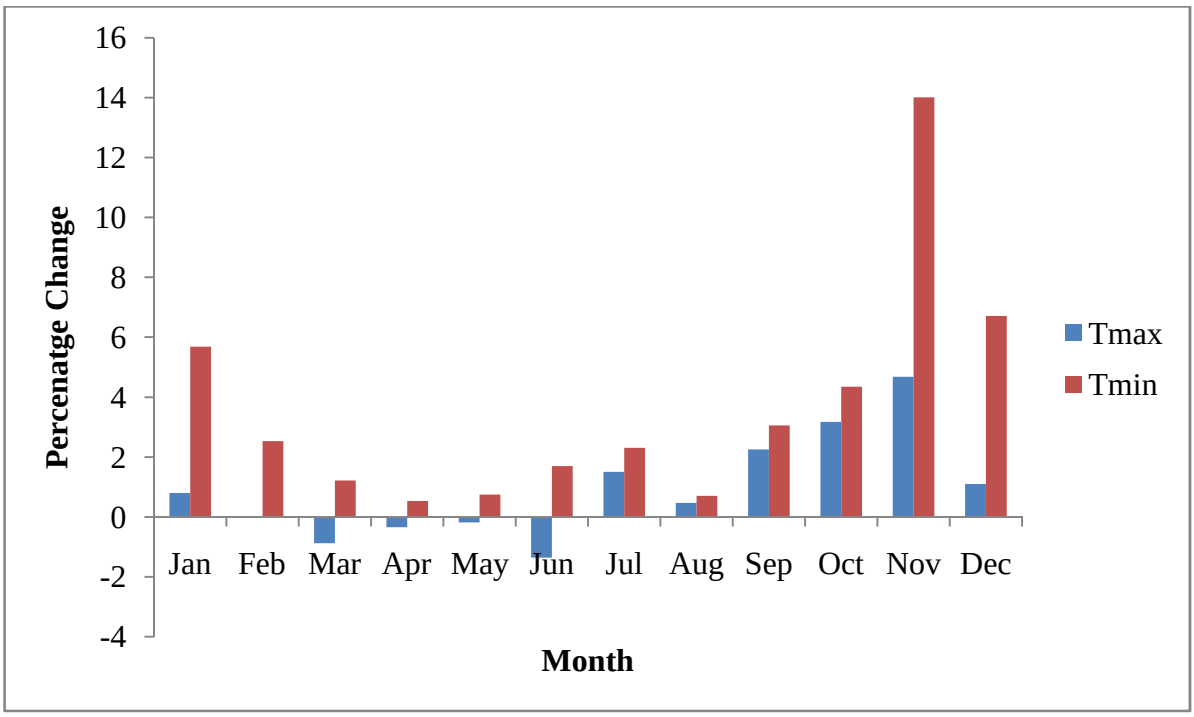

Figure 4.12 Percentage change in maximum and minimum temperature over 51 years

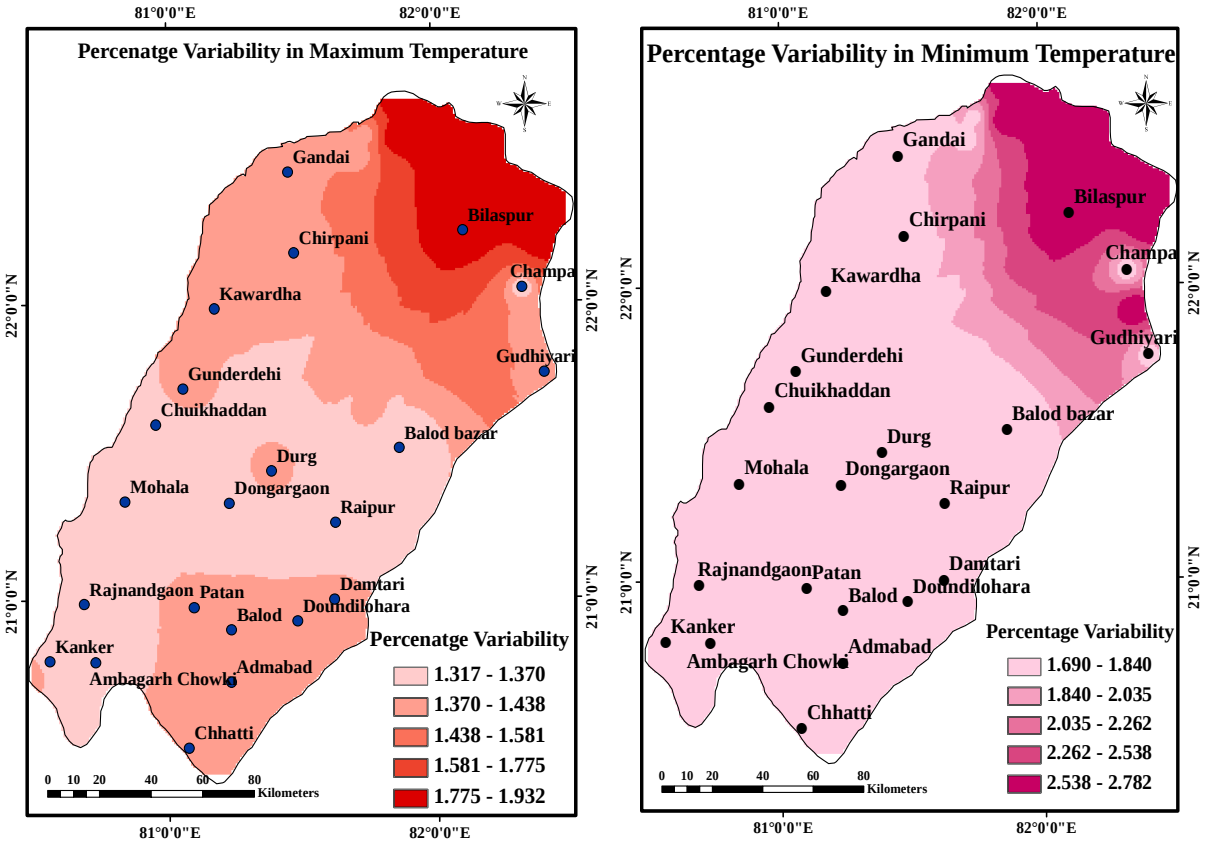

(a) Tmax **(b) Tmin**

Figure 4.13 Inter-annual variability of maximum and minimum temperature

Table 4.3 Sen Slope estimator (°C/100 years) for maximum, minimum, mean temperature for different months

Seasons	Sens Slope (β)		
	Maximum Temperature	Minimum Temperature	Mean Temperature
January	0.423	1.407	0.947
February	0.021	0.766	0.471
March	-0.619	0.476	0.068
April	-0.273	0.256	0.018
May	-0.152	0.402	0.239
June	-1.026	0.895	1.092
July	0.956	1.126	1.140
August	0.288	0.341	0.234
September	1.438	1.444	1.359
October	2.028	1.787	1.919
November	2.750	4.307	3.545
December	0.598	1.611	1.048

4.4.3 Trend Analysis of Relative Humidity

The temporal trend in Relative Humidity (RH) is shown in Figure 4.14. It shows that significantly decreasing RH has been observed for the months of July, September, October and November. Whereas, from March to June non-significant increasing trend have been observed. The MK results indicate that the annual mean RH for all the seasons are in significant decreasing trends. For the overall basin the percentage of stations showing significant decreasing/ increasing trend is depicted in Figure 4.15. For annual trend the

entire river basin shows significant decreasing trend except few stations located in the north western region of the study area (Figure 4.16 a). For monsoon season strongly significant decreasing trend has been observed for the entire basin (Figure 4.16 b). Whereas for winter the non significant decreasing trend and for summer season increasing trend has been observed (Figure 4.16 c, d). The decrease in RH is mainly due rise in temperature of the river basin already discussed in previous section. The RH for annual, winter and monsoon are decreasing whereas for summer it is increasing. The Tmax for summer is decreasing therefore RH is increasing because there is inverse relation exist between the two variables. The results are in conformity with the past study on RH in Mahanadi basin (Singh et.al, 2008a). The Sen's slope is applied to detect the trend magnitude and percentage change. The monthly rate of change over 51 years of period has been presented in Figure 4.17. From Figure 4.17 the larger changing magnitude has been observed for the months of July, September, October and November. The relative percentage of change for the entire basin is spatially presented in Figure 4.18. From this figure it was depicted that the highest percentage change was observed for the entire basin except for northwestern region of the study area which shows the lowest change. The inter-annual variability in relative humidity for the basin ranges from 0.9% to 2.2% (Figure 4.19).

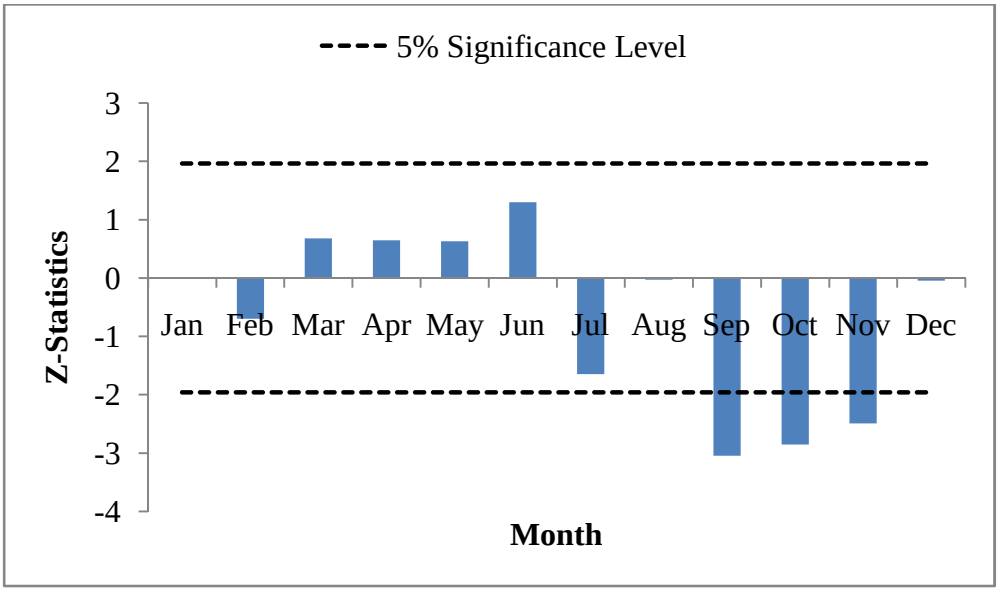

Figure 4.14 Temporal Monthly Relative Humidity Trend at Seonath River Basin over 51 years

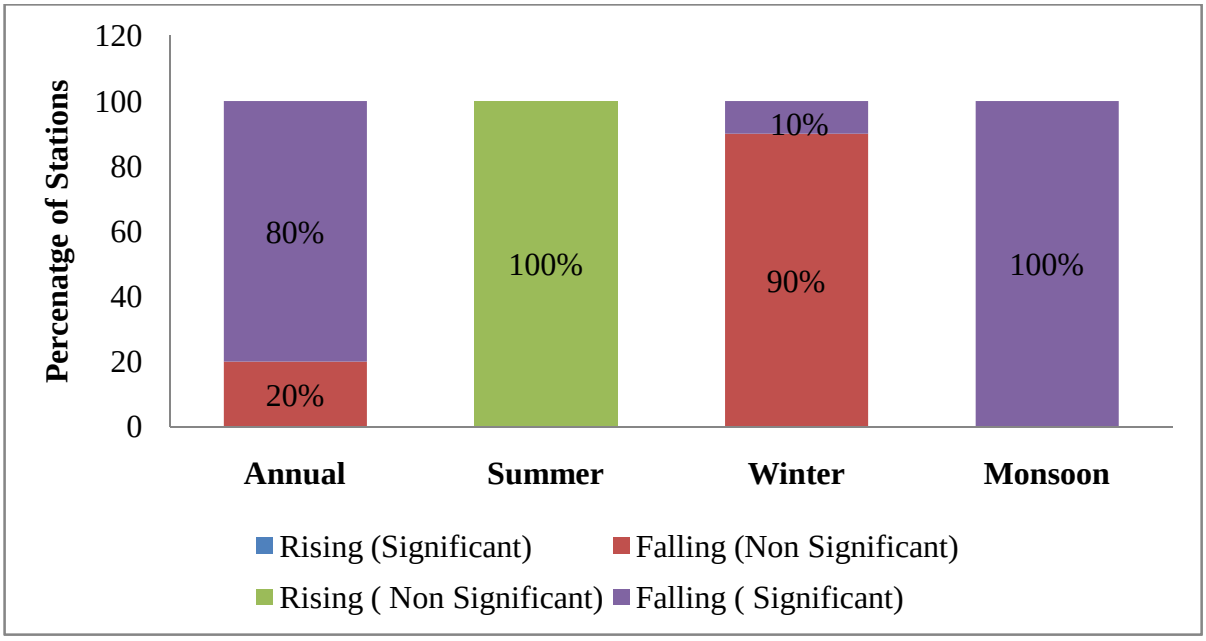

Figure 4.15 Percentage of Stations with significant Trend at Annual and Seasonal Scale

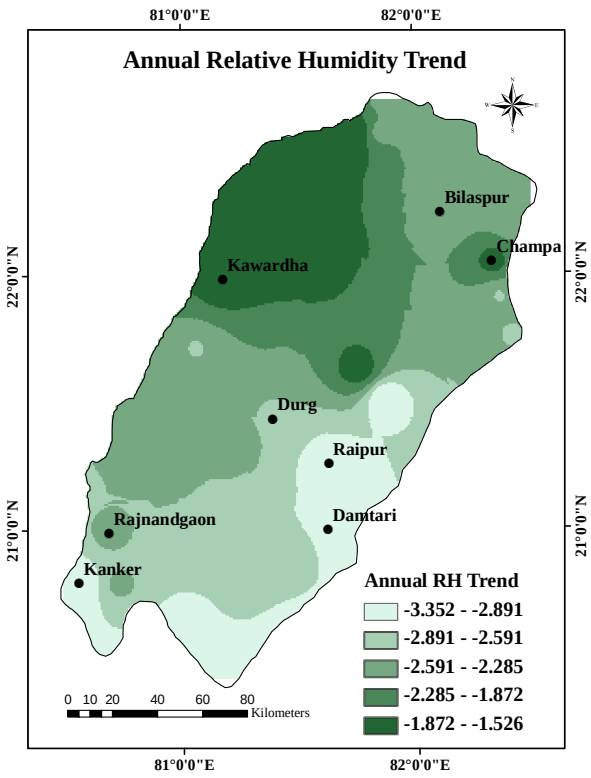

(a) Annual

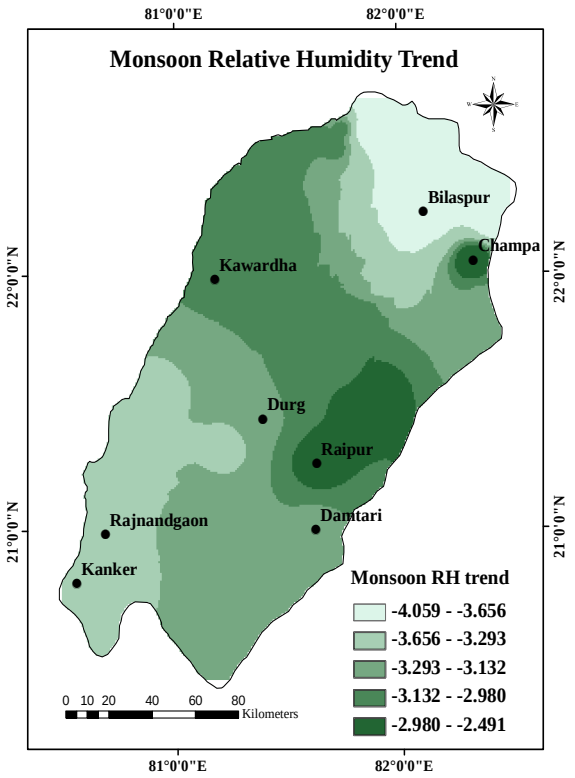

(b) Monsoon

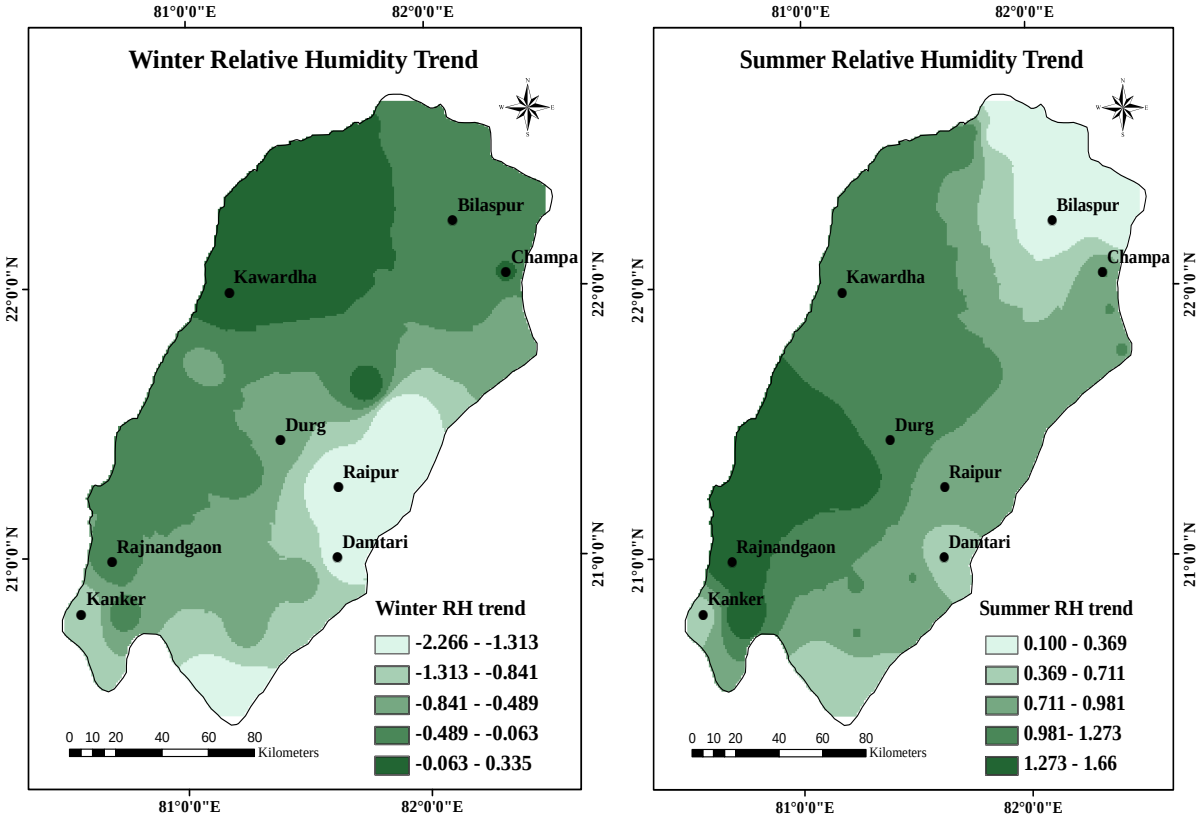

(c) Winter **(d) Summer**

Figure 4.16 Spatial distribution of Annual and Seasonal Relative Humidity Trend

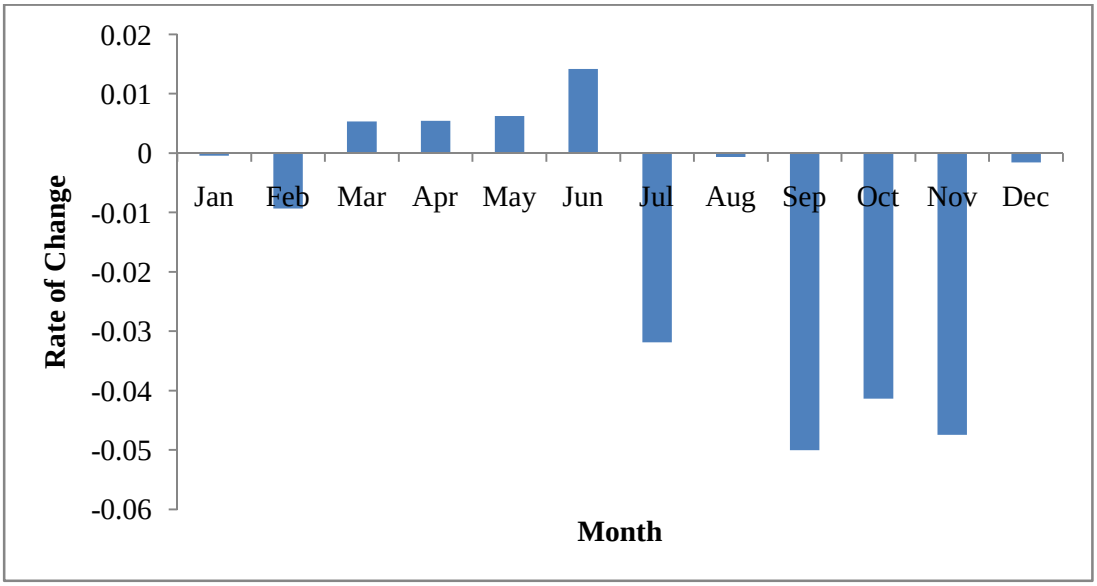

Figure 4.17 Monthly Rate of Change in Relative Humidity over 51 years (1960-2010)

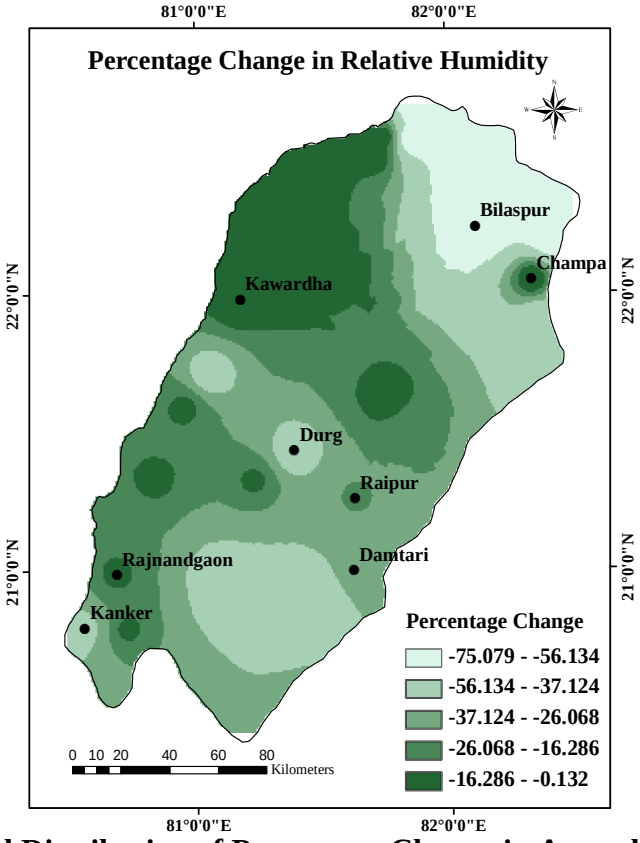

Figure 4.18 Spatial Distribution of Percentage Change in Annual Relative Humidity

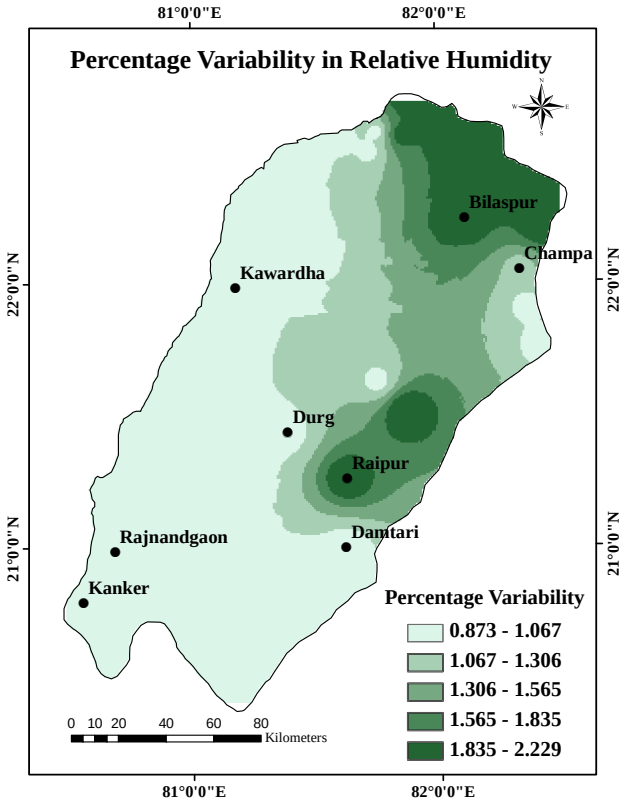

Figure 4.19 Spatial Distribution of Inter-annual Variability in Annual Relative Humidity

4.4.4 Trend Analysis of Wind Speed

The monthly trend statistics by MK test is presented in Figure 4.20 which clearly indicates a significant increasing trend for all the months. The trend in seasonal wind speed is depicted in Figure 4.21. From seasonal analysis of time series for wind speed, strong significant increasing trend has been obtained for monsoon and winter season (Figure 4.21 a and 4.21 b). In summer season some stations located in southwest shows an insignificant increasing trend (Figure 4.21 c). The percentage of stations with rising trend has been 100% for all the seasons (Figure 4.22). The Sen's slope estimates the magnitude of change in wind speed. The monthly change in rate of wind speed over 51 years is shown in Figure 4.23. It is clear from the figure that there is increasing rate of change over the years. It is also depicted from figure that August is having highest rate of change followed by July, June and September. The percentage change is shown spatially (Figure 4.24). From this figure the highest percentage change has been highlighted for the entire basin ranges from 34% to 61%. The highest change has been obtained for Kawardha and lowest for Korba. The spatial variability in wind speed was shown in Figure 4.25. The stations in the northern part of the basin show the highest variability of 23%.

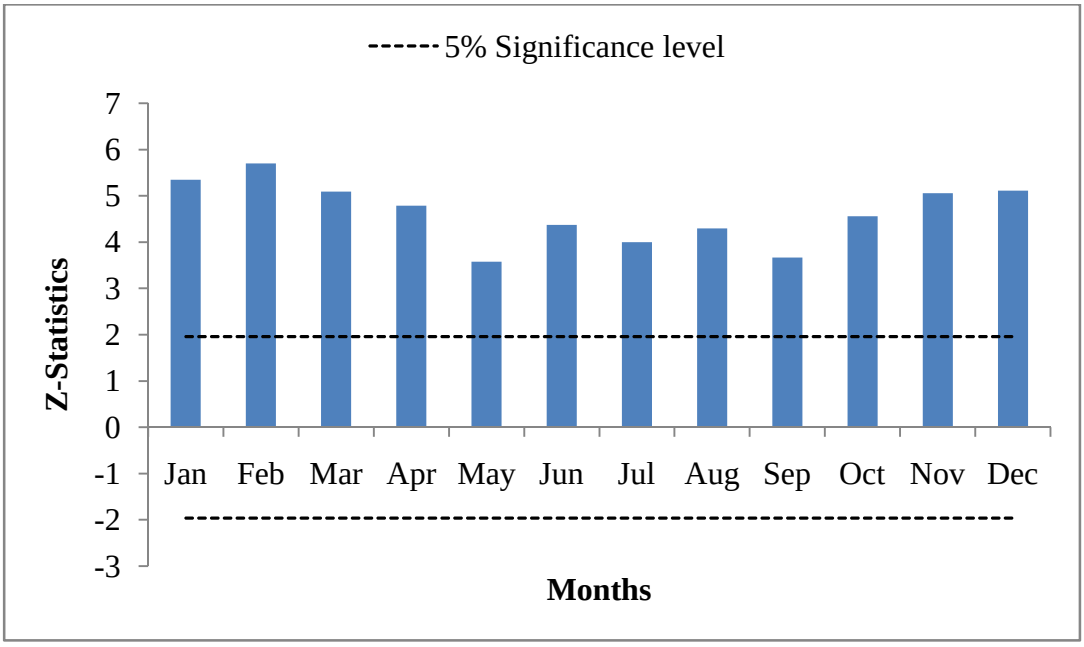

Figure 4.20 Temporal Trend of Wind Speed over 51 years in Seonath river basin

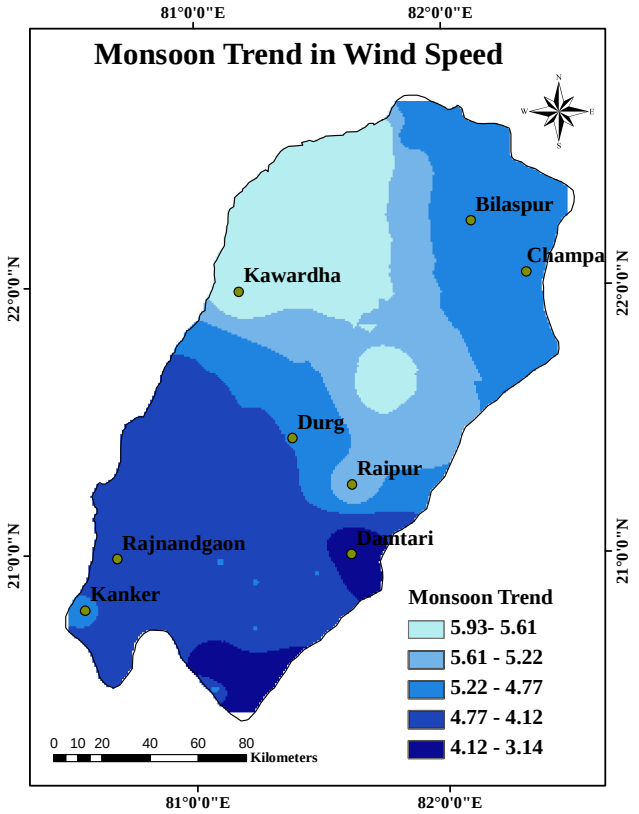

(a) Monsoon

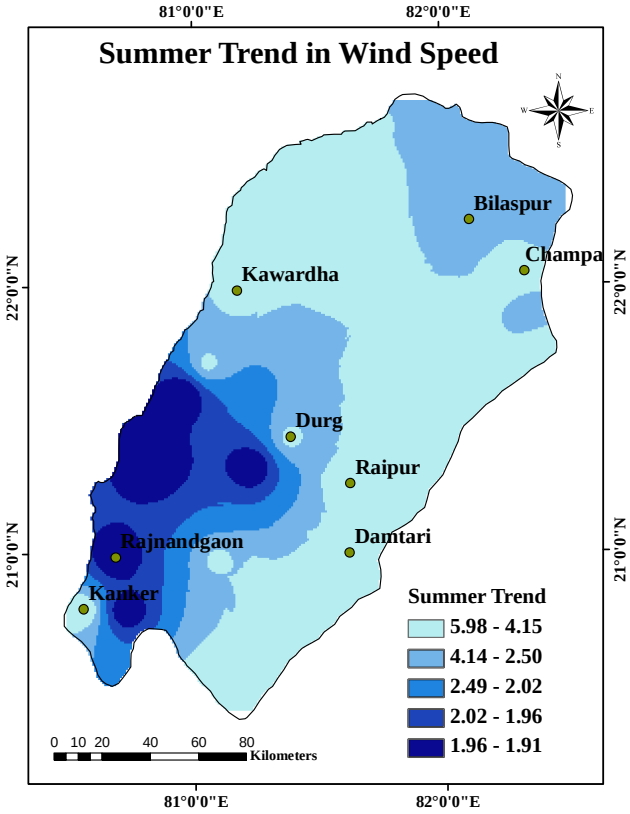

(b) Summer

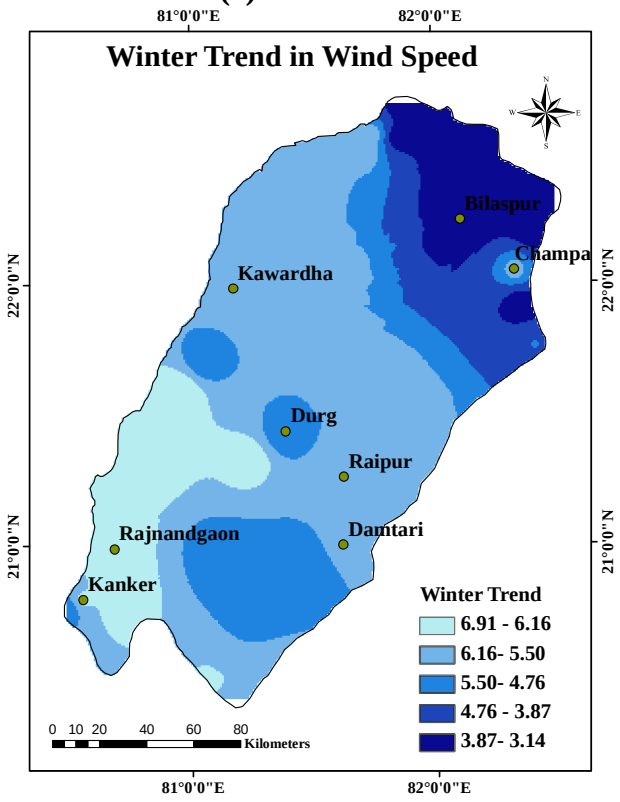

(c) Winter

Figure 4.21 Spatial trend distribution of wind speed for (a) Monsoon (b) Summer (c) Winter over entire Seonath river basin

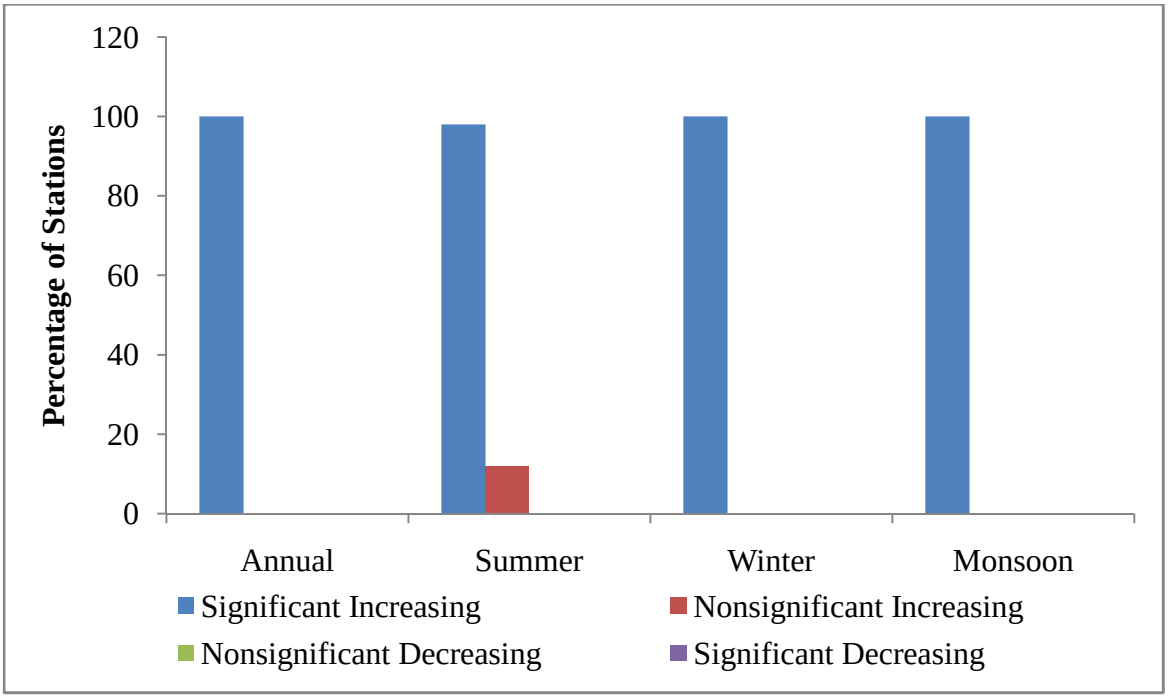

Figure 4.22 Percentage of Stations shows trends in seasonal wind speed

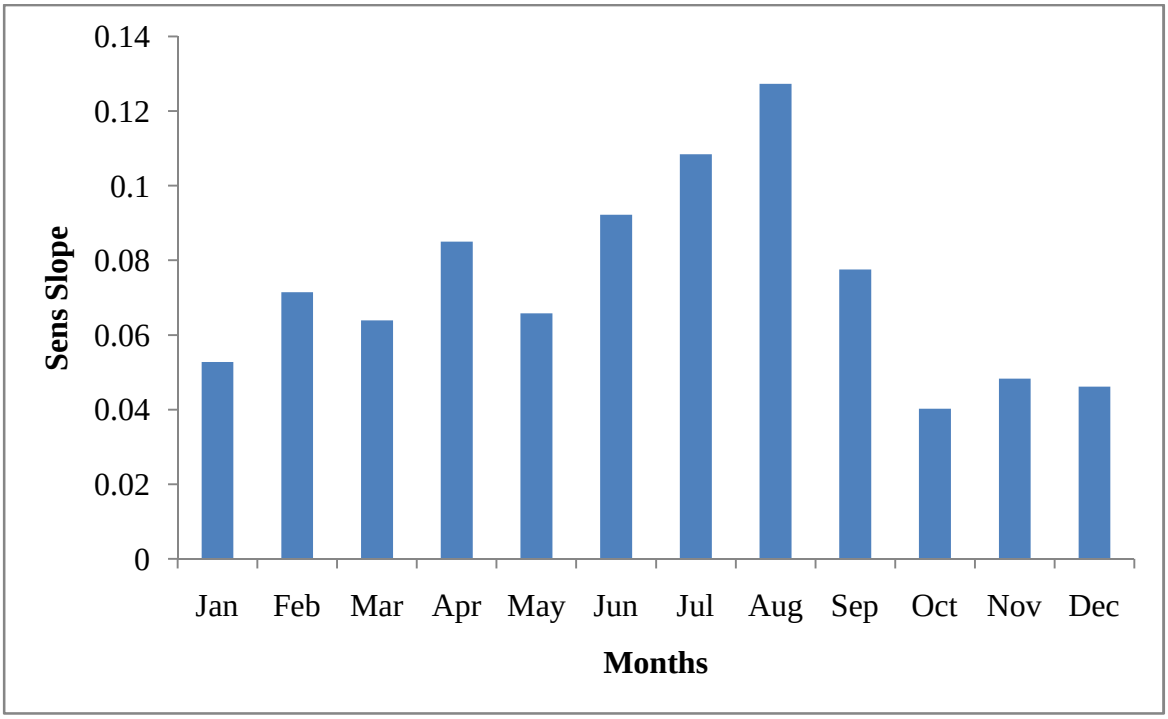

Figure 4.23 Monthly Wind Speed Trend Magnitudes over 51 years

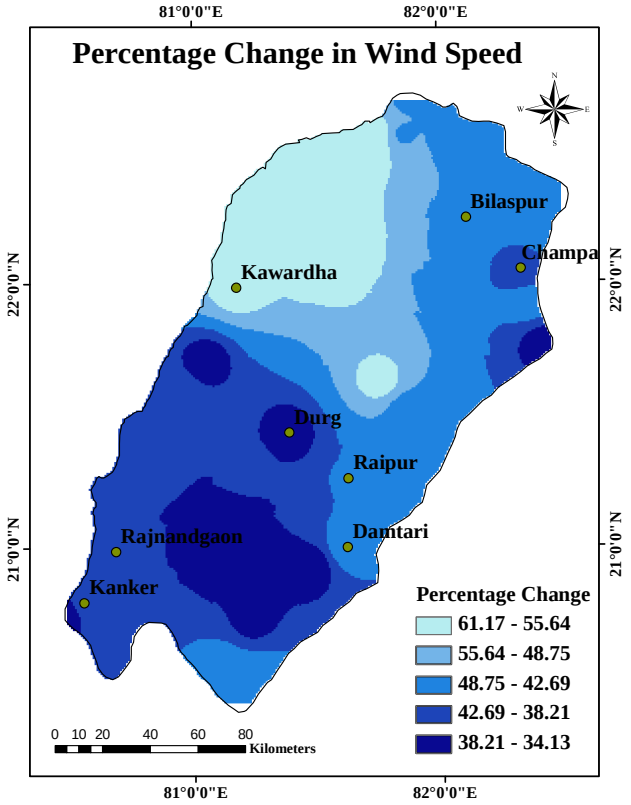

Figure 4.24 Percentage change in Wind Speed over 51 years

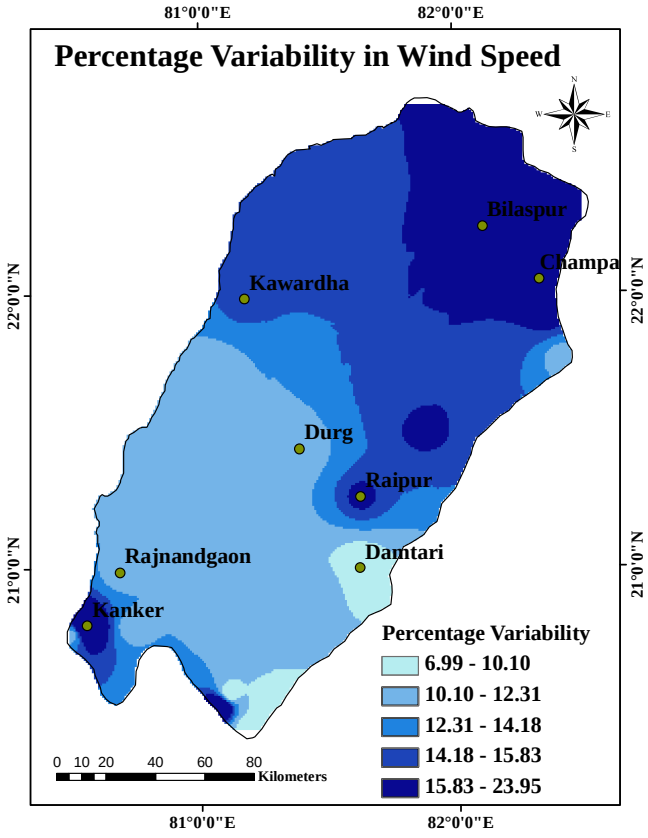

Figure 4.25 Spatial Variability of wind speed in Seonath river basin

4.5 SUMMARY

The application of trend detection techniques in meteorological variables viz., maximum, mean and minimum temperature, rainfall, wind speed and relative humidity in Seonath River Basin has resulted in the detection of long-term trends appearing in the study area during the past several decades. The direction of trends for temperature and wind speed is upward, whereas the direction of trends for rainfall and relative humidity is in general, downward.

On the basis of the analysis for temperature, rainfall, relative humidity and wind speed over the 51 year period, a few general, but important, conclusions can be drawn. First, temperature in the Seonath River Basin has increased, especially during the Monsoon and winter seasons. Second, rainfall has changed during past 51 years, and analysis of the slopes indicated decreasing trend for annual and monsoon season in the study area. Although, there have been significant decrease in relative humidity and increase in wind speed. The results of the trend and variability analysis of climatic variables may lead to develop better understanding for water resources management in the study area.

CHAPTER 5

INTER-COMPARISON OF REFERENCE EVAPOTRANSPIRATION ASSESSMENT METHODS

This chapter deals with comparative study of various methods commonly used for assessment of reference evapotranspiration (ETo). Six methods have been selected for comparison of ET estimates. Also sensitivity analysis of ETo with different meteorological variables (viz. maximum and minimum temperature, relative humidity and wind speed) has been carried out in order to identify key variable(s) having relatively greater influence on ETo. Variation in Class A pan coefficient (Kp) over different months in a year has been studied for more realistic estimation of ETo using pan evaporation data.

5.1 INTRODUCTION

The term evapotranspiration (ET) describes the total evaporation and plant transpiration from the surface to the atmosphere. It is a very important parameter in hydrological cycle and in agriculture (rainfed as well as irrigated). It plays a significant role for the assessment of irrigation water requirement (Mohan and Arumugam, 1996; Tukimat et al., 2012). Therefore, realistic assessment of ET is vital for water budgeting and planning. It has been projected that effect of climate change on water resources will be mainly due to ET. Increase in temperature will provoke higher evapotranspiration which in turn will affect the hydrological system and water resources (Shahid, 2011). Thus, reliable and accurate estimation of ET due to climate change is very important for the long-term water resources management.

There are several methods available in literature for estimation of ETo. Each method is based on certain perception, and has been developed for specific climatic conditions. However, the major concern in estimating ET is the reliability and accuracy of the methods (Burnash, 1995). As some of the methods have been developed for given purposes and for specific climate conditions, they may provide poor estimates of ET for other climatic conditions. From various studies conducted in India (Praveen et.al, 2011) it is established that, Penman-Monteith (Monteith, 1965) method provides relatively more reliable estimates over a broad climatic region. Also, the researchers have studied the accuracy and reliability of this method in other parts of the world and have reported that ETo estimated using Penman-Monteith is relatively more reliable and acceptable (Racz et al., 2013). Some of the

ET estimation methods (including Penman-Monteith method) need measurements of many meteorological variables whereas others require fewer only. Therefore, the selection of ET estimation method depends on availability of meteorological data in respect of different variables. Table 5.1 shows the meteorological variables which are required to be considered in various methods.

Table 5.1 Climatic variables involved in selected methods for ETo estimation

Methods	**T**	**RH**	**Rs**	**WS**	**n**	**P**	**Ep**
Pan Method	---	✓	---	✓	---	---	✓
Penman-Monteith	✓	✓	✓	✓	---	✓	---
Priestley-Taylor	✓	---	✓	---	---	---	---
Turc Method	✓	✓	✓	---	---	---	---
Hargreaves Method	✓	---	---	---	---	---	---
Thornthwaite Method	✓	---	---	---	---	---	---
Blaney-Criddle Method	✓	---	---	---	---	---	---

Abbreviations: T = Temperature, RH = Relative Humidity, Rs = Solar Radiation, WS = Wind Speed, n = Sunshine hours, P = Atmospheric Pressure, Ep = Pan evaporation

Pan evaporation data are widely used all over the world (Irmak et al., 2002) for the estimation of ETo using pan coefficient values. The pan evaporation (Ep) presents a measurement of the combined effect of climatic variables (i.e., air temperature, relative humidity, wind speed and solar radiation) on the evaporation. Therefore pan evaporation data may provide reliable estimates of ETo, provided realistic values of pan coefficients are used in different months.

To understand the relative role of climatic variables in accurate assessment of ETo, sensitivity analysis of ETo with different meteorological variables (viz., maximum and minimum temperature, relative humidity and wind speed) is required. ETo estimated using Penman-Monteith method is considered for the sensitivity analysis as this method provides relatively more accurate assessment of ETo and involves consideration of the measured values of maximum and minimum temperature, relative humidity and wind speed

This chapter presents comparison of performance of six widely used ETo estimation methods, viz., Hargreaves Method, Thornthwaite Method, Blaney-Criddle Method, Priestley-Taylor Method, Penman-Monteith Method and Turc Method. The performance of these ETo estimation methods have been compared with pan evapotranspiration (ETp) estimates for the corresponding period as it is one of the most reliable method for ETo estimation (Irmak et al., 2002 and Rahimikhoob, 2009).

5.2 DATA

The climatic data used in this study consisted of daily maximum and minimum temperature (Tmax and Tmin), relative humidity (RH), wind speed (WS), sunshine hours (n) for eight stations and Class A pan evaporation data for one station (Raipur). Pan Evaporation (Ep) is measured daily at 7.00 AM.

5.3 METHODOLOGY

Various methods for estimation of ETo are presented below and these methods are summarized in the form of flowchart in Figure 5.1.

5.3.1 Estimation of Pan Coefficient (Kp) and Evapotranspiration (ETp)

In this method reference evapotranspiration (ETo) is estimated by multiplying observed pan evaporation (Ep) data with a pan coefficient (Kp). A non-linear regression equation has been developed by Orang (1998) to estimate Kp for Class A pan with green vegetation surrounding condition. The developed equation performs well and accuracy is similar to Allen-Pruitt (1989) equation. The ETo computed using Kp values obtained from Orang method gives more accurate daily, monthly and annual ETo estimates compared to other empirical methods viz., Allen and Pruitt, 1991; Cuenca, 1989; and Snyder, 1992 (Rahimikhoob, 2009). Therefore, for accurate assessment of Kp values Orang method is used for our study area. The pan evapotranspiration (ETp) is obtained by following formula

$$ETp = Ep \times Kp \quad (5.1)$$

Where; ETp = Reference evapotranspiration (mm); Ep = Observed Pan evaporation data for class A pan (mm); Kp = Pan coefficient for class A pan.

Further, pan coefficient has been determined by following formula

$$Kp = 0.5126 - 0.000321U + 0.002889H + 0.031886 \ln(F) \quad (5.2)$$

Where, U = Wind speed (km/day), H= relative humidity (%) and F= upwind fetch distance around the pan. As the pan area is surrounded by dry fallow land, the value of F is taken as 50 m.

5.3.2 Penman-Monteith equation

The Penman-Monteith method is a combination method developed by Penman (1948). It combines the energy balance with mass transfer method and proposes an equation to estimate ETo on daily basis using climatic variables viz. temperature, sunshine hours, relative humidity and wind speed. It is expressed as below:

$$ETo = \frac{0.408\,\Delta(\mathrm{Rn} - \mathrm{G}) + \gamma \frac{900}{\mathrm{T}+273} \mathrm{u2}(\rho s - \rho a)}{\Delta + \gamma(1 + 0.34\mathrm{u2})} \quad (5.3)$$

where, ETo is reference evapotranspiration(mm day^{-1}); Δ is the slope vapor curve (kPa °C^{-1}); Rn is the net radiation of the crop surface (MJm^{-2} day^{-1}); G is the soil heat flux density (MJm^{-2} day$^{-1)}$; T is the air temperature at 2m height (°C); U2 is the wind speed at 2m height (m s^{-1}); ρs is the saturation vapour (kPa); ρa is the actual vapour pressure (kPa); and γ is the psychrometric constant (kPa °C^{-1}).

5.3.3 Priestley-Taylor method

Priestley-Taylor method (Priestley and Taylor, 1972) is a radiation based method to estimate reference evapotranspiration (ETo). They establish that the potential evaporation is 1.26 times lesser than the actual evaporation and thus they replace the aerodynamic terms with constant (1.26). Therefore, the method needs only long-wave radiation and temperature for the assessment of ETo. The equation for calculating ETo is given below:

$$ETo = 1.26\ \frac{\Delta}{\Delta + \gamma}\left(\mathrm{Rn} - \mathrm{G}\right)\frac{1}{\lambda} \quad (5.4)$$

where, Δ is the slope vapor curve (kPa °C^{-1}); γ is the psychrometric constant (kPa °C^{-1}); Rn is the net radiation of the crop surface (MJm^{-2} day^{-1}); G is the soil heat flux density (MJm^{-2} day^{-1}); and λ is the latent heat of vapour (MJ kg^{-1}).

5.3.4 Turc Method

Turc method (Turc, 1961) provides an easy equation for calculating ETo by using only few climatic variables (relative humidity, solar radiation and mean temperature). The

Turc method gives reliable estimates of ETo under humid conditions (Jensen et al., 1990) which is similar to our study area (Seonath river basin). The equation is given as follows:

When, RH < 50%

$$ETo = 0.0133 \frac{Tm}{Tm+15}(Rs + 50) \quad (5.5a)$$

When, RH > 50%

$$ETo = 0.0133 \frac{Tm}{Tm+15}(Rs + 50)(1 + \frac{50-RH}{70}) \quad (5.5b)$$

where, Tm is mean temperature (°C); Rs is the solar radiation of the crop surface (MJm^{-2} day^{-1}); and RH is the relative humidity (%).

5.3.5 Hargreaves Method

Hargreaves is temperature based method proposed by Hargreaves and Samani in 1982. The equation is given as:

$$ETo = 0.0023(Tmax - Tmin)0.5(Tm + 17.8)Ra \quad (5.6)$$

where, Tmax, Tmin and Tm denotes maximum, minimum and mean temperatures (°C); and Ra is the extra terrestrial radiation of the crop surface (MJm^{-2} day^{-1}).

5.3.6 Thornthwaite Method

The Thornthwaite equation is proposed by Thornthwaite (1948). It is based on the empirical correlation between changes in evapotranspiration and mean air temperature. The equation is given as follows:

$$ETo = 16\left(\frac{L}{12}\right)\left(\frac{N}{30}\right)\left(\frac{10Ta}{I}\right)^{\alpha} \quad (5.7a)$$

Where ETo is the monthly potential evapotranspiration (mm/month), Ta is the average daily temperature (°C; if this is negative, use 0) of the month being calculated, N is the number of days in the month being calculated, L is the average day length (hours) of the month being calculated. Where, I is the monthly heat index; and it is estimated by the formula given below:

$$\alpha = (0.675x10^{-7})I^3 - (7.71X10^{-5})I^2 + (1.792X10^{-2})I + 0.49239 \quad (5.7b)$$

$$I = \sum_{i=1}^{12}(T_{ai} / 5)^{1.514} \quad (5.7c)$$

5.3.7 Blaney-Criddle Method

The Blaney-Criddle is the simple temperature based method for the assessment of ET. It is widely method applied before Penman-Monteith method. This equation only considers changes in temperature for specific condition for estimating ETo. The Blaney-Criddle equation is given below:

$$ETo = p(0.46Tm + 8) \quad (5.8)$$

where, p = percentage of average daily annual day time hours due to the latitude of region; and Tm = mean temperature (°C).

5.3.8 Model Evaluation Statistics

The inter-comparison of the ETo estimation methods are estimated using the following statistical measures

5.3.8.1 Mean absolute error (MAE, Johnson et al., 2003), given as

$$MAE = 1 - \frac{\sum_{i=1}^{N}|Oi-Ei|}{\sum_{i=1}^{N}|Oi-\overline{Oi}|} \quad (5.9)$$

5.3.8.2 Root mean square error (RMSE), defined as

$$RMSE = \sqrt{\{\frac{1}{N}\sum_{i=1}^{N}(Oi - Ei)\}} \quad (5.10)$$

5.3.8.3 Sum of squares of errors (SSE), defined as

$$SSE = \sum_{i=1}^{N}(Oi - Ei)^2 \quad (5.11)$$

5.3.8.4 Coefficient of determination (R^2) is defined as the degree of collinearity between observed and predicted data. The value of R^2 lies between 0 and 1.

$$R^2 = 1 - \frac{\sum_{i=1}^{N}(Oi-Ei)^2}{\sum_{i=1}^{N}(Oi-\overline{Oi})^2} \quad (5.12)$$

5.3.9 Sensitivity Analysis

To carry out sensitivity analysis of ETo with climatic variables, partial correlation method is employed. It gives the correlation coefficient (CC) between the variable y and its factors (Wang et al., 2011). Correlation provides a measure of the strength of a linear association between a variable and its effecting parameter. Though, when the effecting parameters are strongly correlated with each other, ordinary correlation technique cannot give the accurate association between the variable and its factors (Janssen et al., 1992). The partial correlation method has been proposed by Iman and Helton (1988) to address this problem by removing the influences of other correlative factors. The partial correlation coefficient (PCC) describes a linear relationship between the variable y and its factors xj after discounting the linear effects on y of the remaining factors. The sensitivity coefficient (S) is also calculated in order to determine the response of calculated ETo to selected meteorological variables. Changes of model outputs and their variability induced by change in climatic variables (X) have been also evaluated. Mean values of climatic variables and ETo values of each model have been calculated. Then we calculate the deviation (Δ) from these means for the daily data of these variables and the ETo values, respectively. In order to reach the best comparability between the effects of changes in all climatic variables, Δ values of each variable and ETo have been converted to percentage changes. The Sensitivity Coefficient (S) has been calculated by the formula given below:

$$S = \frac{\Delta ETo}{\Delta X} \times \frac{X}{ETo} \tag{5.13}$$

Where, ΔX is the relative change of model input value X and ΔETo is the relative change in ETo induced by ΔX. The coefficient of S represents changes in ETo induced by changing meteorological variable (X). If S is 0.4, then a 10 % increase of X would cause a 4 % increase in ETo, while other climatic variables are remain unchanged.

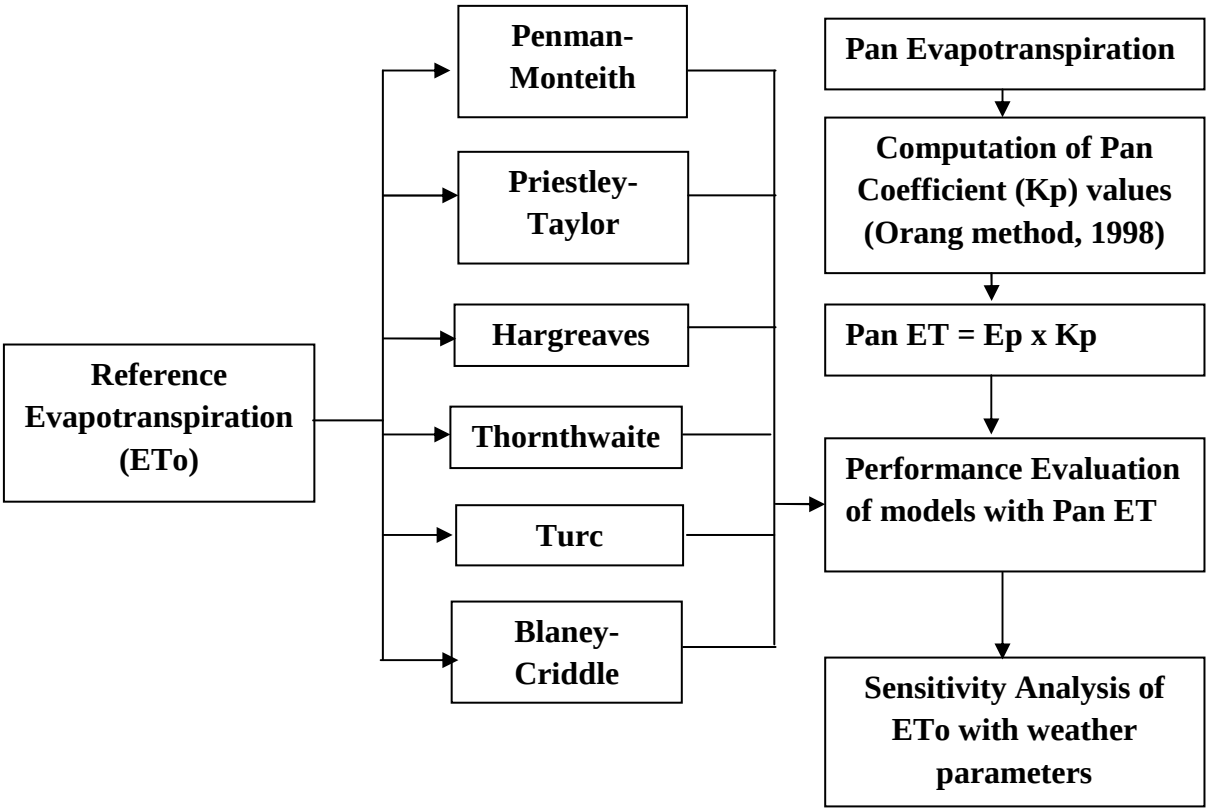

Figure 5.1 Flowchart describing methodology for the present study

5.4 RESULTS

5.4.1 Estimation of Pan Coefficient (Kp)

The ETo computed using Kp values obtained from Orang method. As this method of Kp estimation gives more precise estimates of ETo compared to other empirical methods viz., Allen and Pruitt, 1991; Cuenca, 1989; and Snyder, 1992 (Rahimikhoob, 2009). A non-linear regression equation has been developed by Orang (1998) to estimate Kp for Class A pan with green vegetation surrounding condition. Therefore, pan coefficient values for the study area have been estimated using Orang method. The study shows that the monthly Kp values vary significantly from month to month (0.56 to 0.89) for the study area (Figure 5.2). The highest Kp value is obtained for the month of July whereas it is lowest for the month of November. The estimated monthly pan coefficient values for the study area are considered to be more appropriate than the Kp values (0.60-0.80) for Class A pan mentioned in FAO-24 document (Doorenbos and Pruitt, 1977). The pan coefficient values differ by -6% to 21% when compared with FAO-24 tabulated Kp values.

The estimates of ETo using tabulated FAO-24 Kp values and those using Orang method based Kp values are plotted in Figure 5.3. Use of the FAO recommended values of Kp result in over estimation of the monthly ETo values by 11.8% to 56.3% (Figure 5.3).

The Kp values given in FAO-24 are based on general climatic conditions. Thus for accurate estimation of ETo from pan evaporation data, the estimated Kp values considering local climatic conditions should used for the study area.

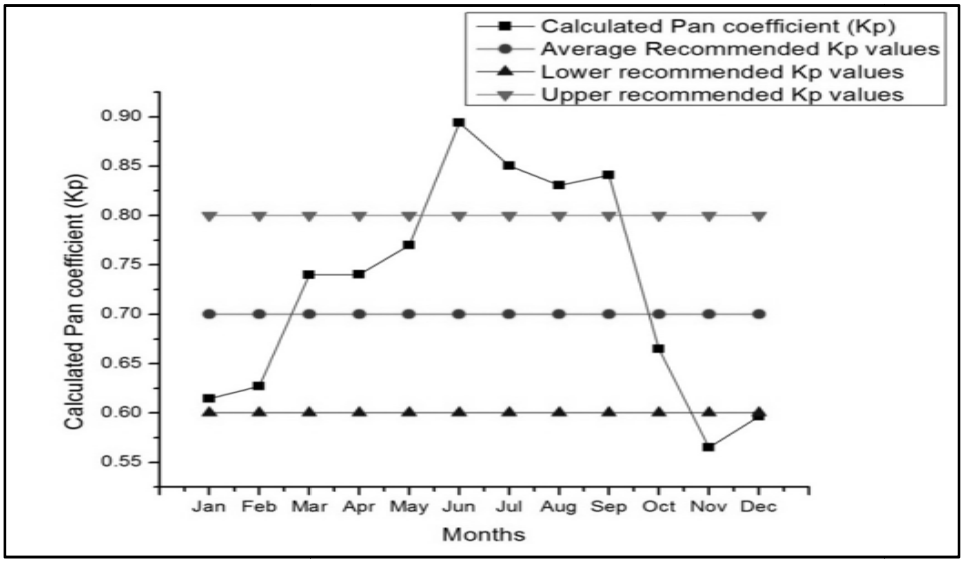

Figure 5.2 Monthly variation of pan coefficients

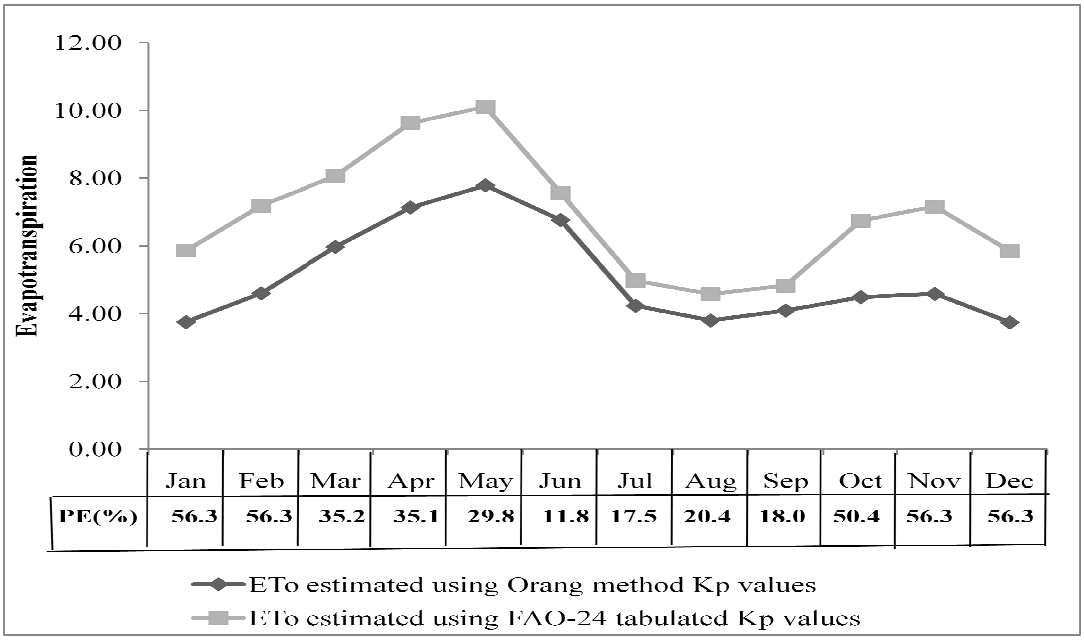

Figure 5.3 Monthly variation of ETo using recommended and estimated Kp values

5.4.2 Comparison of ETo Methods

To measure the consistency and accuracy of ETo methods, the estimates obtained from different methods have been compared with pan evapotranspiration values (ETp). Performance evaluation of ETo methods has been done using four statistical parameters viz., Mean absolute error, Root mean square error, Sum of Square Error (SSE) and coefficient of determination (R^2). Figure 5.4 shows the monthly average reference evapotranspiration values using different methods for the study area. Almost all the methods show the same trend throughout the year. The Penman-Monteith estimates the higher reference evapotranspiration in all the months followed by Hargreaves and Thronthwaite method. Figure 5.5 shows the mean daily reference evapotranspiration and annual evapotranspiration values estimated by different methods for the study area. The annual reference evapotranspiration values reveal the similar prototype. The Penman-Monteith method based ETo values are close to pan evapotranspiration (ETp) values. Whereas the estimates of ETo using Preistly-Tyalor and Blaney-Criddle methods give relatively lower values than pan evapotranspiration values (Figure 5.5). The estimates indicate that the values of ETo in the Seonath River Basin range from 1330.43 mm/year to 1819.33 mm/year. Among the six methods, the Penman-Monteith, Hargreaves, Thornthwaite and Turc, methods illustrate high correlation with reasonable errors (Table 5.2). However, Penman-Monteith method is found to be suitable for estimating ETo in the study area as it gave the closest estimate followed by Hargreaves, Thornthwaite and Turc methods. Penman-Monteith method showed the highest correlation and fewer errors among all the methods used in the present study. Thus estimates of evapotranspiration obtained using Penman-Monteith method are considered more accurate and reliable. If the records of relative humidity and wind speed are not available then Hargreaves and Thornthwaite models can be applied because the capability of both the methods in estimating ETo is more or less similar for the study area. These is in agreement with the results of the study by Toriman et al. (2009) for North Kedah, Malaysia indicated that the Thornthwaite method provides reasonable estimates of ETo in absence of relative humidity and wind speed data. Thus, from Table 5.2, it can be seen that the pan evapotranspiration values show reasonable correlation coefficient with Penman-Monteith, Hargreaves, Thornthwaite and Turc methods indicating that the estimates are reliable. Therefore, considering the pan evapotranspiration (ETp) values, the Penman-Monteith, Hargreaves and Thornthwaite methods performed well with low value of RMSE, MAE, SSE and high correlation coefficient. Further, the analysis

revealed that the estimates of ETo obtained using Blaney-Criddle and Priestly-Taylor methods are comparatively poor. Further to study the impact of key climatic variables in calculation of ETo, sensitivity analysis is required.

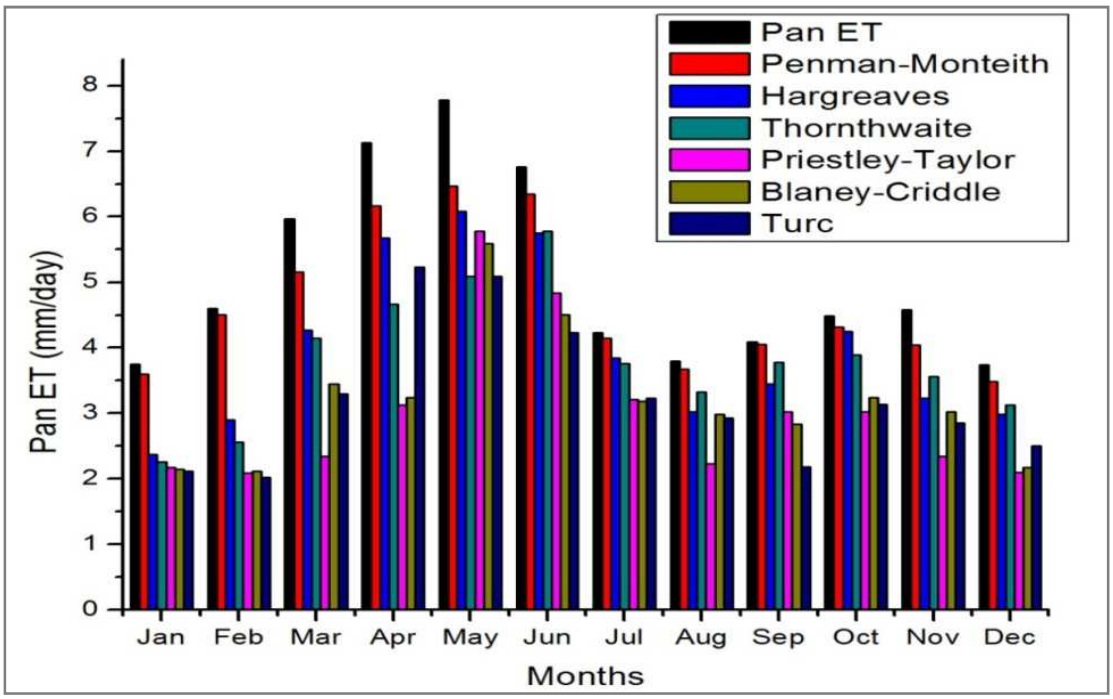

Figure 5.4 Monthly average reference evapotranspiration (ETo) for the study area

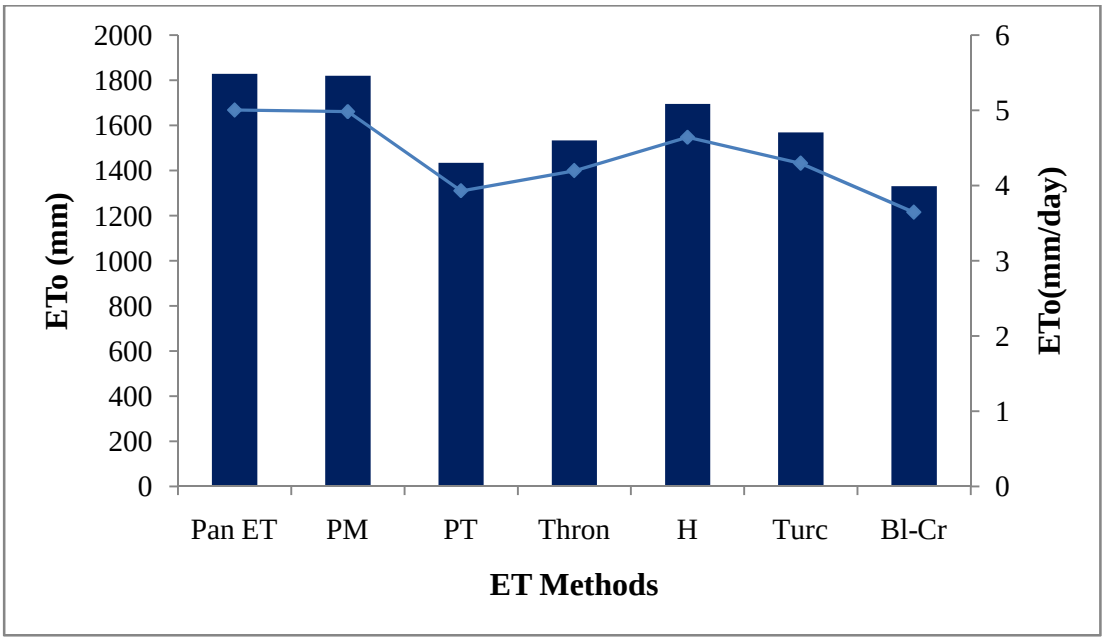

Figure 5.5 Mean and Annual Reference Evapotranspiration for Seonath basin

Abbreviations

P= Pan evaporation method; PM= Penman- Monteith method; H= Hargreaves method; PT= Priestley Taylor method; Bl-Cr= Blanney-criddle method; Turc= Turc Method; Thron=Throntwaite Method

Table 5.2 Errors and correlation between Pan ET and other ET models for Seonath basin

Methods	R^2	RMSE	MAE	SSE
PM	0.962	0.803	0.647	0.659
H	0.878	1.194	1.077	1.137
PT	0.614	1.228	0.932	0.985
Bl-Cr	0.406	1.237	0.981	0.159
Turc	0.776	1.062	0.750	0.922
Thron	0.857	1.393	1.362	1.279

5.4.3 Sensitivity to Climatic Parameters

The partial correlation method is employed to investigate the correlation between ETo and major meteorological variables (Maximum and Minimum Temperature, Relative Humidity and Wind Speed) in the Seonath River Basin. Table 5.3 provides a summary of the correlations between ETo and major meteorological variables on annual and seasonal scales in the Seonath river basin. The negative and positive partial correlation coefficients indicate that positive and negative relationships exist between ETo and the meteorological variables. The larger the values of coefficient, the stronger correlations exist between ETo and the meteorological variables, and the larger the influence of the corresponding meteorological variable on ETo. In the Seonath river basin maximum temperature is dominating factor in estimation of ETo at seasonal and annual scales. As temperature increases, ETo also increases due to low humidity in the atmosphere, large amount of water would be lost from the surface and from plant cells or tissues. Relative Humidity followed by wind speed is another important driving variable for ETo during the year and in all the seasons (Table 5.3). The overall result indicates that the temperature has major effect on ETo and it is least effected by rainfall. Figure 5.6 represents the results of sensitivity analysis of monthly ETo with key climatic variables. The analysis shows that the maximum temperature has maximum effect on the estimation of ETo followed by relative humidity and wind speed. The minimum temperature is found least significant compared to above

variables. On monthly time scale, sensitivity coefficient (S) shows large variation during a year for all the months. The similar results have also been reported by Hupet and Vanclooster, 2001; Gong et al., 2006 and Liqiao et al., 2008. The maximum temperature has the highest sensitivity coefficient (S) during August followed by September and July. The similar patterns of sensitivity coefficients for relative humidity, wind speed and minimum temperature have also been obtained. On annual scale, the spatial distribution of sensitivity coefficients for key climatic variables has been presented in Figure 5.7. The sensitivity of ETo to maximum temperature is highest with S of 1.77 for Bilaspur station which indicate that ETo would increase by 17.7 % in response to the 10 % rise in maximum temperature if other meteorological variables remain constant. Similarly, the sensitivity of ETo to maximum temperature is notably highest for all the stations the value ranges from 1.54 to 1.77 (Figure 5.7). However the next variable which effects ETo the most is relative humidity (RH). The value of S is highest for Rajnandgaon station (-1.28) which means 10% decrease in RH causes ETo to increase by 12.8%. Therefore omission of relative humidity and wind speed (eg. Temperature based methods) in empirical formulae can thus be important reason of uncertainty in ETo estimation. From the previous section Penman-Monteith is best suited method for our study area followed by Hargreaves and Thronthwaite methods. But from the results of sensitivity analysis the ETo is sensitive to relative humidity and wind speed also. Therefore, it is recommended not use these two methods as they donot taken into consideration the relative humidity and wind speed parameters for ETo calculation.

Table 5.3 Correlation Analysis of ETo with Meteorological Variables (Temperature, Rainfall, Relative Humidity and Wind Speed) in Seonath River Basin

Parameters	**Annual**	**Monsoon**	**Winter**	**Summer**
Temperature (Max,°C)	**0.9501**	**0.9373**	**0.9839**	**0.7141**
Temperature (Min,°C)	**0.5874**	**0.6289**	**0.8121**	**0.6438**
Rainfall (mm)	0.1086	0.0816	-0.0501	-0.0353
Relative Humidity (%)	**-0.8117**	**-0.8169**	**-0.8916**	**-0.7303**
Wind Speed (km/hr)	**0.7324**	**0.7298**	**0.7015**	**0.7346**

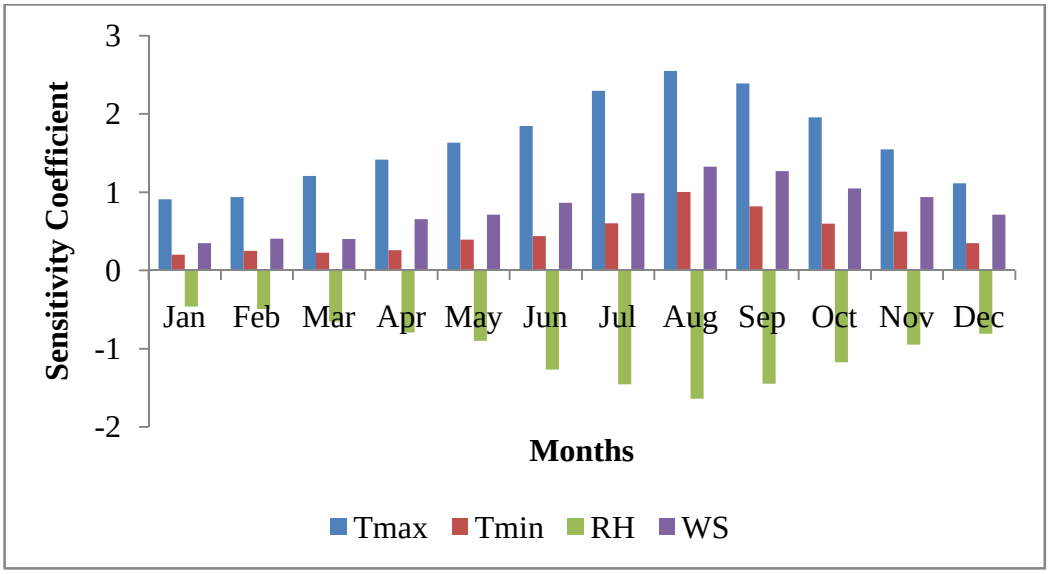

Figure 5.6 Mean monthly sensitivity coefficients for each climate variable in Seonath Basin

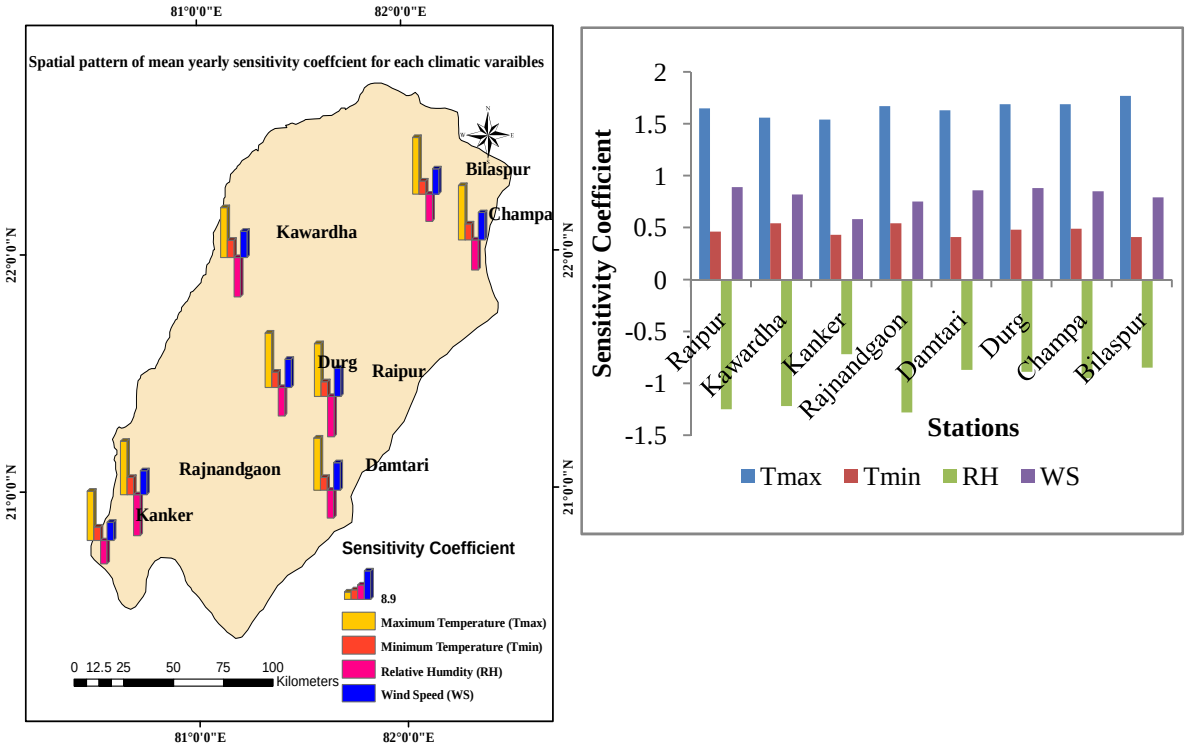

Figure 5.7 Average yearly sensitivity (a) Spatial pattern of % change in ETo with 10% rise in climatic variables (b) Sensitivity coefficient for each climatic variable in Seonath River Basin

5.5 SUMMARY

The complexity and inaccuracies in ETo estimation often appear as major constraints in developing effective water management strategies for maintaining crop water requirement. Therefore in the present study, six ETo estimation methods have been compared with pan evapotranspiration (ETp) values to show the reliability of different ETo estimation methods. The analysis revealed that there are significant variation in the ET estimates obtained using different methods. The Penman-Monteith method is found to be suitable for estimating ETo in the study area as it gave the closest estimate with ETp followed by Hargreaves, Thornthwaite and Turc methods.

The monthly Kp values have also been estimated for the study area. The Kp values vary from -6% to 21% when compared with the average values of Kp values given in the FAO-24 table for Class A pan. Thus for accurate assessment of ETo using observed pan evaporation (Ep) data the computed Kp values for the study area have been used.

The analysis indicates that the estimation ETo is sensitive to maximum temperature followed by relative humidity and wind speed. The estimates of ETo are found least sensitive to minimum temperature in Seonath river basin. Therefore Hargreaves and Thornthwaite methods may not be reliable for estimation of ETo for the study area though they have good correlation values with pan evapotranspiration (ETp) values. The present study is considered to be useful in selection of method for estimation of ETo according to the desired accuracy of estimated ETo for specific purpose and availability of observed meteorological data.

Keeping in the view of research objectives, the next chapter deals with study of Crop Water Requirement (CWR) and Irrigation Water Requirement (IWR) for major crops in Kharif and Rabi seasons in Seonath basin and analysis of trends in ETo and IWR.

CHAPTER 6

LONG TERM TREND ANALYSIS TO DETECT CHANGE IN IRRIGATION WATER REQUIREMENT (IWR)

Surface irrigation schemes comprise of i) surface storage and/or diversion structures, ii) irrigation water distribution, iii) drainage network, iv) on farm development works etc. These schemes involve huge investment of capital and other resources. Irrigation schemes are planned to serve the purpose of providing adequate, timely and reliable water supply for the crops to meet their irrigation water requirement over the life of project (usually 50 to 100 years). Irrigation water requirements of crops are based on average fortnightly or monthly climatic data. Over the year variability is not considered in the irrigation schemes and also, it is assumed that irrigation water requirements shall be same over the years.

Planning horizon of such schemes typically range from 50 years to 100 years during this period change may occur in the regional climate and therefore irrigation water requirements may also change. On supply side, water availability for irrigation may also be adversely affected.

This Chapter presents the study of long term trends in Irrigation Water Requirement (IWR) of Seonath River Basin. The chapter is divided into two sections. First section presents estimation of reference evapotranspiration (ETo), crop coefficient, crop water requirement (CWR) and irrigation water requirement (IWR) and the second section focuses on the long term trend and variability analysis of ETo and IWR.

6.1 INTRODUCTION

Water resources management plays a key role in stable agriculture and sustainable environment. Reliable assessment of evapotranspiration is important for managing the water resources efficiently in agriculture. Evapotranspiration is a key climatic factor for proper irrigation scheduling and appropriate water allocation for various uses (Al-Ghobari, 2000; George et al., 2002; Dinpashoh, 2006). ETo is a function of climatic variables thus, it may be affected by changes in climatic variables. Several region specific studies have been conducted in various parts of the world to determine trends and variability of meteorological variables.

In Chhattisgarh State of India, 80% of the population depends on agriculture for livelihood. Crop production in the region is often adversely affected due to randomness in spatial distribution and magnitude of rainfall, and hence in water availability for crops. Due to changes in pattern of rainfall and evapotranspiration (ET), the paddy cultivation in the basin comes under water stress from time to time which ultimately affects the crop yield. Therefore, understanding ETo dynamics will be critical for managing local water resources and food security issues. Hence, assessment of irrigation water requirement (IWR) at the micro-regional level and its impact on agriculture is necessary for developing strategies for mitigation of water stress in the basin. Keeping this in view, an analysis is carried out to determine the long-term changes, in ETo and IWR due to changes in climatic variables.

6.2 METHODOLOGY

6.2.1 Estimation of ETo

The Penman-Monteith (PM, 1965) method suggested by FAO is one of the widely used methods for determining ETo (Tabari et al., 2011; Wang et al., 2011). From the discussion presented in previous Chapter (Chapter 5) it has emerged that the Penman-Monteith method is most suited for our study area. Further, this method has added advantage of being physically based and explicitly incorporates both physiological and aerodynamic parameters (Xu et al., 2006). The ETo has been estimated using records of meteorological variables for eight stations viz, Bilaspur, Rajnandgaon, Korba, Durg, Raipur, Kanker, Dhamtari and Jhanjgir-Champa. The long term data for the period from 1960 to 2010 has been used to estimate ETo.

6.2.2 Determination of CWR/IWR

IWR is the amount of water stored as soil moisture which is essential consumptively for crop production (USDA, 1970). It is estimated by subtracting the quantity of water available to the crop through rainfall, i.e. rainfed irrigation, from the crop evapotranspiration. Thus, IWR includes assessment of reference evapotranspiration (ETo), crop water requirement (CWR), and effective precipitation. CWR is an empirical estimate of the total quantity of water required for a crop growth in an area under known climatic conditions so that crop production is not limited by lack of water. CWR is calculated using ETo and a crop coefficient (Kc), as follows (USDA, 1993; Doorenbos and Pruitt, 1977):

$$CWR = Kc \times ETo \quad (6.1)$$

Where, CWR = rate of crop evapotranspiration in mm, Kc = crop coefficient relating actual crop evapotranspiration, ETo = reference evapotranspiration for reference crop in mm. Kc is a factor that relates ETo to CWR. Here, the growing season for a particular crop is divided into four stages and crop coefficients are determined at defined increments throughout the growing stage.

The crop coefficient (Kc) is defined as the ratio of the crop evapotranspiration to the reference evapotranspiration when the soil surface is dry but transpiration is occurring at a potential rate, i.e. water is not limiting transpiration (Allen, 2000). Therefore, Kc represents primarily the transpiration component of the crop evapotranspiration (ETc). The Kc given in FAO-56 include only single values for each stage i.e., Kc mid and Kc end. The Kc values associated with a standard sub-humid climate consider the minimum average daytime relative humidity (RH_{min}) of 45% and wind speed ranges from 1–3 m/s and average value of 2 m/s. In FAO-56, Table No. 12 Kc values of about 80 crops are listed. FAO-56 table No. 12 represents the recommended values. For the region where average minimum relative humidity is different from 45% and wind speed is different from 2.0 m/s, the Kc values given in FAO-56 for mid season and late season values must be adjusted according to the local climatic conditions. The Kc values for the mid-season and late season stages are adjusted using the following equation:

$$Kc_{mid} = Kc_{recommended} + [0.04(U_2 - 2) - 0.04(RHmin - 45)]\left(\frac{h}{3}\right)^{0.3} \quad (6.2)$$

Where, $Kc_{recommended}$ is the recommended Kc value by FAO-56 (Allen et al., 1998), U_2 the wind speed at 2 m height (m/s), RH_{min} the minimum relative humidity, and h the mean height of crop during the mid-season or late season stage (m). After adjustment, the daily Kc value is determined by assuming Kc to be constant during the initial and mid-season stages and assuming linear relationship between the Kc value at the end of the previous stage (Kc, prev) and the Kc value at the beginning of the next stage (Kc, next) during the crop development and late season stages. The daily Kc values during the crop development and late season stages could be calculated as:

$$Kci = Kc_{prev} + [\frac{i-\sum(L_{prev})}{L_{stage}}](Kc_{next} - Kc_{prev}) \quad (6.3)$$

Where, i is the day number within the growing season (1, 2, 3 ... length of the growing season), Kci the crop coefficient on day i, L_{stage} the length of the stage under consideration (days), and (Lprev) the sum of the lengths of all previous stages (days).

Effective Precipitation (Pe) is the amount of precipitation that is available to meet the evapotranspiration requirements of crops and it is estimated as (USDA, 1970):

$Pe = R / 125 * (125 - 0.2 * R)$ (R < 250 mm) (6.4a)

$Pe = 125 + 0.1 * R$ (R> 250 mm) (6.4b)

Where, Pe = monthly effective precipitation during the crop duration in mm and R = monthly precipitation in mm. IWR is computed as follows (USDA, 1970). The effective rainfall for crop growing period (Pe) has been estimated on pro rata basis.

$IWR = CWR – Pe$ (6.5)

Where, Pe = Total effective rainfall for a growing period for a given crop, in mm.

6.2.3 Statistical Test for Trend and Variability Analysis

The non parametric Mann-Kendall test is used to detect the trend and Theil–Sen's Slope Estimator is used to estimate the trend magnitude. The variability in climatic parameters has been detected by statistical measure named coefficient of variation (CV). The detailed procedure and formulae of above mentioned statistical methods are described in Chapter 4. The procedure of the present study has been summarized in flowchart given in Figure 6.1.

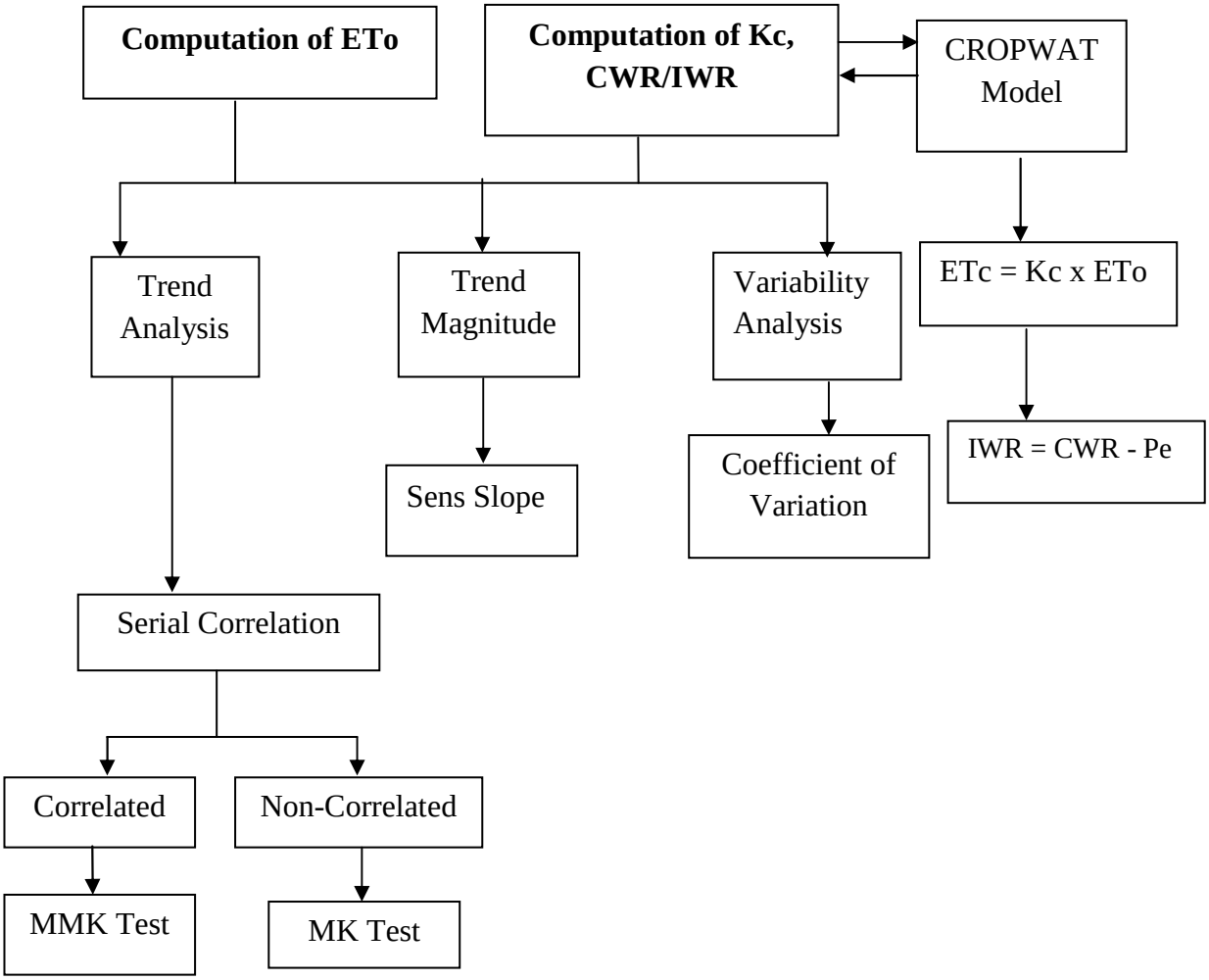

Figure 6.1 Flowchart represent methodology of the study

6.3 RESULTS

6.3.1 Computation of ETo, Kc, CWR, IWR

The ETo has been computed with the Penman-Monteith (PM) method using the CROPWAT 8.0 software employing daily temperature (maximum and minimum values), solar radiation, wind speed and relative humidity (RH) data of eight meteorological stations located over the Seonath River Basin. Table 6.1 describes the statistics of hydro-meteorological variables.

Daily data series of meteorological variables during cropping period have been used to compute CWR. The major part of the basin is covered by agriculture (76%), it can be described as an agricultural basin figure depicted in Chapter 3. The major crops of the

basin are Paddy in Kharif season and wheat and summer paddy in Rabi season as shown in Figure 3.2 in Chapter 3. CWR is computed for each stage of crop growth period, and then summed up to compute total crop water requirement for major Paddy crop of Kharif season. Similarly, CWR for wheat and summer paddy of Rabi season have been estimated for the period from 1960-2010. The effective rainfall (Pe) in the study basin has been computed for all the eight stations using Eq. 6.4a and b. Finally, the IWR is computed for both the seasons separately as a difference of CWR and Pe (IWR= CWR-Pe). Monthly rainfall, ETo and estimates of effective rainfall and details of various growth stages of major Kharif and Rabi season crops are presented in Table 6.2.

In order to estimate CWR, the crop characteristics need to be considered. The crop characteristics are represented in the form of crop coefficient (Kc). The Kc is different for different growth stages i.e. the initial stage, development stage, midseason stage, and the late season stage. The average Kc values for paddy, wheat, summer paddy have been estimated for different growth stages and compared with typical ranges of Kc values reported by the FAO-56 under the standard conditions (Doorenbos and Kassam, 1979). The Kc values suggested in FAO document (Paper No. 56, Table No. 12) for paddy, wheat and summer paddy are 1.10, 1.20 and1.05; 0.3, 1.15, and 0.3; 0.50, 1.05 and 0.70 for the initial, mid-season, and late season stages, respectively. The above Kc values have been adjusted using Eq. 6.2 for the climatic conditions of the study area. After adjustment, the Kc values of Kharif paddy, wheat and summer paddy in the initial, midseason, and late season stages are used to determine daily Kc values. The daily Kc values are determined using Eq. 6.3, and the crop coefficient curve could then be drawn as given in Figure 6.2.

Figure 6.2 presents the average Kc values for different crops compared with FAO-56 recommended Kc values. For Kharif paddy, Kc value for different crop growth stages differs by -1% to -15% with respect to FAO recommended Kc values whereas for Wheat and Summer paddy (rabi crops) difference ranges from -2% to -16% and -9% to -23% respectively with respect to FAO recommended Kc values (Table 6.3). In case of Kharif paddy, the Kc value considerably differs from FAO recommended Kc value for initial stage only. The value of Kc_{ini} is affected by the evaporating power of atmosphere, magnitude of wetting event and time interval between wetting event. The wide variation in Kc values during initial stage of Kharif paddy is due to the fact that during this period (i.e., 15th June to 10th July) decreasing evapotranspiration rate for the entire basin (discussed in Chapter 4) cause lower value of Kc_{ini} than the FAO recommended Kc values. During this period

decrease in evapotranspiration is observed for the entire Seonath basin due to low temperature and low wind speed magnitude and increase in relative humidity (Table 6.1) compared to FAO standard climatic condition. The estimated values of crop coefficients for rabi wheat and summer paddy at developmental stage differ significantly from those suggested by FAO. These differences can be attributed to factors such as higher temperature, lower relative humidity, different cultivars, and increased soil evaporation (FAO-56). Also the Kc values for rabi wheat and summer paddy during crop developmental stage are lower than the FAO Kc values, because the actual field conditions are drier than the standard conditions referred in FAO document. The actual field conditions (Seonath river basin) are drier due to rise in winter temperature, decrease in relative humidity and in turn increase in evapotranspiration of the basin. Thus, the dry condition during this stage corresponds to the decrease in Kc value.

The adjusted Kc values are lower than those suggested by FAO-56 for each crop during the different crop growth stages. This is mainly due to humid climate of Seonath river basin and lower mean wind speed (1.7-1.0 m/s) and higher mean minimum relative humidity (79-41%) during Kharif and rabi season. Therefore, it is recommended to use adjusted Kc values for accurate estimation crop water requirement.

6.3.2 Implication for Irrigation Planning

The CWR estimated using FAO recommended Kc values are significantly higher as compared to CWR estimated by region specific Kc values (Figure 6.3). This overestimation of CWR implies lower irrigation area compared to the area which can be realistically brought under irrigation. For eg. if 650 mm of CWR which is estimated using FAO recommended Kc values irrigates 1 ha of rice field. However with the same depth of CWR (650 mm) more area would be under irrigation and increase in aggregate returns if CWR is estimated using site specific Kc values. Therefore region specific Kc values play an important role for better use of existing irrigation facilities and economic planning and management of any irrigation project.

6.3.3 Effect of Climate Change on Kc Values

Since Kc value can vary significantly with the change in meteorological variables therefore estimates of Kc values under climate change scenario have been determined for the study area. The Kc values for three crops viz., Kharif rice, rabi wheat and summer paddy

have been calculated for future period of 2011-2100 (Figure 6.4). As seen in Figure 6.4 a, b and c, the Kc values for future period are close to FAO recommended Kc values. The future Kc values are relatively higher when compared with present estimated Kc values. This is because increase in precipitation in the future scenario would cause increase in wetness condition of soil surface (Figure 6.5). Therefore for future years, FAO-56 recommended Kc values are well suited for the study area.

Figure 6.6 depicts the monthly variation of average rainfall and evapotranspiration (ETo) in the basin. In this Figure, ETo is seen to be higher than rainfall during January to June and during October to December, indicating water requirements for irrigation, that is, IWR, during these periods. However, during the remaining period (i.e., from the beginning of July to September) the monthly rainfall is more than ETo and therefore, IWR may be low or negligible during this period, or it may be needed for prolonged dry spells during monsoon season, if any.

Table 6.1 Statistic of (seasonal) meteorological variables used for the computation of ETo, CWR, IWR

Meteorological Variables/Parameters	Kharif Season (Late June to October)					Rabi Season (November to April)				
	Max	Min	Average	SD	Skew	Max	Min	Mean	SD	Skew
Rainfall (mm)	1303.6	599.67	879.93	168.42	0.64	184.53	11.16	79.64	42.6	0.23
Minimum Relative Humidity (%)	72.97	69.01	71.44	0.84	-0.82	50.51	48.05	49.28	0.62	-0.13
Temp (Max, °C)	33.05	31.20	32.18	0.46	-0.10	31.73	29.76	30.69	0.47	-0.13
Temp (Min, °C)	24.34	22.57	23.34	0.38	0.35	16.81	15.03	16.06	0.46	-0.14
Sunshine (hrs)	9.50	0.30	5.25	3.03	0.11	10.10	4.50	8.73	1.26	-1.81
Wind Speed (km/hr)	16.40	1.33	6.14	2.09	0.51	25.07	0.78	3.59	3.45	5.95
Effective Rainfall(mm)	693.56	395.84	547.75	61.94	0.12	174.59	11.08	75.96	40.6	0.18

Table 6.2 Average monthly values of rainfall, Pe and ETo for the computation of CWR/IWR

Months	Rainfall (mm)	Effective Rainfall (Pe, mm)	Reference Evapotranspiration (ETo, mm)	Cropping Season
June	175.509	114.772	202.777	Kharif Season (Mid June-Oct)
July	268.483	141.227	131.125	
August	255.545	137.429	117.659	
September	139.842	97.766	121.764	
October	43.123	36.779	138.993	
November	10.008	9.182	121.302	Rabi Season (Nov-Mid Apr)
December	8.939	8.271	108.062	
January	12.791	11.814	111.575	
February	13.809	12.787	126.117	
March	16.560	15.223	184.881	
April	19.191	17.697	213.835	Non Cropping season (Mid Apr-May)
May	35.556	31.633	241.238	

Table 6.3 Percentage change in computed Average crop coefficient (Kc) values with FAO recommended Kc values at different growth stages of major crops in Seonath River Basin.

Major Crops of Seonath Basin	Percentage change in Computed Kc value and FAO Kc values			
	Percentage Change in Kc_{ini} compared with Kc_{recom}	Percentage Change in Kc_{dev} compared with Kc_{recom}	Percentage Change in Kc_{mid} compared with Kc_{recom}	Percentage Change in Kc_{end} compared with Kc_{recom}
Paddy	**-15.25**	-2.30	-4.80	-1.31
Wheat	-2.43	**-16.31**	-3.39	-3.42
Summer Paddy	-9.38	**-23.22**	**-15.25**	**-15.47**

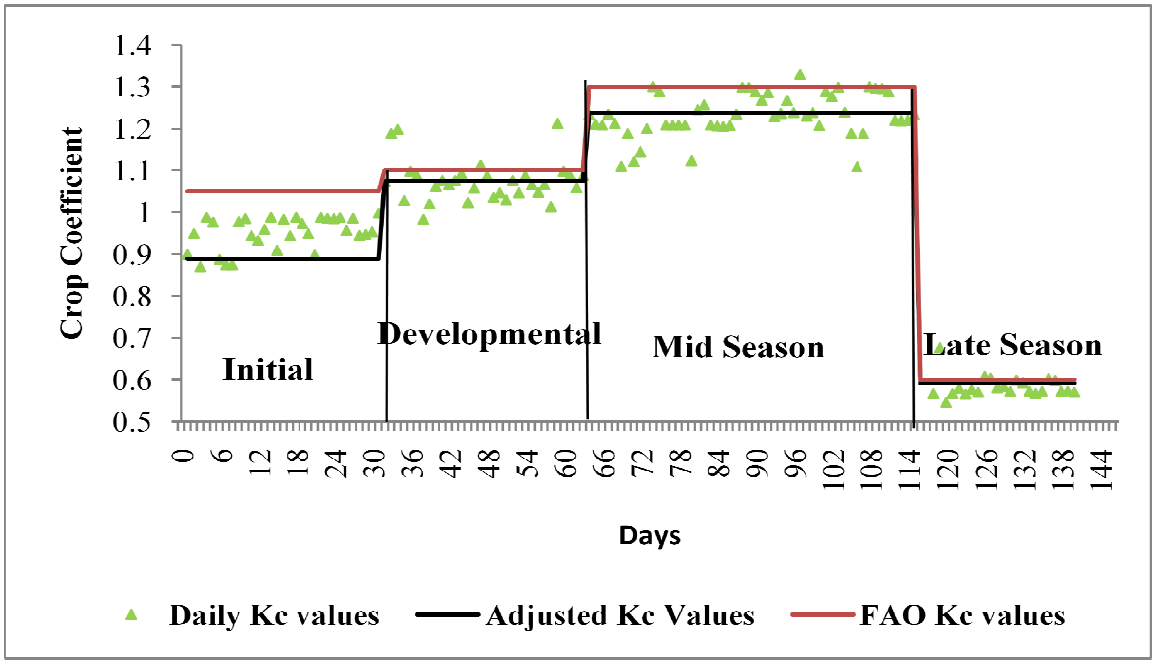

Figure 6.2(a) Crop coefficient (Kc) curve for Rice using growth stage lengths of 31, 32, 52, and 25 days

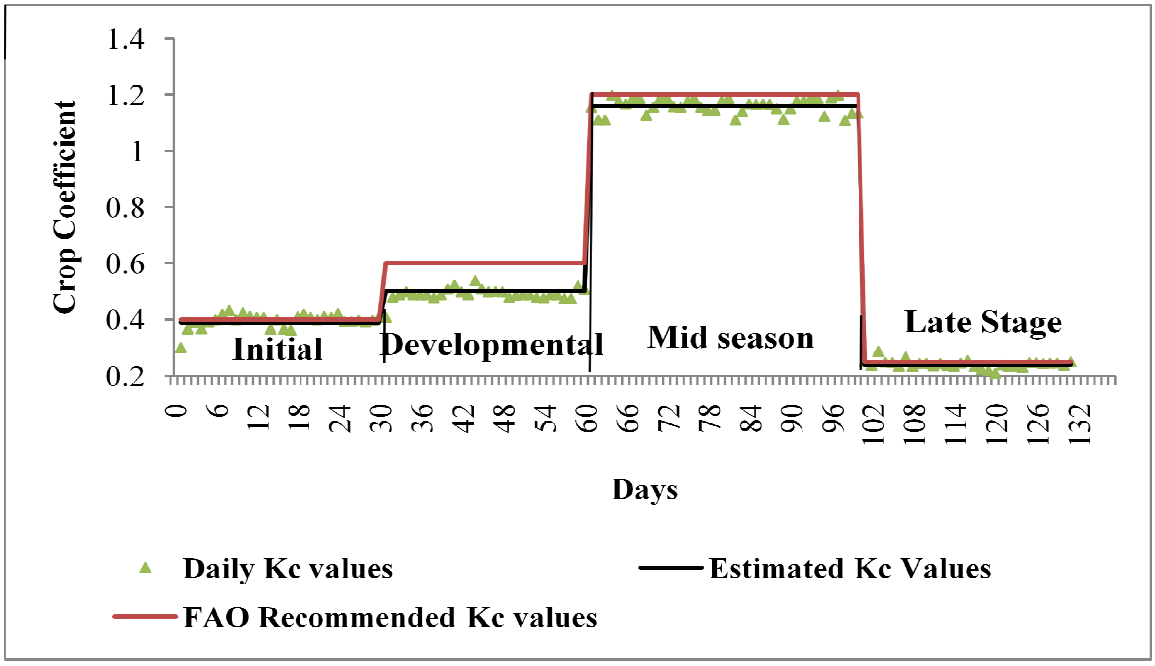

Figure 6.2(b) Crop coefficient (Kc) curve for wheat using growth stage lengths of 30, 30, 40, and 30 days

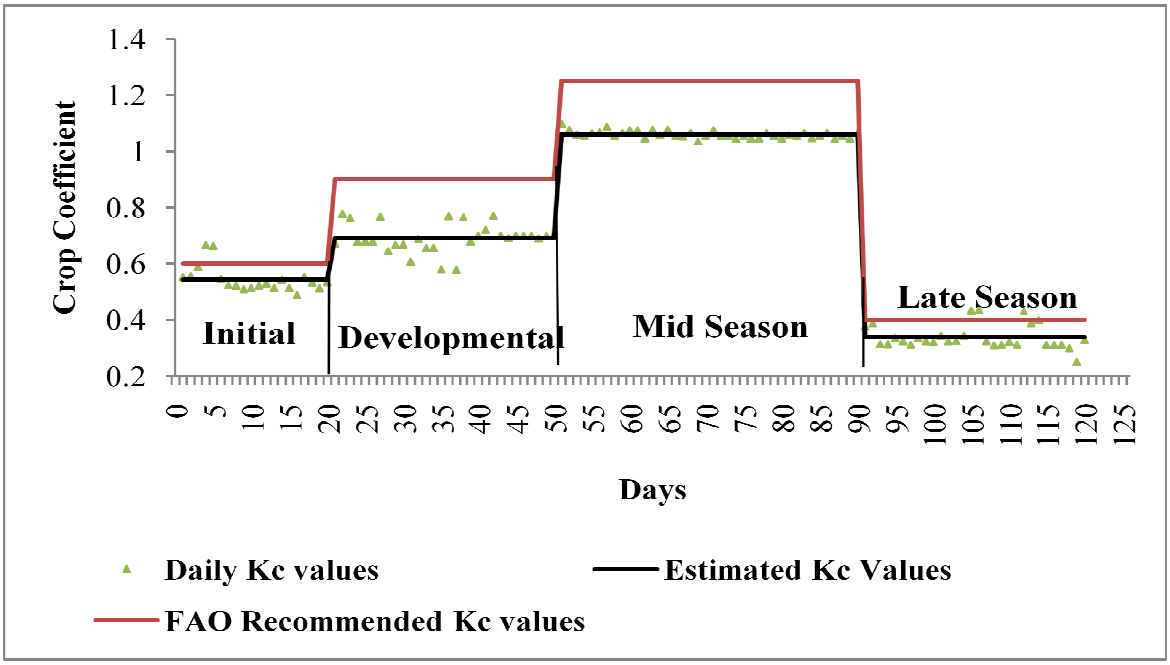

Figure 6.2(c) Crop coefficient (Kc) curve for summer paddy using growth stage lengths of 20, 30, 40, and 30 days

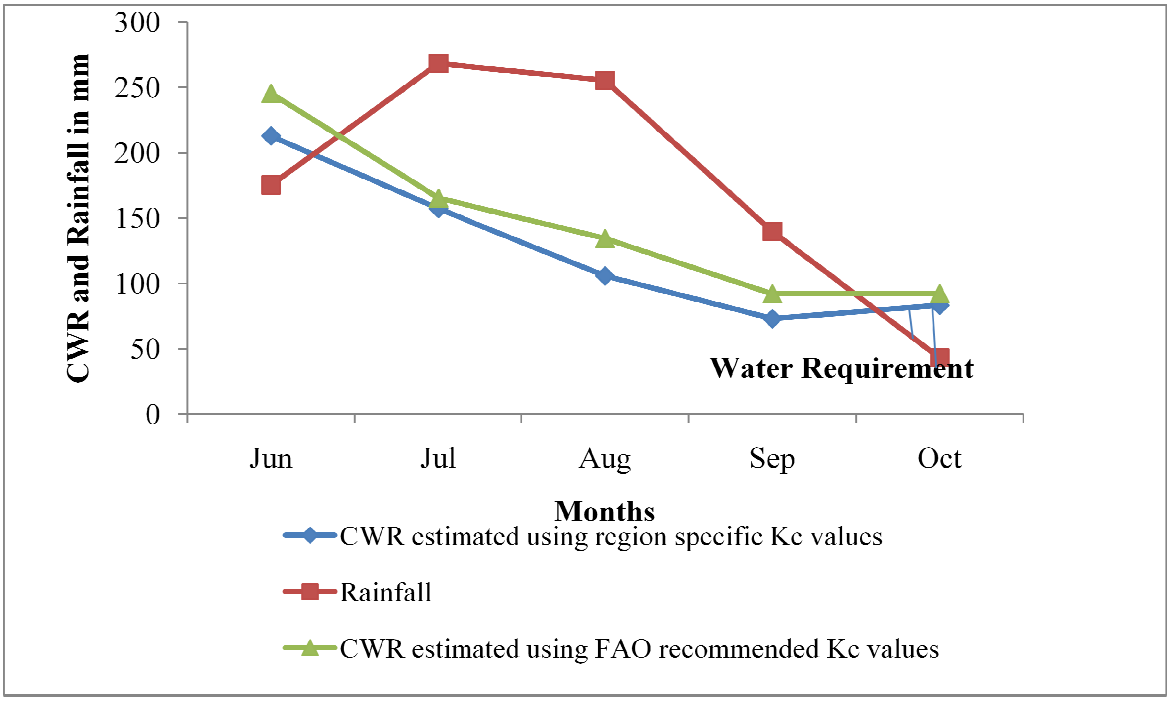

a) Kharif Season

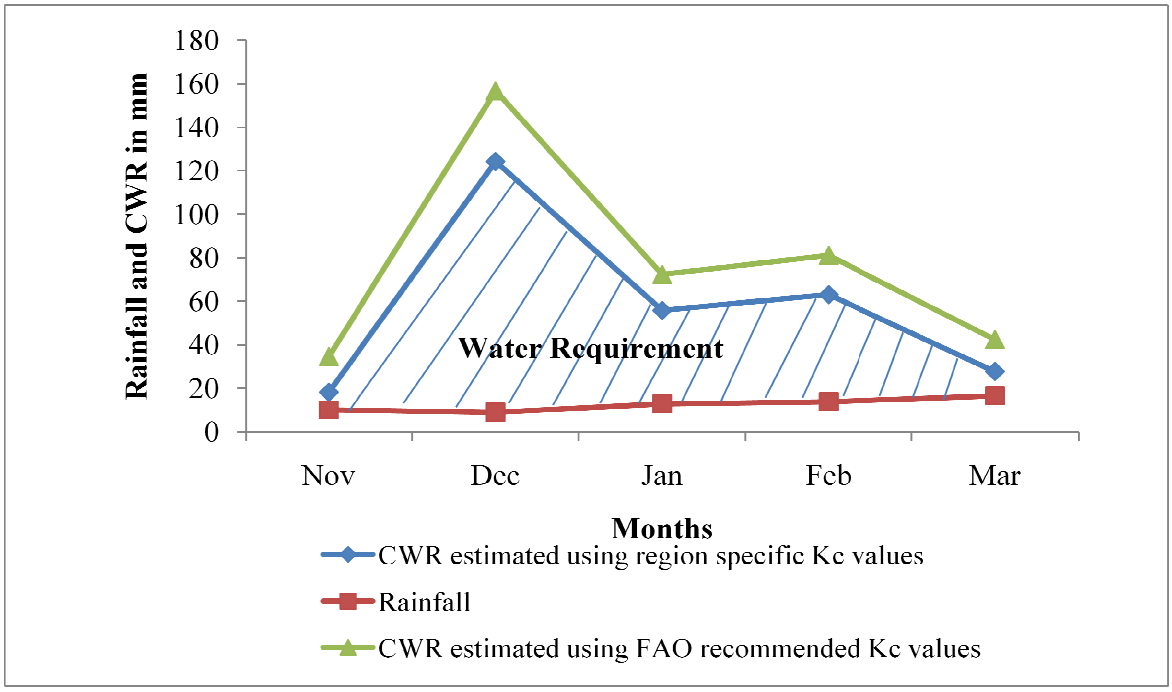

b) Rabi Season

Figure 6.3 Monthly variation of CWR estimated using FAO recommended and region specific Kc values. The hatched area shows the amount of crop water requirement

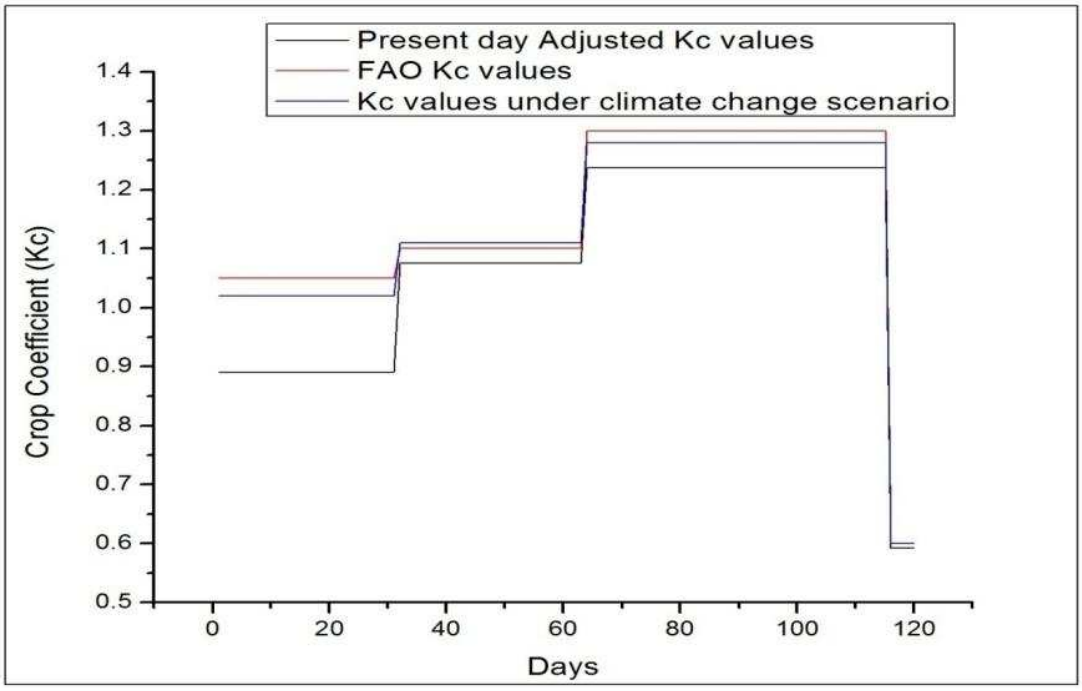

(a) Kharif Rice

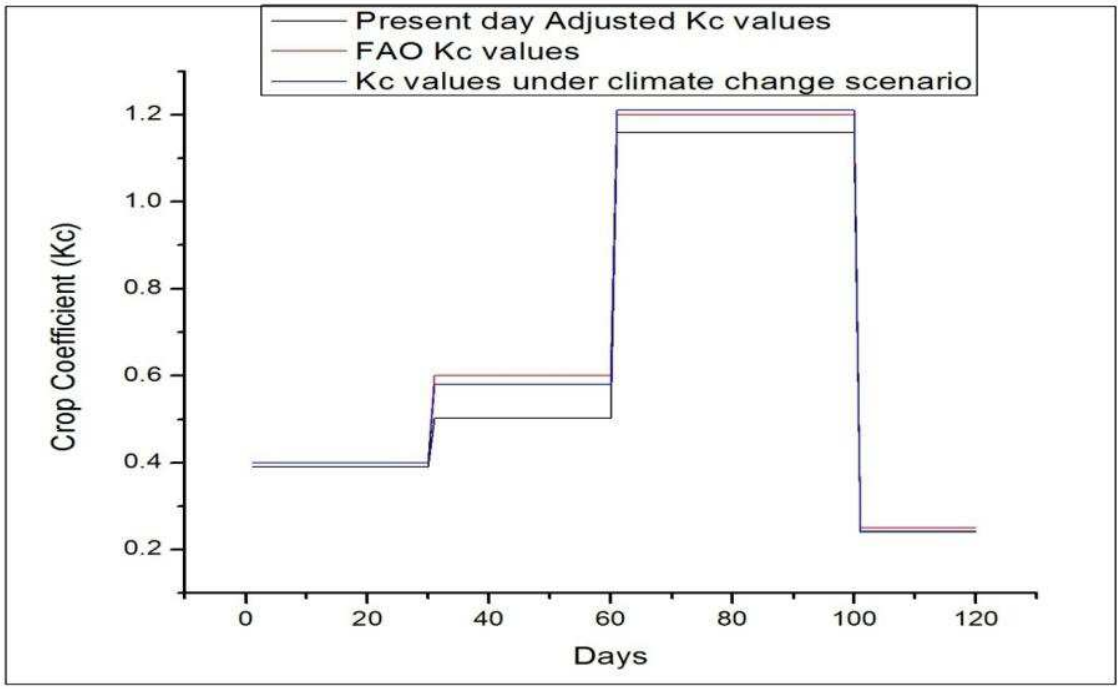

(b) Rabi Wheat

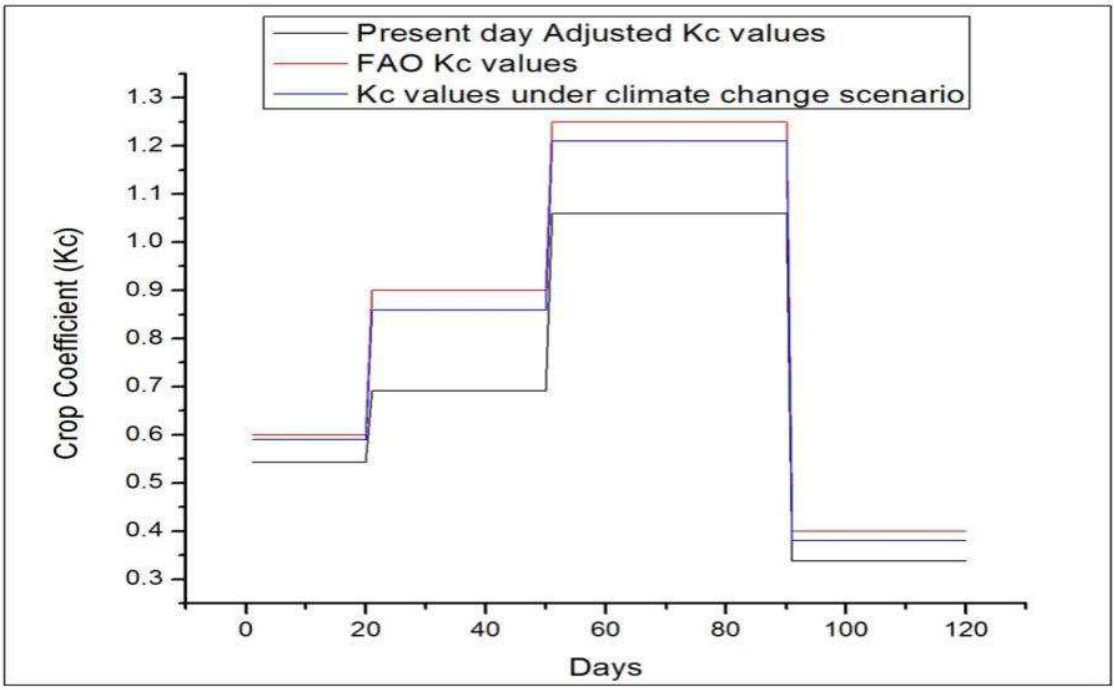

(c) Summer Paddy

Figure 6.4 Kc values under climate change scenario

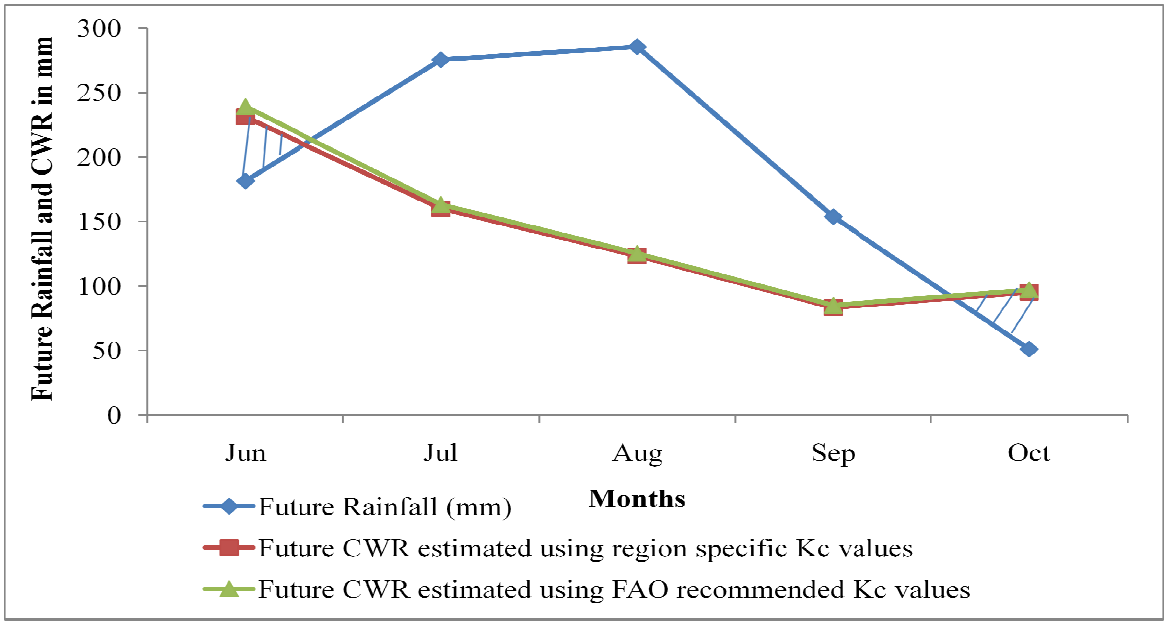

a) Kharif Season

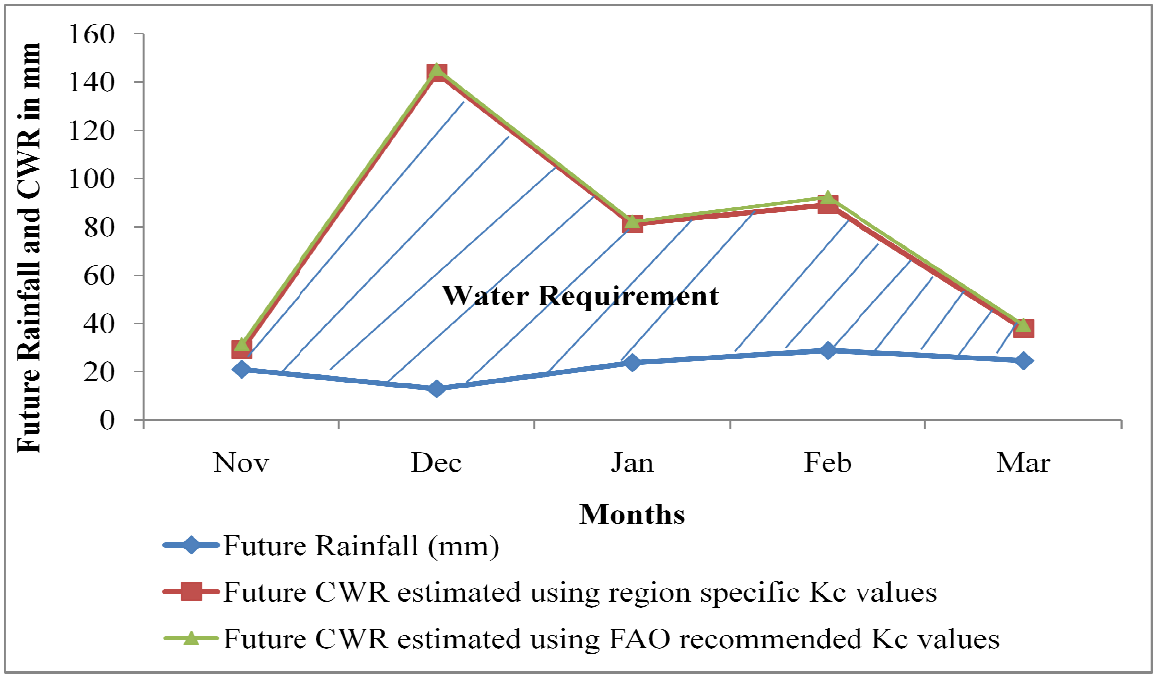

b) Rabi Season

Figure 6.5 Monthly variation of future CWR estimated using FAO recommended and region specific Kc values. The hatched area shows the amount of crop water requirement

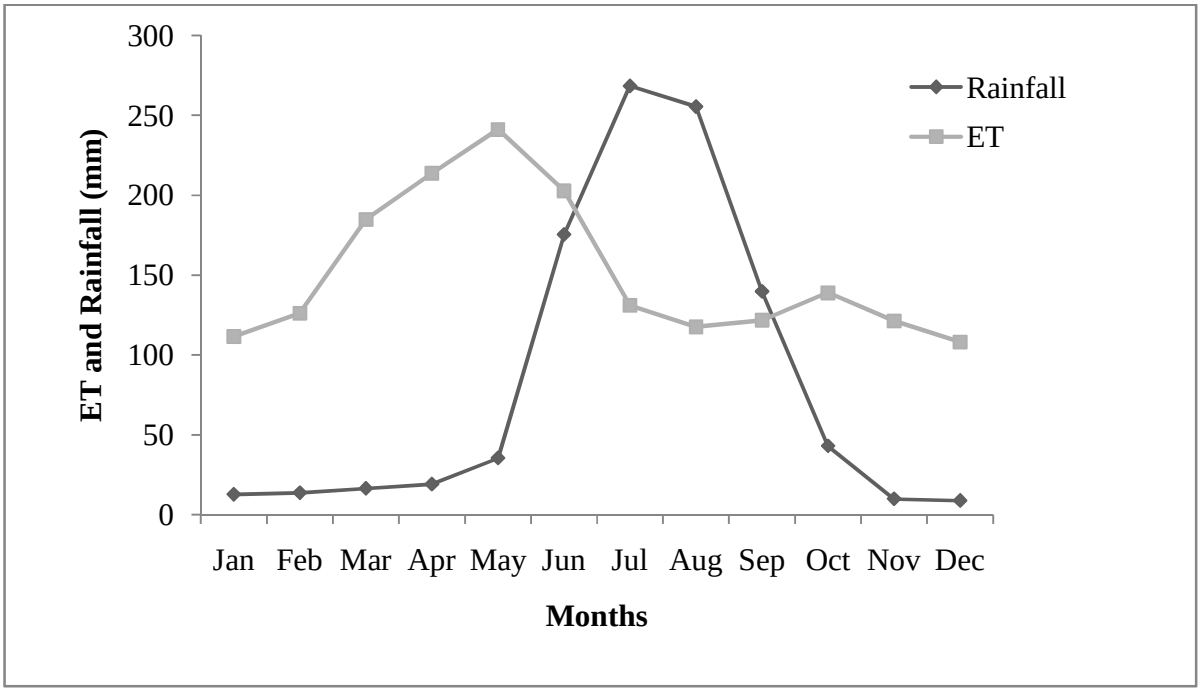

Figure 6.6 Monthly Variations of ET and Rainfall

6.3.4 Reference Evapotranspiration Trend

The Mann-Kendall's test is applied to detect trends in reference evapotranspiration (ETo) for all the selected stations falling in Seonath River basin, Chhattisgarh. The spatial distribution of trends in annual and seasonal ETo is shown in Figure 6.7. From Figure 6.7 the increasing trend is observed for all the seasons except for summer season which shows non-significant decreasing trend. For annual series significant increasing trend has been observed in the stations located in Southwest part of the study area. However non-significant increasing trend of ETo are found in other parts of the study area. On the seasonal scale large differences are found in the spatial distribution of trends in ETo. For the summer season the most of the stations shows non-significant decreasing trend (Figure 6.7 d). The summer ETo has decreasing trend because of decrease in maximum temperature and increase in relative humidity over Seonath basin during summer season (discussed in Chapter 4). For the winter months increasing trends of ETo have been observed for stations located at Raipur, Kawardha, Jhajgir-Champa and Damtari (Figure 6.7 c). The rest of the stations showed non-significant increasing trend. The monsoon season exhibits significant increasing trend of ETo. However, the trends at Bilaspur district are found to be non-significant

increasing (Figure 6.7 b). The monsoon season showed the similarities in the spatial pattern with respect to annual ETo. The percentage of stations in the study area exhibiting rising and falling trend using MK test are presented in Figure 6.8. In the monsoon season, significant rising trends of ETo exhibits in 92% of the stations. However non-significant increasing trend of annual and winter ETo values are found in 67% and 58% of the stations, respectively. Non significant decreasing trends in 87% of the stations could be noticed in summer ETo values (Figure 6.8). Overall annual, winter and monsoon ETo values have increasing trends in the basin. However, ETo in summer season showed decreasing trend.

The monthly ETo trend for each month are given in Table 6.4. Both upward and downward trends are evident in different stations and months. Almost all the stations exhibit significant increasing trends from September to November except for Bilaspur station. The estimates of ETo for the months of December, January, February, July and August show non-significant increasing trend. However significant increasing ETo trend have emerged for the months of August, September and October. The Kharif crops have maximum growth (developmental stage) during the month of August and therefore more water is transpired from the plant canopy. In summary, the results show that the average monthly ETo for the period of 51 years has significant increasing trend for September, October, November (Table 6.4).

Figure 6.9 shows trend magnitude of monthly estimates of ETo. The decreasing trend magnitude is noticed for March, April and June and rest of the months show increasing trend with highest magnitude for the month of August followed by September and October. Figure 6.10 shows the percentage change in ETo over 51years. The percentage change is highest for two districts viz., Rajnandgaon and Kanker. However, Bilaspur district has emerged with lowest percentage change in ETo with the magnitude ranging between 0.91% to 4.61%. Overall result indicates that the ETo value have increased in Seonath River Basin over the period of 51years.

The overall trend and percentage change for annual and seasonal ETo of the basin have been summarized in Table 6.5. The increasing trend magnitude and percentage change on annual and seasonal ETo have emerged very clearly except for summer season which show decreasing trend. This may be due to decreasing trend in summer maximum temperature in study basin (discussed in detail in Chapter 4). The significant increasing trends in ETo values have been observed for monsoon and winter season (Table 6.5, Column 2). The percentage variability in ETo values have been found highest for monsoon followed by winter season (Table 6.5, Column 4).

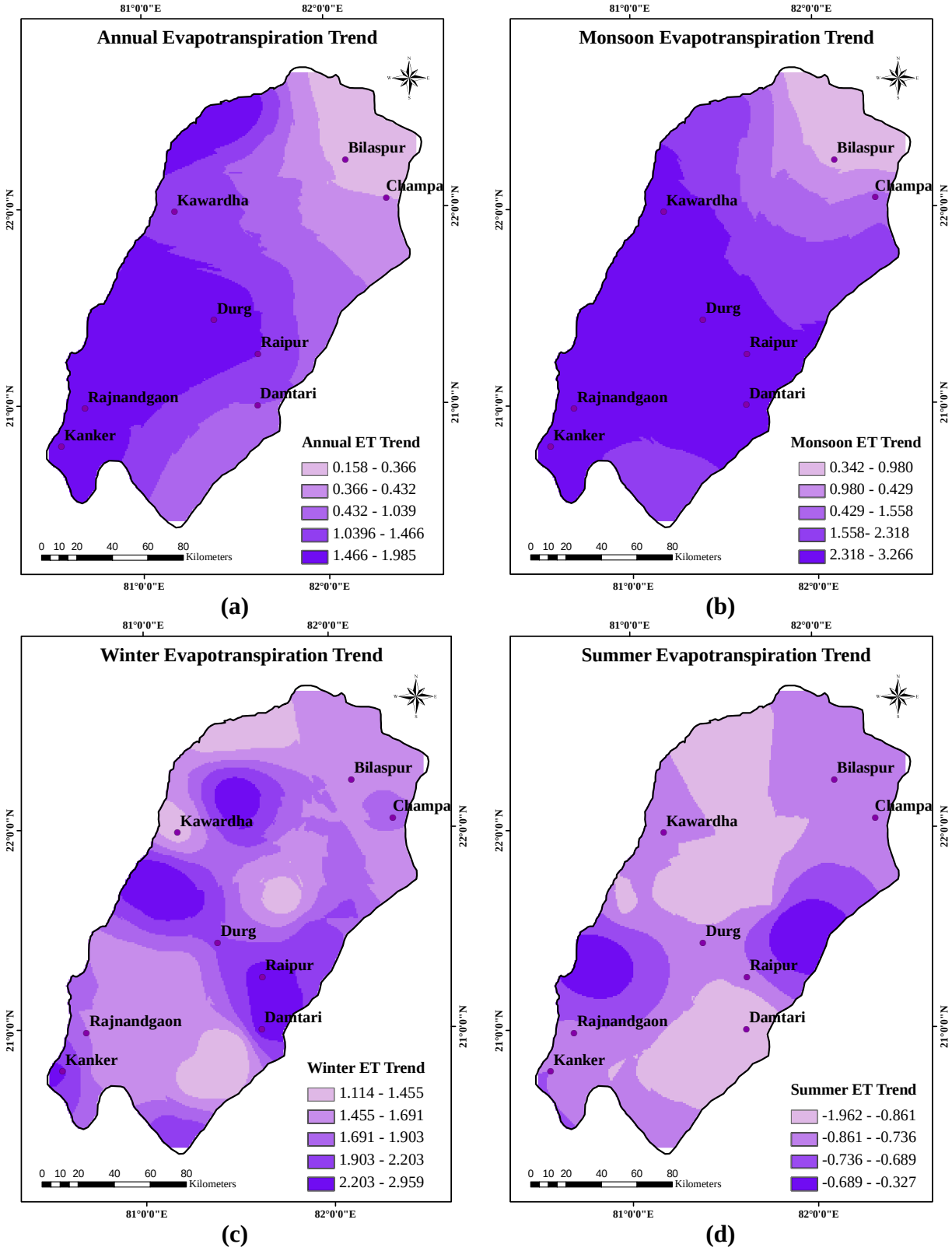

Figure 6.7 Plots of Kendall Z statistic for the annual and seasonal ETo trend during 1960-2010 (a) Annual; (b) Monsoon; (c) Winter; (d) Summer

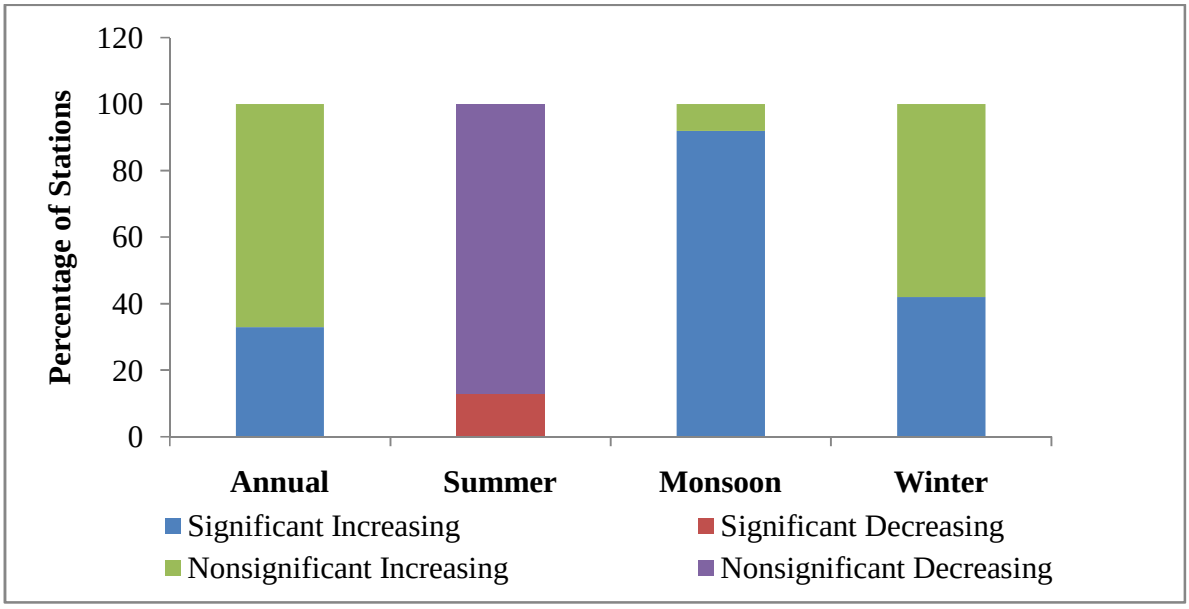

Figure 6.8 Percentage of stations showing increasing and decreasing trend for the Seonath river basin

Table 6.4 Monthly ETo trends by Mann–Kendall test (Bold value indicates significant level)

Months	Raipur	Bilaspur	Durg	Dhamtari	Kanker	Kawardha	Korba	Rajnandgaon
Jan	0.31	0.16	0.75	0.90	0.83	0.82	1.31	0.19
Feb	0.10	0.52	0.22	0.27	0.59	0.04	0.67	0.35
Mar	-0.88	-0.91	-0.86	-0.53	0.02	-1.00	-1.41	-0.48
Apr	-0.40	-0.31	-0.56	-0.25	0.03	-0.79	-0.94	-0.64
May	-0.36	-1.45	-0.04	-0.04	0.34	-0.24	-0.49	-0.03
Jun	-0.17	**-3.22**	-0.60	-0.31	-0.24	-0.91	-0.81	-0.72
Jul	**2.06**	1.31	1.23	1.66	1.84	0.37	0.10	1.42
Aug	**2.35**	1.53	**2.60**	**2.79**	**3.28**	**2.15**	1.86	**2.97**
Sep	**3.24**	0.91	**3.15**	**3.38**	**3.29**	**3.23**	**2.89**	**3.04**
Oct	**2.69**	**2.10**	**2.10**	**2.03**	**2.00**	**2.14**	**2.23**	1.91
Nov	0.73	1.70	0.74	0.40	0.38	1.26	1.03	0.73
Dec	0.61	0.84	0.15	0.33	0.66	0.05	0.41	0.05

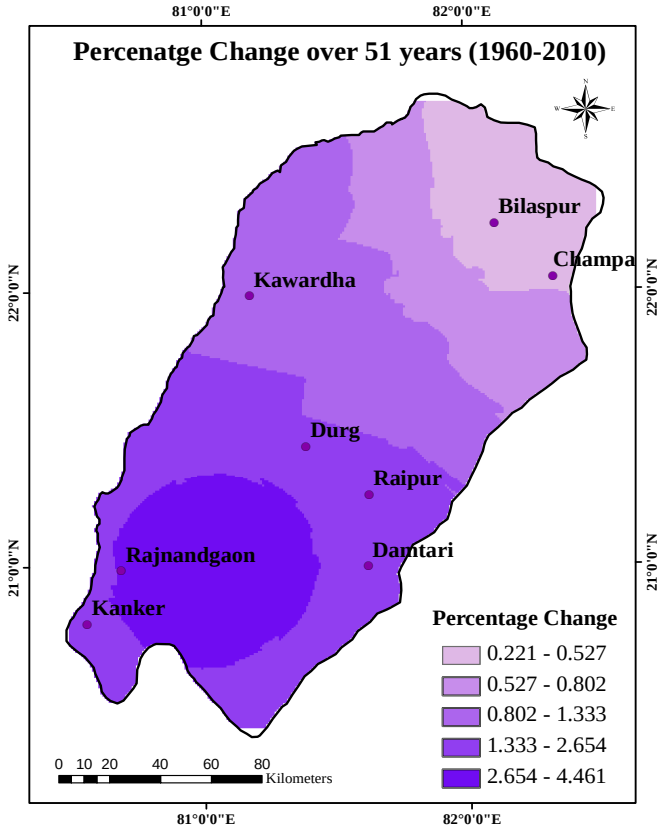

Figure 6.9 Percentage change in annual (ETo) for the Seonath river basin

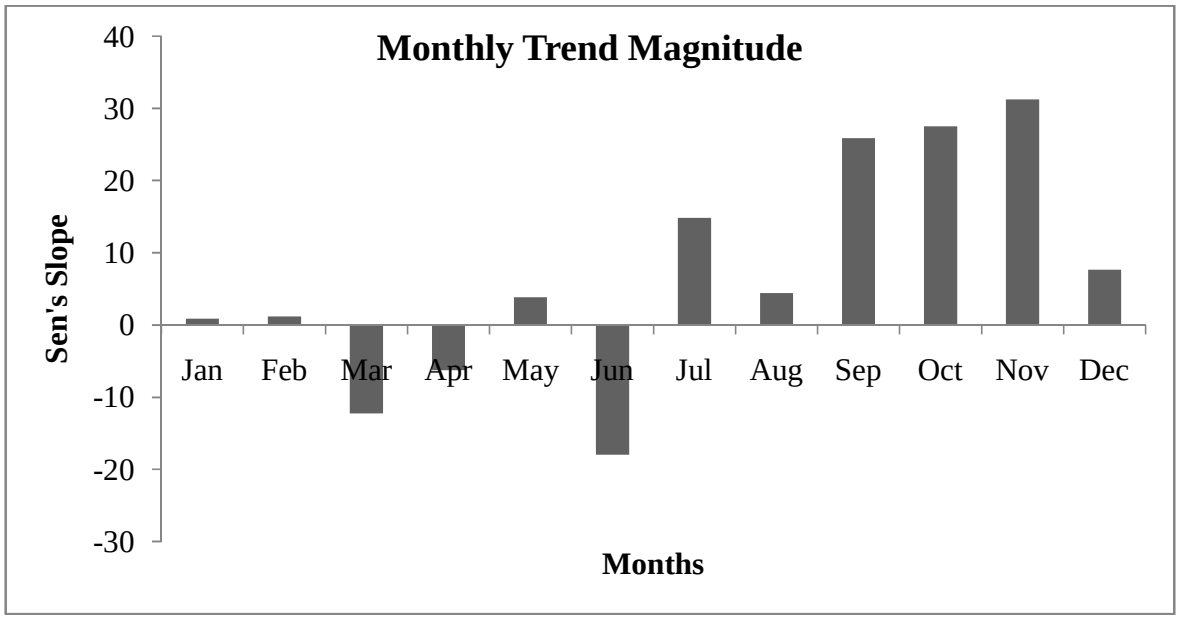

Figure 6.10 Monthly ETo trend slope values over 51 years (1960–2010) for the Seonath river basin

Table 6.5 Results of regional average annual and seasonal ETo for entire Seonath Basin

Seonath River Basin	Z-values MK	Sen's Slope (β)	% Change over 51 year	% Variability over 51 year
	Col. 1	***Col.2***	***Col.3***	***Col.4***
Annual	1.56	13.14	1.43	1.17
Summer	-0.43	-10.51	-0.78	2.01
Winter	**1.96**	21.02	3.08	2.77
Monsoon	**2.37**	22.0	3.07	2.88

Bold value indicates significant increasing/decreasing trend

6.3.5 Analysis of Annual ETo Variability Pattern

Knowledge on the variation in ETo is essential from agricultural point of view for precise estimation of supplemental water requirements. The study of ETo variability pattern using Coefficient of Variation (CV) for a period of 1960-2010 (51 years) for Seonath river basin indicates that the inter-annual variability is highest for the entire river basin (Figure 6.11). The highest (3.4-3.6%) annual ETo variability is seen in stations located at southern part of the basin while rest of the stations exhibits almost same inter-annual variability ranges from 1.0%-1.8%. Overall it can be stated that high variation in ETo is observed for the entire Seonath River Basin.

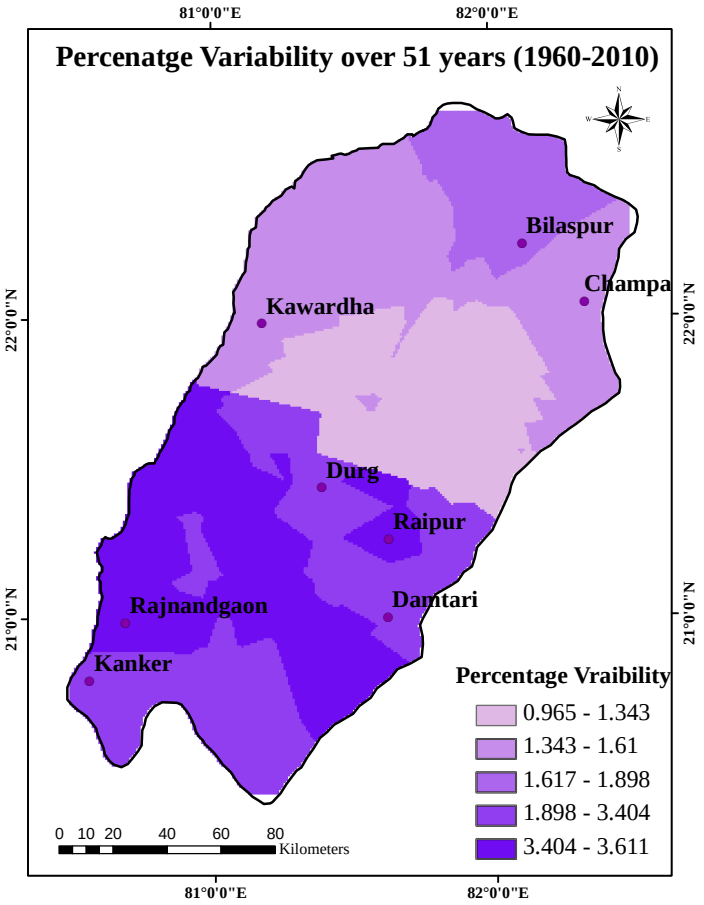

Figure 6.11 Spatial distribution of inter-annual variability of annual ETo (CV)

6.3.6 Trends in Irrigation Water Requirement (IWR)

The estimated annual IWR is shown in Figure 6.12. It can be seen from the figure that IWR has generally increased for the entire study period. The IWR of the Kharif Paddy is relatively higher for the later stage of the crop growth period. For Rabi cropping season (wheat and summer paddy) it has been found that the required Irrigation Water Requirement (IWR) is of the same order throughout the growing season, but marginally higher during the developmental stage. The overall IWR at annual time steps indicated the irrigation requirement to be more for Rabi crops (Figure 6.13). Overall, the analysis of long term IWR has revealed that the water requirement for agricultural crops in most parts of the study area have shown increasing trend.

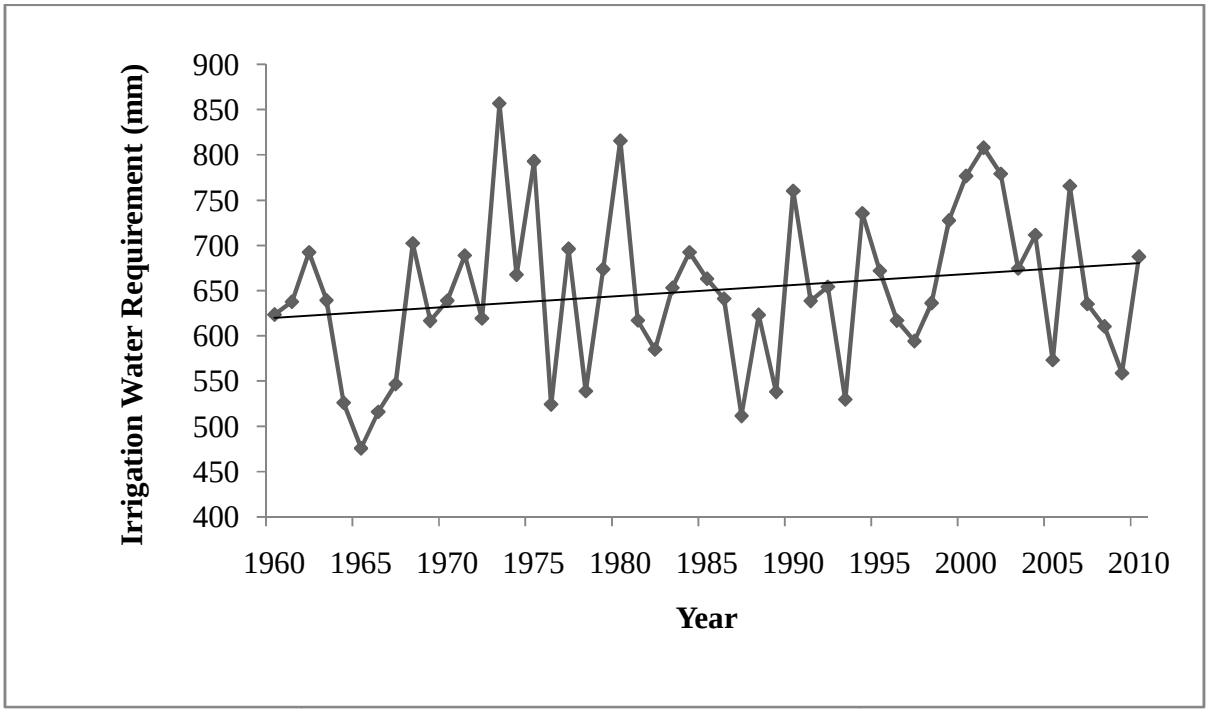

Figure 6.12 Trends in Irrigation Water Requirement for Seonath river basin

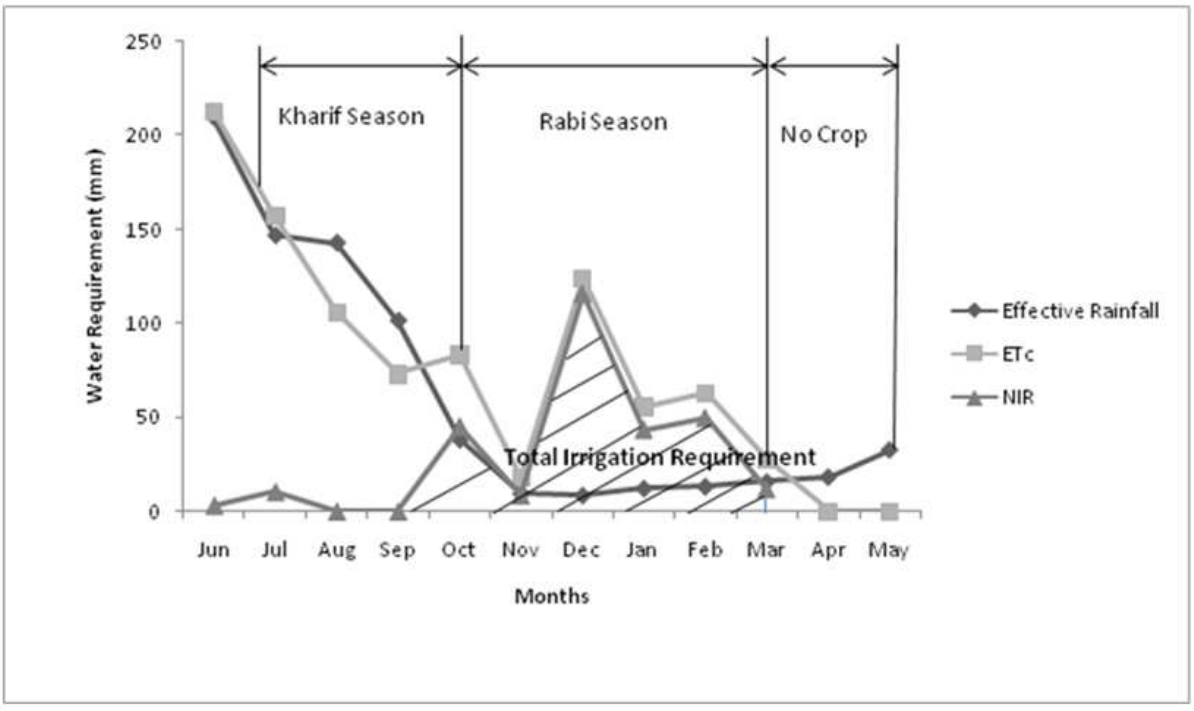

Figure 6.13 Total IWR. The hatched area shows the amount of Irrigation requirements

6.3.7 Changes in IWR over the period 1960–2010

In order to detect changes in IWR, the MK-test and Sen's slope have been used for the 51-year period (1961-2010). Changes in IWR are investigated for Kharif (Paddy) and Rabi (wheat and summer paddy) cropping seasons using meteorological data for eight weather stations within the basin. The estimates of IWR for Kharif Paddy growing season in all the stations have increasing trend except for Korba station. The estimates of IWR for Korba basin have indicated non-significant decreasing trend (Figure 6.14a).For the Rabi season IWR trend is indentified for two crops wheat and summer paddy. For wheat crop, significant increasing trends of IWR have been found for five stations (viz., Bilaspur, Raipur, Durg, Dhamtari and Rajnandgaon) and the increasing trends have been found non-significant for three stations (Korba, Kawardha and Champa). Similarly for summer paddy significant increasing trend have emerged for upper half (northern parts) of the basin whereas the estimates of IWR for lower half (southern part) of the basin show non-significant increasing trend (Figure 6.14 b, c). The percentage of stations with rising and falling trend is shown in Figure 6.15. For Kharif season positive trend have been detected in 88% of the stations, and remaining 12% of the stations showed decreasing trend. For rabi wheat crop analysis revealed that the significant increasing trend are dominant, (with 63% of the stations). Whereas, for summer paddy 50% of the stations show significant increasing trend and rest 50% stations shows non-significant increasing trend (Figure 6.15).The IWR for Kharif and Rabi seasons are increasing at the rate of 3.627 mm/yr and 1.264 mm/yr respectively. These changes are characterized by a relative increase in IWR by 47%, while rabi IWR by 23%. The change in magnitude of IWR for Kharif and Rabi crops for each station are presented in Table 6.6. Among the crop growing seasons, the highest absolute maximum values of percentage change have emerged during Kharif season. This highest percentage change in Kharif IWR is likely to have significant adverse impact on rainfed agriculture in future. This may necessitate shifting the existing focus from irrigation in Rabi season to supplemental irrigation in Kharif (monsoon) season crops.

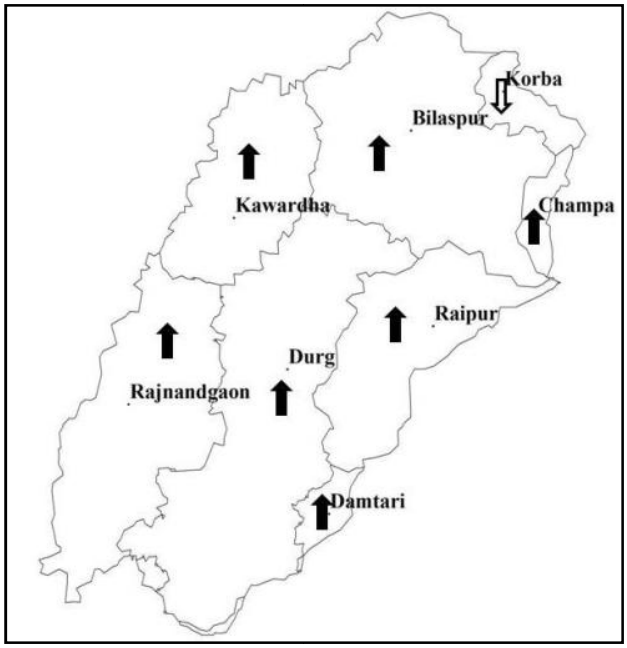

(a) Kharif IWR trend(Paddy)

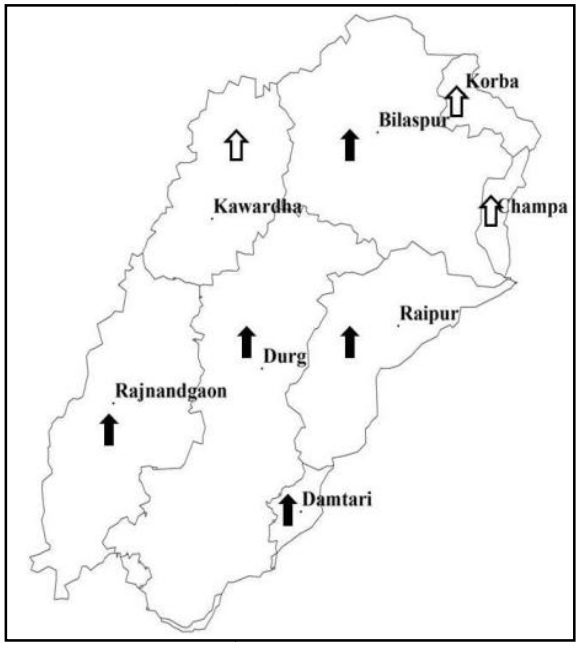

(b) Rabi IWR trend (wheat)

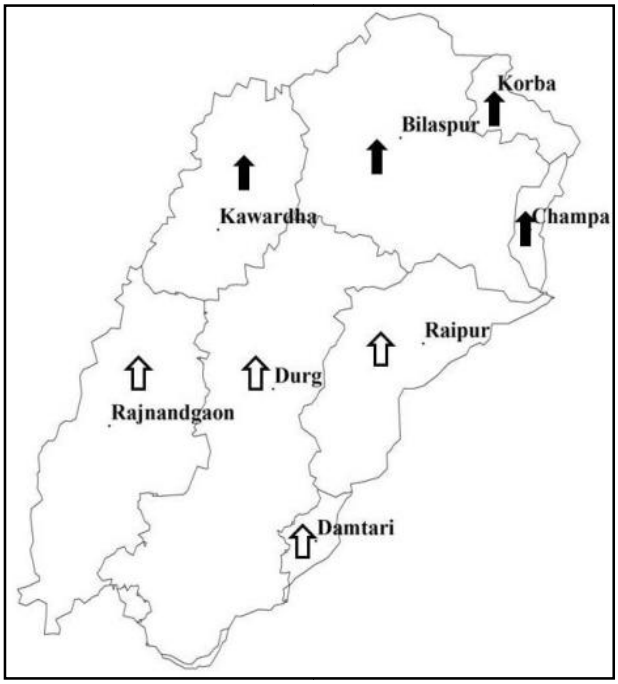

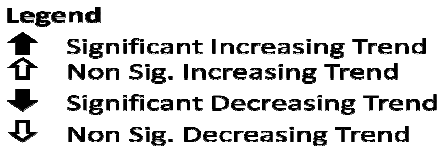

(c) Rabi IWR (Summer Paddy)

Figure 6.14 Trend in Irrigation Water Requirements (a) Kharif Crop (Paddy) (b) Rabi Crop (Wheat) (c) Rabi Crop (Summer Paddy)

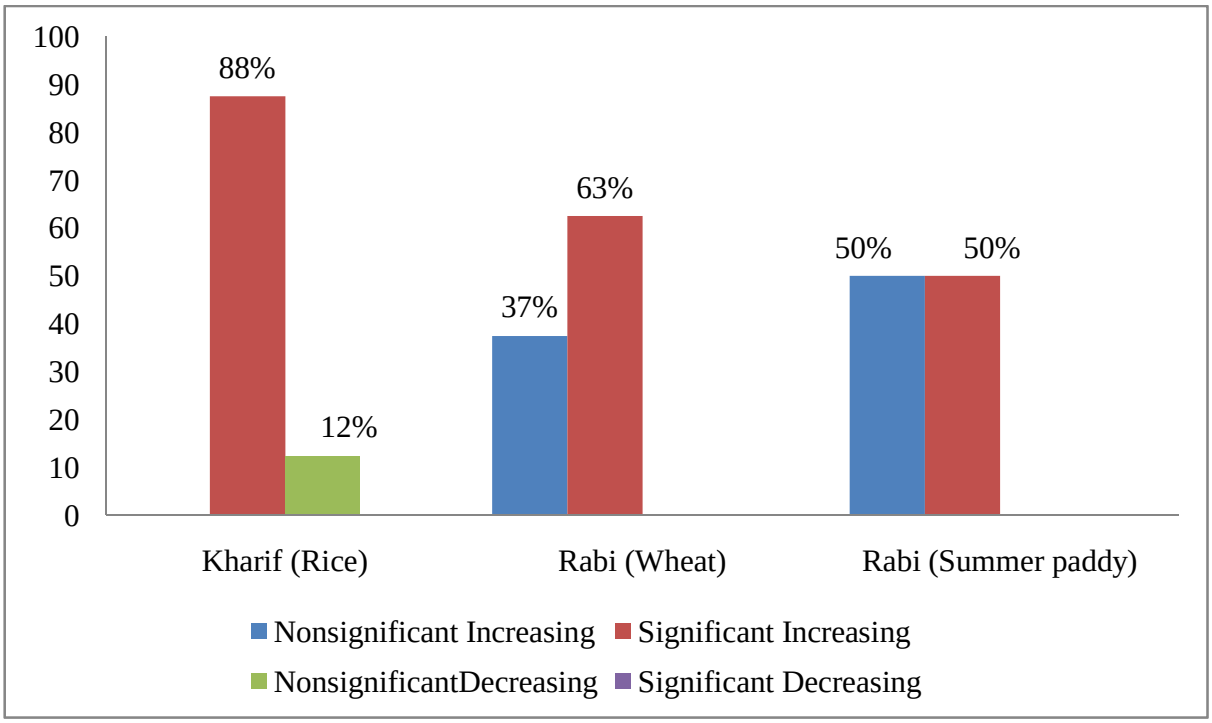

Figure 6.15 Percentage of station with increasing/decreasing trend

Table 6.6 Sen's Slope of Monsoon and Post Monsoon IWR over the period of 1960-2010

Station	Kharif IWR		Rabi IWR (Wheat)		Rabi IWR (Summer Paddy)	
	Sen's Slope (β) (mm/yr)	% Change	Sen's Slope (β)	% Change	Sens Slope (β) (mm/yr)	% Change
Raipur	0.869	30.973	0.565	9.299	0.567	6.438
Bilaspur	1.726	23.087	0.0156	0.289	0.003	0.0386
Durg	3.627	7.313	0.0570	0.869	0.048	0.515
Damtari	0.366	48.371	0.597	9.807	0.628	7.121
Champa	1.894	28.406	0.218	3.487	0.258	2.842
Kawardha	1.082	29.533	0.190	3.563	0.201	2.542
Korba	0.460	10.699	0.429	9.608	0.417	6.138
Rajnandgaon	3.671	47.092	1.264	22.853	1.236	15.099

6.4 SUMMARY

This chapter presents the estimates of ETo, CWR and IWR including determination of region specific crop coefficients and effective rainfall. The ETo has been computed using FAO-56 Penman-Monteith method. The crop coefficients during crop growing season and CWR have been computed for major crops viz. Kharif Paddy, wheat and summer paddy. The climatic condition of Seonath river basin (study area) differs from the standard climate considered in FAO paper-56 (Allen et al., 1998) because of lower mean wind speed (1.7-1.0 m/s) and higher mean minimum relative humidity (79-41%) during Kharif and rabi season. Hence, the adjusted Kc values are lower than those suggested by FAO-56 for each crop during the different crop growth stages. The CWR computed using Kc in FAO-56 gives significantly different (higher) values. It is therefore recommended to use adjusted Kc values for accurate estimation crop water requirement.

The Mann-Kendall (MK) and Modified Mann-Kendall (MMK) tests are applied to detect the trend in annual, seasonal and monthly ETo and IWR estimates over 51 years (1960–2008) in the Seonath River Basin, Chhattisgarh (India). The slopes of trend lines are computed using the Theil–Sen's slope estimator. The increasing tends in ETo have been found for winter and monsoon season except for summer season which shows non-significant decreasing trend. Annual analysis of ETo series indicated that the increasing trend. On the monthly time scale, increasing trends have been identified in ETo values in majority of the months. The significant positive trend magnitude is found for the months of September, October and November. The Coefficient of Variability (CV) revealed that inter-annual variability of ETo has been high in the whole river basin. The southern part of the basin shows highest variability (3.4-3.6%).

The analysis has revealed that IWR has increasing trends for Kharif Paddy crop as well as for Rabi season crops (wheat and summer paddy). Overall, the results of this study showed an increase in irrigation water requirement, because of increase/change in meteorological variables (viz., rainfall, Tmax and Tmin, relative humidity and wind speed). Therefore, changing irrigation requirement appraisals presented in this study would be useful for future irrigation management systems for the Seonath River Basin.

In the next chapter an attempt has been made to correlate the Curve Number (CN) parameter of the SCS-CN methodology with IWR in order to investigate a simple methodology for determination of CWR and IWR using rainfall runoff records. To this end, a model is explored between potential maximum retention (S) and ETo, and the dependence of ETo on S will be used for correlating S with IWR.

CHAPTER 7

RELATIONSHIP BETWEEN IRRIGATION WATER REQUIREMENT AND SCS-CURVE NUMBER

This chapter presents the development of simple model for estimation of Irrigation Water Requirement (IWR) and Soil Conservation Service-Curve Number (CN). To this end the proposed model is validated using large rainfall-runoff dataset of Seonath river basin.

7.1 INTRODUCTION

Irrigation Water Requirement (IWR) is one of the most important components for regional water budget and one of the key measurements for planning and management of water resources. It is of significance to assess the amount and changes of IWR especially for those areas where the conflicts between water demands and supply are serious. The study site is Seonath Rivers Basin falling in Chhattisgarh State of India. Nearly, the livelihood of 80% population in the study basin depends on agriculture. The basin receives an average annual rainfall of the order of 1255 mm. Nearly 88% of annual rainfall is received in monsoon period i.e., June-September. The average rainfall in non rainy season (October-May) is insignificant and it is only 12% of the annual rainfall. Therefore the basin often faces dry conditions during winter and summer seasons. It often encounters with water shortage in rural and urban areas and the problem becomes more adverse in summer season in low rainfall years. It is reported that the study area faces frequent droughts and thus crop production is adversely affected from time to time. Due to uneven and erratic distribution of rainfall, the pattern of water utilization in agriculture has also changed. It is reported that the water utilization in the basin has increased with time. Thus, it is essential to study the changes in ET is to work out the supplemental water requirement of different crops during their critical growth periods.

Thus, for the assessment of future water and crop production, it is necessary to estimate the water requirement of irrigated agriculture. For estimation of IWR, reference evapotranspiration (ETo) forms to be the key component. Despite availability of a number of models in literature, the assessment of evapotranspiration (ET) is a complex task as it involves spatial and temporal heterogeneity in meteorological and climatic parameters, soil

moisture status, plant water availability, surface cover type, soil classes etc. (Makkeasorn et al., 2006).

In field, it is widely believed that the lysimeter provides the most reliable assessment of ET if surface cover condition of the catchment perfectly matches its inside cover condition. It is however expensive in terms of its installation and requires high operational skills. Therefore, the measurement using lysimeter is not very common for routine measurements. Consequently, several empirical and semi-empirical approaches have been suggested from time to time for different regions based on available meteorological data. However, a few or sometimes only one meteorological station represents the climate of the entire watershed. All empirical methods however work in a certain range of conditions and none can be recommended as the best one due to their limitations and complexity. Therefore, care should be taken not to use them outside the prescribed range (Beven, 2001).

ET can be estimated using energy balance, mass transfer, combination of energy balance and mass transfer based empirical and semi-empirical approaches (Brutsaert, 1982; Allen et al., 1989; Jensen et al., 1990; Morton, 1994; Xu and Singh, 2002). The simple methods like Blaney-Criddle (1950), Thornthwaite (1948), and Hargreaves (1982) used only temperature data, are not very accurate especially under extreme climatic conditions. These methods underestimate (up to 60%) ET in windy, dry, and sunny areas, while in calm, humid, and cloudy areas, they overestimate (up to 40%) (Brutsaert, 1982). The combined approach (Penman, 1948) is however considered as the most physically satisfying approach (Jensen et al., 1990; Smith et al., 1991; Shuttleworth, 1993; Beven, 2001). The Penman-Monteith (PM) model recommended by FAO (Allen et al., 1998) is commonly used for estimation of reference evapotranspiration (ETo). It is however more data demanding and data sensitive compared to other methods. There are situations when more data demanding complex ET estimation methods cannot be used due to non availability of accurate and long term data. Thus, there is need to investigate simpler methods to derive irrigation water requirement on seasonal scale and also be compatible with the available complex methods. To this end, Mishra et al. (2014) suggested there are strong relationships between the SCS-CN (SCS, 1971) runoff curve number (CN) (for a watershed at any time scale including the seasonal (Mishra et al., 2008) and potential evapotranspiration (PET). It is obvious that the popular SCS-CN method is simple and easy to use. As ET is prime component for the estimation of IWR. Accordingly, an attempt has been made in this study to establish relationship between IWR and CN.

7.2 METHODOLOGY

For the derivation of IWR and CN relationship the values of ETo, CWR, IWR and CN for Kharif and Rabi season crops for each year are required. The estimates of ETo, CWR and IWR are discussed in detail in previous Chapter. The methodology used in this chapter is summarized in flowchart given in Figure 7.1.

7.2.1 Determination of Curve Number (CN)

The SCS-CN method (SCS, 1956) employs the water balance equation and two fundamental hypotheses described, respectively, as follows:

$$P = I_a + F + Q \tag{7.1}$$

The first hypothesis states that the ratio of direct runoff to potential maximum runoff is equal to the ratio of infiltration to potential maximum retention and, according to the second hypothesis; the initial abstraction is some fraction of the potential maximum retention. These are respectively expressed as:

$$\frac{Q}{P - I_a} = \frac{F}{S} \tag{7.2}$$

$$I_a = \lambda S \tag{7.3}$$

Where, P = total precipitation (mm), Ia = initial abstraction (mm), F = cumulative infiltration (mm), Q = direct runoff (mm), and S = potential maximum retention (mm), and λ = initial abstraction coefficient (= 0.2, a standard value). A combination of Eqs. 7.1 and 7.2 leads to the popular form of the SCS-CN method:

$$Q = \frac{(P - I_a)^2}{P - I_a + S} = \frac{(P - \lambda S)^2}{P + (1 - \lambda)S} \tag{7.4}$$

Here, P ≥ Ia, Q = 0 otherwise. From the observed rainfall-runoff data, the SCS-CN parameter S can be determined as follows (Hawkins 1993) with λ=0.2:

$$S = 5[(P + 2Q) - \sqrt{Q(4Q + 5P)}] \tag{7.5}$$

S can be transformed to CN scale using the following empirical relation:

$$CN = \frac{25400}{S + 254} \tag{7.6}$$

where, S (mm) and CN is a non-dimensional parameter. A detailed description of the application procedure is available elsewhere (McCuen, 1982; Ponce, 1989; Mishra and Singh, 2003a; Michel et al., 2005).

Originally, the event-based SCS-CN methodology was developed for small ungauged agricultural watersheds. Ponce and Hawkins (1996) suggested the methodology to be suitable for areas less than 250 km^2. Eq. 7.4 however does not restrict its applicability based on watershed size and rain duration (Mishra et al., 2008, 2014). Its capabilities, limitations, uses, and its revisions are reported elsewhere (McCuen, 1982; Steenhuis et al., 1995; Ponce and Hawkins, 1996; Bonta, 1997; Yu, 1998; Mishra and Singh, 1999, 2002, 2003a, b, Mishra et al., 2004a, 2006; and Michel et al., 2005). Williams and Laseur (1976), Soni and Mishra (1985), Mishra and Singh (2004b), Geetha et al. (2008), Mishra et al. (2008) and several others have employed the SCS-CN methodology for long-term hydrologic simulation in catchments of a few thousand sq.kms.

7.2.2 Relationship between CN and IWR

Mishra et al. (2014) suggested CN-PET relationship based on the water balance equation (Eq. 7.1) and the proportionality hypothesis (Eq. 7.2). The maximum amount of moisture available as rainfall (P) can be lost only when the direct surface runoff (Q) is equal to zero. In other words, P = Ia + S. Here, the maximum infiltration losses F will equal S (in magnitude) which includes the initial moisture (Mishra and Singh, 2002). From Eq. 7.2, as $Q \rightarrow (P-Ia)$, $F \rightarrow S$. Since Ia = 0.2S, the maximum water loss = 1.2S. In terms of antecedent moisture condition (AMC), it is equal to $1.2S_I$. For longer time scale reasons, the subscript I here is taken to refer to AMC condition (fully dry condition) of the watershed. Alternatively, S_I corresponds to the capacity of the fully saturated condition. Since, by definition, PET corresponds to unlimited amount of moisture supply to vegetation. Due to certain limitations PET concept has been gradually replaced by the terms, such as reference crop evapotranspiration (Jensen et al., 1990), or surface dependent evapotranspiration (Federer et al., 1996). The assumption in the proposed ETo computation is that the rainfall (P) is always greater than or equal to $1.2S_I$ during the whole period. Here, Ia accounts for all such initial water losses, for example, interception, evaporation, surface detention, and infiltration,

describable in terms of evaporation and not available for either plant use or runoff generation (Mishra and Singh, 2003a). The water that can transpire through vegetation during the storm duration can be equal to S_I, if the moisture is fully available. Thus, the sum of Ia and S (or CN) for dry condition describes the potential amount of evapotranspiration that can occur in a watershed during the period of consideration. Mathematically, the relation between ET and S has been described as follows (Mishra et al., 2014)

The governing equations for the root-zone soil moisture W and evapotranspiration E (ET) by Mintz and Walker, 1993 are given as follows:

$$E_T + E_S = \beta_{T,S}\left(E^* - E_I\right) \tag{7.6a}$$

$$\beta_{T,S} = \frac{W}{W^*} \tag{7.6b}$$

$$ET = E_I + E_T + E_S \tag{7.6c}$$

where E_T is the transpiration (moisture transferred from the soil to the atmosphere through the root-stem-leaf system of vegetation); E_s is the soil evaporation (moisture transferred from the soil to the atmosphere by hydraulic diffusion through the pores of the soil); E_I is the interception loss (water evaporated from the wet surface of the vegetation and wet surface of the soil) during rain storm; E_S is the coefficient of transpiration plus soil evaporation, taken as a function of soil wetness; E* is the potential evapotranspiration; W is the root-zone moisture at the end of the day; and W* is the root-zone storage capacity.

From Eqs. 7.6a and 7.6c,

$$\beta_{T,S} = \frac{ET - E_I}{E^* - E_I} \tag{7.7}$$

Combination of Eqs. 7.6b and 7.7 gives

$$\frac{ET - E_I}{E^* - E_I} = \frac{W}{W^*} \tag{7.8}$$

The right hand term of Eq. 7.8 represents, by above definition, the ratio of F (= W) to S (= W*). Thus, Eq. 7.8 states that, similar to the SCS-CN proportionality hypothesis (Eq. 7.2), the ratio of actual evapotranspiration to the reference evapotranspiration is equal to the ratio

of actual infiltration (or moisture retention) to the potential maximum retention. A substitution of Eq. 7.2 into Eq. 7.8 leads to

$$\frac{ET - E_I}{E^* - E_I} = \frac{F}{S} = \frac{Q}{P - I_a} \tag{7.9}$$

When further coupled with Eq. 7.4, Eq. 7.9 yields the following:

$$ET = E_I + \frac{(P - I_a)(ETo - E_I)}{P - I_a + S} \tag{7.10}$$

Here, E_I, by definition, represents the interception loss (water evaporated from the wet surface of the vegetation and wet surface of the soil) during the rain storm. It is however a representation of the above described SCS-CN initial abstraction (Ia) that includes not only interception losses but also surface detention, initial infiltration, and evaporation. This is the water loss abstracted initially and not contributing to either direct runoff or infiltration. On the other hand, E_T and E_S are the water losses occurring during the whole period of rain storm. Thus, within the frame-work of SCS-CN terminology, E_I can be taken as to represent Ia. Therefore, Eq. 7.10 can be recast as:

$$ET = I_a + \frac{(P - I_a)(E^* - I_a)}{P - I_a + S} \tag{7.11}$$

Where, P > ETo > Ia, ET = 0 otherwise. Taking Ia = 0.2S allows determination of ET from known P, E*, and S (or CN). Eq. 15 also exhibits an implicit relationship between ET and Ia and S and, in turn, CN.

In Equation (7.11), S is a function of ET/ETo. IWR is a function of CWR which, in turn, is a function of ET. Expressed mathematically,

$$S \text{ (or CN)} = f(ET, ETo) \tag{7.12}$$

$$CWR = f(ETo) = f(S \text{ or CN}) \tag{7.13}$$

Therefore,

$$IWR = f(CWR) = f(S \text{ or CN}) \tag{7.14}$$

The sum of Ia and S multiplied with suitable crop coefficient value describes amount of water required to compensate the evapotranspiration loss from the cropped field. The net irrigation water requirement of each crop is calculated by subtracting the effective rainfall from the actual crop evapotranspiration. Thus, a mathematical relation is also developed between IWR and S, as described below:

$$P = Ia + S \text{ (if, } Q \rightarrow 0, F \rightarrow S) \quad (7.15)$$

$$ETo = Ia + S = 1.2S_I \quad (7.16)$$

$$Pe = P - Ia = S \quad (7.17)$$

$$IWR = CWR\text{-}Pe \quad (7.18)$$

Substituting, the value of ETo and Pe in Eqs 7.18 we get Eq. 7.19 which can be described in the form described below:

$$IWR = Kc \times (1.2\ S) - S = S\ (1.2Kc - 1) \quad (7.19)$$

7.2.3 Performance Evaluation

7.2.3.1 Nash-Sutcliffe efficiency (NSE)

The Nash-Sutcliffe efficiency (NSE) is a normalized statistic that determines the relative magnitude of the residual variance ("noise") compared to the measured data variance ("information") (Nash and Sutcliffe, 1970). NSE is computed as shown in Eq 7.20:

$$NSE = 1 - \left| \frac{\sum_{i=1}^{N} (Oi - Ei)^2}{\sum_{i=1}^{N} (Oi - \overline{Ei})^2} \right| \quad (7.20)$$

7.2.3.2 Coefficient of determination (R^2)

The coefficient of determination (R^2) (Moriasi et al., 2007; Krause et al., 2005) is used to evaluate the model performance. R^2 describes the proportion of the variance in measured data explained by the model. R^2 ranges from 0 to 1, with higher values indicating less error variance, and typically values greater than 0.5 are considered acceptable (Santhi et al., 2001, Van Liew et al., 2003). Although R^2 have been widely used for model evaluation, these statistics are oversensitive to high extreme values (outliers) and insensitive to additive and proportional differences between model predictions and measured data (Legates and McCabe, 1999).

7.2.3.3 Index of agreement (d)

The index of agreement (d) has been developed by Willmott (1981) as a standardized measure of the degree of model prediction error and varies between 0 and 1. A computed value of 1 indicates a perfect agreement between the measured and predicted values, and 0 indicates no agreement at all (Willmott, 1981). The index of agreement represents the ratio between the mean square error and the "potential error" (Willmott, 1984). The index of agreement can detect additive and proportional differences in the observed and simulated means and variances; however, d is overly sensitive to extreme values due to the squared differences (Legates and McCabe, 1999). Legates and McCabe (1999) suggested a modified index of agreement (d1) that is less sensitive to high extreme values because errors and differences are given appropriate weighting by using the absolute value of the difference instead of using the squared differences.

7.2.3.4 Percent bias (PBIAS)

Percent bias (PBIAS) measures the average tendency of the simulated data to be larger or smaller than their observed counterparts (Gupta et al., 1999). The optimal value of PBIAS is 0.0, with low-magnitude values indicating accurate model simulation. Positive values indicate model underestimation bias, and negative values indicate model overestimation bias (Gupta et al., 1999). PBIAS is calculated with Eq. 7.21

$$PBIAS = 1 - \frac{\sum_{i=1}^{N}(Oi-Ei)*100}{\sum_{i=1}^{N}(Oi)} \quad (7.21)$$

7.2.3.5 Root Mean Square Error (RMSE)

RMSE is an error index used in model evaluation. RMSE values of 0 indicate a perfect fit. Singh et al. (2004) state that RMSE values less than half the standard deviation of the measured data may be considered low and that either is appropriate for model evaluation.

$$RMSE = \sqrt{\{\frac{1}{N}\sum_{i=1}^{N}(Oi - Ei)\}} \quad (7.22)$$

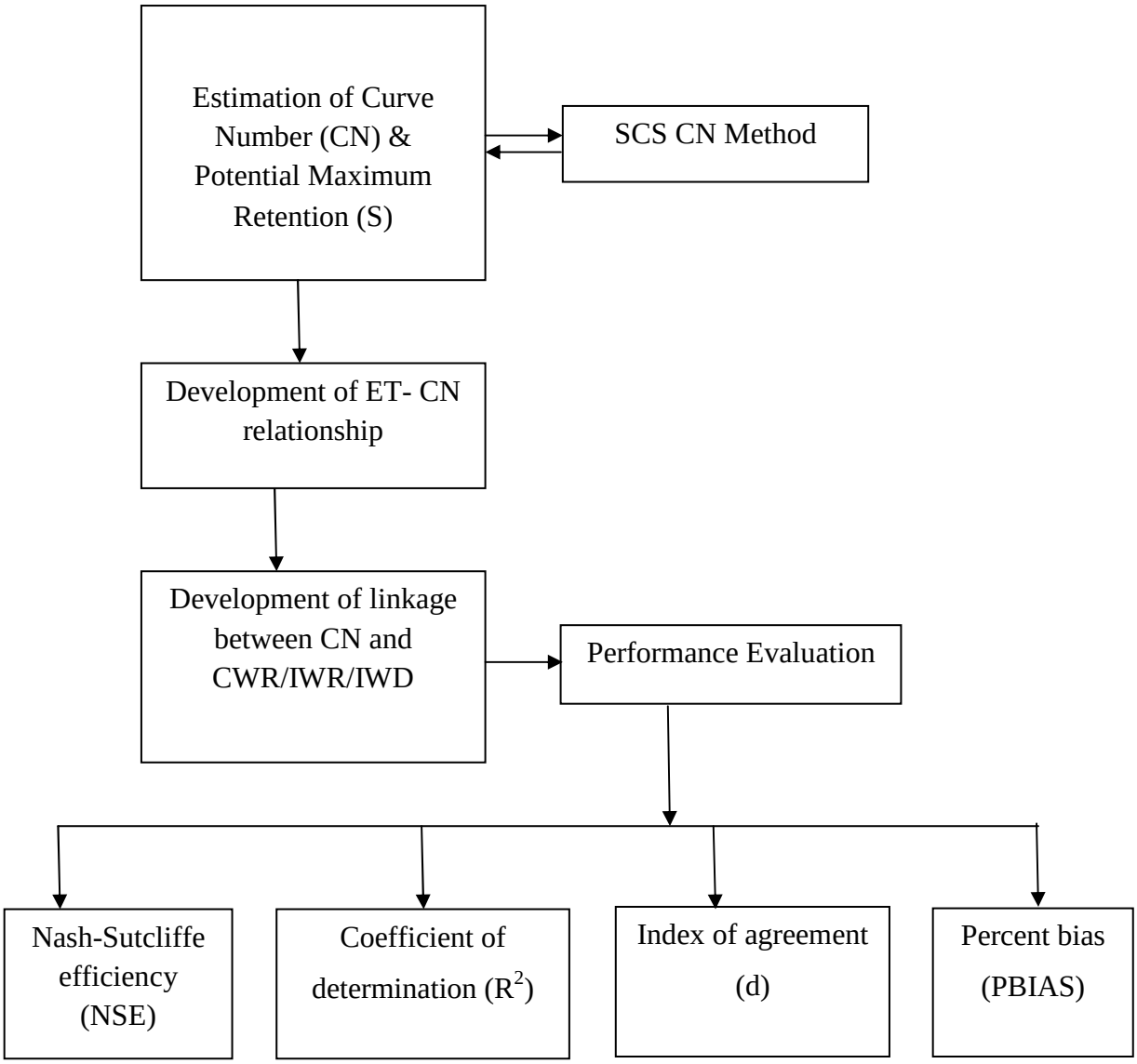

Figure 7.1 Flowchart describing methodology to establish IWR-CN relationship

7.3 RESULTS

For derivation of CN-IWR relationship, the 50 years of dataset is divided into two parts. The first 30 years of data (1960-1989) have been used for deriving the relationship, and the remaining 20 years of data (1990-2010) for its validation. Also validation is done for datasets of four different periods (i.e., 1990-1994, 1995-1999, 2000-2004 and 2005-2010) in order to avoid the effect of trend in the data series. To this end, yearly IWR and CN values for major crops in Kharif (Paddy) and Rabi seasons (Wheat and Summer Paddy) in Seonath basin have been computed as follows.

7.3.1 Determination of CN

CN values have been derived from Eqs. 7.5 and 7.6 using seasonal rainfall-runoff data for both monsoon and post-monsoon seasons separately. To this end, base flow has been excluded from the total daily runoff values. Then annual series of (accumulated) seasonal rainfall-runoff data for each year has been prepared for both seasons separately. It provides the estimates of S or CN values for rainy season and non rainy season for every year. Since the seasonal rainfall generated runoff represents the characteristics of whole watershed, CN values derived also represent the seasonal watershed characteristic. For derivation of CN-IWR relationship, two separate series of rainfall-runoff data for both seasons have been prepared to determine corresponding CN values (Eqs. 7.5 and 7.6) for each season.

Here instead of using daily rainfall runoff data to derive CN, seasonal values are used. As IWR is calculated on seasonal basis for two seasons viz. monsoon and post-monsoon. To follow the same scale seasonal CN is derived and used in the study to derive a relationship between IWR-CN.

7.3.2 Relationship between CN and IWR

For derivation of CN-IWR relationship, the CWR have been computed for crop growth stage (Table 7.1) for deriving the values of IWR. The CN-values derived from 30 years (1960-1989) rainfall-runoff data for each monsoon and post-monsoon season have been plotted against the corresponding IWR values (Table 7.2a and 7.2b), yielding a relation in power form.

$$IWR = \alpha S^{\beta} \qquad (7.23)$$

Where, α and β are the coefficient and exponent, respectively. Since there exists an inverse relationship between S and CN (Eq. 7.6), Eq. 7.16 suggests IWR to be high for the watershed of low CN, and vice versa. When S approaches zero, IWR also approaches zero and it is physically describable in terms of IWR being nil for the fully saturated (wet) watershed. On the other hand, when S approaches infinity, IWR also approaches infinity as the soil is able to absorb the whole amount of rain water supplied. The range of IWR and CN is presented in Table 7.3. As seen from Figures. 7.2 a and 7.2 b, the values of α and β are 0.007 and 2.984 and 96.56 and 0.431 for monsoon and post-monsoon seasons,

respectively. The above value indicates that α is inversely proportional to β. The value of α increase as the value of S is increasing. Thus, α is an indicator of S. As IWR is a function of S, therefore with the increase of IWR the value of α will be more. Eq. 7.23 is fitted with R^2 of 0.970 and 0.926 for monsoon and non-monsoon seasons, respectively. These reasonably high values of R^2 indicate that there is a strong relationship between CN and IWR for both the seasons.

Table 7.1 Computation of CWR for Kharif Paddy (P), Rabi Wheat (W) and Summer Paddy (SP) for each stages of crop growth period (1960-1989, calibration period)

Year	Crop Water Requirement (CWR, mm)											
	Initial Stage			Development Stage			Mid Season Stage			Late Season Stage		
	P	W	SP	P	W	SP	P	W	SP	P	W	SP
1960	353.2	53.8	57.35	142.1	109.9	106.03	107.6	53.46	84.710	79.53	67.79	119.74
1961	350.8	53.4	57.14	141.0	109.5	110.18	107.6	55.46	88.264	81.86	70.91	115.64
1962	333.7	51.9	56.17	139.3	107.6	108.18	104.4	53.74	84.531	79.63	67.93	120.71
1963	353.1	52.8	58.33	141.8	111.8	107.25	109.8	54.18	85.608	84.97	68.30	114.86
1964	364.4	54.0	56.98	145.9	109.2	105.42	107.4	52.05	82.512	82.25	66.88	120.55
1965	348.3	54.0	58.6	135.9	112.4	106.15	105.3	54.00	84.493	83.25	66.69	117.74
1966	351.0	54.7	56.40	136.9	108.1	107.49	110.1	54.02	83.962	81.72	66.46	115.56
1967	339.3	52.7	55.26	141.0	105.9	102.93	104.4	53.51	85.480	83.32	67.56	118.30
1968	349.5	53.4	58.21	141.7	111.5	109.36	106.3	54.88	86.721	81.77	69.47	117.33
1969	346.0	51.6	55.9	138.	107.1	105.7	107.8	53.4	85.339	83.0	68.5	113.95
1970	345.2	54.2	56.52	136.2	108.3	109.00	108.7	54.16	83.967	83.53	66.82	119.37

1971	353.9	53.0	55.82	147.3	106.9	106.47	108.4	54.67	86.963	84.23	69.03	114.32
1972	370.3	53.0	57.31	145.6	109.8	104.44	110.2	53.97	85.131	85.14	66.94	119.29
1973	365.1	54.3	57.47	134.2	110.1	106.31	109.2	54.69	86.211	80.93	67.93	116.84
1974	352.6	55.9	56.93	137.9	109.1	106.03	114.5	53.78	84.657	80.74	67.20	113.52
1975	353.1	54.2	55.42	139.5	106.2	104.77	104.4	53.76	86.655	83.18	69.42	121.39
1976	340.9	52.7	57.00	139.7	109.2	105.25	106.6	53.21	83.521	84.74	66.32	118.84
1977	323.1	54.4	57.45	140.0	110.1	102.87	113.7	53.25	85.385	83.49	67.84	115.39
1978	383.5	54.5	56.70	144.7	108.6	110.26	112.5	54.79	85.401	82.30	68.20	117.89
1979	362.7	54.0	57.35	150.6	109.9	106.72	114.1	54.08	85.779	80.37	68.49	125.64
1980	362.1	51.4	57.89	159.1	110.9	108.22	124.3	54.43	87.791	84.81	71.19	121.79
1981	350.5	53.5	55.56	146.3	106.5	105.74	102.8	54.21	87.220	85.21	69.82	120.03
1982	346.4	53.2	57.89	138.4	110.9	105.78	106.9	53.62	84.647	86.30	67.36	116.09
1983	340.9	52.8	57.12	137.5	109.4	107.17	107.7	54.95	88.076	82.63	70.33	117.12
1984	338.7	54.1	56.75	130.9	108.7	103.46	104.8	52.83	84.991	81.95	68.20	114.59
1985	352.4	51.5	56.93	144.1	109.1	107.57	104.2	54.97	85.947	85.49	67.62	116.49
1986	323.5	52.4	58.12	137.8	111.4	110.14	105.7	55.20	85.344	81.84	67.42	119.43
1987	346.1	53.5	57.86	137.1	110.9	107.69	107.4	54.41	85.953	87.09	68.57	114.38
1988	359.1	52.8	57.21	134.5	109.6	107.98	117.5	53.49	85.033	84.25	68.92	116.73
1989	367.0	52.6	57.70	144.3	110.6	105.91	109.9	53.13	85.108	79.53	68.80	115.64

Table 7.2(a) Computation of ETo, CWR, IWR, CN for derivation of CN-IWR relation for monsoon season

Year	Rainfall (mm)	Runoff (mm)	Potential Maximum Retention (S, mm)	Curve Number (CN)	ETo (mm)	CWR (mm)	Effective Rainfall (Pe, mm)	IWR (mm)
1960	1159.25	1127.16	27.262	90.307	718.09	682.60	621.844	167.9
1961	669.995	635.705	29.628	89.553	725.22	681.35	485.508	179.1
1962	599.676	575.704	20.547	92.515	689.99	657.20	395.845	62.09
1963	1130.05	1094.24	30.517	89.274	731.83	689.68	633.165	192.2
1964	1303.64	1275.71	23.626	91.489	707.07	700.13	638.041	102.9
1965	777.316	748.050	25.042	91.025	708.07	672.85	535.742	120.6
1966	855.541	828.930	22.665	91.807	702.89	679.88	549.109	88.56
1967	1205.51	1182.82	19.164	92.984	676.89	668.18	579.621	20.74
1968	1045.90	1011.82	29.051	89.736	724.59	679.43	598.538	176.3
1969	893.751	862.613	26.592	90.522	712.65	675.01	590.295	139.7
1970	854.939	828.349	22.647	91.813	702.50	673.88	526.093	87.56
1971	978.033	951.629	22.423	91.887	700.82	693.92	580.225	81.18
1972	811.557	780.367	26.704	90.486	714.19	711.35	568.479	142.8
1973	883.923	844.289	34.091	88.166	757.04	689.59	624.914	261.3
1974	685.644	655.476	25.932	90.736	712.14	685.87	509.573	137.1
1975	1122.70	1083.54	33.438	88.366	748.09	680.36	659.620	205.9

1976	918.059	891.541	22.551	91.845	700.89	672.06	532.291	84.72
1977	945.746	915.854	25.469	90.886	708.56	660.43	572.872	130.7
1978	976.073	953.086	19.474	92.879	682.79	723.11	539.451	56.51
1979	732.016	703.635	24.306	91.266	707.35	707.94	534.371	113.7
1980	1046.50	1009.57	31.547	88.951	738.45	730.44	627.533	195.4
1981	958.650	926.735	27.225	90.319	715.91	684.99	575.562	147.7
1982	742.990	716.178	22.917	91.724	705.50	678.22	510.275	96.33
1983	899.952	867.921	27.369	90.272	720.73	668.82	572.494	173.5
1984	836.975	811.172	21.973	92.037	696.73	656.55	535.918	80.89
1985	961.764	926.978	29.735	89.519	725.26	686.43	605.257	183.6
1986	870.922	846.926	20.386	92.570	684.87	648.97	534.989	60.76
1987	658.691	629.716	24.907	91.069	707.67	677.89	471.908	113.9
1988	688.988	660.840	24.142	91.320	707.07	695.54	503.344	109.4
1989	736.983	711.526	21.735	92.117	695.67	700.89	521.719	64.67

Table 7.2(b) Computation of ETo, CWR, IWR, CN for derivation of CN-IWR relation for post monsoon season

Year	Rainfall	Runoff	S (mm)	CN	ETo	CWR	Pe (mm)	IWR
1960	26.527	6.340	37.787	87.049	584.848	652.857	26.116	611.5
1961	111.696	75.516	39.033	86.679	585.685	660.572	106.482	473.3
1962	57.902	12.368	89.439	73.957	601.236	650.925	55.935	551.4

1963	26.957	6.668	37.405	87.163	584.735	653.230	26.405	619.7
1964	34.598	13.247	31.894	88.844	580.532	647.693	33.672	586.8
1965	13.767	1.561	30.313	89.338	578.531	654.240	13.650	630.2
1966	24.567	6.042	34.241	88.121	581.720	646.733	24.163	607.8
1967	92.179	53.899	45.131	84.912	590.046	641.720	86.415	476.8
1968	75.795	39.617	45.557	84.791	590.375	661.025	73.724	526.1
1969	28.385	6.689	40.862	86.142	586.571	641.788	27.937	595.6
1970	44.681	14.173	50.101	83.524	591.066	652.407	43.908	580.3
1971	130.333	69.968	74.848	77.239	595.101	647.320	123.415	455.4
1972	131.357	92.863	40.381	86.282	586.353	649.987	122.122	488.4
1973	85.955	35.995	71.179	78.111	593.244	653.970	82.830	530.2
1974	81.812	44.402	46.092	84.640	590.480	647.265	79.884	513.5
1975	121.677	67.311	66.237	79.316	593.090	651.888	116.249	458.4
1976	103.193	69.517	36.413	87.461	582.378	646.214	99.305	479.5
1977	110.888	65.683	52.884	82.767	591.244	646.772	106.879	482.3
1978	139.232	98.542	42.654	85.621	587.327	656.471	133.081	423.1
1979	114.430	69.029	52.532	82.862	591.157	662.059	110.178	476.5
1980	123.513	60.745	81.842	75.631	597.137	663.739	117.769	479.4
1981	127.535	89.543	40.029	86.385	585.820	652.672	121.696	439.5
1982	131.249	90.784	43.037	85.511	588.624	649.586	126.061	427.6
1983	128.062	88.295	42.378	85.701	587.231	657.082	122.997	446.9
1984	154.437	89.589	76.816	76.779	596.464	643.769	145.409	397.4

1985	75.974	42.099	41.230	86.034	586.970	650.246	73.981	526.1
1986	184.536	126.031	62.722	80.196	592.555	659.492	174.596	355.0
1987	125.911	94.530	31.681	88.910	579.230	653.322	120.384	469.3
1988	60.376	27.993	43.643	85.336	589.425	651.900	58.665	560.1
1989	53.617	24.173	40.300	86.306	586.003	649.547	52.502	565.4

Table 7.3 Range of IWR and CN for Seonath River Basin

Factors	Monsoon Season	Post Monsoon
Coefficient (α)	0.007	96.56
Exponent (β)	2.984	0.431
IWR range (mm)	57-192	423-620
Range of CN	89-93	76-89

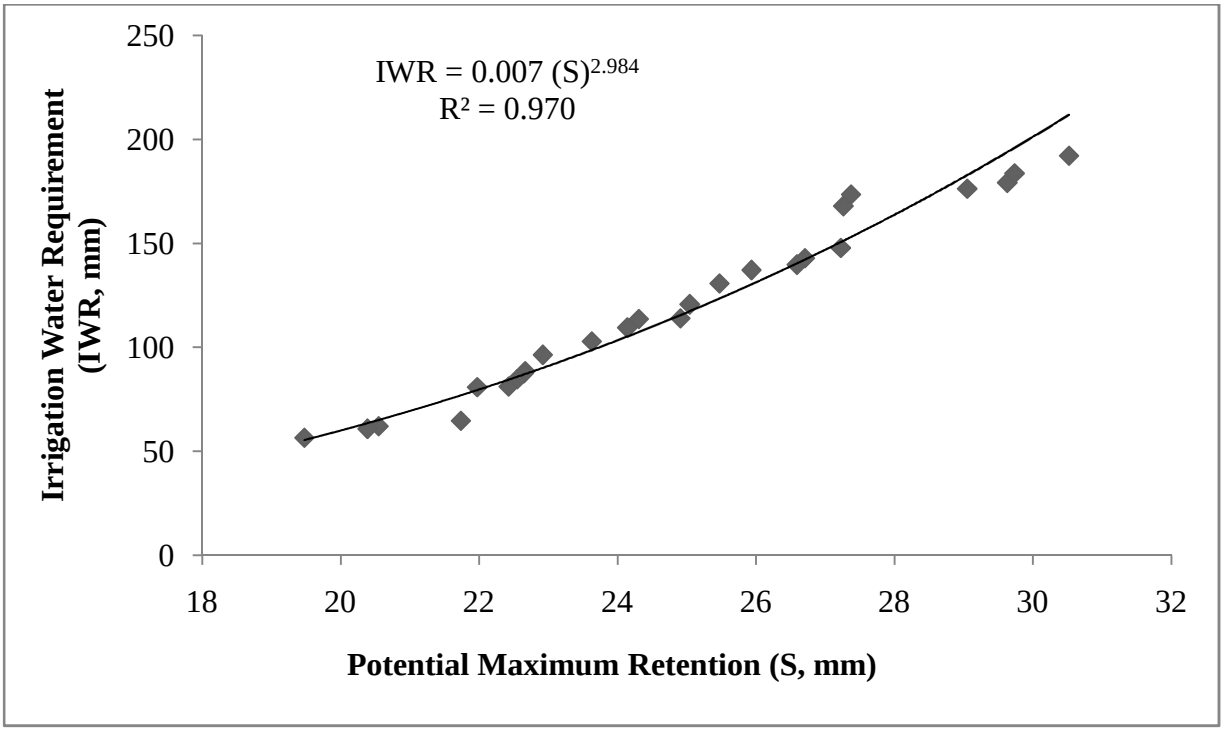

(a) Monsoon

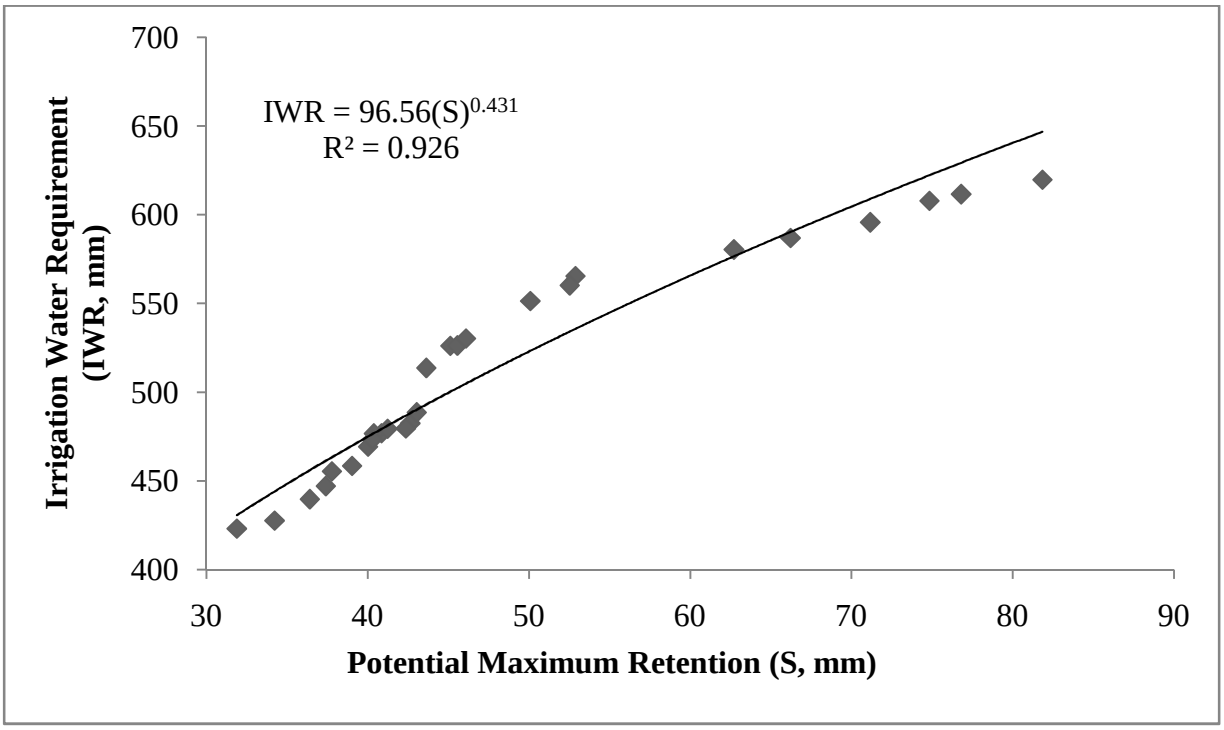

(b) Post-Monsoon

Fig. 7.2 Development of a relationship between IWR and S for (a) Monsoon (b) Post-monsoon seasons.

7.3.3 Validation of the Proposed Relationship

The above derived relation is validated using the data of 20 years (from 1990-2010) and the results are shown in Figs. 7.3 a and 7.3 b for monsoon and non-monsoon seasons, respectively. The developed model is evaluated with statistical measures and errors (Table 7.4). The PBIAS values for calibration period is -2.37% for monsoon and for post-monsoon period, it is 0.26% whereas 3.22% and 0.52% for validation period respectively. However highest values of NSE and R^2 values indicate the very good performance rating. The calculated values of Index of agreement (d) for monsoon and post-monsoon season is 0.99 which is close to 1 which indicates perfect agreement between the measured and simulated values. A close match with R^2 of 0.957 for monsoon season and R^2 of 0.954 for non-monsoon season warrants the applicability of the CN-IWR relationship to the studied basin. Again shorter period of dataset is used to validate the relationship. The 4 datasets (1990-1994, 1995-1999, 2000-2004 and 2005-2010) have been used to assess the accuracy of the proposed model. The values of R^2 and NSE ranging from 0.965-0.975, 0.948-0.963 and 0.915-0.964, 0.867-0.969 have been achieved for monsoon and post-monsoon season respectively except for the period (2000-2004, Figures 7.4 a and b). The lower values of $R^2$and NSE have been observed during the period (2000-2004) because there are few severe drought years. In the years 2000-2004 there are exceptionally dry conditions which led to very high estimates of IWR and consequently there is crop failure. It is noticed that the seasonal rainfall is less than corresponding mean rainfall in the order of -43.86%, -45.41 and -48.15% in the post-monsoon season of 2000, 2001 and 2002 respectively. The values of percentage departure for monsoon season in above years were -33.12%, -34.58% and 35.47% respectively. The details of percentage deviation of rainfall for monsoon and post-monsoon seasons are presented in Table 7.5. Therefore the proposed relationship is having low R^2 values for drought years forms the major limitation of the proposed model.

To show the existence of relationship between CN and IWR the major factors which affect CN are considered in order to evaluate their impact on IWR. It is obvious that the CN value is low for sandy soil (group A) and high for clayey (soil group D). However, the water holding of the sandy soil is low compared to clayey soil. Therefore comparatively, less water is available for crop in sandy soil. Thus the irrigation requirement for crops grown in sandy soil would be more as compared to clayey soil. This indicates that the CN and IWR have inverse relationship. Further, a soil with greater salt content often leads to clogging of soil pores resulting in reduction of hydraulic conductivity and, in turn, infiltration and

consequently leads to more CN values. On the other hand presence of salts cause low evaporation from soil under given meteorological conditions due to inclusion of one more resistance caused by salt crust. Thus, ET reduces with increase in salt content and would result lesser IWR. This again supports strong inverse relationship between IWR and CN.

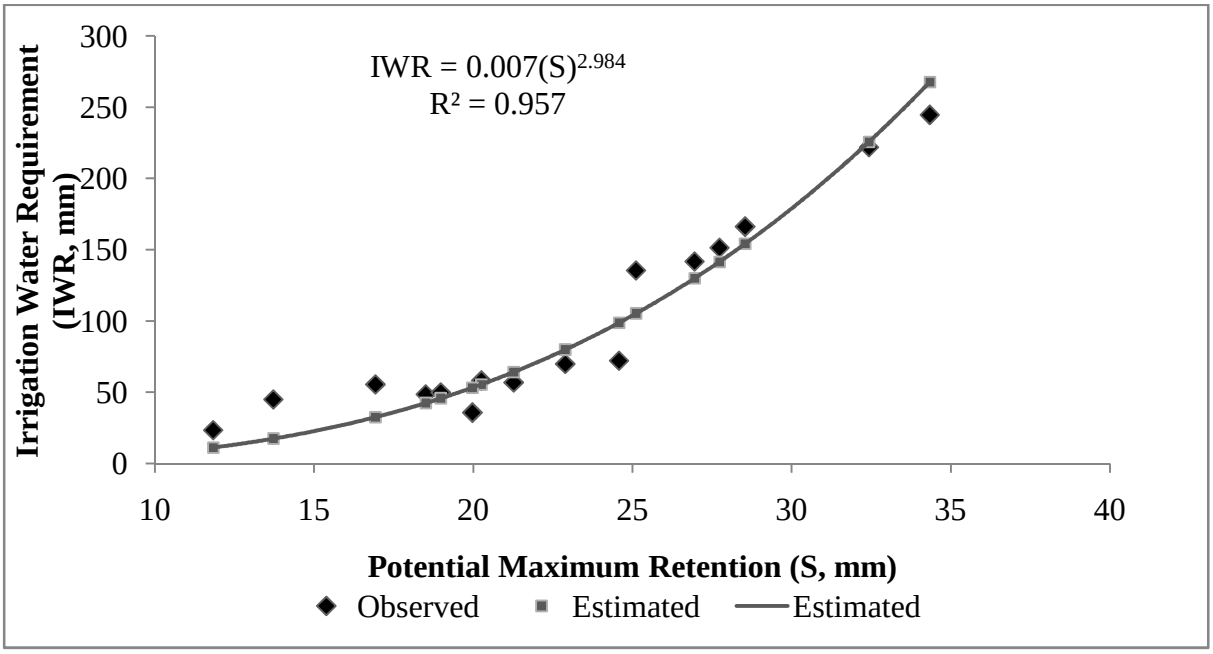

(a) Monsoon

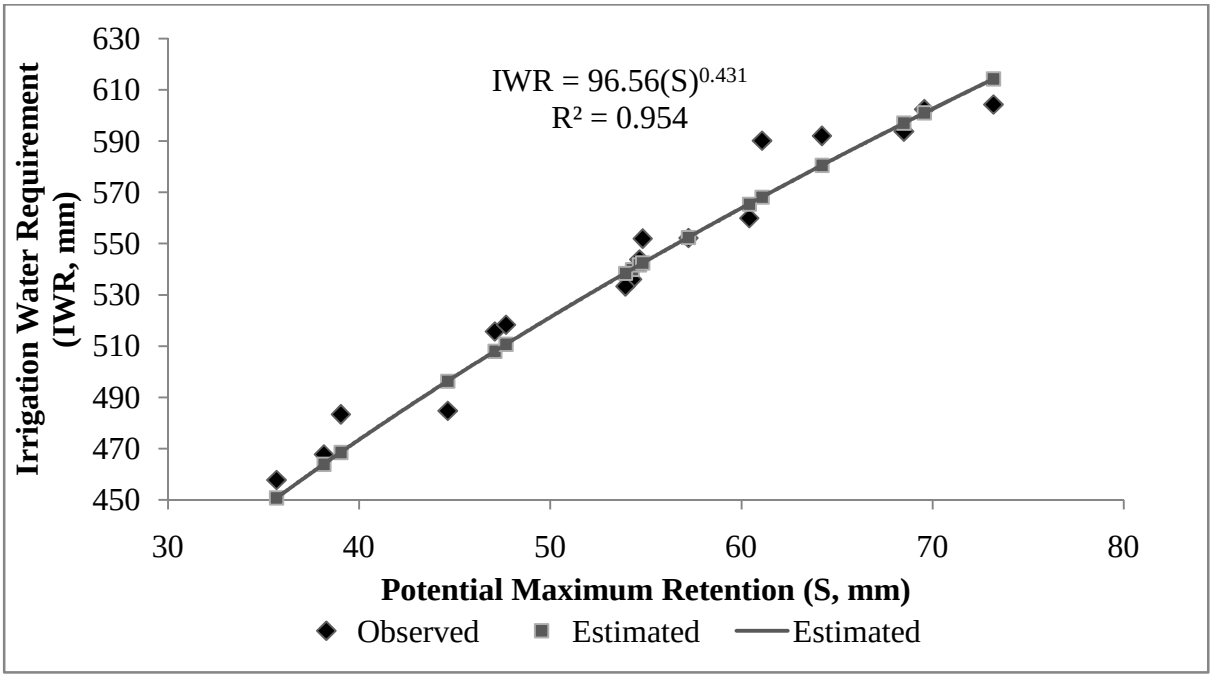

(b) Post Monsoon

Figure 7.3 Validation of IWR-S relationship for (a) monsoon and (b) non-monsoon seasons

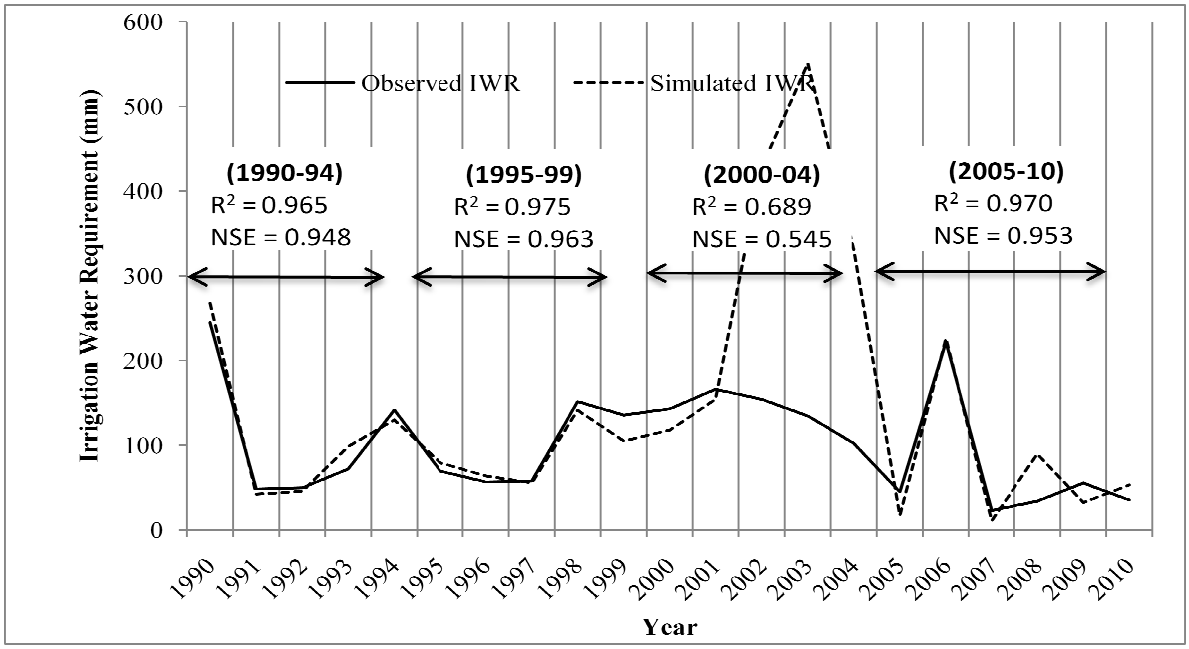

(a) Monsoon

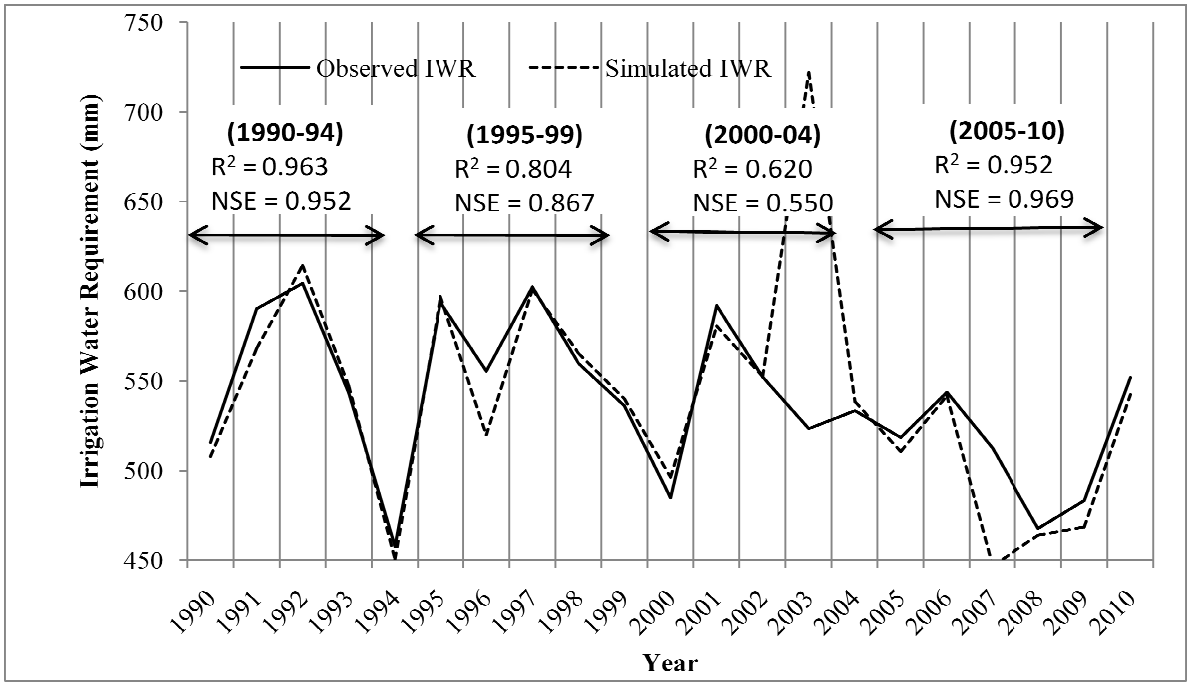

(b) Post-Monsoon

Figure 7.4 Validation of proposed model for 4 datasets (1990-94, 1995-99, 2000-04, 2005-10) for (a) Monsoon (b) Post-Monsoon seasons

Table 7.4 Performance Evaluation of Developed Model

Evaluation Statistics	Seasons			
	Monsoon		Post Monsoon	
	Calibration	Validation	Calibration	Validation
Coefficient of Determination (R^2)	0.970	0.956	0.925	0.953
Nash-Sutcliffe efficiency (NSE)	0.984	0.936	0.839	0.961
Index of agreement (d)	0.999	0.998	0.998	0.999
Percent bias (PBIAS)	-2.376	3.217	0.261	0.522
Root Mean Square Error (RMSE)	6.769	7.438	2.107	6.185

Table 7.5 Rainfall deviation for monsoon and post-monsoon season

Year	Monsoon		Post Monsoon	
	Rainfall Deviation (%)	Drought Type	Rainfall Deviation (%)	Drought Type
2000	-33.12	Mild	-43.86	Moderate
2001	-34.56	Moderate	-45.41	Severe
2002	-35.47	Moderate	-48.15	Severe
2003	-13.65	No Drought	-25.86	Mild
2004	-15.30	No Drought	-24.47	No Drought

7.3.4 Advantages and Limitations of Proposed Model

The proposed model provides very good relationship between IWR and CN. Therefore, it may be reasonable substitute for complex IWR assessment, particularly in the area where meteorological parameters are not easily available. In addition, the model is able to make quick assessment of water requirement for the crops in a given region and therefore it may be useful in the design and management of irrigation systems. The use of model may be limited to sub humid climatic regions of India. Further studies are required for assessment of its applicability to other regions. In addition, since parameter λ is a regional parameter that depends on geological and climatic factors and hence a vital parameter in ET/CWR/IWR estimation, results may be improved by using value other than the standard value of 0.2 for other climatic regions. Moreover, it is feasible to quantitatively study the effect of climate change on hydrologic systems employing CN-IWR relationship. The basin used in this study is an agricultural basin with slight or no alteration in land use, and thus, the efficiency of the proposed model need to be examined in future.

7.4 SUMMARY

In this chapter, the results of analysis have been discussed and a relationship between IWR and SCS-CN parameter i.e. potential maximum retention (S) has been proposed. Mathematical and physical justification of IWR-CN rationale invokes the existence of a relationship between the seasonal IWR and runoff curve numbers (or potential maximum retention). The proposed model of relationship was calibrated and verified by employing a large set of hydro-meteorological data of Seonath river basin in Chhattisgarh State in India. Subsequently, the curve numbers derived from rainfall-runoff data exhibit a strong correlation (of power form) with IWR derived using standard method. High R^2 and NSE values support a strong relationship to exist and work satisfactorily. Thus, IWR-CN relationship is very useful especially for field engineers in irrigation planning and water resource management.

CHAPTER 8

STATISTICAL DOWNSCALING OF CLIMATIC VARIABLES, THEIR FUTURE PREDICTION AND IMPACT ON IRRIGATION WATER REQUIREMENT

This Chapter is divided into two sections. First part presents downscaling of daily climatic variables viz., precipitation, maximum temperature (Tmax), minimum temperature (Tmin), relative humidity (RH) and wind speed (WS) for Seonath River Basin in Chhattisgarh State of India using different downscaling methods. The inter-comparison of statistical downscaling methods has been carried out to identify best prediction model for the study area. The study compares four statistical downscaling methods using results from Global Circulation Models (GCMs). The climatic variables are generated for the period 2011–2100 under climate change projections for a future scenario A2. The second part of the chapter presents projected climate change scenarios of rainfall as well as other meteorological variables which influence the evapotranspiration (viz., RH, WS, Tmax and Tmin). Subsequently, the projected estimates of above climatic variables have been used to assess the impacts of climate change on irrigation water requirement (IWR) in Seonath Basin.

8.1 INTRODUCTION

Global Circulation Models (GCM) is used to project the changes in atmospheric variables under the climate change scenarios defined by the Intergovernmental Panel for Climate Change (IPCC). These climate projections are defined at a coarse grid (approximately 150–300 km) and are often biased and hence cannot be used directly in hydrological models for climate change impact assessments (Fowler et al., 2007). Thus there is a need for downscaling of GCM data. More recently, downscaling has found wide application in hydro-climatology for scenario generation and simulation/ prediction of regional precipitation, low-frequency rainfall events, mean, minimum and maximum air temperature, soil moisture, runoff and streamflow, water quality and many more.

There are two main downscaling approaches i) dynamic and, ii) statistical downscaling. In the dynamic downscaling method a Regional Climate Model (RCM) is embedded into GCM. The RCM is essentially a numerical model in which GCMs are used

to fix boundary conditions. The major disadvantage of RCM, which limits its use in climate impact studies, is due to its high computational cost and complex design. Furthermore, RCM is rigid in terms of expanding the region or moving to a somewhat different region needs rebuilding of complete experiment (Crane and Hewitson, 1998). The second approach to downscaling, termed statistical downscaling, involves deriving empirical relationships that transform large-scale features of the GCM (Predictors) to regional-scale variables (predictands) such as precipitation, temperature and streamflow. There are three implicit assumptions involved in statistical downscaling (Hewitson and Crane, 1996). First, the predictors are variables of relevance and are realistically modeled by the host GCM. Second, the empirical relationship is valid also under altered climatic conditions. Third, the predictors employed fully represent the climate change signal.

A large number of techniques have been developed for statistical downscaling. These can be categorised into three main classes: i) weather typing schemes, ii) weather generators and, iii) regression models (Fowler et al., 2007). The Regression models directly calculate a correlation between the regional climatic variable (e.g. rainfall) and large-scale atmospheric variables. Stochastic weather generators (WG) are statistical methods that predict climatic variables based on statistical characteristics of the variable (Burton et al., 2008; Kilsby et al., 2007; Semenov and Stratonovitch, 2010). Weather typing includes grouping days into a finite number of distinct weather category or “states” based on their synoptic resemblance (Wilby et al., 2004). GCM or RCM are then used to estimate the change in the frequency of weather types in order to estimate climate change (Fowler et al., 2007).

In the past studies, hydro-meteorological variables were downscaled using linear regression (Benestad et al., 2007; Cannon and Whitfield, 2002; Cheng et al., 2008; Goyal and Ojha, 2010; Najafi et al., 2011), PCA (Tolika et al., 2006; Wetterhall et al., 2006), CCA (Tolika et al., 2006), ANN (Goyal and Ojha, 2012; Tisseuil et al., 2010; Tripathi et al., 2006), and SVM (Anandhi et al., 2009; Chen et al., 2008; Ghosh and Mujumdar, 2008; Najafi et al., 2011; Tripathi et al., 2006). Among them, ANN based downscaling techniques have gained wide recognition owing to their ability to capture nonlinear relationships between predictors and predictand (Cannon and Whitfield, 2002; Tisseuil et al., 2010). Despite a number of advantages, the traditional neural network methods have numerous disadvantages including the possibility of getting trapped in local minima and subjectivity in the choice of model architecture (Suykens, 2001). Recently, Vapnik (1998) developed a

novel machine learning algorithm, called SVM, which provides an elegant solution to these problems. The SVM has theoretically proved better than other techniques in transfer functions in climate impact studies in hydrology (Tripathi et al., 2006).

The rising CO_2 and climate change due to global warming directly affect both rainfall and evapotranspiration, consequently the irrigation water requirement. Moreover, the irrigation water requirements of the crops change as a function of climate change. Several authors have focused on assessing the impacts of climate change on agriculture, over the past decade. Most of these studies concentrated on estimating the changes in crop productivity. Assessment studies focusing on the impacts of climate change on irrigation requirement using GCM outputs are becoming more accepted in recent years. This study is undertaken to examine and compare four statistical downscaling methods and identify the best model for future prediction. Further, the predicted climatic variables viz., Tmax, Tmin, RH and WS have been used to estimate changes in reference evapotranspiration (ETo) and to assess their impact on IWR for major crops in Seonath Basin.

8.2 MATERIAL AND METHODS

In this chapter four models have been selected viz, ANN, Model Tree, Multiple linear Regression (MLR) and Least Square Support Vector Machine (LS-SVM) to downscale the climatic variables. The methodology of the present study is presented in the form of flowchart (Figure 8.1).

8.2.1 Dataset

In this study to forecast the rainfall, Tmax, Tmin, RH and WS the daily data of eight meteorological stations have been used. In this study, the outputs of Hadley Center's GCM (HadCM3) have been utilized for A2 Scenario. A2 scenario is based on the assumption that the atmospheric CO2 concentrations will reach 850 ppm in the year 2100 in a world characterized by high population growth, medium GDP growth, high energy use, medium/high land-use changes, low resource availability and slow introduction of new and efficient technologies, which matches with the Indian condition. Therefore, in the present study, only A2 scenario data of HadCM3 are used. Large-scale NCEP reanalysis atmospheric data have been used as the model predictors. Spatial resolution (dimensions of grid box) of HadCM3 outputs is 3.75° (long.) × 2.5° (lat.), whereas it is 2.5° (long.) × 2.5° (lat.) for NCEP data. Therefore, projected large-scale predictors of NCEP on HadCM3 computational grid box have been used. These data and HadCM3 daily simulations are

supported and distributed by the Canadian Climate Change Scenarios Network (CCCSN) (http://www.cccsn.ec.gc.ca) and also the Canadian Climate Impacts Scenarios (CCIS) website (www.cics.uvic.ca/scenarios/sdsm/select.cgi). There are 26 different predictors for each grid box in this database. For each station, nine boxes covering the study area have been selected.

8.2.2 Methodology

The various steps involved in the estimation of future daily meteorological variables are as follows: 1) Both predictors and predictands (1961−2001) are normalized using their respective means and standard deviations for further analysis. 2) The physical relationship and cross correlation method is used to select appropriate predictors at different pressure level and grid point 3) Performed Principal Component Analysis (PCA) to reduce the dimensions of the standardized predictor data, i.e. NCEP/NCAR reanalysis climate data set, pertaining to the study area and preserve the eigen vectors obtained therein. The dimensionally-reduced climate variables represent a large fraction of the variability contained in the original data. 4) Training of the model(s) i.e, calibration (1961-1990) to establish relationship between the input data containing current day standardized and dimensionally-reduced climate predictors along with previous day(s) rainfall state and the output data containing the current day rainfall state. 5) Obtained principal components of GCM data by performing PCA of the GCM data with the help of principal directions (eigen vectors) obtained during PCA of NCEP/NCAR reanalysis data. 6) Used the trained model to derive present day rainfall state of the river basin with the help of principal components obtained from GCM output and rainfall state of the previous day. 7) Applied bias correction for the predicted output data to obtain bias-corrected future data. The various models employed in this study are described in next section. 8) Validated the results with remaining set of data i.e., 1991-2001.

8.2.2.1 Least Square Support Vector Machine (LS-SVM)

The Least Square Support Vector Machine (LS-SVM), which has been used in this study. It provides a computational advantage over standard SVM by converting quadratic optimization problem into a system of linear equations (Suykens, 2001). The LS-SVM optimization problem for function estimation is formulated by minimizing the cost function $\psi_L(w,e)$.

$$\boldsymbol{\psi} \mathrm{L}(\mathrm{w}, \mathrm{e}) = \frac{1}{2}\, \mathrm{w}^{\mathrm{T}}\mathrm{w} + \frac{1}{2}\mathrm{C}\sum_{\mathrm{i}=1}^{\mathrm{N}} \mathrm{ei}^2$$

subjected to the equality constraint

$$y_i - \bar{y_i} = e_i \ \mathrm{i}= 1 \ldots \mathrm{N} \tag{8.1}$$

Important differences with standard SVMs are the equality constraints and the quadratic loss term e^2_i , which greatly simplifies the problem. The solution of the optimization problem is obtained by considering the Lagrangian as

$$\mathrm{L}(\mathrm{w}, \mathrm{b}, \mathrm{e}, \alpha) = \frac{1}{2}\, \mathrm{w}^{\mathrm{T}}\mathrm{w} + \frac{1}{2}\mathrm{C}\sum_{\mathrm{i}=1}^{\mathrm{N}} \mathrm{ei}^2 - \sum_{\mathrm{i}=1}^{\mathrm{N}} \alpha_{\mathrm{i}} \{\bar{\mathrm{y}}_{\imath} + \mathrm{e}_{\mathrm{i}} - \mathrm{y}_{\mathrm{i}}\} \tag{8.2}$$

where α_i are Lagrange multipliers. The conditions for optimality are given by

$$\left\{\begin{array}{c} \frac{\partial L}{\partial w} = w - \sum_{i=1}^{N} \alpha_i \phi(x_i) = 0 \\ \frac{\partial L}{\partial b} = \sum_{i=1}^{N} \propto_i = 0 \\ \frac{\partial L}{\partial ei} = \alpha_i - Cei = 0 \ \ i = 1, \ldots N \\ \frac{\partial L}{\partial xi} = \bar{y_i} + e_i - y_i = 0 \ \ \ i = 1, \ldots N \end{array}\right\} \tag{8.3}$$

The above conditions of optimality can be expressed as the solution to the following set of linear equations after elimination of w and e_i.

$$\begin{bmatrix} 0 & \overrightarrow{1^T} \\ \vec{1} & \Omega + C^{-1}I \end{bmatrix} \begin{bmatrix} b \\ \propto \end{bmatrix} = \begin{bmatrix} 0 \\ y \end{bmatrix},$$

$$\text{Where, } \mathrm{y} = \begin{bmatrix} y_1 \\ y_2 \\ \vdots \\ y_N \end{bmatrix}; \overrightarrow{1} = \begin{bmatrix} 1 \\ 1 \\ \vdots \\ 1 \end{bmatrix}_{N\times N} ; \alpha = \begin{bmatrix} \propto_1 \\ \propto_2 \\ \vdots \\ \propto_N \end{bmatrix}; I = \begin{bmatrix} 1 & 0 & \cdots & 0 \\ 0 & 1 & \cdots & 0 \\ \vdots & \vdots & \vdots & \vdots \\ 0 & 0 & \cdots & 1 \end{bmatrix}_{N\times N} \tag{8.4}$$

In Eq. (8.5), Ω is obtained from the application of Mercer's theorem.

$$\Omega \mathrm{i}.\mathrm{j} \ = \ \mathrm{K}(\mathrm{xi}, \mathrm{xj}) = \ \phi\ (\mathrm{xi})\mathrm{T}\ \phi(\mathrm{xj}) \forall \mathrm{i}, \mathrm{j} \tag{8.5}$$

The resulting LS-SVM model for function estimation is

$$f(x) = \sum \alpha_i\, K(xi, x) + b^* \tag{8.6}$$

where αi and b* are the solutions to Eq. (8.5). It is worth mentioning that developing LS-SVM with RBF kernel involve selection of RBF kernel width r and parameter C.

8.2.2.2 Artificial Neural Network Model

Artificial neural network is simply understood as a nonlinear statistical data modeling tool that presents complex relationships between predictors (input layer) and predictants (output layer) through a synapse system (hidden layers) connecting predictors with predictants, or the so-called required outputs. As a result, ANN has demonstrated its wide range of application to solve complicated problems in many fields, for instance, engineering and environment.

The RBF network consists typically of two layers, where the hidden layer nodes contain prototype vectors (or basis centres), which are in effect hidden layer weights. The distance between the input and the prototype vector determines the activation level of the hidden layer with the non-linearity provided by a basis function. The activation function in the output layer can be non-linear, however, training is considerably faster if an ordinary linear weighted sum of these activations are performed, and this approach is consequently adopted. The main parameter that needs to be set is the number of nodes in the hidden layer. In this study 30 nodes have been used for the prediction.

The MLP network is not necessarily restricted to one hidden layer, although it has been demonstrated that any continuous function can be mapped to an arbitrary degree of accuracy by a single hidden layer (Hornik et al., 1989). The configuration used in this investigation is a single hidden layer. The ANN model has been trained using MLP back-propagation algorithm network with simple structure, four nodes in the input layer, single hidden layer with seven nodes and one node in the output layer. Input to the model is the present-day rainfall data (t) and the 3-day lagged rainfall [(t-1)(t-2)(t-3)], while the output is rainfall of the next day (t+1). The transfer function used is the sigmoid function with 500 numbers of epochs.

8.2.2.3 Multiple Linear Regression (MLR)

The most common and basic linear transfer function is the MLR. A predictand, y, from an observation site in a local region can be downscaled using the following MLR equation (von Storch, 1999; Hessami et al., 2008)

$$y = X\beta + \varepsilon; \qquad (8.7)$$

where, ε [n x 1] is a residual vector of MLR and the parameter vector β [q x 1] can be estimated by the ordinary least squares estimation method below (Chatterjee and Price, 1977)

$$\hat{\beta} = (X^T X)^{-1} X^T y \quad (8.8)$$

The variance–covariance matrix for the vector of coefficients of the MLR with OLS estimate, $\hat{\beta}$ is given by the following

$$Var(\widehat{\beta}) = \sigma^2 (X^T X)^{-1} \quad (8.9)$$

Where, σ^2 is the variance of the error term of the MLR model.

From Eq. 8.9, the standard error of an estimate parameter, $\hat{\beta}$ (m= 1, 2,…, q) is given by (Chatterjee and Price, 1977)

$$\text{se}(\widehat{\beta_m}) = \frac{\sigma}{\sqrt{\sum_{i=1}^{N} (X_{mi} - \overline{X_m})^2 (1 - C_m^2)}} \quad (8.10)$$

where, σ is the standard error of the predictand y from the MLR model, and C^2_m is the R^2 (coefficient of determination, the square of the correlation coefficient between the model outcomes and predictand values) of the regression when X_m is a dependent variable and the other X_js ($j \neq m$) are independent variables. If X_m is correlated to the other independent variables, C^2_m becomes larger and that increases the standard error of $\widehat{\beta_m}$: However, several factors influence se($\widehat{\beta_m}$) other than C^2_m . For example, increased standard error (σ) of the MLR model because of poor accuracy also increases the standard error of ($\widehat{\beta_m}$): Furthermore, the variability of independent variable X_m, as given by $\sum(X_{mi} - \overline{X_m})^2$, is inversely related to se($\widehat{\beta_m}$). Therefore, if the new $X_{mi} \neq \overline{X_m}$; including new records of X_{mi} by increasing the sample size increases the variability and decreases se($\widehat{\beta_m}$).

8.2.2.4 Model Tree Method

Model tree is a method of language change described by an analogy with the concept of family tree. It has originally developed by Quinlan (1992). Model trees combine a conventional decision tree with the possibility of generating linear regression functions at the leaves. Only few papers in water-related applications are present, for example, Kompare et al. (1997) and Solomatine and Dulal (2003) for rainfall-runoff modelling and Bhattacharya and Solomatine (2002) for modelling the stage discharge relationship.

If the tree model which is generated has an excess quantity of leaves, it may lead to be an overfit model. The model can then be made more robust by pruning the leaves. Pruning, in a general sense, means to cut off or remove dead or living parts or branches of a plant, to improve shape or growth. Thus, in a similar way here the lower sub-trees are merged into a single node.

The Smoothing process is used to compensate for the sharp discontinuities that will inevitably occur between adjacent linear models at the leaves of the pruned trees. Smoothing is accomplished by producing linear models for each internal node, as well as for the leaves at the time the tree is built (Witten and Frank, 2000). It has been observed experimentally that smoothing increases the accuracy of prediction. In this study the model tree with pruning and with smoothing (MTPS) is employed for future prediction.

For all above described downscaling models the programming is written in MATLAB R2009a.

8.2.2.5 Bias Correction

In this study non-linear correction method suggested by Leander and Buishand (2007) have been used. Using this method GCM simulated daily climatic variables are bias corrected by a power law relationship $P^* = aP^b$. In this method statistics such as mean, standard deviation and coefficient of variation have been matched with corresponding value calculated from observed values. Therefore this method is used in the study as consider all the statistics for bias correction.

The constant “a” and “b” are calculated by in the following steps. i) the exponent “b” is calculated by iteration, so that the coefficient of variation of the predicted time series (daily climatic variables) matches with observed dataset. It is obtained by Brent’s method (Press et al., 1986). The exponent “b” is the only function of coefficient of variation; (ii) the coefficient “a” is calculated so that the average of the simulated values is equal to the average observed value. This aforesaid method of power law relationship is not applicable for the correction of climatic factors viz., temperature, relative humidity and wind speed because these climatic variables are considered to be normally distributed. Therefore, correction of normally distributed data set using power law relationship gives the data set which is not normally distributed. For this reason we use another method for correcting these climatic variables. The correction of climatic factors (temperature, relative humidity

and wind speed) only involves shifting and scaling to adjust the mean and variance (Leander and Buishand, 2007). The formula for correction is given below:

$$P_{corr} = \overline{P}_{obs} + \left(\frac{\sigma (P_{obs})}{\sigma (P_{gcm})} \right) \times (P_i - \overline{P_{obs}}) + (\overline{P_{obs}} - \overline{P_{gcm}}) \quad (8.11)$$

Where, P_{SDcorr} = Bias Corrected Climatic variables; $\overline{P}_{obs}$ = Mean daily observed climatic variables; $\overline{P}_{gcm}$ = Mean daily predicted climatic variables obtained from GCM; $\sigma(P_{obs})$ = Standard Deviation of the observed climatic variables; $\sigma(P_{gcm})$ = Standard Deviation of the predicted climatic variables obtained from GCM; P_i = uncorrected daily or monthly climatic variables from HadCM3 data. The above mentioned method for bias correction is widely acceptable and used by many researchers in the recent years (Terink et al., 2010; Raneesh and Thampi, 2013).

8.2.2.6 Model Evaluation Statistics

The inter-comparison of the models is evaluated using the following statistical measures.

1) Coefficient of Determination (R^2)

It is defined as the degree of collinearity between simulated and observed data. The value of R^2 lies between 0 and 1. The value tends to 1 represents the highest correlation.

$$R^2 = 1 - \frac{\sum_{i=1}^{N}(Oi - Ei)^2}{\sum_{i=1}^{N}(Oi - \overline{Oi})^2} \quad (8.12)$$

2) Nash-Sutcliffe efficiency (NSE)

The Nash-Sutcliffe efficiency (NSE) is a normalized statistic that determines the relative magnitude of the residual variance ("noise") compared to the measured data variance ("information") (Nash and Sutcliffe, 1970). NSE indicates how well the plot of observed versus simulated data fits the 1:1 line. NSE is computed as shown in Eq 7.20:

$$NSE = 1 - \left| \frac{\sum_{i=1}^{N}(Oi - Ei)^2}{\sum_{i=1}^{N}(Oi - \overline{Ei})^2} \right| \quad (8.13)$$

The better suited model for the study area could thus be obtained and it has been employed to estimate the climatic variables for future years (2011-2100) for each station. Subsequently, the above predicted meteorological variables have been used in estimation of ETo and IWR for major crops have been computed. Further, long term changes in IWR have been computed to investigate the impacts of climate change on IWR in the study area.

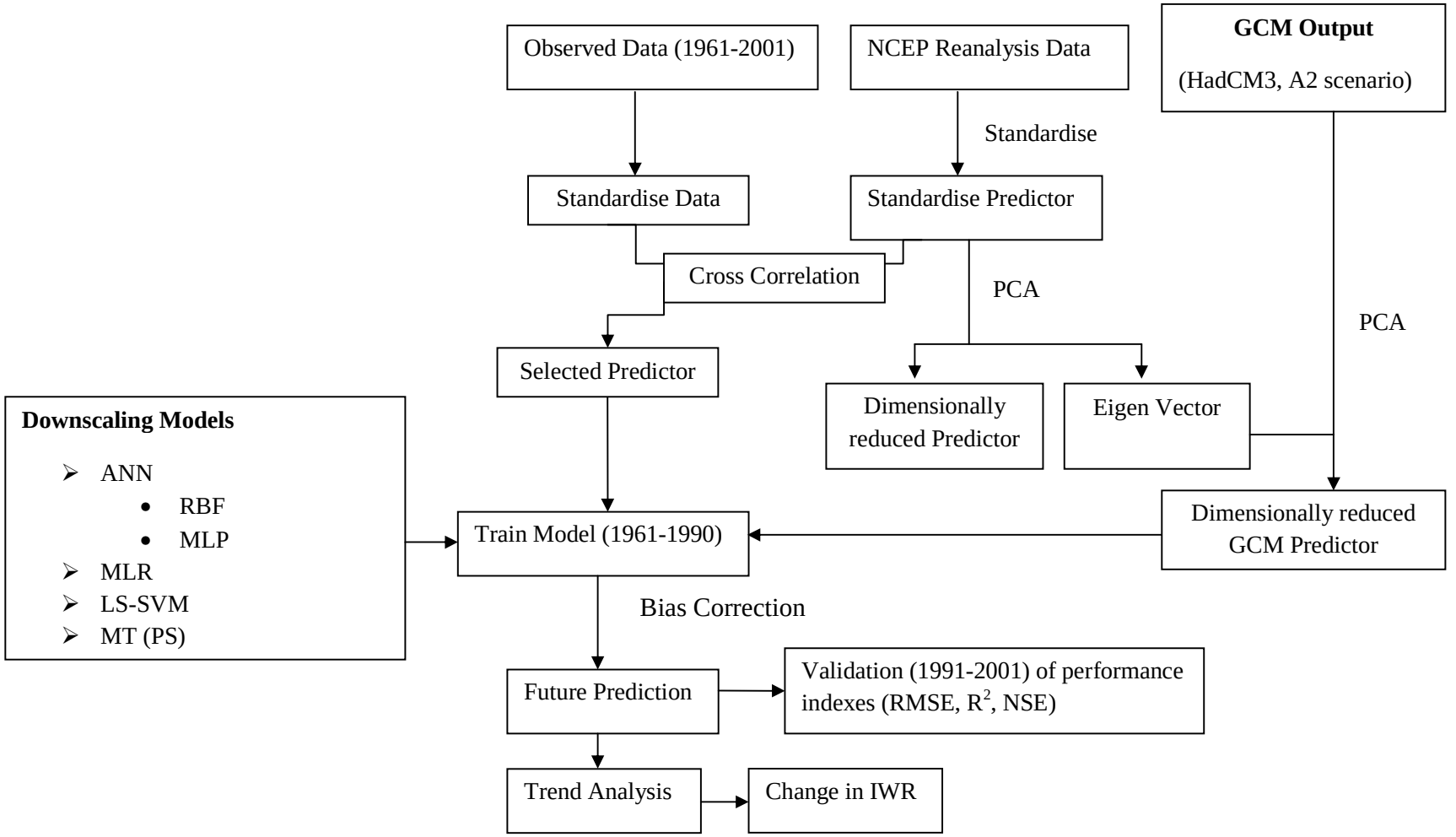

Figure 8.1 Statistical downscaling framework

8.3 RESULTS AND DISCUSSION

8.3.1 Inter-comparison of Statistical Downscaling Models

The four statistical downscaling methods previously described have been applied to eight stations of different climatic variables viz, Tmax, Tmin, Tmean, Rainfall, Relative Humidity, Wind Speed. The NSE and R^2 values for the calibration sets of meteorological variables are shown in Fig. 8.2 and the validation results are shown in Fig. 8.3. The calibration and validation results clearly indicate that for each climatic variable LS-SVM is performing best followed by MT and ANN (MLP). Lower values of NSE and R^2 are obtained for ANN (RBF) method for almost all the meteorological variables. The station-wise performance indexes for each model of different climatic variables are presented in Appendix A.

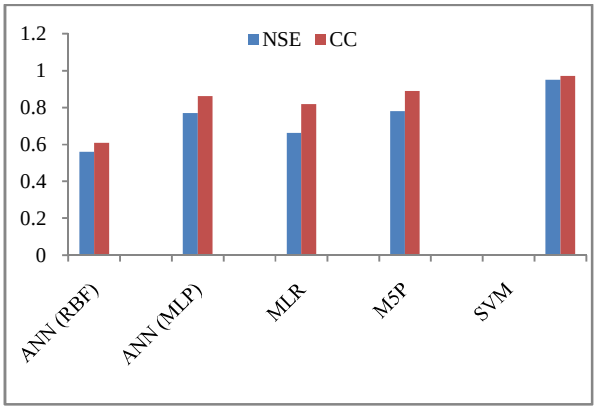

(a) Rainfall

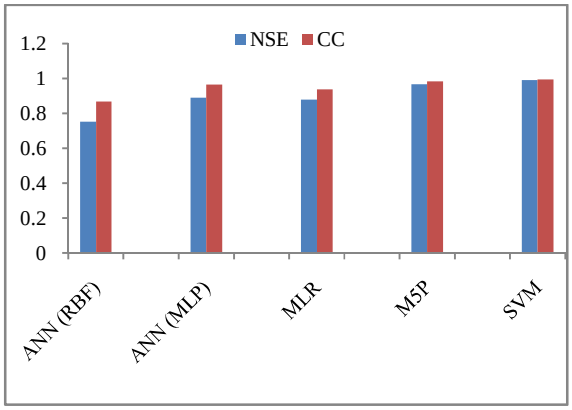

(b) Tmax

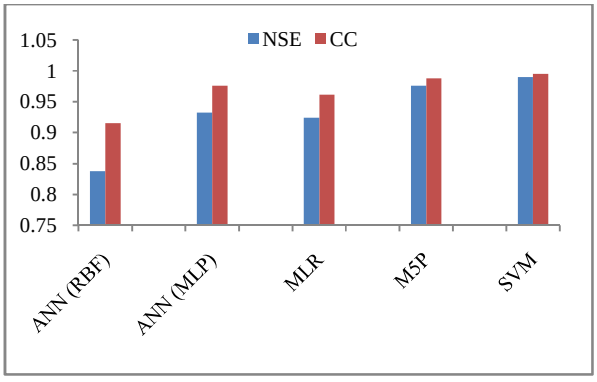

(c) Tmean

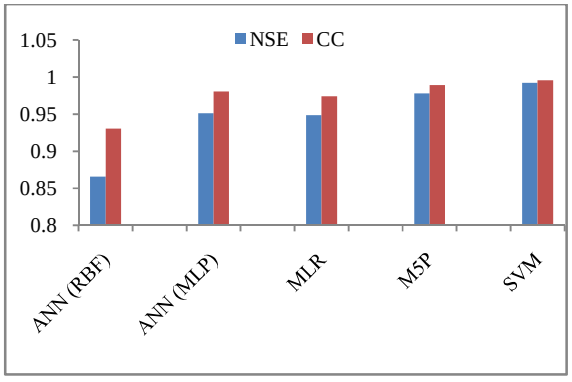

(d) Tmin

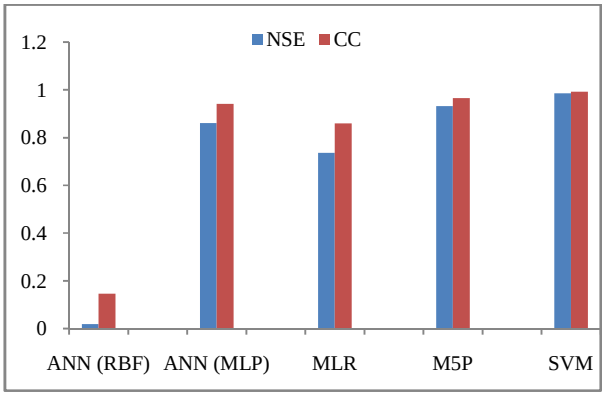

(e) Relative Humidity

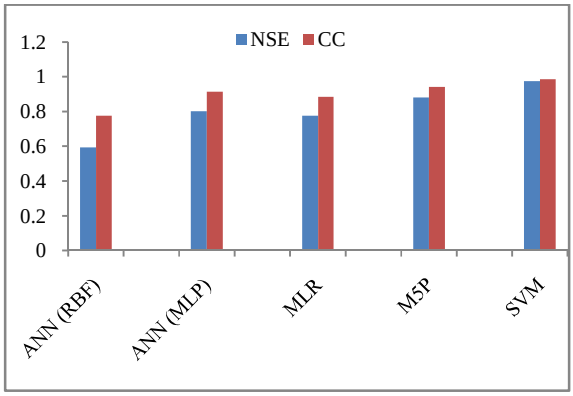

(f) Wind Speed

Fig. 8.2. NSE and R^2 calibration values for four downscaling methods

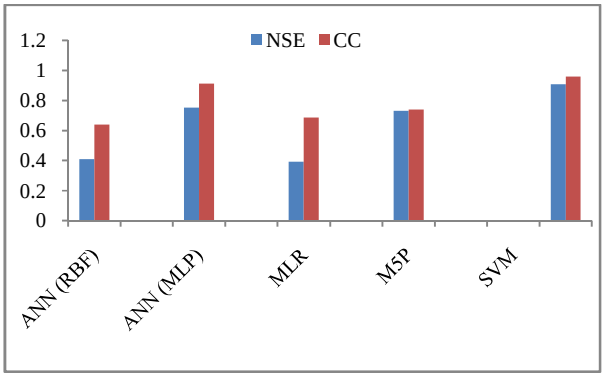

(a) Rainfall

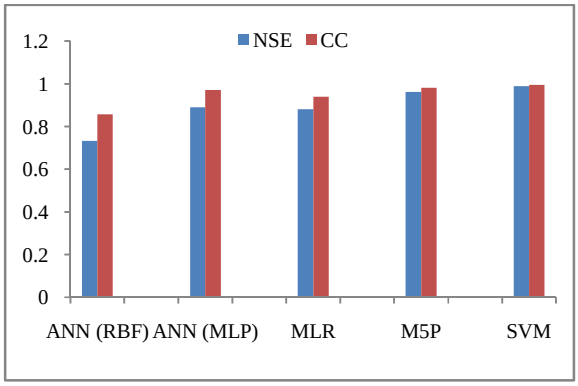

(b) Tmax

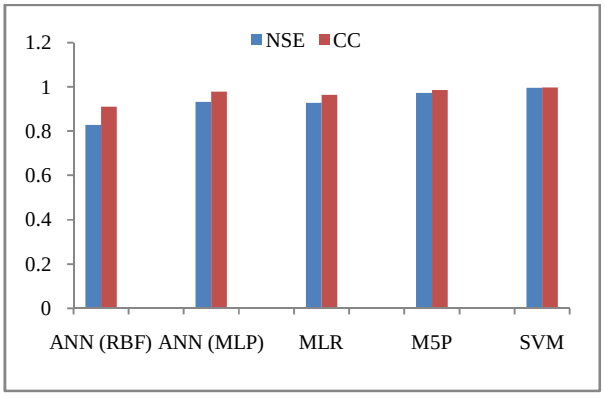

(c) Tmean

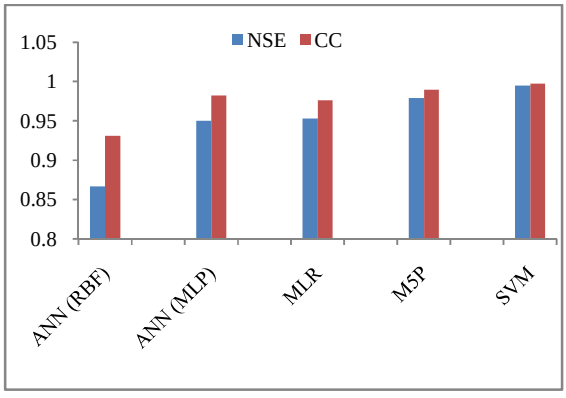

(d) Tmin

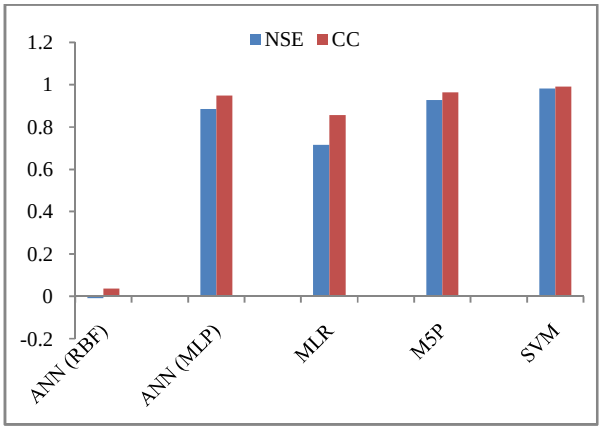

(e) Relative Humidity

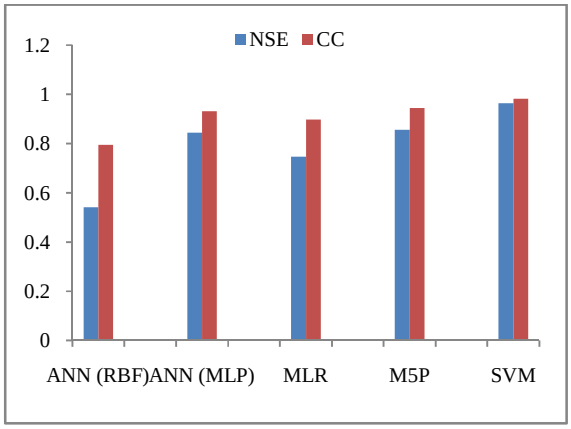

(f) Wind Speed

Fig. 8.3. NSE and R^2 validation values for four downscaling methods

Therefore from overall study it is clear that LS-SVM method is most suitable for our study area (also reported by Sachindra et al., 2013). The MT technique was also perform better and gives higher R^2 values above 0.90. The least performing model for the study area is ANN using RBF kernel which gives the lowest values of R^2 and NSE.

The climatic variables (Tmax, Tmin, Tmean, rainfall, RH and WS) are estimated using LS-SVM method. As from the above section it is clear from the results that LS-SVM method is most suitable method for our study area. The prediction of climatic variables has been done by the LS-SVM method explained in section 8.2.

8.3.2 Selection of Predictor Variables

The selection of suitable predictor variables is the most significant step for downscaling of various predictands (meteorological variables). The selection of predictors varies from region to region based on the type of predictand and the characteristics of the large-scale atmospheric circulation. Wetterhall et al. (2005) reported that any type of predictor variables can be used if, a physical relationship exists between the predictor and the predictand. Wibly et al. (2004) suggested that predictors should be selected using the following criteria: (1) the large-scale predictors should be physically relevant to the local-scale features and realistically simulated by GCMs, (2) the predictors are readily available from the archives of GCM output and reanalysis datasets, and (3) strongly correlated with the predicted. The predictor variables

are selected on the basis of physical relationship with predictands i.e., temperature, rainfall, wind speed and relative humidity (Table 8.1). The abbreviation of predictor variables are also presented in Table 8.2. The physical basis for selection of the listed predictor variables in table 8.2 is described as follows.

The suitable predictor variables for temperature prediction are selected based on physical processes. The temperature at any place depends upon circulation variables (i.e., represented by geopotential, or the wind component) and other variables such as temperature (through geopotential heights at various levels and precipitable water content in the atmosphere). Further, the temperature that occurs at any location is a result of the net radiation available and the way that radiation is budgeted. The net radiation (latent heat, sensible heat and horizontal heat transfer) depends on gains of solar and terrestrial energy. The available energy is then used for sensible heat transfer and evaporation. Therefore, in the present study, the potential predictors selected are air temperature (°C), geopotential height (meter), precipitable water content (kg/m^2), zonal and meridional wind velocities (m/s) at different pressure levels.

Likewise for rainfall suitable predictors are selected based on physical processes. The total rainfall at a place and its form depend upon a number of meteorological factors, such as the wind, temperature, humidity and pressure in the volume region enclosing the clouds and the ground surface at a given place. The occurrence of rainfall is a convection process and he physical features that dominate convective processes are: (1) changes in the pressure fields as proxied with the geo-potential height fields, (2) a transport mechanism, either the meridional or zonal winds that can advect moisture into the region, (3) a moisture mechanism as measured through specific humidity and (4) air temperature at various height levels. Therefore, in the present study, the probable predictors extracted from the NCEP and HadCM3 are air temperature, geo-potential height, specific humidity, zonal and meridional wind velocities at different pressure levels, precipitable water content and surface pressure (Table 8.2).

The selection of probable predictor variables is based on the physical relationship with the predictand (relative humidity). Humidity signifies the amount of water vapor present in the atmosphere. The relative humidity at any place is strongly related to temperature (Wypych, 2010). At a given location moisture-holding capacity of the atmosphere and the pressure varies

with temperature. The pressure gradient influences the circulation, which consecutively affects the moisture holding capacity of atmosphere and thus affects humidity. At the pressure height of 925 mb, the boundary layer (near surface effect) is significant. The latent heat signifies the amount of moisture leaving from the surface to the air. Therefore in the present study the probable predictors selected are surface air temperature (°C), air temperature (°C) at 925 mb, specific humidity (925 mb) and latent heat flux (Table 8.1).

For downscaling of wind speed, predictor variables viz., zonal and meridional velocities at 925 mb are selected as suitable predictors also reported by Anandhi (2010). The correlation coefficients between suitable predictor variables and predictands have been presented in Annexure B for each station. The predictor with high correlation values are selected for downscaling. Further PCA method is applied to selected predictors to extract principal components (PCs) which are orthogonal. A feature vector is formed for each record using PCs. The feature vector is used as an input to the LS-SVM model, whereas, predictands (rainfall, Tmax, Tmin, relative humidity and wind speed) constitutes the output of the model.

Table 8.1 Selected Predictor Variables for downscaling of predictands

S.No.	Selected predictor variables from NCEP and HadCM3 daily datasets	Predictands
1.	Prw, Ua 200, Ua 925, Va 200, Va 925, Zg 200, Zg 500, Zg 925, Ta 200, Ta 500, Ta 700, Ta 925, LH	Temperature
2.	Prw, Ua 200, Ua 925, Va 200, Va 925, Zg 200, Zg 500, Zg 925, Ta 200, Ta 500, Ta 700, Ta 925, Hus 850, Hus 925, Ps	Rainfall
3.	Ta 925, Hus 925, Ta sur, and LH	Relative Humidity
4.	Ua 925 and Va 925	Wind Speed

Table 8.2 Abbreviation of selected predictor variables

S.No.	Abbreviation	Description
1.	Hus 850	Specific humidity at 850 hPa
2.	Hus 925	Specific humidity at 925 hPa
3.	Prw	Precipitable water content
4.	Ps	Surface pressure
5.	Ta 200	Air temperature at 200 hPa
6.	Ta 500	Air temperature at 500 hPa
7.	Ta 700	Air temperature at 700 hPa
8.	Ta 925	Air temperature at 925 hPa
9.	Ta sur	Surface air temperature
10.	Zg 200	Geopotential height at 200 hPa
11.	Zg 500	Geopotential height at 500 hPa
12.	Zg 925	Geopotential height at 925 hPa
13.	Ua 200	Zonal wind at 200 hPa
14.	Ua 925	Zonal wind at 925 hPa
15.	Va 200	Meridional wind at 200 hPa
16.	Va 925	Meridional wind at 925 hPa
17.	LH	Latent Heat Flux

8.3.3 Impact of Climate Change on Meteorological Variables

Here the dataset is divided into two sections one for training (1961-1990) and other for testing (1991-2001). Figure 8.4 shows the comparison of observed vs predicted variables. The highest values of R^2 (0.98) and NSE (0.99) for rainfall shows the good correlation between predicted and observed data. Whereas for temperature the R^2 value of 0.98 for Tmax and Tmin and for Tmean its values is 0.93. For RH the R^2 value is 0.97 and for WS its value is 0.98. All the meteorological variables are well simulated by LS-SVM downscaling method (Figure 8.4) for the training period of 1961 to 1991. The station wise downscaling results are presented in Annexure C.

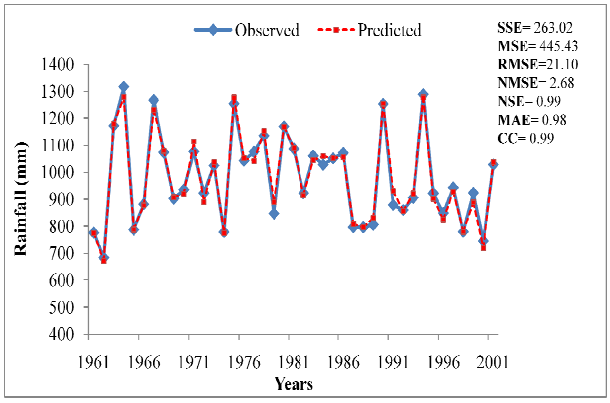

(a) Rainfall

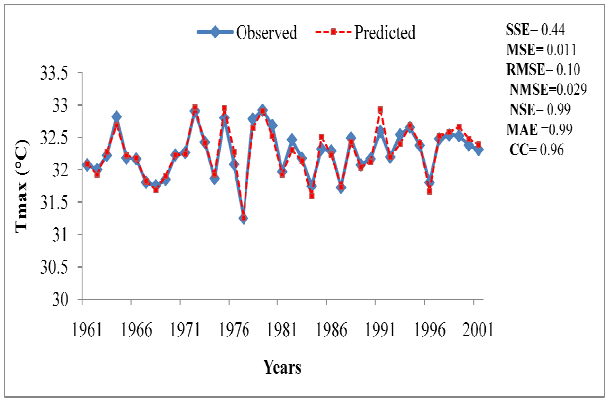

(b) Maximum Temperature (Tmax)

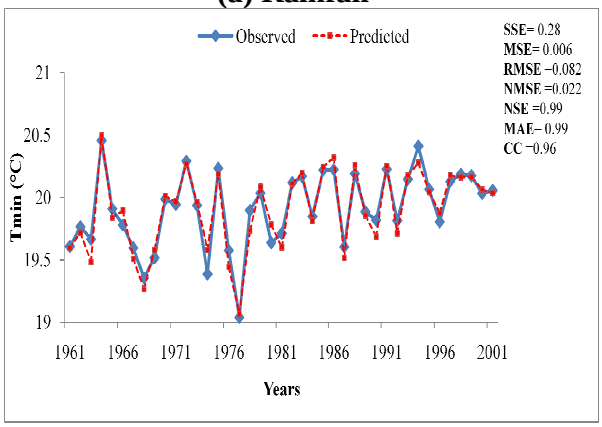

(c) Minimum Temperature (Tmin)

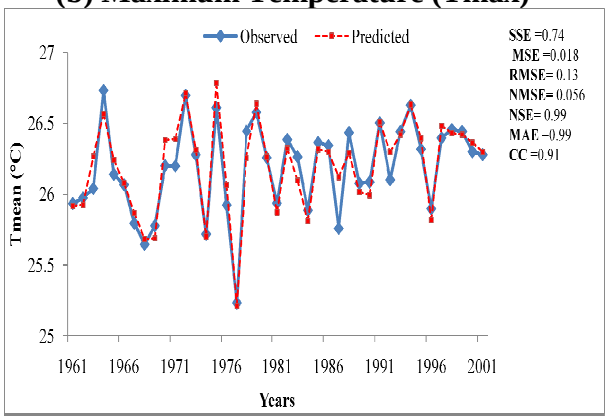

(d) Mean Temperature (Tmean)

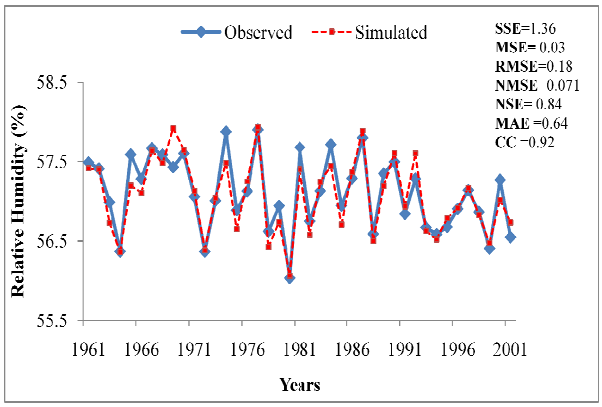

(e) Relative Humidity (RH)

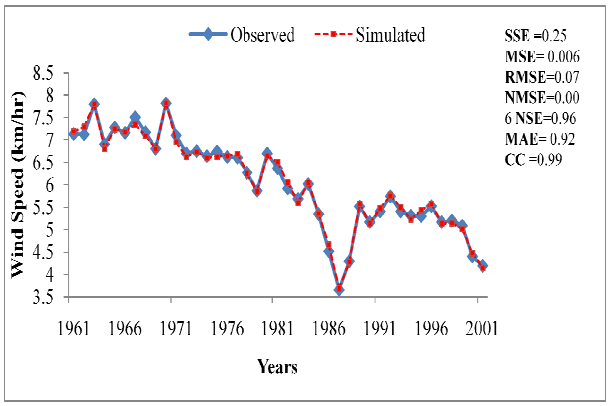

(f) Wind Speed (WS)

Figure 8.4 Downscaling results of meteorological variables for the entire basin

All future projections are for the A2 scenario and divided into nine decades (2011-2020, 2021-2030, 2031-2040, 2041-2050, 2051-2060, 2061-2070, 2071-2080, 2081-2090, and 2091-2100) have been represented in box-plot format. Figure 8.5 represents the future projections for all the meteorological variables. The projected rainfall is started increasing from 2020s and

increased upto 2050. The rainfall is started decreasing from 2071 period. There is decrease in rainfall for the period of 2091-2100 (Figure 8.5 a). For the maximum temperature the increasing trend has been observed for the entire projected period but the highest temperature change is observed for two decades i.e., 2021-2030 and 2031-2040 (Figure 8.5 b). For the minimum and mean temperature the overall increasing trend has been observed but for Tmin the highest temperature rise is for the period of 2061-2070 (Figure 8.5 c, d). The projected RH is higher for during the period of 2011 to 2040. From 2041 to 2070 the RH is comparatively lower then again increase in RH after year 2071 (Figure 8.5 e) whereas for WS shows a decreasing trend (Figure 8.5 f).

The trend and change in magnitude for temperature, rainfall, wind speed and relative humidity for the future scenarios are shown in Table 8.3. For the projected rainfall there is generally little change over the future periods. The changes in precipitation are highest for 2020s and 2050s period whereas 2090s will have little impact for both rabi and Kharif seasons (Table 8.3, Col. 1). For 2020s and 2050s periods rainfall show significant increasing trend whereas for 2090s period shows non-significant increasing trend. The predicted decadal rate of change in rainfall during Kharif and rabi varies from 2.74 to 7 mm/decade and 5mm to 12 mm/decade for 2020s and 2050s periods respectively. The maximum temperature (Tmax) shows a significant increasing trend for 2020s and 2050s period during both Kharif and rabi season whereas for 2090s period, non-significant increasing trend has been obtained (Table 8.3, Col. 3). The rate of change for Tmax varies from 0.1°C/decade to 0.5°C/decade for kharif and 0.01°C/decade to 0.3°C/decade for rabi season. The change in magnitude for minimum temperature for kharif season is varies from 0.2°C/decade to 0.75°C/decade, whereas for rabi season the rate of change varies from 0.02°C/decade to 0.57°C/decade. It can be inferred that warming is more pronounced during the night (when temperature is lower) than day. The relative humidity forecasts represent a significant decreasing trend for Kharif season, whereas for rabi season non-significant decreasing trend have been observed for two decades i.e., 2020s and 2090s period. There is very little change in projected RH for the entire growth period (Table 8.3, Col. 8). The projected wind speed shows non-significant increasing trend for the entire basin. Wind speed projections are highly uncertain with extremes in 2090s during Kharif season whereas for rabi season the uncertainty is for 2020s and 2050s period. No significant trend is observed for wind speed (Table 8.3, Col. 10). The monthly change factors for

temperature, rainfall, wind speed and relative humidity for the future scenarios are presented in Annexure D.

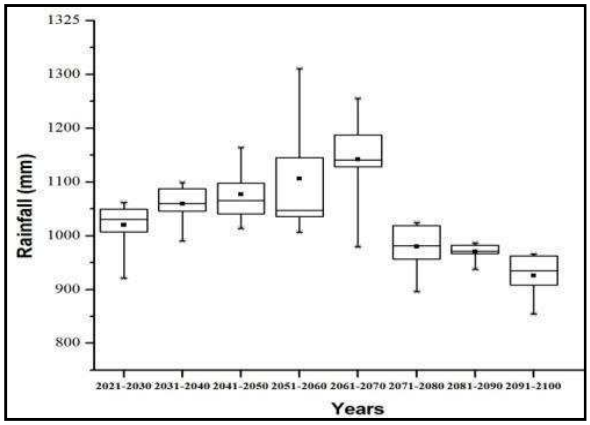

(a) Rainfall

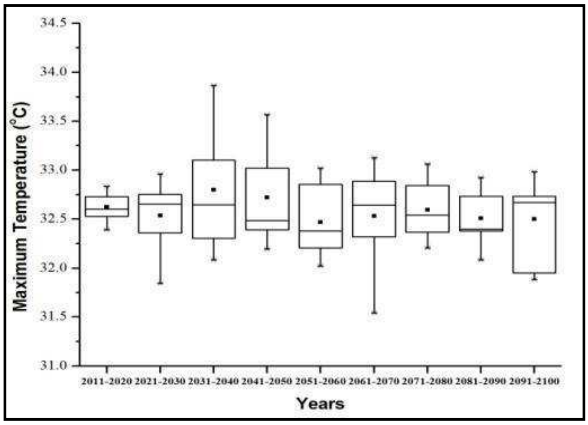

(b) Maximum Temperature (Tmax)

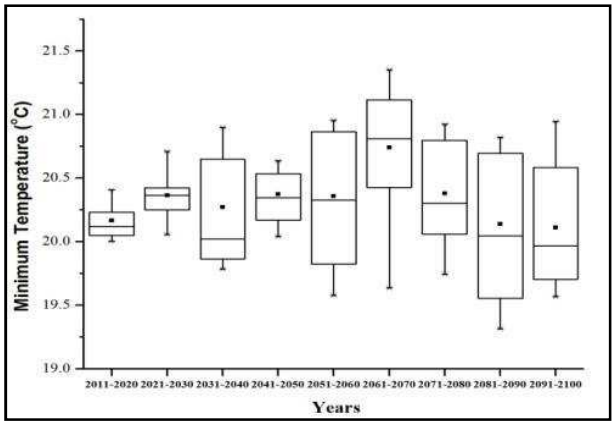

(c) Minimum Temperature (Tmin)

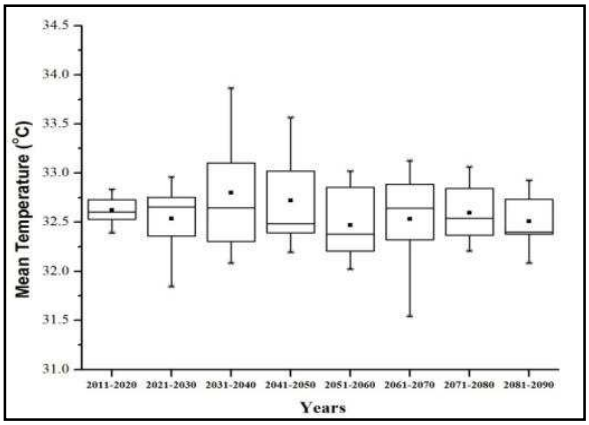

(d)Mean Temperature (Tmean)

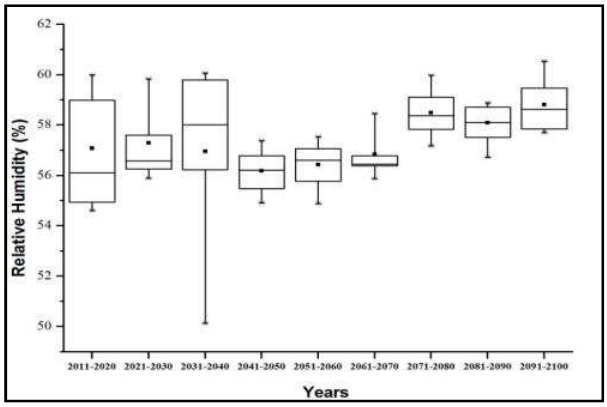

(e) Relative Humidity (RH)

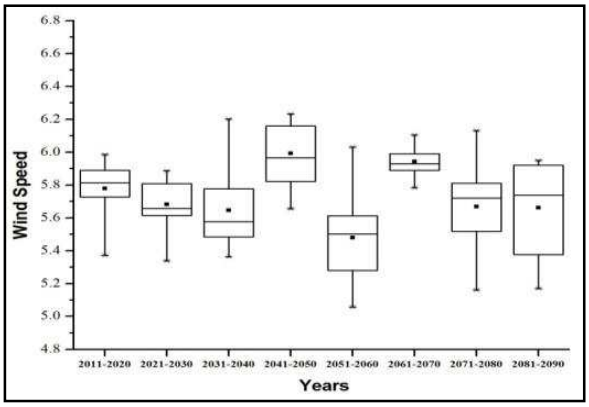

(f) Wind Speed (WS)

Figure 8.5 Future projections of climatic variables from HadCM3 GCM output with A2 scenario for entire basin

Table 8.3 Seasonal trends in climatic variables for future (2011-2100)

Seonath River Basin		Rainfall		Tmax		Tmin		Relative Humidity		Wind Speed	
		MK Test	β (mm/dec)	MK Test	β (°C/dec)	MK Test	β (°C/dec)	MK Test	β (%/dec)	MK Test	β (%/dec)
		Col.1	Col.2	Col.3	Col. 4	Col.5	Col.6	Col.7	Col.8	Col.9	Col.10
Kharif Season	2020s	**2.55**	2.74	**1.96**	0.263	**3.75**	0.44	**-3.87**	-0.55	1.96	0.2
	2050s	**4.16**	6.97	**2.06**	0.520	**1.96**	0.75	**-3.89**	-0.48	1.56	0.2
	2090s	1.26	0.11	0.21	0.149	1.63	0.20	**-4.72**	-0.57	1.05	0.6
Rabi Season	2020s	**3.33**	4.84	**3.66**	0.13	6.40	0.20	-0.35	-0.08	1.58	0.7
	2050s	**4.35**	11.85	**3.83**	0.33	5.94	0.57	**-4.14**	-0.53	1.30	0.8
	2090s	1.70	0.85	1.21	0.01	3.30	0.10	-1.69	-0.23	1.17	0.13

8.3.4 Impact of Climate Change on Reference Evapotranspiration (ETo)

The ETo is a key factor for estimating irrigation water requirement. Thus, the trend of projected ETo is necessary to evaluate for the assessment of IWR. The reference evapotranspiration estimated from the projections of Tmax and Tmin, RH and WS using the evapotranspiration method (Penman-Monteith) and observed meteorological data for the period of 1960 to 2010 is shown in Figure 8.6. The future projections of reference evapotranspiration predicted to increase for all months. Particularly, the change of evapotranspiration is more in the months of May to August due to the large projected changes of Tmax and Tmin variables. The rate of change is increasing from May to September. The peak ETo is observed for the month of June 25 mm/100 years (Figure 8.7). The rate of change on annual and seasonal scales for two decades 2011-2054 and 2055-2100 are spatially shown in Figure 8.8. From Figure 8.8 (a) the annual ETo trend is significantly increasing for the northern part of the study area whereas other parts of the basin show non-significant increasing trend. From Figure 8.8 b the lower region of the basin shows a significant increasing trend. Monsoon ETo for the period of 2011-2054 shows non-significant increasing trend for all the stations exception has been observed for bilaspur and kanker stations, which show significant increasing trend (Figure 8.8 c). However for the period of 2055-2099 the entire basin shows significant increasing trend except bilaspur station, which shows non-significant increasing trend (Figure 8.8 d). In post

monsoon season overall significant increasing trend was obtained for the first decade i.e., 2011-2054 (Figure 8.8 e). Whereas for second decade form 2055-2099 non-significant increasing trend have been obtained for the entire basin except for Bilaspur station which shows significant increasing trend (Figure 8.8 f).

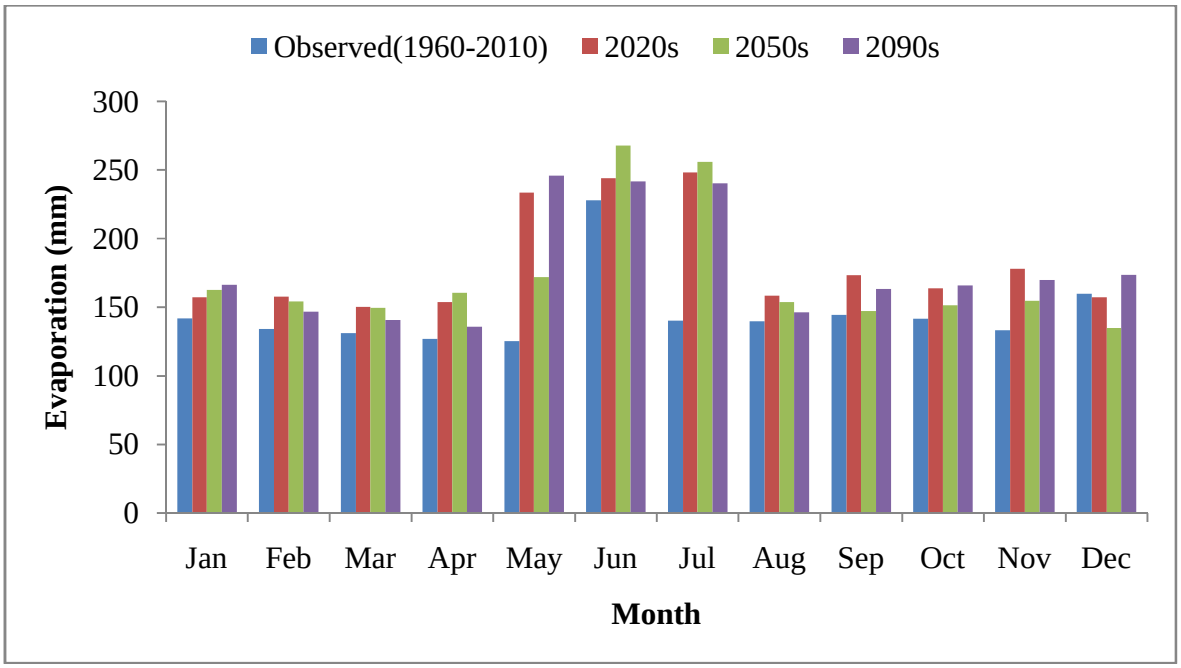

Figure 8.6 Monthly reference evapotranspiration for Seonath River Basin estimated from HadCM3 GCM output for A2 scenario

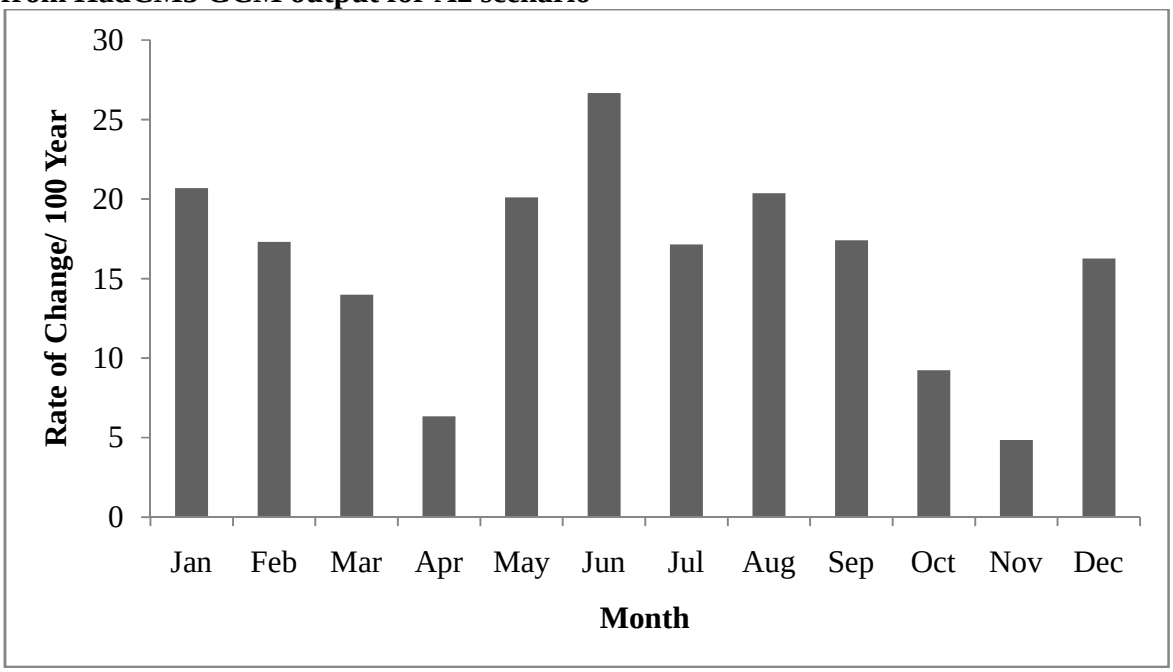

Figure 8.7 Rate of Change in Reference Evapotranspiration over 100 years

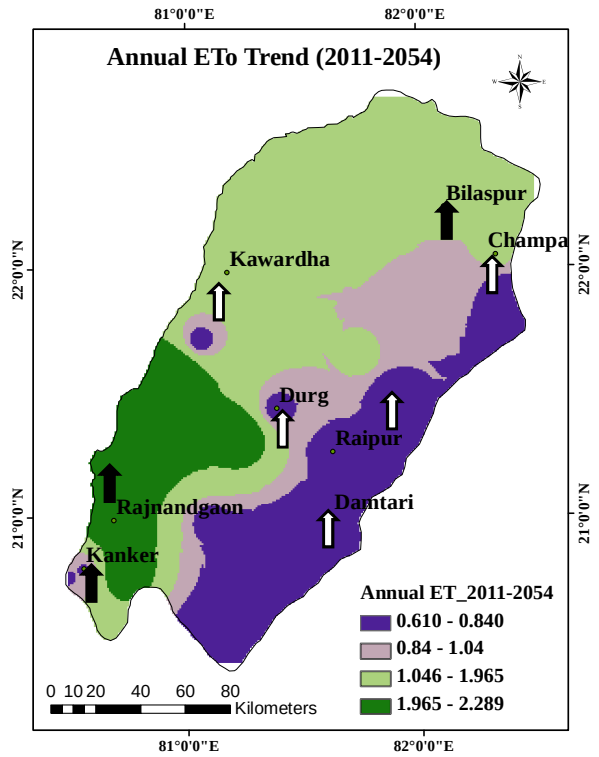

(a) Annual (2011-2054)

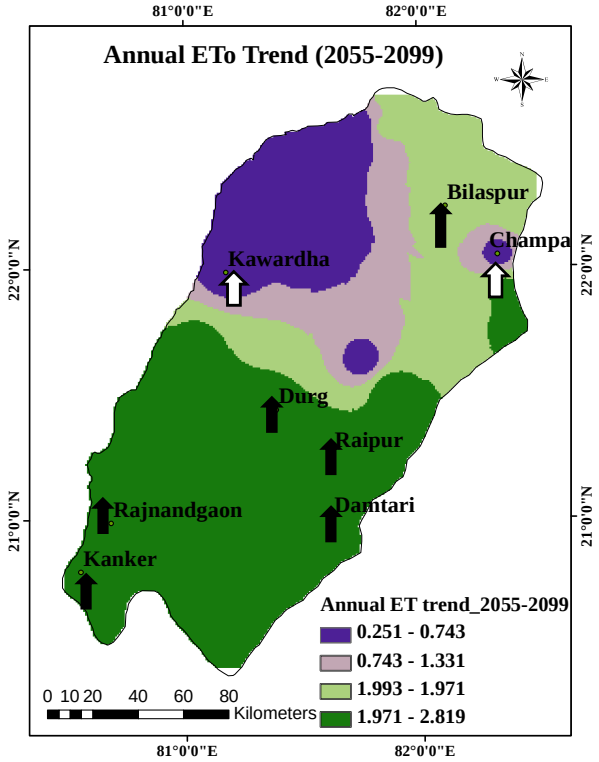

(b) Annual (2055-2099)

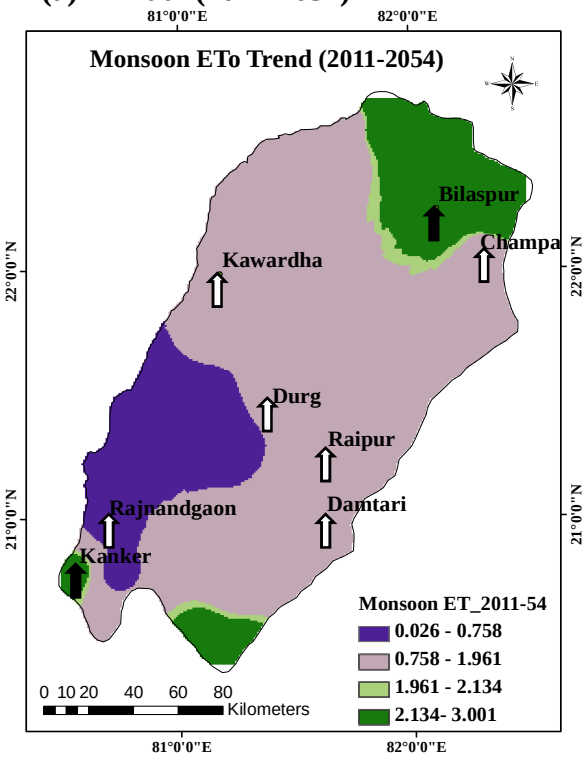

(c) Monsoon (2011-2054)

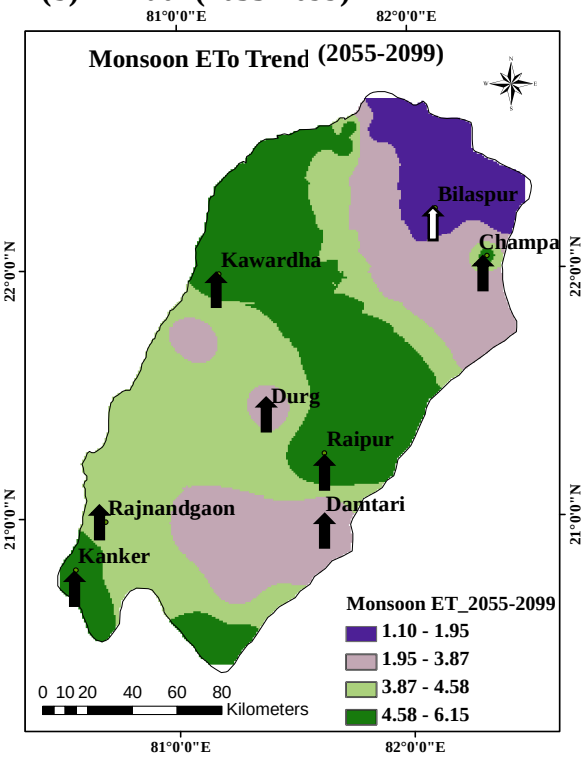

(d) Monsoon (2055-2099)

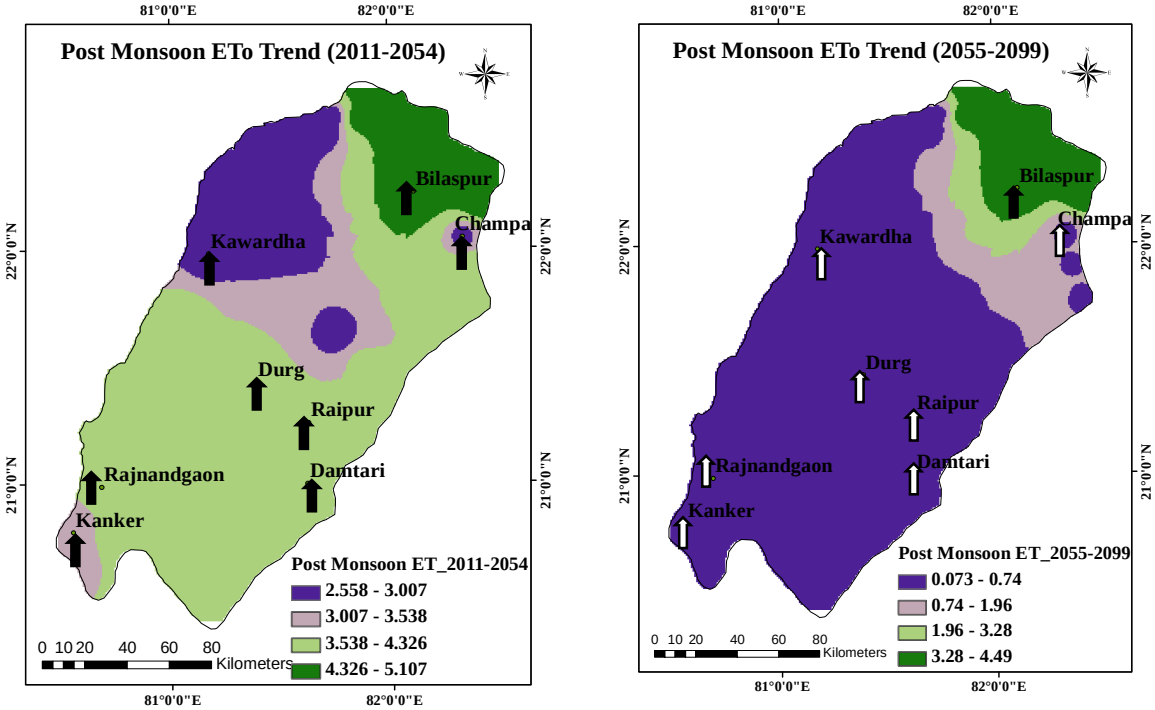

(e) Post Monsoon (2011-2054) **(f) Post Monsoon (2055-2099)**

Figure 8.8 Reference Evapotranspiration trend on annual and seasonal scales for two decades

8.3.5 Impact of Climate Change on Irrigation Water Requirement (IWR)

The irrigation water requirements are computed for Paddy (Kharif), Wheat and summer paddy (Rabi crops) at eight locations of the river basin. The monthly ETo is corrected with crop coefficients for each crop to compute the Crop Water Requirement (CWR) which in turn can be used to compute the irrigation water requirement of the crop. The monthly IWR have been estimated from the projections of rainfall at each of the location downscaled from LS-SVM model and CWR projections (The calculation of CWR and crop coefficient is detailed in Chapter 6). The projected percentage variations of IWR for eight locations are shown in Figures 8.9 a, b and c respectively, for Kharif paddy, wheat and summer paddy. The projected percentage variations of IWR for Kharif paddy during three decades i.e., 2020s, 2050s and 2090s for eight locations are also shown in Figures 8.10 a, b, c in the form of bar chart. It is clear from the figure that for Kharif paddy percentage change is highest for 2020s period for all the stations then 2050s and variation has been decreased in last decades (2090s) (Figure 8.9 a). For wheat crop the variability is highest for 2020s and 2050s period and least variation has been

observed for 2090s period (Figure 8.9 b). Whereas for summer paddy 2020s and 2050s period show highest variability (Figure 8.9 c). The predicted change in IWR at each location is a function of rainfall at that location and the ETo.

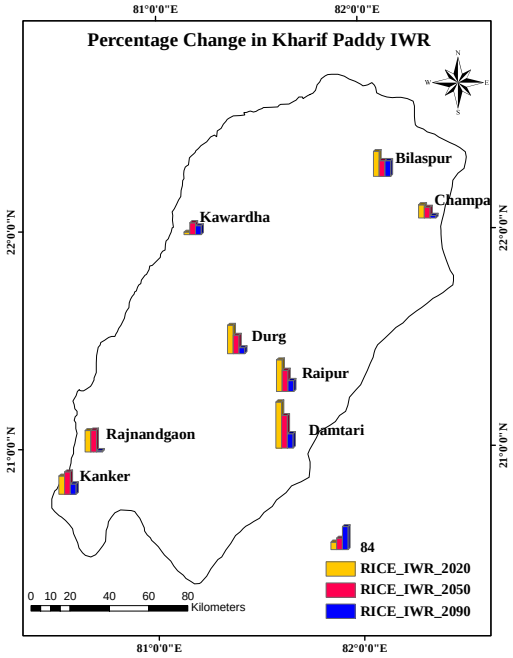

a) Kharif Paddy

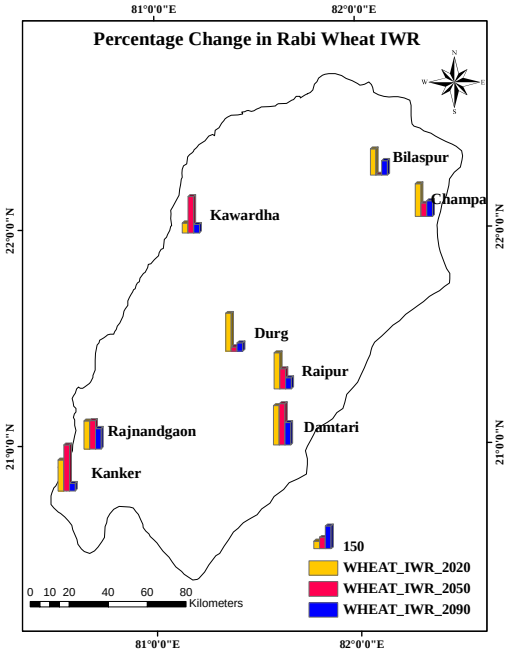

b) Rabi Wheat

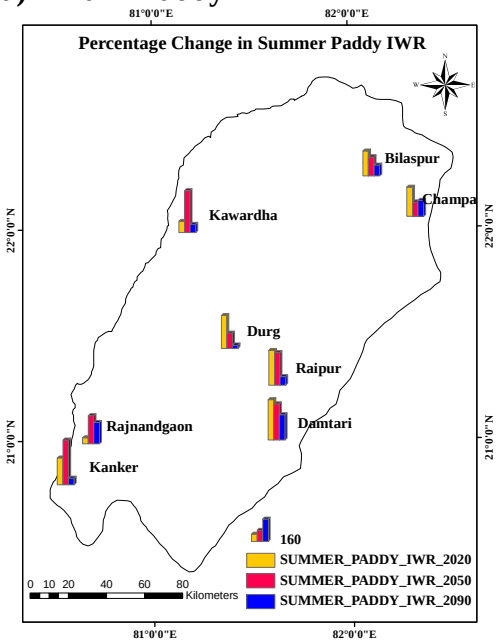

c) Summer Paddy

Figure 8.9 Percentage Change in IWR for Kharif Paddy, Wheat and Summer Paddy

8.3.5.1 Kharif Irrigation Water Requirement (Paddy)

The crop growing period of Kharif paddy in Chhattisgarh state is from mid July to October. (Details of crop growth period are given in Chapter 6). The trends in irrigation water requirement is presented in three decades 2020s, 2050s, 2090s for eight location in Seonath River Basin depicted in Figure (8.10). It is clear from the figure that IWR is increasing in future years when compared with present IWR. The highest IWR has been observed for 2090s as for the same decade the rainfall is decreasing. In 2050 IWR is comparatively least. The spatial distribution of rate of change in IWR for paddy is shown in Figure 8.11 a. For the upper half of the basin experiences the significant increased IWR. Whereas rest of the regions show non-significant increasing trend. As the temperature of the basin is increasing thereby ETo of the basin is high for monsoon period hence IWR for paddy crop is increasing for the future scenario.

8.3.5.2 Rabi Irrigation Water Requirement (Wheat)

The IWR for wheat crop is estimated and projected IWR for wheat crop is compared with present day water requirement. From the figure it is clear that water requirement is highest for the period of 2050s and 2090s. 2020s require least IWR compared to 2050s and 2090s but increase in IWR has been observed for all the three decades (Figure 8.12). The change in IWR is spatially shown in Figure 8.11 b. The central and southern part of basin shows the increasing IWR trend. From the figure 8.11 b in 2020s the change varies from 3 mm to 14 mm. However for 2050s period the rate of change varies from 0 to 16 mm/year. The highest change is observed for the lower half of the basin. Overall a non-significant increasing trend has been observed for the entire basin. For last decade i.e., 2090s period IWR trend is increasing for five of the stations the range varies from 5 mm to 12 mm.

8.3.5.3 Rabi Irrigation Water Requirement (summer paddy)

The comparative IWR for summer paddy with present and projected IWR is shown in figure 8.13. From Figure 8.13 the water requirement is highest for 2050s period for all the locations. The next highest decade for IWR is 2090s. Little increase 2020s IWR when compared with present day IWR for summer paddy. The spatial variation of IWR for three decades (2020s, 2050s and 2090s) is depicted in Figure 8.10 c. From Figure 8.10 c for 2020s period the

rate of change in IWR has been varied from 1.5 mm to 15.5 mm. The southern and central half of the basin show significant increasing trend in IWR. However for 2050s period the upper half of the basin shows no change whereas rest of the parts shows significant increasing trend. The maximum change in this period was 16 mm/year which is in the lower part of the basins. For 2090s period the change in IWR for different locations varies from 2 mm to 17 mm/year. But highest change has been observed for lower half of the basin. Overall basin show a significant increasing trend.

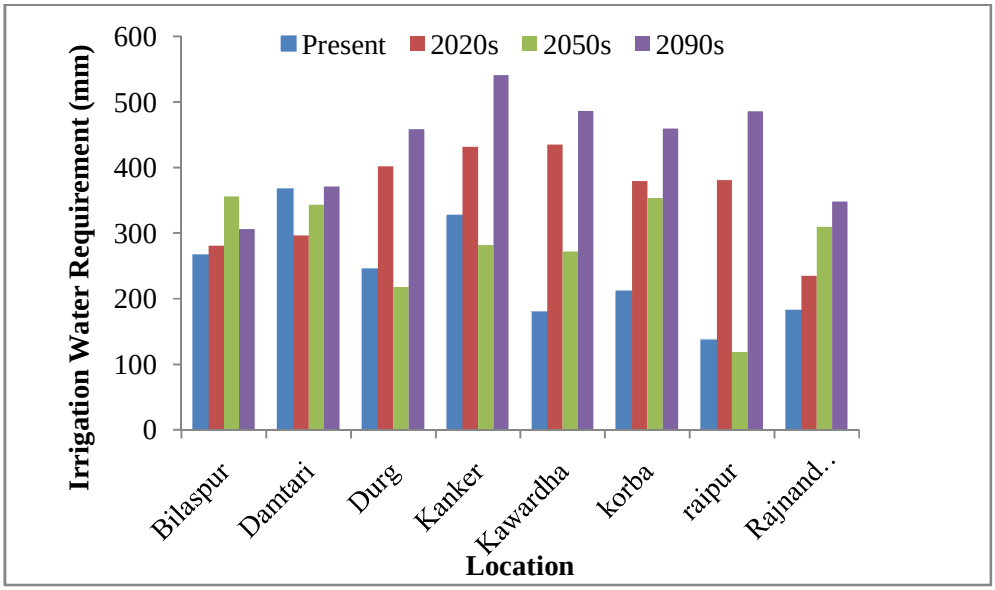

Figure 8.10 Irrigation Water Requirement of Kharif Paddy

(a)

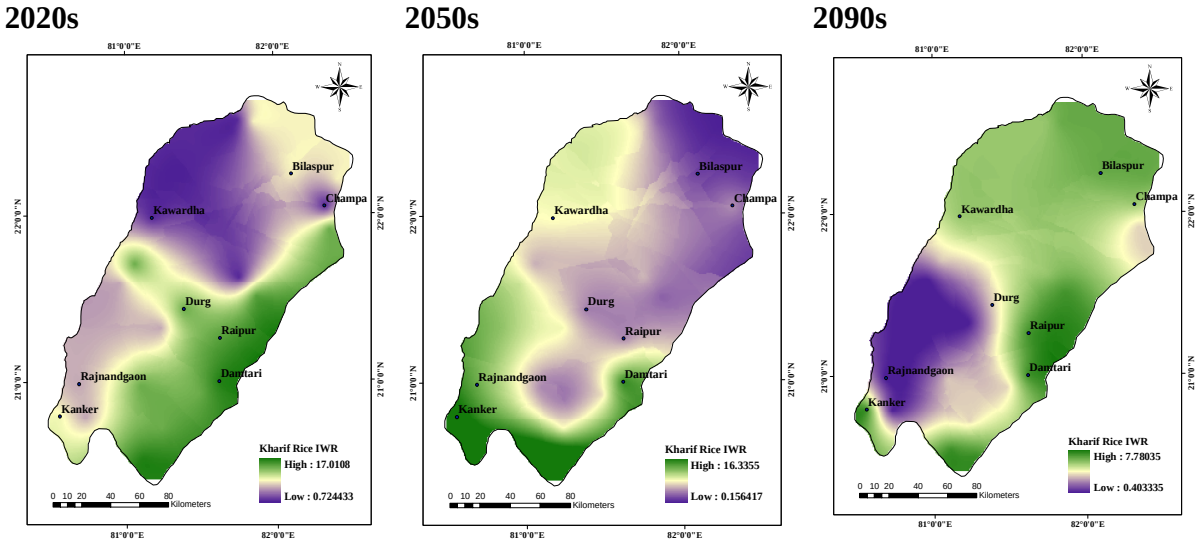

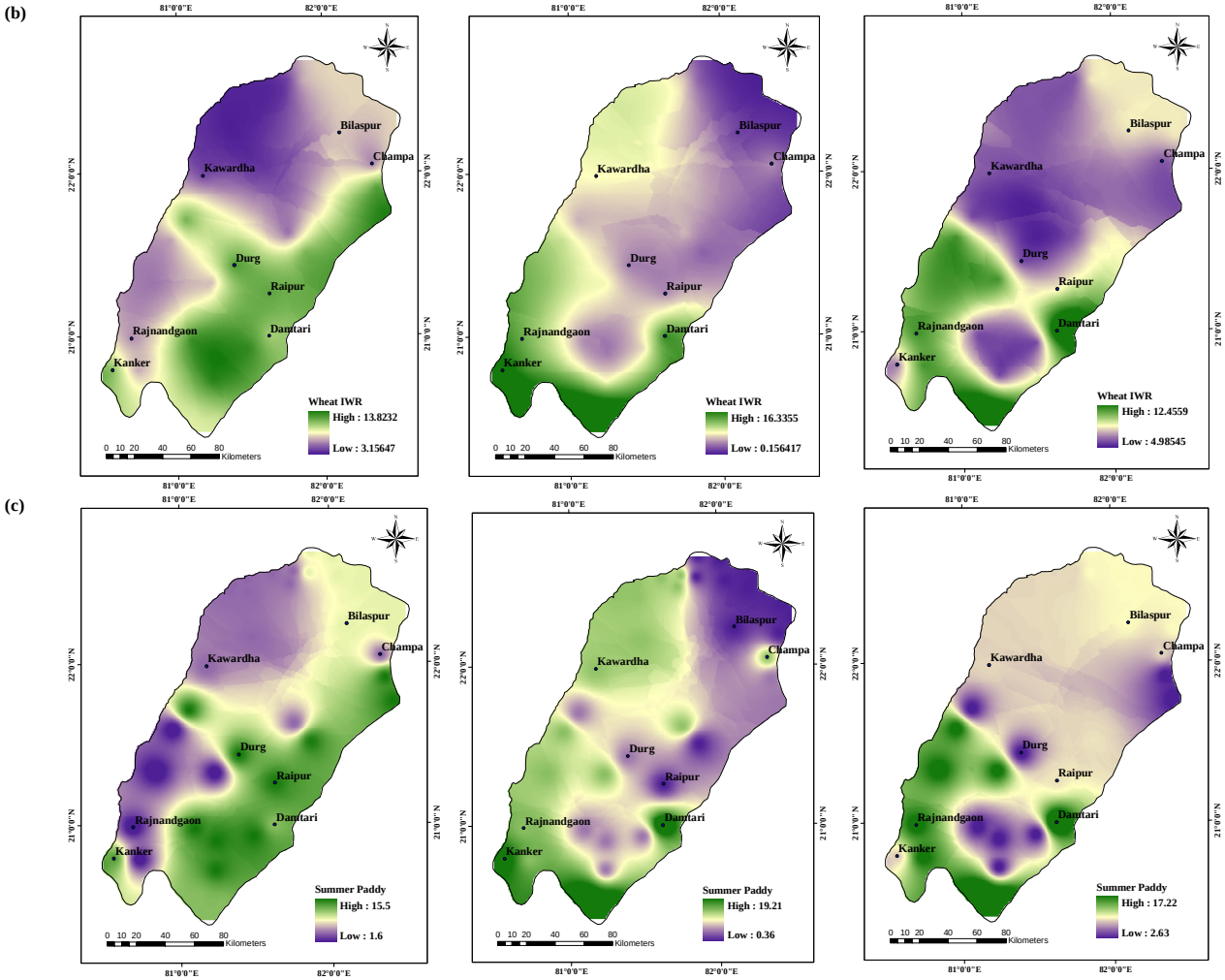

Figure 8.11 Spatial distribution of Future Irrigation Water Requirement for (a) Kharif (Paddy) (b) Rabi (Wheat) (c) Rabi (Summer Paddy)

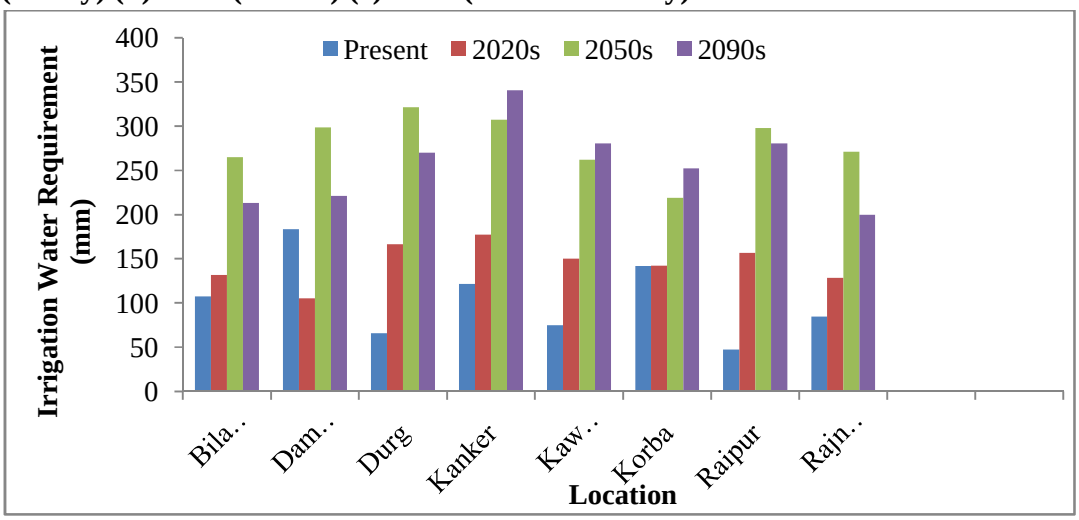

Figure 8.12 Irrigation Water Requirement of Rabi Wheat

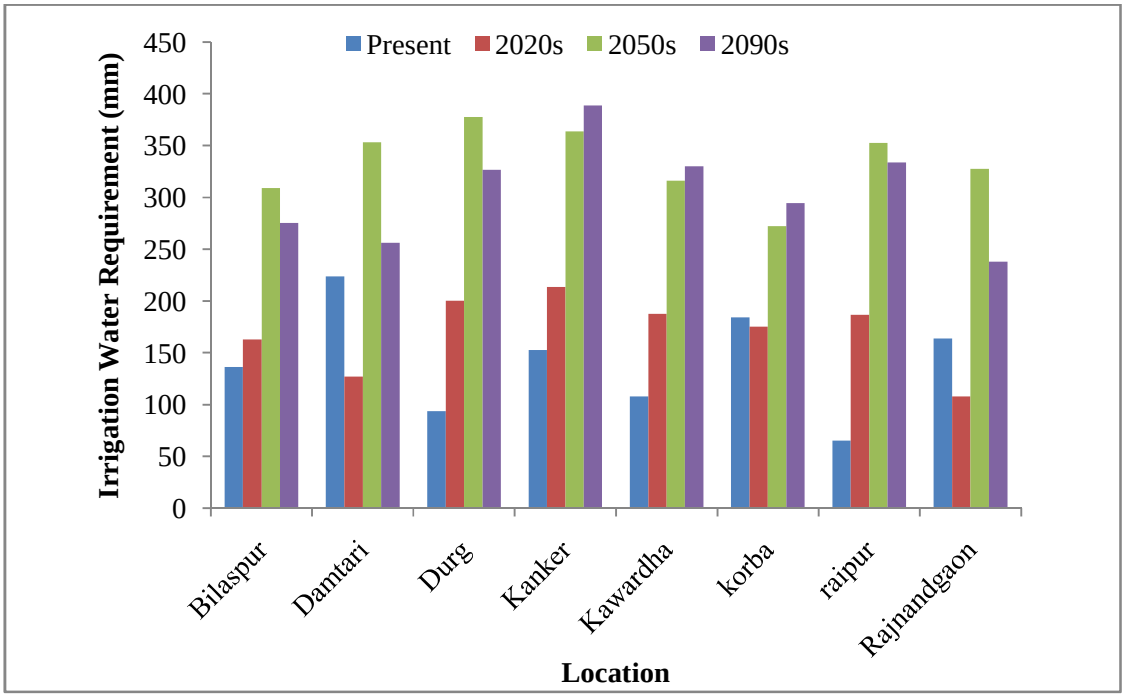

Figure 8.13 Irrigation Water Requirement of Rabi Summer Paddy

8.4 SUMMARY

In the present study inter-comparison of four statistical downscaling models have been done to identify the best prediction model. It has been predicted that LS-SVM method is the suitable model for further analysis. The LS-SVM model is used for predicting the future irrigation water requirement in the river basin. The expected changes of rainfall, RH, WS, Tmax and Tmin are modeled by using LS-SVM, with HadCM3 GCM output for the A2 scenario. The ETo projections are modeled with an evapotranspiration model (Penman-Monteith equation) accounting for the projected changes in temperature, RH, solar radiation and WS. The irrigation water requirement is quantified by accounting for projected rainfall and ETo. The monthly irrigation water requirement of Kharif (Paddy) and Rabi crops (Wheat and summer paddy) are quantified for downscaling eight locations covering the entire Seonath river basin. The annual irrigation water requirements for Kharif paddy, Wheat and summer paddy are predicted to increase in the Seonath river basin. The kharif IWR has been projected to increase by an average (and range) of 84% (8-168%), 71% (39-82%) and 32% (5–57%) in the 2020s, 2050s and 2090s respectively from a baseline of 67 mm. For Rabi Wheat crop IWR change increase by 201% (67-262%), 163% (6-307%) and 91% (50-150%) for three decades.

However for summer paddy the increase in IWR ranges from 184% (44-287%), 215% (103-319%) and 90% (21-181%) for 2020s, 2050s and 2090s periods respectively. This projected change in irrigation requirement will be helpful in planning of irrigation projects. In this study estimation of future irrigation water requirement by using single GCM output (HadCM3) and a single scenario (A2 scenario). It is reported by various researchers (Simonovic and Davies, 2006; Ghosh and Mujumdar, 2007) that the variation between different GCMs over regional climate change projections indicates a major cause of uncertainty. Further studies are essential for assessment of future irrigation requirement using different GCMs with scenarios to understand the underlying GCM and scenario uncertainty. The results of this study provide guidelines for the decision makers to accommodate sufficient amount of water in those months when rainfall only will not be adequate to fulfill the water requirements for crops.

CHAPTER 9

SUMMARY AND CONCLUSIONS

The accessibility of abundant water resources to meet agriculture water demand is globally a challenging issue due to change in climate. It is widely believed that the variability of meteorological factors and climate change are leading to change in irrigation water demand. There is a need to critically assess variation in Irrigation Water Requirement (IWR) over the years to plan agricultural water management and irrigation scheduling policies to cope with climate change. Seonath river basin is the longest tributary of Mahandi river system. It is located between latitudes 20°16' N to 22°41' N and Longitudes 80°25' E to 82°35' E. The total drainage area of the basin is 30,860 sq. km. The mean annual rainfall in the basin varies from 1005 mm to 1255 mm. The major part of annual rainfall occurs during three months i.e., July-September. The river gets dried by mid-winter season and both rural and urban areas in the basin are often subjected to severe water crisis during the summer season due to erratic nature of rainfall. The pattern of water utilization for agriculture has also changed over the years due to change in climatic variables. Hence there is a need to understand the region specific alteration in irrigation water requirement due to climatic variability for development and management of sustainable water resources.

This study has been undertaken to evaluate the impact of climate change on Irrigation Water Requirement in Seonath River Basin located in Chhattisgarh state of India. The specific objectives of the study are 1) Analysis of temporal trends and spatial variability of climatic variables viz., maximum, minimum and mean temperature (Tmax, Tmin, Tmean), relative humidity, rainfall and wind speed in the study area. 2) Estimation of region specific pan coefficient (Kp) on monthly basis to compute reference evapotranspiration (ETo). Inter-comparison of available models for estimation of ETo and conducting sensitivity analysis of ETo with respect to key climatic variables. 3) Analysis of site specific crop coefficients, crop water requirement (CWR) and Irrigation Water Requirement (IWR) for major crops using the observed agro-climatic data and analysis of long term trend in ETo and IWR. 4) Development of relationship between curve number (CN) parameter of Soil Conservation Service Curve Number (SCS-CN) methodology and CWR/IWR. 5) Application of different statistical downscaling models and their inter-comparison to predict future climatic variability and its impact on IWR. Summary conclusions on various aspects of the study and major contribution of this research work are presented below.

9.1 SPATIAL AND TEMPORAL TRENDS IN CLIMATIC VARIABLES

Scientific assessment of spatial variability and temporal trends in climatic variables are needed for sustainable planning and management of irrigated agriculture. The analysis and results of the study are summarized below

9.1.1 Rainfall Trend

The trends in annual and seasonal rainfall time series from 1960-2010 have been analyzed using Mann–Kendall test and the Sen's Slope estimator for 24 stations in the Seonath river basin. The analysis indicated a decreasing trend in the annual rainfall series. The results of the annual rainfall series show that there is a significant decreasing trend in annual rainfall at 75% of the stations located in northern part of basin and non-significant decreasing trend in annual rainfall at 17% of the stations located in southern part of basin. Moreover, the decreasing trends in seasonal rainfall for most of the stations are significant according to the statistical tests, in the winter (87%), monsoon (83%) seasons and summer (83%).

The magnitude of decreasing trends in annual rainfall is -2.4 mm/year and for monsoon it is -2.79 mm/year. Decrease in monsoon rainfall at the rate of 2.74 mm/year is likely to have significant adverse impact on rainfed agriculture in future.

9.1.2 Temperature Trend

Rising trend over the years has been observed in mean seasonal maximum temperature for monsoon and winter, whereas, there is decreasing trend over the years in mean summer maximum temperature. However, mean seasonal minimum and mean seasonal average temperatures show rising trend for the entire basin. Few stations located in Northern part of the basin show non-significant rising trend in mean seasonal temperature. The minimum temperature has increased more as compared to maximum temperature over 51 years period of analysis. The percentage change in minimum temperature is highest for the month of November followed by December and January. The variability is observed to be more pronounced in minimum temperature ranging from 1.69% to 2.78%. For annual maximum and minimum temperature, the upper half of the basin shows more variability with highest magnitude of variability 1.93%. The study shows that the mean annual temperature is likely to increase by 1.98°C in next 100years. However winter temperature may increase by 2.06°C, monsoon temperature may increase by 4.73°C and summer

temperature may decrease by -0.528°C over the study area. Overall there is an increase in Tmax on annual and seasonal scale except for summer whereas for Tmin and Tmean, overall significant increasing trend is observed for the entire Seonath River basin.

The monsoon temperature is expected to increase by 4.73°C over 100 years. This rise in temperature may cause significant increase in the irrigation water requirements and rainfed agriculture may get adversely affected. Therefore irrigation planning for Rabi as well as for Kharif crops need to be analyzed for the study area.

9.1.3 Relative Humidity (RH) Trend

Monthly trend analysis of Relative Humidity (RH) shows significant decreasing trend in RH for months of July, September, October and November. Whereas, from March to June insignificant increasing trends are observed. All stations show significant decreasing trend in annual RH except few stations in the north western part of the study area which shows non-significant decreasing trend. For monsoon season, strongly significant decreasing trend is observed for the entire basin. Whereas for winter season, non-significant decreasing trend and for summer season increasing trend have been observed. The highest change in magnitude of RH has been observed for July, September, October and November months. The inter-annual variability in RH of the basin ranges from 0.9 to 2.2%.

9.1.4 Wind Speed (WS) Trend

The wind speed is one of the key variable which cause water vapour transpiration from plant leaves into atmosphere. Thus, monthly and seasonal assessment of trends in wind speed and its variability is important in order to quantify its effect on ET. On seasonal basis, strongly significant increasing trend is obtained for wind speed in monsoon and winter season all over the basin. On monthly time scale, the highest rate of change is seen in August followed by July, June and September. The percentage change is highest for the entire basin ranging from 38% to 61%.

Highest inter-annual variability (23%) is observed in monthly wind speed in northern part of the river basin. Overall there is increasing trend in monthly and seasonal wind speed for the entire basin.

9.2 INTER-COMPARISON OF ETo ASSESSMENT METHODS

Evapotranspiration is directly related to crop water requirement and is an important parameter in hydrological studies. Therefore, accurate estimation of ETo is of significant importance. To measure the consistency and accuracy of ETo methods, the estimates obtained from six different methods (Hargreaves, Thornthwaite, Blaney-Criddle Method, Priestley-Taylor Method, Penman-Monteith Method and Turc Method) have been compared with pan evaporation data (Ep). The following inferences could be drawn from this analysis

1. The pan coefficient (Kp) have been estimated as the ratio between ETo and pan evaporation (Ep) for the study area. The study shows that the Kp varies significantly from month to month (0.56 to 0.89) for the study area. The estimated monthly pan coefficients values for the study area are considered to be more appropriate than the Kp values (0.60-0.80) given in literature for Class A pan. The highest Kp value is obtained for July month whereas it is lowest for the month of November. Thus, use of the FAO recommended values of Kp result in over estimation of the monthly ETo values by 11.8% to 56.3%. Thus for accurate estimation of ETo from pan evaporation data, the estimated Kp values considering local climatic conditions should be used for the study area.
2. According to statistical performance evaluation of six ETo estimated methods, Penman-Monteith, Hargreaves and Thornthwaite methods have performed well with low value of RMSE, MAE, SSE and high correlation coefficient. The radiation-based Priestley-Taylor and temperature based Blaney-Criddle method indicate lowest correlation values.
3. Sensitivity analysis of ETo to different meteorological variables viz, Tmax, Tmin, RH and WS has been performed. The temperature is found to be the most important driving parameter which affects ETo and followed by relative humidity. In the Seonath river basin maximum temperature is dominating factor in estimation of ETo at seasonal and annual scales. As temperature increases, ETo also increases. Bilaspur station shows highest sensitivity coefficient of 1.77 in relation to temperature. It means ETo would increase by 17.7% in response to the 10% rise in maximum temperature if other meteorological variables remain constant. However Rajnandgaon station shows the highest value of sensitivity coefficient in relation to RH (-1.28) which means 10% decrease in RH causes ETo to increase by 12.8%.

Hargreaves and Thornthwaite methods are therefore not recommended for this study area as these donot take into consideration the RH parameter.

9.3 ASSESSMENT OF CROP COEFFICIENT, CWR, IWR AND THERE LONG TERM TREND

9.3.1 Assessment of Crop Coefficient (Kc)

In order to estimate CWR, the crop characteristics in the form of crop coefficient (Kc) need to be considered. The value of Kc varies for different growth stages i.e. the initial stage, development stage, midseason stage, and the late season stage. In this study, the Kc values recommended by FAO paper No. 56 have been adjusted according to climatic conditions of the study area. The average Kc values for major crops (Kharif Paddy, Wheat and Summer paddy) for crop growth stages viz, initial, development, mid and late season are computed. These average Kc values for different crops are then compared with recommended Kc values in FAO-56. For Kharif paddy, percentage change in adjusted Kc value with respect to FAO recommended Kc values during different crop growth stages varies from -1% to -15% whereas for rabi crops (Wheat and Summer paddy) it range from -2% to -16% and -9% to -23% respectively. The adjusted Kc values are lower than those suggested in FAO-56 for each crop during the different crop growth stages. This is mainly due to humid climate of Seonath river basin and lower mean wind speed (1.7-1.0 m/s) and higher mean minimum relative humidity (79-41%) during Kharif and rabi season. The CWR computed using FAO approach (FAO, paper No-56) gives significantly different (higher) values. It is therefore recommended to use the adjusted Kc values for our study area for precise estimation of CWR and subsequently for computation of supplemental water requirement.

9.3.2 Trend Analysis of Reference Evapotranspiration (ETo)

Trend and variability of annual and monthly ETo time series have been analyzed for 8 stations for which data are available. The increase in ETo is 13.4 mm/year on annual time scale. On the seasonal scale, summer ETo trend is decreasing (-10.4 mm/year). The winter and monsoon ETo show increase at the rate of 21 mm/year and 22 mm/year respectively. The estimates of ETo for the months of December, January, February, July and August show non-significant increasing trend. However significant increasing ETo trend has emerged for the months of September October and November. The highest (3.4-3.6%) variability in annual ETo is seen in the stations located at southern part of the basin while

rest of the stations exhibits almost same inter-annual variability ranges from 1.0%-1.8%. Overall a high variation in ETo is observed for the entire Seonath river basin. The results of this study will be useful for the reliable estimation of irrigation water requirement.

9.3.3 Trend Analysis of Irrigation Water Requirement (IWR)

IWR of the Kharif Paddy is relatively higher for the later stage of the crop growth period compared to previous crop growth period. For Rabi cropping season (wheat and summer paddy) it has been found that the irrigation water requirement is of the same order throughout the growing season, but marginally higher during the developmental stage. In order to detect trends in IWR, the MK-test and Sen's slope have been used to analyze the time series for the 51-year period. There is increasing trend in IWR for both Kharif and Rabi seasons. For Kharif season increasing trend is detected at 88% of the stations, and remaining 12% of the stations show non-significant increasing trend. Further, significant positive slopes are dominant for wheat crop, (with 63% of the stations). For summer paddy, 50% of the stations show significant increasing trend and rest 50% shows non-significant increasing trend. The IWR for Kharif and Rabi seasons are increasing at the rate of 3.627 mm/yr and 1.264 mm/yr respectively. These changes are characterized by a relative increase in Kharif IWR by 47%, while Rabi IWR by 23%.

9.4 IWR-CN RELATIONSHIP

Over the last 50 years several empirical and semi-empirical methods for ETo estimation have been developed in different parts of the world but none can be suggested as the best one for any area or any season in terms of its accuracy. In this study, the curve numbers derived from rainfall-runoff data on seasonal scale (Kharif and Rabi season) is related to IWR of same scale. High R^2 values of 0.970 for Kharif season and 0.926 for Rabi season are found for calibration period. The results are validated with R^2 values of 0.957 and 0.954 for Kharif and Rabi seasons, respectively; indicating the existence of a strong CN-IWR relationship.

The supportive results of the proposed model assume to be a good substitute for complex IWR assessment, particularly in the area where meteorological parameters are not easily obtainable. In addition, the developed model can be utilised for the crop water use studies, and especially in the design and management of irrigation systems.

9.5 PREDICTION OF CLIMATE CHANGE IN FUTURE

1. The four statistical downscaling models viz., Artificial Neural Network (RBF), Multilayer Perception (MLP), Multiple Linear Regression (MLR), Model Tree (MT), Least Square Support Vector Machine (LS-SVM) are used for comparative study. The best prediction model for the study area is LS-SVM. The results indicate that for each climatic variable, LS-SVM is performing best followed by MT and ANN (MLP). Lower values of NSE and R^2 are obtained for ANN (RBF) method for almost all the meteorological variables therefore not recommended for our study area.
2. Increase in annual rainfall is statistically predicted from year 2020s upto 2090. The annual rainfall is predicted to decrease for the period of 2091-2100. The predicted decadal change in rainfall varies from 2.74 to 7 mm/decade for 2020s and 2050s period. However for maximum temperature, the increasing trend is predicted for the entire projected period but the highest temperature change predicted for two decades i.e., 2021-2030 and 2031-2040. The rate of change varies from 0.1°C/decade to 0.5°C/decade for monsoon and 0.01°C/decade to 0.3°C/decade for post monsoon season. For the minimum and mean temperature the overall increasing trend is observed but for Tmin the highest temperature rise is expected in the period of 2061-2070. The change in magnitude for minimum temperature for monsoon season varies from 0.2°C/decade to 0.7°C/decade, whereas for post monsoon season the minimum temperature varies from 0.02°C/decade to 0.5°C/decade. It can be inferred that warming is more pronounced during the night (when temperature is lower) than day. The relative humidity forecasts represent a significant decreasing trend for Kharif season, whereas for rabi season non-significant decreasing trend have been observed for two decades i.e., 2020s and 2090s period. The projected wind speed shows non-significant increasing trend for the entire basin. Wind speed projections are highly uncertain with extremes in 2090s during Kharif season whereas for rabi season the uncertainty is for 2020s and 2050s period.
3. The reference evapotranspiration are predicted to increase in future for all months. Particularly, the change in evapotranspiration is more in the months of May to August due to the large projected changes in Tmax and Tmin variables. The rate of change in ETo is increasing from May to September. There could be an increase of 25 mm in ETo in June month over a period of 100 years

4. The monthly irrigation water requirement in future has been estimated from the projections of rainfall at each of the location downscaled from LS-SVM model and CWR projections. The annual irrigation water requirements for Kharif paddy, wheat and summer paddy are predicted to increase in the entire river basin. The IWR for Kharif crops (Monsoon season) is projected to increase by an average (and range) of 84% (8-168%), 71% (39-82%) and 32% (5–57%) in the 2020s, 2050s and 2090s respectively whereas for Rabi crops (Winter season) wheat crop IWR is predicted to increase by 201% (67-262%), 163% (6-307%) and 91% (50-150%) for the three decades (2020s, 2050s, 2090s). However for summer paddy the increase in IWR ranges from 184% (44-287%), 215% (103-319%) and 90% (21-181%) for 2020s, 2050s and 2090s periods respectively. Knowledge on future change in irrigation requirements will be useful in sustainable improvement and management of basin water resources and in developing adaptive policies for operation of irrigation schemes.

9.6 CONCLUSIONS

The following conclusion could be drawn from the study:

1. The analysis indicated that decrease in monsoon rainfall (2.79 mm/yr) is likely to have significant adverse impact on rainfed agriculture. This may necessitate to focus for supplemental irrigation planning in Kharif season crops too.

2. Investigation of results revealed that the temperature changes may have significant impacts on rainfed crop cultivation due to increase in evapotranspiration. Monsoon temperature is expected to increase by 4.73°C over 100 years and it may cause significant increase in the IWR and water shortages.

3. Use of monthly value of pan coefficient (Kp) leads to more precise assessment of evapotranspiration compared to single value for all months (0.70). Estimates of ETo using monthly Kp values indicated large variation in ETo from month to month ranging from -6% to 21%.

4. The analysis revealed that there is increase in IWR for Kharif and rabi crops in most of the region due to high variability of rainfall pattern, rise in temperature, wind speed and decrease in RH. These results shall be helpful in more realistic planning and effectual utilization of basin water resources.

5. A relationship between SCS-CN and IWR has been developed. It may provide a simple substitute to the complex procedure for IWR estimation. CN based IWR estimation would be simple and useful.

6. Four statistical downscaling methods have been taken for comparative study. The results of analysis indicated that for each climatic variable, LS-SVM is performing best. The monthly IWR in future have been predicted using the projections of rainfall (downscaled from LS-SVM model) and CWR projections.

7. The future projection (2001-2100) of IWR for Kharif and rabi crops derived from LS-SVM models show increasing trend. This knowledge on future change in IWR shall be useful for sustainable development and management of water resources and in developing adaptive policies for operation of irrigation schemes.

9.7 MAJOR RESEARCH CONTRIBUTIONS

The major research contributions of the present study are summarized below:

1. Long term spatial trends in spatially distributed climatic variables have been established.
2. Estimation of monthly pan coefficients (Kp) values for easy and perfect assessment of ETo using available pan evaporation data in the study area.
3. Inter-comparison of ETo estimation methods and identification of best suitable model for the study area and its sensitivity to different climatic variables.
4. Estimation of crop coefficients of major crop for the study area for accurate estimation of CWR and subsequently IWR of the study area.
5. Exploration of trend and variability in ETo and IWR in context of long term changes in climatic variables of the study area.
6. Development of relationship between SCS-CN and IWR which could substitute the complex procedure for IWR. CN based IWR estimation is simple, reliable and particularly useful in areas where data on a number of meteorological parameters may not be available.
7. Inter-comparison of four downscaling models and identification of model. Future prediction of rainfall, maximum and minimum temperature, relative humidity and wind speed by LS-SVM downscaling models by HadCM3 GCM data for A2 scenario. Estimation of ETo using climatic variables and in turn CWR for future assessment of IWR for the study area.

9.8 SCOPE FOR FUTURE RESEARCH

1. For an accurate estimation of the IWR, the soil moisture dynamics of individual crops also need to be considered in the impact assessment studies.
2. This study may be extended to study impact of climate change on spatial distribution of drought vulnerability and IWR during drought years.
3. Further studies are required for assessment of applicability of the proposed IWR-CN relation to other regions. In addition, since parameter λ is a regional parameter that depends on geological and climatic factors and hence an important parameter in ET/CWR/IWR estimation, results may be improved with the use of a value other than the standard value of 0.2 for other climatic regions.
4. In this study, only one GCM data i.e., HadCM3 has been used. It is suggested to apply different GCMs data to make a comparison between different models to check inter-models consistency. Hence, this work may be extended in the future by including different GCMs data and for different scenarios for future estimation of climatic variables.

BIBLIOGRAPHY

1. Al-Ghobari HM, 2000. Estimation of reference evapotranspiration for southern region of Saudi Arabia. Irrig Sci., 19, pp: 81–86.

2. Allen R, Pereira LS, Raes D, Smith M. 1998. Crop evapotranspiration: guidelines for computing crop water requirements. Irrigation and Drainage Paper, 56. FAO, Rome, Italy, pp: 300.

3. Allen RG, Jensen ME, Wright JL, Burman, RD. 1989. Operational estimates of reference evapotranspiration. Agron. J. 81: 650–662.

4. Allen RG, Pruitt WO. 1991. FAO-24 reference evapotranspiration factors. J Irrig Drain Eng 117(5), pp: 758–773.

5. Allen RG, Smith M, Pereira LS, Perrier A. 1994. An Update for the Calculation of Reference Evapotranspiration. ICID Bulletin. 43(2), pp: 35-92.

6. Allen RG. 2000. Using the FAO-56 Dual Crop Coefficient Method over an Irrigated Region as Part of an Evapotranspiration Intercomparison Study. J. of Hydrol. 229, pp: 27-41.

7. Amatya DM, Skaggs RW, Gregory JD. 1995. Comparison of methods for Ref-ET. J. Irrig. Drain. Eng. 121, pp: 427–435.

8. Anandhi A, Srinivas VV, Nagesh Kumar D, Nanjundiah RS. 2009. Role of predictors in downscaling surface temperature to river basin in India for IPCC SRES scenarios using support vector machine, Int. J. Climatol. 29, pp: 583-603.

9. Anandhi A. 2010. Assessing impact of climate change on season length in Karnataka for IPCC SRES scenarios. J. Earth Syst. Sci. 119(4), pp: 447–460

10. Arnell NW, Hudson DA, Jones RG. 2003. Climate change 256scenarios from a regional climate model: Estimating change in runoff 257 in southern Africa, J. Geophys. Res., 108(D16), 4519, doi:10.1029/ 258 2002JD002782.

11. Arnell NW. 2004. Climate change and global water resources: SRES emissions and socio-economic scenarios, Global Environ. Change, 14(1), pp: 31–52, doi:10.1016/j.gloenvcha.2003.10.006.

12. Arnold JG, Allen PM, Bernhardt G. 1993. A comprehensive surface-groundwater flow model. J. Hydrology.142, pp: 47-69.

13. Aron G, Miller AC Jr, Lakatos DF. 1977. Infiltration formula based on SCS curve number. Journal of the Irrigation and Drainage Division, American Society of Civil Engineers 103(IR4), pp: 419–427.

14. Ayanlade A, Odekunle OT. 2009. GIS Approach in Assessing Seasonal Rainfall Variability in Guinea Savanna Part of Nigeria. 7th FIG Regional Conference Spatial Data Serving People: Land Governance and the Environment – Building the Capacity Hanoi, Vietnam.

15. Bai W, Feng S, Kang S. 2006. Reference crop evapotranspiration in Shanxi Province based on GIS. Transactions of the CSAE, 2210, pp: 57–61 in Chinese.

16. Bandyopadhyay A, Bhadra A, Raghuwanshi NS, Singh R 2009. Temporal Trends in Estimates of Reference Evapotranspiration over India, J. Hydrologic Engineering, 14(5), pp: 508–515.

17. Bardossy A, Bogardi I, Matyasovszky I. 2005. Fuzzy rule-based downscaling of precipitation. Theor. Appl. Climatol., 82, pp: 119-129.

18. Barnett TP, Adam JC, Lettenmaier DP. 2005. Potential impacts of a warming climate on water availability in snow-dominated regions, Nature 438 (7066), pp: 303-309.

19. Basistha A, Arya DS, Goel NK. 2009. Analysis of historical changes in rainfall in the Indian Himalayas. Int. J. Climatol., 29, pp: 555–572.

20. Benestad R. 2007. Novel methods for inferring future changes inextreme rainfall over Northern Europe, Clim. Res., 34, pp: 195–210, doi:10.3354/cr00693.

21. Beven KJ. 2001. Rainfall–runoff modelling: the primer. Wiley, New York. 360.

22. Bhattacharya B, Solomatine DP. 2002. Application of artificial neural networks and M5 model trees to modelling stage-discharge relationship. Proc., 2nd Int. Symp. on Flood Defence, Beijing, China, B. S. Wu, Z. Y. Wang, G. Q. Wang, G. H. Huang, H. W. Fang, and J. C. Huang, eds., Science Press New York.

23. Bhunya PK Mishra SK, Berndtsson R. 2003. Simplified 2PGD for derivation of SUH, JHE, ASCE, 8(4), pp: 226-230.

24. Bhutiyani MR, Kale VS, Pawar NJ. 2007. Long term trends in maximum, minimum and mean annual air temperatures across the Northwestern Himalaya during the twentieth century, Climatic Change, 85, pp:159-177.

25. Birsan M, Molnar P, Burlando P, Pfaundler M. 2005. Streamflow trends in Switzerland. J. Hydrol. 314, pp: 312-329.

26. Blaney HF, Criddle WP. 1950. Determining water requirements in irrigated areas from climatological and irrigation data. USDA (SCS) TP-96, 48.

27. Bois B, Pieri P, Van Leeuwen C, Gaudillere JP. 2005: XIV International GESCO Viticulture Congress, Geisenheim, Germany, 23–27 August, 2005, pp: 187–193.

28. Bonta JV. 1997. Determination of watershed curve number using derived distributions. J. Irrig Drain Engg., ASCE, 123 (1), pp: 234-238.

29. Bosznay M. 1989. Generalization of the SCS curve number method. Journal of Irrigation and Drainage Engineering Division, ASCE, 115(IR1), pp: 139-144.

30. Bradley RS, Diaz HF, Eischeid JK, Jones PD, Kelly PM, Goodess CM. 1987. Precipitation fluctuations over northern hemisphere land areas since the mid-19th century. Science, 237, pp: 171-175.

31. Brouwer C, Heibloem M (1986) Irrigation water needs. Irrigation Water Management Training Manual 3, Food and Agriculture Organization of the United Nations, Rome.

32. Brown RA, Rosenberg NJ. 1999. Climate change impacts on the potential productivity of corn and winter wheat in their primary United States growing regions. Climate Change 41, pp: 73–107.

33. Brutsaert W. 1982. Evaporation into the Atmosphere: Theory, History, and applications. Reidel, Hingham, MA, pp: 229.

34. Buma J, Dehn M. 2000. Impact of climate change on a landslide in South East France, simulated using different GCM scenarios and downscaling methods for local precipitation. Clim. Res., 2000, 15, pp: 69–81.

35. Burman RD, Laramie WY, Nixon PR, Wright JL, Pruitt WO. 1983. Water Requirements. In: Jensen, M.E. (ed.) 1983. Design and operation of farm Irrigation Systems, Chapter 6, ASAE Monograph No.3. USA.

36. Burn DH, Cunderlik JM, Pietroniro A. 2004. Hydrological trends and variability in the Liard river basin. Hydrolo. Sci. J. 49, pp: 53–67.

37. Burn DH, Hesch NM. 2007. Trends in evaporation for the Canadian Prairies. J. Hydrol., 336, pp: 61-73.

38. Burnash RJC. 1995. The NWS River forecast system - catchment modeling. In V. P. Singh (Ed.), Computer Models of Watershed Hydrology (pp. 311–366). Water Resources Publications, Highlands Ranch, CO.

39. Burton A, Kilsby CG, Fowler HJ, Cowpertwait PSP, O'Connell PE. 2008. Rain Sim: A spatio temporal stochastic rainfall modeling system. Environmental Modeling and Software, 23, pp: 1356-1369.

40. Byun HR, Han YH. 1994. On the existence of the seasonal drought in the Korean peninsula. Journal of Korean Meteorological Society, 30, pp: 457-467. (In Korean with English abstract).

41. Byun HR, Lee DK, Jeong CH. 1992a. A study on the atmospheric circulation during the dry period before the Changma. Part I: existence and characteristics. Journal of Korean Meteorological Society 28, pp: 72-85. (In Korean with English abstract).

42. Byun HR, Lee DK, Jeong CH. 1992b. A study on the atmospheric circulation during the dry period before the Changma. Part II: compared with those before and after the period.

Journal of Korean Meteorological Society, 28, pp: 86-102. (In Korean with English abstract).

43. Byun HR, Lee DK. 2002. Defining three rainy seasons and the hydrological summer monsoon in Korea using available water resources index. Journal of the Meteorological Society of Japan, 80(1), pp: 33-44.

44. Byun HR. 1996. On the atmospheric circulation caused the drought in Korea. Journal of Korean Meteorological Society, 32, pp: 455-469. (In Korean with English abstract).

45. Cannon AJ, Whitfield PH. 2002. Downscaling recent stream-flow conditions in British Columbia Canada using ensemble neural network models. Journal of Hydrology 259, pp: 36–151.

46. Cavazos T. 1997. Downscaling large-scale circulation to local winter rainfall in north-eastern Mexico. International Journal of Climatology 17, pp: 1069–1082.

47. Chatterjee S, and Price B. 1977. Regression Analysis by Example. New York: Wiley. (Section 3.7, p.68ff of 2nd ed.(1991).).

48. Chattopadhyay, N. and Hulme, M. (1997). Evaporation and potential evapotranspiration in India under conditions of recent and future climate change, Agricultural and Forest Meteorology, 87, pp: 55-73.

49. Chaudhary A, Abhyankar VP. 1979. Does precipitation pattern foretell Gujarat climate, becoming arid, Mausam, 30, pp: 85-90.

50. Chen H, Xu CY, Guo SL. 2012. Comparison and evaluation of multiple GCMs, statistical downscaling and hydrological models in the study of climate change impacts on runoff, Journal of Hydrology 434–435, pp: 36–45.

51. Chen S, Liu Y, Thomas A. 2006. Climatic change on the Tibetan Plateau: potential evapotranspiration trend from 1961–2006. Climatic Change 76, pp: 291–319. DOI: 10.1007/s10584-006-9080-z.

52. Chen X, Li Y, Harrison R, Zhang YQ. 2008. Type-2 fuzzy logic-based classifier fusion for support vector machines. Applied Soft Computing, 8(3), pp: 1222–1231.

53. Cheng C, Li G, Li Q, Auld H. 2008. Statistical downscaling of hourly and daily climate scenarios for various meteorological variables in South Central Canada. Theoretical and Applied Climatology. 9(1), pp: 129-147.

54. Cheng J, Shi Z, Zhu Y. 2007. Assessment and mapping of environmental quality in agricultural soils of Zhejiang Province. J. Environ. Sci., 191, pp: 50–54.

55. Choudhury BU, Das A, Ngachan SV, Slong A, Bordoloi LJ Chowdhury P. 2012. Trend Analysis of Long Term Weather Variables in Mid Altitude Meghalaya, North-East India. Journal of Agricultural Physics, 12(1), pp: 12-22.

56. Chow VT. 1964. Handbook of applied hydrology. McGraw Hill Book Co, New York.

57. Christiansen JE, Hargreaves GH. 1969. Irrigation requirements from evaporation. Trans. Int. Comm. On Irrig. and Drain., Vol. III, 23, pp: 569-596.

58. Christiansen JE. 1968. Pan evaporation and evapotranspiration from climatic data. J.Irrig. and Drain. Div., 94, pp: 243-256.

59. Cleugh HA, Leuning R, Mu Q, Running SW. 2007. Regional evaporation estimates from flux tower and MODIS satellite data. Remote Sensing of Environment 106 (3), pp: 285–304.

60. Cohen S, Stanhill G. 2002. Evaporative climate changes at Bet-Dagan Israel, 1964–1998. Agricultural and Forest Meteorology 111, pp: 83–91. DOI: 10.1016/S0168-1923(02)00016-3.

61. Cong ZT, Yang DW. 2009. Does evaporation paradox exist in China? Hydrology and Earth System Sciences 13, pp: 357–366. DOI: 10.5194/hessd-5-2111-2008.

62. Conway D, Wilby RL, Jones PD. 1996. Precipitation and air flow indices over the British Isles. Climate Research, 7, pp: 169-183.

63. Corte-Real J, Qian B, Xu H. 1998. Regional climate change in Portugal: precipitation variability associated with large-scale atmospheric circulation. International Journal of Climatology 18, pp: 619–635.

64. Coulibaly P, Dibike YB, Anctil F. 2005. Downscaling Precipitation and Temperature with Temporal Neural Networks, J. Hydrometeor, 6, 483–496, doi: http://dx.doi.org/10.1175/JHM409.1.

65. Crane RG, Hewitson BC. 1998. Doubled CO_2 precipitation changes for the Susquehanna basin: downscaling from GENESIS general circulation model. International Journal of Climatology, 18, pp: 65-76.

66. Cuenca RH. 1989. Irrigation system design: an engineering approach. Prentice-Hall, Englewood Cliffs, pp: 133

67. Cuenca RH. 1989. Irrigation system design: an engineering approach. Prentice-Hall, Englewood Cliffs, New Jersey.

68. Cunderlik JM, Burn DH. 2004. Linkages between regional trends in monthly maximum flows and selected climatic variables. ASCE J.of Hydrol. Engg., 9(4), pp: 246–256.

69. Das DC, Sarkar TK, Mukhopadhaya DP. 2009. Drought in Chhattisgarh. J. Soil Water Conserv. 8(1), pp: 25-32.

70. Dash SK, Kulkarni MA, Mohanty UC, Prasad K. 2009. Changes in the characteristics of rain events in India, J. Geophy. Res., 114, D10109, doi: 10.1029/2008JD010572.

71. De Silva CS, Weatherhead EK, Knox JW, Rodriguez-Diaz JA. 2007. Predicting the impacts of climate change—a case study on paddy irrigation water requirements in Sri Lanka. Agricultural Water Management 93(1–2), pp: 19–29.

72. Deng ZQ, Patil A. 2011. Assessment of water quality variation in Amite River watershed under changing climate and land use. Water quality: current trends and expected climate change impacts. IAHS Publ; pp: 348.

73. Dettinger MD, Cayan DR, Meyer MK, Jeton AE. 2004. Simulated hydrologic responses to climate variations and change in the Merced, Carson, and American river basins, Sierra Nevada, California, pp: 1900–2099, Clim. Change, 62(1–3), 283–3doi:10.1023/B:CLIM. 0000013683.13346.4f.

74. Dhorde A, Dhorde A, Gadgil AS. 2009. Long-term Temperature Trends at Four Largest Cities of India during the Twentieth Century, J. Ind. Geophys. Union, 13(2), pp: 85-97.

75. Dibike YB, Coulibaly P. 2005. Hydrologic impact of climate change in the Saguenay watershed: comparison of downscaling methods and hydrologic models, Journal of Hydrology 307 (1-4), pp: 145-163.

76. Dinpashoh Y, Jhajharia D, Fard AF, Singh VP, Kahya E. 2011. Trends in reference crop evapotranspiration over Iran. J. of Hydrol. 399, pp: 422–433.

77. Dinpashoh Y. 2006. Study of reference crop evapotranspiration in I.R of Iran. Agric. Water Manage., 84, pp: 123–129.

78. Doll P, Siebert S. 2002. Global modeling of irrigation water requirements. Water Resources Research, 38(4), pp: 1-8

79. Doll P. 2002. Impact of climate change and variability on irrigation requirements: A global perspective. Climatic Change. Kluwer Academic Publishers. Printed in the Netherlands. 54, pp: 269–293.

80. Doorenbos J, Kassam AH. 1979. Yield Response to Water. FAO, Irrig. Drain. Paper No. 33, FAO, Rome, Italy, pp: 193.

81. Doorenbos J, Pruitt WO. 1975. Guidelines for predicting crop water requirements, Irrigation and Drainage Paper no. 24, FAO-ONU, Rome, Italy, pp: 168.

82. Doorenbos J, Pruitt WO. 1977. Guidelines for predicting crop water requirements. FAO, Rome, Irrig. Drain. Paper No. 24, pp: 144.

83. Douglas EM; Vogel R.M. Knoll, C.N., 2000. Trends in flood and low flows in the United States: impact of spatial correlation. J. Hydrol. 240, 90–105.

84. Duhan D, Pandey A, Pandey RP. 2012. Analysing trends in reference evapotranspiration and weather variables in the Tons River Basin in Central India. Stoch Environ Res Risk Assess, DOI 10.1007/s00477-012-0677-7.

85. Easterling WE, Crosson PR, Rosenberg NJ, McKenney MS, Katz LA, Lemon KM. 1993. Agricultural impacts of and response to climate change in the Missouri-Iowa-Nebraska-Kansas (MINK) region. Climate Change 24, pp: 23–61.

86. Elgaali E, Garcia LA, Ojima DS. 2007. High resolution modeling of the regional impacts of climate change on irrigation water demand. Climate Change 84, pp: 441–461.

87. FAO, 1975. Production vegetale et protection des plantes. Surveillance agromrteorologique pour la prevision des recoltes, N°117.

88. Faucher M, Burrows WR, Pandolfo L. 1999. Empirical-statistical reconstruction of surface marine winds along the western coast of Canada. Clim. Res., 11, pp: 173-190.

89. Federer CA, Vorosmarty C, Fekete B. 1996. Intercomparison of Methods for Calculating Potential Evaporation in Regional and Global Water Balance Models. Water Resour. Res, 32, pp: 2315-2321.

90. Fowler HJ, Kilsby CG, O'Connell PE. 2000. A stochastic rainfall model for assessment of regional water resource systems under changed climatic conditions. Hydrological and Earth Systems Science, 4, pp: 263-282.

91. Fowler, HJ, Blenkinsopa S, Tebaldib C.2007. Linking climate change modelling to impacts studies: recent advances in downscaling techniques for hydrological modeling. Int. J. Climatol. 27, pp: 1547–1578.

92. Fu G, Stephen CP, Yu J. 2009. A critical overview of pan evaporation trends over the last 50 years. Climatic Change, 97, pp: 193-214.

93. Gadgil A. 1986. Annual and weekly analysis of rainfall and temperature for Pune: A multiple time series approach. Inst. Indian Geographers, 8(1).

94. Gao G, Chen DL, Ren GY, Chen Y, Liao YM. 2006. Spatial and temporal variations and controlling factors of potential evapotranspiration in China: 1956–2000. Journal of Geographical Sciences 16, pp: 3–12. DOI: 10.1007/s11442-006-0101-7.

95. Garbrecht J, Van Liew M, Brown GO. 2004. Trends in precipitation, streamflow and evapotranspiration in the great plains of the United States. Journal of Hydrologic Engineering, 9, pp: 360-367.

96. Gaur ML, Mathur BS. 2003. Modeling event-based temporal variability of flow resistance coefficient. J. Hydrologic Engg.8 (5), pp: 266-277.

97. Geeta K, Mishra SK, Eldho TI, Rastogi AK, Pandey RP. 2008. SCS-CN-based continuous simulation model for hydrologic forecasting. Water Res. Manage., 22, pp: 165-190.

98. Geetha K, Mishra SK, Eldho TI, Rastogi AK, Pandey RP 2007. Modifications to SCS-CN Method for Long-Term Hydrologic Simulation. Journal of Irrigation and Drainage Engineering, 133(5), pp: 475-486.

99. Georgakakos KP, Smith DE. 2001. Soil Moisture Tendencies into the Next Century for the Conterminous United States. Journal of Geophysical Research-Atmospheres, 106(D21), pp: 27367-27382.

100. George BA, Reddy BRS, Raghuwanshi NS, Wallender WW. 2002. Decision support system for estimating reference evapotranspiration. J. Irrig Drain. Eng. 128, pp: 1–10.

101. George BA, Reddy BRS, Raghuwanshi NS, Wallender WW. 2002. Decision support system for estimating reference evapotranspiration. J. Irrig Drain. Eng. 128, pp: 1–10.

102. Ghosh S, Mujumdar PP. 2007. Nonparametric Methods for Modeling GCM and Scenario Uncertainty in Drought Assessment, Water Resources Research, 43, W07405, doi:10.1029/2006WR005351.

103. Ghosh S, Mujumdar PP. 2008. Statistical downscaling of GCM simulations to streamflow using relevance vector machine. Advances in Water Resources 31, pp: 132-146.

104. Gidrometeoizdat. 1967. The water resources and water balance of the territory of the Soviet Union, Leningrad, Russia, 199.

105. Gilbert RO. 1987. Statistical methods for environmental pollution monitoring. Van Nostrand Reinhold, New York, 336.

106. Goel Arun. 2012. Application of support vector machine techniques for prediction of discharge in triangular weir, Water and Energy International, 69(9), pp: 45-51.

107. Gong LB, Xu CY, Chen DL, Halldin S, Chen YQD. 2006. Sensitivity of the Penman-Monteith reference evapotranspiration to key climatic variables in the Changjiang (Yangtze River) basin. Journal of Hydrology, 329 (3-4), pp: 620–629. DOI:10.1016/j.jhydrol.2006.03.027.

108. Govindaraju RS, Rao AR. (eds.). 2000. Artificial neural networks in hydrology, Kluwer Academic Publishers, Dordrecht.

109. Goyal MK, Ojha CSP. 2010. Evaluation of linear regression methods as downscaling tools in temperature projections over the Pichola Lake Basin in India. Hydrological Processes. 25(9), pp: 1453–1465.

110. Goyal MK, Ojha CSP. 2012. Downscaling of Surface Temperature for Lake Catchment in Arid Region in India using Linear Multiple Regression and Neural Networks. International Journal of Climatology, Wiley InterScience on behalf of Royal Meteorological Society (RMetS), 32(4), pp: 552–566.

111. Grotch S, MacCracken M. 1991. The use of general circulation models to predict regional climatic change. J Clim 4, pp: 286–303.

112. Gupta HV, Sorooshian S, Yapo PO. 1999. Status of automatic calibration for hydrologic models: Comparison with multilevel expert calibration. J. Hydrologic Eng. 4(2), pp: 135-143.

113. Haberlandt U. 2007. Geostatistical interpolation of hourly precipitation from rain gauges and radar for a large-scale extreme rainfall event. J. Hydrol., 332, pp: 144–157.

114. Hakan A. 2010. Trend analysis of hydro-meteorological parameters in climate regions of Turkey. Conference on Water Observation and Information System for Decision Support, May, 25-29, BALWOIS, Republic of Macedonia, pp: 1- 11.

115. Hamed KH, Rao AR. 1998. A modified Mann-Kendall trend test for auto correlated data. J. of Hydrol. 204, pp: 182–196.

116. Hargreaves GH, Samani ZA. 1982. Estimating of potential evapotranspiration. J. Irrig. Drain. Engg-ASCE 108, pp: 223-230.

117. Hargreaves GH, Samani ZA. 1985. Reference crop evapotranspiration from temperature. Applied Engrg. in Agr., Am. Soc. Agr. Engr, 1(2), pp: 96-99.

118. Harmsen EW, Miller NL, Schlegel NJ, Gonzalez JE. 2009. Seasonal climate change impacts on evapotranspiration, precipitation deficit and crop yield in Puerto Rico. Agricultural Water Management 96, pp: 1085–1095.

119. Hassan H, Aramaki T, Hanaki K, Matsuo T, Wilby RL. 1998. Lake stratification and temperature profiles simulated using downscaled GCM output. J. Water Sci. Technol. 38, pp: 217–226.

120. Hawkins RH. 1978. Runoff curve numbers with varying site moisture. J Irrig Drain Eng 104(4), pp: 389–398.

121. Hawkins RH. 1979. Runoff curve numbers from partial area watersheds, J. Irrig. Drain. Div., 105(4), pp: 375-389.

122. Hawkins RH. 1993. Asymptotic determination of runoff curve numbers from data. J Irrig Drain Engg. 119(2), pp: 334–345.

123. Hawkins RH. 2001. Discussion of Another look at SCS-CN method by Mishra S.K. and Singh V.P., Journal of Hydrologic Engineering, ASCE, 6(5), pp: 451.

124. Hay LE, Clark MP, Wilby RL, Gutowski WJ, Leavesley GH, Pan Z, Arritt RW. 2002. Use of regional climate model output for hydrologic simulations, J. Hydrometeorol., 3(5), pp: 571–590, doi: 10.1175/ 1525-7541(2002)003<0571: UORCMO>2.0.CO; 2.

125. Hegerl GC, Zwiers FW, Braconnot P, Gillett NP, Luo Y. 2007. Understanding and Attributing Climate Change. In: Climate Change 2007: The Physical Science Basis, Solomon, S., (Ed.). IPCC, New York, pp: 663-746.

126. Helsel DR, Hirsch RM. 1992. Statistical Methods in Water Resources. Elsevier, Amsterdams, the Netherlands, Elsevier Publishers, pp: 529.

127. Hershfield DM. 1964. Effective rainfall and irrigation water requirement. Proceedings of the ASCE. J Irrig Drain Div 90, pp: 33–37.

128. Hessami M, Gachon P, Ouarda TBMJ, St-Hilaire, A. 2008. Automated regression-based statistical downscaling tool. Environmental Modelling & Software. 23(6), pp: 813-834. doi>10.1016/j.envsoft.2007.10.004

129. Hewitson BC, Crane RG. 1996. Climate downscaling: techniques and application. Clim Res 7, pp: 85–95.

130. Hingane LS, Rupa Kumar K, Ramana Murthy BV. 1985. Long-term trends of surface air temperature in India, J. Climatology, 5, pp: 521-528.

131. Hingane LS. 1995. Is a signature of socio-economic impact written on the climate?, Climatic Change, pp: 91-101.

132. Hirsch RM, Slack JR, Smith RA. 1982. Techniques of trend analysis for monthly water quality data. Water Resour. Res. 18 (1), pp: 107–121.

133. Hjelmfelt AT. 1980. Curve number procedure as infiltration method, Journal of the Hydraulics Division, 106(6), pp: 1107-1110.

134. Hjelmfelt AT. 1991. Investigation of curve number procedure. J Hydraul Eng 117(6), pp:725–737.doi:10.1061/(ASCE)0733-9429(1991)117:6(725).

135. Holland GJ, Done J, Bruyere C, Cooper C, Suzuki A. 2010. Model investigations of the effects of climate variability and change on future Gulf of Mexico tropical cyclone activity. OTC Metocean.

136. Hornik K, Stinchcombe MB, White H. 1989. Multilayer feed forward network are universal approximators. Neural Networks, 2(5), pp: 359-366.

137. Hulme M, Osborn TJ, Johns TC. 1998. Precipitation sensitivity to global warming: comparison of observations with HadCM2 simulations. Geophys Res Lett 25(17), pp: 3379-3382.

138. Huth R. 1999. Statistical downscaling in central Europe: evaluation of methods and potential predictors. Climate Research, 13, pp: 91-101.

139. Iman RL, Helton JC, 1988. An investigation of uncertainty and sensitivity analysis techniques for computer models."Risk Analysis, 8(1), pp: 71–90.

140. IPCC. 2007. Climate Change 2007: Synthesis Report. Contribution of Working Groups I, II and III to the Fourth Assessment Report of the Intergovernmental Panel on Climate Change. [Core Writing Team, Pachauri, R.K and Reisinger, A. (eds.)]. IPCC, Geneva, Switzerland, pp: 104.

141. Irmak S, Haman D, Jones W. 2002. Evaluation of Class A pan coefficients for estimating reference evapotranspiration in humid location. J. Irrig Drain Engg. 128(3), pp:153–159

142. Irmak S, Payero JO, Martin DL, Irmak A, Howell TA. 2006. Sensitivity Analyses and Sensitivity Coefficients of Standardised daily ASCE- Penman-Monteith Equation. J. Irrig. Drain. Eng., ASCE, 132(6), pp: 564-578.

143. Jain MK, Mishra SK Babu PS, Venugopal K, Singh VP. 2006. Enhanced runoff curve number model incorporating storm duration and a nonlinear Ia-S relation. J. Hydrol. Eng. 11(6), pp: 631-635.

144. Jain SK, Kumar V. 2012. Trend analysis of rainfall and temperature data for India. Current Science, 102(1), pp: 37-49.

145. Jang M, Choi J, Lee J. 2007. A spatial reasoning approach to estimating paddy rice water demand in Hwanghaenam-do, North Korea. Agric. Water Manage., 893, pp:185–198.

146. Janssen PHM, Heuberger PSC, and Sanders, R., 1992. "UNCSAM 1.1: A software package for sensitivity and uncertainty analysis." Rep. No. 959101004, National Institute of Public Health and Environmental Protection, Bilthoven, The Netherlands.

147. Jasper K, Calanca PL, Gyalistras D, Fuhrer J. 2004. Differential impacts of climate change on the hydrology of two alpine river basis. Clim Res, 26, pp: 113–129.

148. Jat MK, Khare D, Garg PK, Shankar V. 2009. Remote sensing and GIS-based assessment of urbanisation and degradation of watershed health. Urban Water Journal, 6(3), pp: 251-263, doi: 10.1080/15730620801971920.

149. Jensen ME, Burman RD, Allen RG. 1990. Evapotranspiration and irrigation water requirements, ASCE- Manuals and Reports on Engineering Practice 70, New York, USA, pp: 332.

150. Jensen ME, Haise HR. 1963. Estimating evapotranspiration from solar radiation. Proc. J. Irrig. and Drain. Div., Am. Soc. Civ. Engr., 89(IR4):15-41, Closure, 91(IR1),pp: 203-205.

151. Jhajharia D, Dinpashoh Y, Kahya E, Singh VP, Fakheri-Fard A. 2011. Trends in reference evapotranspiration in the humid region of northeast India. Hydrological Processes. DOI: 10.1002/hyp.8140 Burn DH, Hesch NM. 2007. Trends in evaporation for the Canadian Prairies. J Hydrol, 336, pp: 61-73.

152. Jiang T, Chen YD, Xu C, Chen X, Chen X, Singh VP. 2007. Comparison of hydrological impacts of climate change simulated by six hydrological models in the Dongjiang Basin, South China. J. Hydrol. 336, 316–333.

153. Jin JM, Wang SY, Gillies RR. 2011. An Improved Dynamical Downscaling for the Western United States, Climate Change - Research and Technology for Adaptation and Mitigation, Juan Blanco and Houshang Kheradmand (Ed.), ISBN: 978-953-307-621-8, InTech, pp: 23-38.

154. Joachims T, 1999. Making large scale support vector machine learning practical. Advances in Kernel Methods-Support Vector Learning, Scholkopf et al., Eds. MIT Press, Cambridge, MA, pp: 169-184.

155. Johnson MS, Coon WF, Mehta VK, Steenhuis TS, Brooks ES, Boll J. 2003. Application of two hydrologic models with different runoff mechanisms to a hillslope dominated watershed in the northeastern US: a comparison of HSPF and SMR. Journal of Hydrology, 284, pp: 57–76, DOI:10.1016/j.jhydrol.2003.07.005.

156. Karpouzos DK, Kavalieratou S, Babajimopoulos C. 2010. Trend analysis of precipitation data in Pieira Region (Greece). European Water. E.W. Publications. 30, pp: 31-40.

157. Katz RW, Brown BG. 1992. Extreme events in a changing climate: variability is more important than averages. Climatic Change 21, pp: 289-302.

158. Kay AL, Davies HN, Bell VA, Jones RG. 2009. Comparison of uncertainty sources for climate change impacts: flood frequency in England. Clim. Change 92, pp: 41–63.

159. Kettle H, Thompson R. 2004. Empirical modeling of summer lake surface temperatures in southwest Greenland. Limnol. Oceanogr. American Society of Limnology and Oceanography, Inc, 49(1), 2004, 271–282.

160. Kilsby CG, Jones PD, Burton A, Ford AC, Fowler HJ, Harpham C, James P, Smith A, Wilby RL. 2007. A daily Weather Generator for use in climate change studies. Environmental Modelling and Software, 22, pp: 1705–1719.

161. Kim MK, Kang IS, Park CK, Kim KM. 2004. Super ensemble prediction of regional precipitation over Korea, Int. J. Climatol., 24(6), pp: 777 – 790.

162. Knisel WG (ed). 1980. CREAMS. A field scale model chemical, runoff and erosion from agricultural management systems. Conservation Research Report, No. 26. USDA, Washington, DC.

163. Kompare B, Steinman F, Cerar U, Dzeroski S. 1997. Prediction of rainfall runoff from catchment by intelligent data analysis with machine learning tools within the artificial intelligence tools. Acta Hydrotechnica, 16, 16 (in Slovene).

164. Krause P, Boyle DP, Base F. 2005. Comparison of different efficiency criteria for hydrological model assessment. Adv. in Geosci., 5, pp: 89–97.

165. Kumar V, Jain SK, Singh Y. 2010. Analysis of Long-term rainfall trends in India. Hydrol. Sci. J. 55(4), pp: 484–496.

166. Kuo SF, Ho SS, Liu CW (2006) Estimation irrigation water requirements with derived crop coefficients for upland and paddy crops in ChiaNan irrigation association, Taiwan. Agric Water Manage 82, pp: 433–451.

167. Lal M. 2001. Climatic change Implications for India's water resources, J. Indian Water Resources Society, 21, pp: 101-119.

168. Landsea CW, Gray WM. 1992. The strong association between western sahelian monsoon rainfall and intense Atlantic hurricanes. A merucan Meteorological society, 5, pp: 435- 453.

169. Leander R, Buishand TA. 2007. Resampling of regional climate model output for the simulation of extreme river flows. Journal of Hydrology, 332, pp: 487-496.

170. Lebel TG, Bastin G, Obled C, Creutin JD. 1987. On the accuracy of areal rainfall estimation: a case study. Water Resour. Res. 23, pp: 2123–2134.

171. Lee Y, Hsieh W, Huang C. 2005. SSVR: A smooth support vector machine for insensitive regression. IEEE Transactions on Knowledge and Data Engineering, 17, pp: 678-685.

172. Legates DR, McCabe GJ. 1999. Evaluating the use of "goodness-of-fit" measures in hydrologic and hydro-climatic model validation. Water Resources Res. 35(1), pp: 233-241.

173. Lehner B, Doll P, Alcamo J, Henrichs T, Kaspar F. 2006. Estimating the impact of global change on flood and drought risks in Europe: A continental, integrated analysis, Clim. Change, 75(3), pp: 273–299, doi: 10.1007/s10584-006-6338-4.

174. Ley TW, Hill RW, Jensen DT. 1994. Errors in Penman-Wright Alfalfa Reference Evapotranspiration Estimates: Effects of Weather Sensor Measurement Variability. Trans. ASAE, 37(6), pp: 1863-1870.

175. Libiseller C, Grimval A. 2002. Performance of partial Mann-Kendall test for trend detection in the presence of covariates. Environmetr. 13, pp: 71–84.

176. Liu BH, Xu M, Henderson M, Gong WG. 2004. A spatial analysis of pan evaporation trends in China, 1955–2000. Journal of Geographical Sciences 109:D15102. DOI: 15110.11029/12004JD004511.

177. Liu S, Mo X, Lin Z, Xu Y, Ji J, Wen G, Richey J. 2010. Crop yield response to climate change in the Huang-Huai-Hai plain of China. Agricultural Water Management 97(8), pp: 1195–1209.

178. Lu J, Sun G, McNulty SG, Amatya DM. 2005. A comparison of six potential evapotranspiration methods for regional use in the South eastern United States, Journal American Water Resources Association 41, pp: 621-633.

179. Ludwig R. et al. 2009. The role of hydrological model complexity and uncertainty in climate change impact assessment. Adv. Geosci.21, pp: 63–71.

180. Maheras P. 1988. Changes in precipitation conditions in the Western Mediterranean over the last century. Journal of Climatology 8, pp: 179–189.

181. Maidment DR. 1991. GIS and Hydrologic modeling, Proc., 1st Int. Conference on GIS and Envir. Modeling, Boulder, Colorado, USA, pp: 147–167

182. Makkeasorn A, Chang NB, Beaman M, Wyatt C, Slater C. 2006. Soil moisture estimation in a semiarid watershed using RADARSAT-1 satellite imagery and genetic programming. Water Resources Research, 44, doi: 10.1029/2005WR004033.

183. Makkink GF. 1957, Testing the Penman Formula by Means of Lysimeters, J. Instit. Water Engineers 11, pp: 277–288.

184. Mall RK, Bhatia R, Pandey SN. 2007. Water resources in India and impact of climate change, Jalvigyan Sameeksha, 22, pp: 157–176.

185. Mangasarian OL, Musicant DR. 1999. Successive over relaxation for support vector machines. IEEE Transactions on Neural Networks, 10(5), pp: 1032-1037.

186. McAlpine CA, Syktus J, Deo RC, Lawrence P J, McGowan HA, Watterson IG, Phinn S R. 2007. Modeling the impact of historical land cover change on Australia's regional climate, Geophysical Research Letters, Vol. 34, L22711, pp: 1-6 doi:10.1029/2007GL031524.

187. McCuen R. 1973. The role of sensitivity analysis in hydrologic modelling., J. Hydrol., 18, pp: 37–53.

188. McCuen RH. 1982. Hydrologic Analysis and Design. Prentice Hall Inc., Englewood Cliffs, New Jersey07632, USA.

189. McCuen RH. 2002. Approach to confidence interval estimation for curve numbers. Journal of Hydrologic Engineering, 7(1), pp: 43-48.

190. Mearns LO, Rosenzweig C, Goldberg R. 1997. Mean and variance change in climate scenarios: methods, agricultural applications, and measures of uncertainty. Climatic Change 35, pp: 367–396.

191. Michel C, Vazken A, Charles P. 2005. Soil Conservation Service number method: How to mend among soil moisture accounting procedure. Water Resour. Res 41(2).

192. Mintz Y, Walker GK. 1993. Global fields of soil moisture and land surface evapotranspiration derived from observed precipitation and surface air temperature. Journal of Applied Meteorology, 32, pp: 1305-1334.

193. Minville M, Krau S, Brissette F, Leconte R. 2008. Behaviour and performance of a Nordic water-resource system under adapted operating policies in a climate change context. Water Resour. Manage. 24 (7), pp: 1333–1352.

194. Mirza MQ, Warrick RA, Ericksen NJ, Kenny GJ. 1998. Trends and persistence in precipitation in Ganges, Brahmaputra and Meghna river basins, Hydrological Sciences, 43, pp: 845-858.

195. Mishra AK, Ozger M, Singh VP. 2009. Trend and persistence of precipitation under climate change scenarios for Kansabati basin, India, Hydrological Processes, 23, pp: 2345–2357.

196. Mishra SK, Pandey RP, Jain MK, Singh VP. 2008. A rain duration and modified AMC-dependent SCS-CN procedure for long rainfall-runoff events. Water Resour. Res. 22 (7), pp: 861-876.

197. Mishra SK, Rawat SS, Chakraborty S, Pandey RP, Jain MK. 2014. Relation between Runoff Curve Number and PET. J. of Hydrolog. Engg., 19(2), pp: 355-365.

198. Mishra SK, Singh VP. 1999. Behaviour of SCS-CN method in C- -λ spectrum,' Submitted to Int. Conf. Water, Environment, Ecology, Socio-economics, and Health Engineering, Oct. 18-21, Korea.

199. Mishra SK, Singh VP. 2002. SCS-CN method: Part-I: Derivation of SCS-CN based models. Acta Geophysica Polonica 50 (3), pp: 457-477.

200. Mishra SK, Singh VP. 2003b. SCS-CN method Part-II: Analytical treatment, Acta Geophysica Polonica 51(1), pp: 107-123.

201. Mishra SK, Singh VP. 2004a. Validity and extension of the SCS-CN method for computing infiltration and rainfall-excess rates. Hydrol. Processes 18(17), pp: 3323-3345.

202. Mishra SK, Singh VP. 2004b. Long-term hydrologic simulation based on the Soil Conservation Service curve number. Hydrol. Processes 18, pp: 1291-1313.

203. Mishra SK, Singh, VP. 2003a. Soil conservation Service Curve Number (SCS-CN) Methodology, Kluwer Academic Publishers, P. O. Box 17, 3300 AA Dordrecht, The Netherlands.

204. Mishra SK, Tyagi JV, Singh VP, Singh R. 2006. SCS-CN-based modeling of sediment yield. J. of Hydrol. 324, pp: 301-322.

205. Mishra SK. 1998. Operation of a multipurpose reservoir. Unpublished PhD thesis, University of Roorkee, India.

206. Mockus V. 1949. Estimation of total (and peak rates of) surface runoff for individual storms. Interim Survey Rep. Grand (Neosho) River Watershed, Exhibit A in Appedix B, US. Department of Agriculture, Washington, D.C.

207. MOEF. 2004. India's initial national communication to the United Nations framework convention on climate change, Executive Summary, New Delhi.

208. Moglen GE. 2000. Effect of orientation of spatially distributed curve numbers in runoff calculations. Journal of the American Water Resources Association 36(6), pp: 1391–1400.

209. Mohan S, Arumugam N. 1996. Relative importance of meteorological variables in evapotranspiration: Factor analysis approach. Water Resources Management, 10 (1), pp: 1–20.

210. Monteith, J. L. (1965). Evaporation and environment. In G. E. Fogg (Ed.), Symposium of the Society for Experimental Biology, The State and Movement of Water in Living Organisms, Vol. 19. Academic Press, Inc., NY, pp: 205–234.

211. Mooley DA, Parthasarthy B. 1984. Fluctuations of all India summer monsoon rainfall during 1871-1978, Climatic Change, 6, pp: 287-301.

212. Moore RJ, Clarke RT. 1981. A distribution function approach to rainfall–runoff modeling. Water Resources Research 17(5), pp: 1367–1382.

213. Moore RJ. 1983. The Probability-Distributed Approach to Spatial Conceptual Rainfall–Runoff Modeling, Report to Flood Protection Commission, Ministry of Agriculture, Fisheries and Food, Institute of Hydrology: Wallingford.

214. Moore RJ. 1985. The probability-distributed principle and runoff production at point and basin scales. Journal of Hydrological Sciences 30(2), pp: 273–297.

215. Moran MS, Peters-Lidard CD, Watts JM, McElroy S. 2004. Estimating soil moisture at the watershed scale with satellite-based radar and land surface models. Canadian Journal of Remote Sensing, 30(5), pp: 805−826.

216. Moriasi DN, Arnold JG, Van Liew MW, Bingner RL, Harmel RD, Veith TL. 2007. Model Evaluation Guidelines for Systematic Quantification of Accuracy in Watershed Simulations, American Society of Agricultural and Biological Engineers. ISSN 0001−2351, Vol. 50(3), pp: 885−900.

217. Morton FI. 1994. Evaporation research- A critical review and its lessons for the environmental sciences. Critical Reviews in Environmental Science and Technology 24 (3), pp: 237–280.

218. Nagler P, Scott R, Westenberg C, Cleverly J, Glenn E, Huete A. 2005. Evapotranspiration on western U.S. rivers estimated using the enhanced vegetation index from MODIS and data from eddy covariance and Bowen ratio flux towers. Remote Sensing of Environment 97, pp: 337–351.

219. Najafi MR, Moradkhani H, Wherry SA. 2011. Statistical Downscaling of Precipitation using Machine Learning with Optimal Predictor Selection. Journal of Hydrologic Engineering 16, pp: 650–664.

220. Nash JE, Sutcliffe JV. 1970. River flow forecasting through conceptual models part I-A discussion of principles, Journal of Hydrology, 10 (3), pp: 282–290.

221. Novotny EV, Stefan HG. 2007. Stream flow in Minnesota: indicator of Climate Change. J. of Hydrol. 334, pp: 319–333.

222. Oki T, Kanae S. 2006. Global hydrological cycles and world water resources, Science, 313(5790), pp: 1068–1072, doi:10.1126/science.1128845.

223. Olsson J. et al. 2004. Neural Networks for rainfall forecasting by atmospheric downscaling. J. Hydrol. Engg., 9(1), pp: 1-12.

224. Orang M (1998) Potential accuracy of the popular non-linear regression equations for estimating pan coefficient values in the original and FAO-24 tables. Unpublished Report, California Department of Water Resources, Sacramento, CA.

225. Osborn TJ, Hulme M, Jones PD, Basnett TA. 2000. Observed trends in daily intensity of United Kingdom precipitation. International Jornal of Climatology; 20; pp: 347-364.

226. Pandey VK, Tirkey G, Tripathi MP. 2011. Watershed parameterization using geographic information system and satellite remote sensing. In ‘Engineering Interventions in Agriculture’, NSAE-2011, pp: 360-368.

227. Pandit A, Gopalakrishnan G. 1996. Estimation of Annual Storm Runoff Coefficients by Continuous Simulation. ASCE Journal of Drainage and Irrigation Engineering, 122(4), pp: 211-220.

228. Pant GB, Kumar KR. 1997. Climates of South Asia, John Wiley & Sons Ltd., West Sussex, UK.

229. Parry ML, Rosenzweig C, Iglesias A, Livermore M, Fischer G. 2004. Effects of climate change on global food production under SRES emissions and socio-economic scenarios. Global Environmental Change 14(1), pp: 53–67.

230. Partal T, Kahya E. 2006. Trend analysis in Turkish precipitation data. Hydrol. Processes 20, pp: 2011–2026.

231. Patra JP, Mishra A, Singh R, Raghuwanshi NS. 2012. Detecting rainfall trends in twentieth century (1871–2006) over Orissa State, India, Climatic Change, 111, pp: 801–817.

232. Patricola CM, Cook KH. 2010. Northern African climate at the end of the twenty-first century: an integrated application of regional and global climate models. Climate Dyn., 35, pp: 193–212.

233. Patwardhan AS, Nieber JL, Johns EL. 1990. Effective rainfall estimation methods. J Irrig Drain Eng 116(2), pp: 182–193.

234. Penman HL. 1948. Natural evaporation from open water, bare soil, and grass. Proc. Roy. Soc. London A193, pp: 120-146.

235. Penman HL. 1963. Vegetation and Hydrology. Tech. Common. 53, Commonwealth Bureau of Soils, Harpenden, England.

236. Peterson TC, Golubev VS, Groisman PY. 1995. Evaporation losing its strength. Nature 377, pp: 687–688. DOI: 10.1038/377687b0.

237. Piper B. 1989. Sensitivity of Penman Estimates of Evaporation to Errors in Input Data. Agri. Water Manag., 15, pp: 279-300.

238. Platt J. 1998. Fast training of support vector machines using sequential minimal optimization. Scholkopf et al., Eds. Advances in Kernel Methods-Support Vector Learning, MIT Press, Cambridge, MA, pp: 185-208.

239. Ponce VM, Hawkins RH. 1996. Runoff curve number: Has it reached maturity. J. of Hydrolog. Engg., ASCE 1(1), pp: 11-19.

240. Ponce VM. 1989. Engineering Hydrology: Principles and practices. Prentice Hall Inc., Englewood Cliffs, New Jersey 07632, USA.

241. Poulin A, Brissette F, Leconte R, Arsenault R, Malo JS. 2011. Uncertainty of hydrological modelling in climate change impact studies in a Canadian, snow-dominated river basin, Journal of Hydrology 409, pp: 626–636.

242. Praveen P, Sachin Kumar MD, Puttaswamy H, Patil VM, Kumar R. 2011. Estimation of Evapotranspiration Rate by Different Methods for Paddy Crop in South Kodagu, Central Western Ghats. Plant Sciences Feed. 1 (1) pp: 1- 5.

243. Prestt AJ. 1986. Irrigation Scheduling by Evaporation Pan. Zimbabwe Agric. Journal 83(2), pp: 67-72

244. Priestley CHB, Taylor RJ. 1972. On the assessment of surface heat flux and evaporation using large scale parameters. Monthly Weather Review, 100, pp: 81–92.

245. Qudin L., et al. 2005. Which potential evapotranspiration input for a lumped rainfall-runoff model? Part 2-Towards a simple and efficient potential evapotranspiration model for rainfall-runoff modeling. J. Hydrol., 303(1–4), pp: 290–306.

246. Quinlan JR. 1992. Learning with continuous classes. Proceedings 5th Australian Joint Conference on Artificial Intelligence. World Scientific, Singapore, pp: 343-348.

247. Racz C, Nagy J, Dobos AC. 2013. Comparison of Several Methods for Calculation of Reference Evapotranspiration. Acta Silv. Lign. Hung., Vol. 9, pp: 9–24.

248. Raghavendra VK. 1974. Trends and periodicities of rainfall in sub-divisions of Maharashtra state. Indian J. Met. Geophys., 25, pp: 197–210.

249. Raghuwanshi NS, Singh R, Reddy LS. 2006. Runoff and Sediment Yield Modeling Using Artificial Neural Networks: Upper Siwane River, India. J. Hydrol. Eng., 11(1), pp: 71–79.

250. Rahimikhoob A. 2009. An evaluation of common pan coefficient equations to estimate reference evapotranspiration in a subtropical climate (north of Iran). Irrig. Sci., 27, pp: 289–296.

251. Rallison RE. 1980. Origin and evolution of the SCS runoff equation. In: Proceedings of symposium on watershed management. ASCE, New York, pp: 912–924.

252. Ramasastry KS, Seth SM. 1985. Rainfall runoff relationships. Rep. RN-20, National Institute of Hydrology, Roorkee, Uttrakhand, India.

253. Rana G, Katerji N. 1998. A Measurement Based Sensitivity Analysis of the Penman-Monteith Actual Evapotranspiration Model for Crops of Different Height and in Contrasting Water Status. Theoret. Appl. Climatol., 60, pp: 141-149.

254. Raneesh KY, Thampi SG. 2013. Bias Correction for RCM Predictions of Precipitation and Temperature in the Chaliyar River Basin. J Climatol Weather Forecasting, 1(2), pp: 1-6.

255. Rao AR, Hamed KH, Chen HL. 2003. Nonstationarities in Hydrologic and Environmental Time Series. Kluwer Academic Publishers: The Netherlands, pp: 362.

256. Rao PG. 1993. Climate changes and trends over a major river basin in India. Clim. Res., 2, pp: 215-223.

257. Rathod IM, Aruchamy S. 2010. Spatial analysis of rainfall variation in Coimbatore District, Tamil Nadu using GIS, International Journal of Geomatics and Geoscience, 1(2), pp: 106-118.

258. Rayner DP. 2007. Wind run changes: the dominant factor affecting pan evaporation trends in Australia. Journal of Climate 20, pp: 3379–3394. DOI:10.1175/JCLI4181.1.

259. Rehana S, Mujumdar PP. 2012. Regional impacts of climate change on irrigation water demands. Hydrol. Process., DOI: 10.1002/hyp.9379.

260. Rind D, Goldberg R, Ruedy R. 1989. Change in climate variability in the 21st century. Climatic Change 14, pp: 5–37.

261. Roderick ML, Rotstayn LD, Farquhar GD, Hobbins MT. 2007. On the attribution of changing pan evaporation. Geophysical Research Letters 34: L17403. DOI: 17410.11029/12007GL031166.

262. Rodriguez Diaz JA, Weatherhead EK, Knox JW, Camacho E. 2007. Climate change impacts on irrigation water requirements in the Guadalquivir river basin in Spain. Regional Environmental Change 7, pp: 149–159.

263. Rodriguez-Puebla C, Encinas AH, Nieto S, Garmendia J. 1998. Spatial and temporal patterns of annual precipitation variability over the Iberian Peninsula. International Journal of Climatology 18, pp: 299–316.

264. Rosenzweig C, Parry ML. 1994. Potential impact of climate change on world food supply. Nature 367, pp: 133–138.

265. Rupa Kumar K, Krishna Kumar K, Pant GB. 1994. Diurnal asymmetry of surface temperature trends over India, Geophysical Research Letters, 21, pp: 677–680.

266. Rupa Kumar K, Pant GB, Parthasarathy B, Sontakke NA. 1992. Spatial and sub seasonal patterns of the long term trends of Indian summer monsoon rainfall, International J. Climatology, 12, pp: 257-268.

267. Sachindra DA, Huang F, Barton A, Perera BJC. 2013. Least square support vector and multi-linear regression for statistically downscaling general circulation model outputs to catchment streamflows. Int. J. Climatol., 33, pp: 1087-1106.

268. Saghravani SR, Mustapha S, Ibrahim S, Randjbaran E. 2009. Comparison of daily and monthly results of three evapotranspiration models in tropical zone: A case study. American Journal of Environmental Sciences, 5, pp: 698-705.

269. Saltelli A, Chan K, Scott M. 2004. Sensitivity Analysis. John Wiley and Sons Publishers, N. Y.

270. Santhi C, Arnold JG, Williams JR, Dugas WA Srinivasan R, Hauck, LM. 2001. Validation of the SWAT model on a large river basin with point and nonpoint sources. J. American Water Resources Assoc. 37(5), pp: 1169-1188.

271. Sarkar RP. Thapliyal V. 1988. Climate change and variability, Mausam, 39, pp: 127-138.

272. Sato T, Kimura F, Kitoh A.2007. Projection of global warming onto regional precipitation over Mongolia using a regional climate model, J. Hydrol., 333, doi:10.1016/j.jhydrol.2006.07. 023.

273. Saxton KE. 1975. Sensitivity Analysis of the Combination Evapotranspiration Equation. Agric. Meterol., 15, pp: 343-353.

274. Schmidt M, Glade T. 2003. Linking global circulation model outputs to regional geomorphic models: a case study of landslide activity in New Zealand. Clim. Res., 25, pp: 135-150.

275. Schneider LE, McCuen RH. 2005. Statistical guidelines for curve number generation. Journal of Drainage and Irrigation Engineering. 131(3), pp: 282-290.

276. Schoof JT, Pryor SC. 2001. Downscaling temperature and precipitation: A comparison of regression-based methods and artificial neural networks. International Journal of Climatology 21, pp: 773–790.

277. Schwartz P, Randall D. 2003. An abrupt climate change scenario and its implications for United States national security. 1st Edn., Diane Publishing Co., USA., pp: 22.

278. Semenov MA, Porter JR. 1994. The implications and importance of non-linear responses in modelling of growth and development of wheat. In Predictability and Non-linear Modelling in Natural Sciences and Economics, Grasman J, van Straten G (eds). Pudoc: Wageningen.

279. Semenov MA, Stratonovitch P. 2010. The use of multi-model ensembles from global climate models for impact assessments of climate change. Clim. Res. 41, pp: 1-14.

280. Seneviratne SI., et al. 2012. Changes in climate extremes and their impacts on the natural physical environment, in Managing the Risks of Extreme Events and Disasters to Advance Climate Change Adaptation: A Special Report of Working Groups I and II of the Intergovernmental Panel on Climate Change (IPCC), edited by C. B. Field et al., pp: 109–230, Cambridge Univ. Press, Cambridge, U. K.

281. Shahid S. 2011. Impact of climate change on irrigation water demand of dry season Boro rice in northwest Bangladesh. Climate Change 105, pp: 433–453.

282. Sharma KD, Soni B. 2006. (editors), Land Use Diversification for Sustainable Rainfed Agriculture, Atlantic Publishers and Distributors, New Delhi, 410027.

283. Shuttleworth WJ. 1993. Evaporation, in: Maidment DR. (Ed.), Handbook of Hydrology. McGraw-Hill, New York.

284. Simonovic SP, Davies EGR. 2006. Are we modelling impacts of climatic change properly?, Hydrological Processes 20, pp: 431-433.

285. Singh B, Maayar ME, André P, Bryant CR, Thouez JP. 1998. Impacts of a GHG-induced climate change on crop yields: Effects of acceleration in maturation, moisture stress, and optimal temperature. Climate Change 38, pp: 51–86.

286. Singh J, Knapp HV, Demissie M. 2004. Hydrologic modeling of the Iroquois River watershed using HSPF and SWAT. ISWS CR 2004-08. Champaign, Ill.: Illinois State Water Survey. Available at: www.sws.uiuc.edu/pubdoc/CR/ ISWSCR2004-08.pdf.

287. Singh P, Kumar V, Thomas T, Arora M. 2008a. Changes in rainfall and relative humidity in different river basins in the northwest and central India. Hydrol. Processes 22, pp: 2982–2992.

288. Singh P, Kumar V, Thomas T, Arora M. 2008b. Basin-wise assessment of temperature variability and trends in the northwest and central India. Hydrolo. Sci. J. 53, pp: 421–433.

289. Singh VP, Chowdhury PK. 1986. Comparing some methods of estimating mean areal rainfall. Water Resour. Bull. 22, pp: 275–282.

290. Singh VP.1989, Hydrologic Systems, Vol. II, Watershed Modelling, Prentice-Hall, Inc.

291. Sinha Ray KC, De US. 2003. Climate change in India as evidenced from instrumental records, WMO Bulletin, 52(1), pp: 53-58.

292. Sinha Ray KC, Mukhopadhayay RK, Chowdhury SK. 1997. Trends in maximum minimum temperatures and sea level pressure over India, INTROPMET-97, IIT New Delhi, pp: 2-5.

293. Smajstrla AG, Zazueta FS, Schmidt GM. 1987. Sensitivity of Potential Evapotranspiration to Four Climatic Variables in Florida. Soil and Crop Sci. Soc. of Florida, 46, pp: 21-26.

294. Smith MR, Allen RG, Monteith JL, Pereira LS, Segeren A. 1991. Rep. on the Expert Consultation on Procedures for Revision of FAO Guidelines for Predicting Crop Water Requirements. FAO, Land and Water Devel. Div., Food and Agricultural Organization of the United Nations, Rome.

295. Snyder RL. 1992. Equation for evaporation pan to evapotranspirationconversions. J Irrig Drain Eng 118(6), pp: 977–980.

296. Soil Conservation Services, 1956. National Engineering Handbook, Supplement A, Section 4, Chapter 10, Hydrology, Soil Conservation Service, USDA, Washington, D.C.

297. Solomatine DP, Dulal KN. 2003. Model tree as an alternative to neural network in rainfall-runoff modelling. Hydrological Sciences J. 48(3), pp: 399–411.

298. Soni B, Mishra GC. 1985. Soil water accounting using SCS hydrologic soil classification, case study. National Institute of Hydrology, Roorkee (India).

299. Srivastava HN, Sinha Ray KC, Dikshit SK, Mukhopadhaya RK. 1998. Trends in rainfall and radiation over India, Vayu Mandal, Jan-Jun, pp: 41-45.

300. Stamm GG. 1967. Problems and procedures in determining water supply requirements for irrigation projects. Chap. 40 in irrigation.

301. Steele-Dunne S, Lynch P, Mcgrath R, Semmler T, Wang S, Hanafin J, Nolan P. 2008. The impacts of climate change on hydrology in Ireland, J. Hydrol., 356(1–2), pp: 28–45, doi:10.1016/j.jhydrol.2008.03.025.

302. Steenhuis TS, Winchell M, Rossing J, Zollweg JA, Walter MF. 1995. SCS runoff equation revisited for variable-source runoff areas. J. Irrig. Drain. Eng., 10.1061/(ASCE)0733-9437(1995)121:3(234), pp: 234–238.

303. Steiner L, Howell TA, Schneider AD. 1991. Lysimetric Evaluation of Daily Potential Evapotranspiration Models for Grain Sorghum. Agron. J., 83, pp: 240-247.

304. Subash N, Sikka AK. 2013. Trend analysis of rainfall and temperature and its relationship over India. Theor Appl Climatol., DOI 10.1007/s00704-013-1015-9.

305. Suykens JAK. 2001. Non linear modeling and support vector machine, IEEE Instrumentation and Measurement Technology Conference, Budapest, Hungary, pp: 287-294.

306. Tabari H, Aeini A, Talaee PH, Some'e S. 2011. Spatial distribution and temporal variation of reference evapotranspiration in arid and semi-arid regions of Iran. Hydrol. Process. DOI: 10.1002/hyp.8146.

307. Tabari H, Grismer EM, Trajkovic S (2011a) Comparative analysis of 31 reference evapotranspiration methods under humid conditions. Irrig. Sci. DOI: 10.1007/s00271-011-0295-z.

308. Tekwa, IJ, Bwade EK. 2011. Requirement of Maize (Zea mays) using Pan Evaporation Model in Maiduguri, Northeastern Nigeria. Agricultural Engineering International. The CIGR E-Journal. Manuscript No. 1552. 13(1), pp: 7.

309. Terink W, Hurkmans RTWL, Torfs PJJF, Uijlenhoet R. 2010. Evaluation of a bias correction method applied to downscaled precipitation and temperature reanalysis data for the Rhine basin. Hydrol. Earth Syst. Sci., 14, pp: 687–703.

310. Thapliyal V, Kulshreshtha SM. 1991. Climate changes and trends over India, Mausam, 42, pp: 333-338.

311. Thomas A. 2000. Spatial and temporal characteristics of potential evapotranspiration trends over China. International Journal of Climatology 20(4), pp: 381–396. DOI: 10.1002/(SICI)1097-0088 (20000330)20:4<381::AID-JOC477>3.0.CO;2-K.

312. Thornthwaite CW. 1948. An approach toward a rational classification of climate. Geogr. Rev. 38, pp: 55-94.

313. Tisseuil C, Vrac M, Lek S, Wade AJ. 2010. Statistical downscaling of river flows. J Hydrol, 385, pp: 279–291.

314. Tolika K, Maheras P, Vafiadis M, Flocas HA, Arseni-Papadimitriou A. 2006. An evaluation of a General Circulation model (GCM) and the NCEP-NCAR Reanalysis data for winter precipitation in Greece, International Journal of Climatology, 26, pp: 935-955.

315. Toriman, M. E., Mokhtar, M., Gasim, M. B., Abdullah, S. M. S., Jaafar, O. & Aziz, N. A. A. (2009). Water resources study and modeling at North Kedah: a case of Kubang Pasu and Padang Terap water supply schemes. Research journal of earth sciences, 1 (2), 35–42.

316. Tripathi S, Srinivas VV, Nanjundiah RS. 2006. Downscaling of precipitation for climate change scenarios: a support vector machine approach. Journal of Hydrology 330(3–4), pp: 621–640.

317. Tukimat NNA, Harun S, Shahid S. 2012. Comparison of different methods in estimating potential evapotranspiration at Muda Irrigation Scheme of Malaysia. J. Agr. Rural Develop. Trop. Subtrop. 113 - 1 (2012) 77–85.

318. Turc L. 1961. Evaluation des besoins en eau d'irrigation, évapotranspiration potentielle, formulation simplifié et mise à jour. Ann. Agron., 12, pp: 13-49 (in French).

319. Tyagi JV, Mishra SK, Sing R, Singh VP. 2008. SCS-CN based time-distributed sediment yield model. Journal of Hydrology 352, pp: 388–403.

320. U.S. Department of Agriculture. 1970. Soil Conservation Service, Irrigation Water Requirements, Technical Release no. 21 88.

321. U.S. Department of Agriculture. 1993. Natural Engineering Handbook, Part 623, Irrigation water requirement, Chapter 2: Natural Resources Conservation Service, pp: 284.

322. USDA, the United States Department of Agriculture. 1967. Irrigation water requirements. Technical Release 21. USDA Soil Conservation Service, Washington DC.

323. Van Liew, Michael W, Garbrecht J. 2003. Hydrologic simulation of the little Wachita river experimental watershed using SWAT. J American Water Resources Association 39 (2), pp: 413-426.

324. Van Mullem JA. 1989. Applications of the Green Ampt infiltration model to watersheds in Montana and Wyoming. MS thesis, Montana State University, Bozeman MT.

325. Vapnik V. 1998. Statistical Learning Theory, John Wiley, New York, NY.

326. Vennila G, Subramani T, Elango L. 2007. Rainfall Variation Analysis of Vattamalaikarai Sub-basin, Tamil Nadu, India, Journal Of Applied Hydrology, Vol. XX, No.3, pp: 50-59.

327. Ventura F, Rossi Pisa P, Ardizzoni E. 2002. Temperature and precipitation trends in Bologna (Italy) from 1952 to 1999. Atmospheric Research; 61; pp: 203-214.

328. Vinnikov KY, Robock A, Qiu S, Entin JK, Owe M, Choudhury BJ, et al. 1999. Satellite remote sensing of soil moisture in Illinois, USA. Journal of Geophysical Research, 104, pp: 4145−4168.

329. Von Storch H. 1999. On the use of 'inflation' in statistical downscaling. J Clim (in press).

330. Vorosmarty CJ, Federer CA, Schloss AL. 1998. Potential evapotranspiration functions compared on US watersheds: Possible implications for global-scale water balance and terrestrial ecosystem modeling, Journal of Hydrology, 207, pp: 147-169.

331. Wang W, Peng S, Yang T, Shao Q, Xu J, Xing W. 2011. Spatial and Temporal Characteristics of Reference Evapotranspiration Trends in the Haihe River Basin, China. J. Hydrolo. Engg. DOI: 10.1061/(ASCE)HE.1943-5584.0000320., pp: 239-252.

332. Weisse R, Oestreicher R. 2001. Reconstruction of potential evaporation for water balance studies. Clim. Res.,16, pp: 123-131.

333. Wetterhall F, Bardossy A, Chen D, Halldin S, Xu CY. 2006. Daily precipitation-downscaling techniques in three Chinese regions.Water Resour Res 42, W11423. DOI 10.1029/2005WR004573.

334. Wetterhall F, Halldin S, Xu CY. 2005. Statistical precipitation downscaling in central Sweden with the analogue method, J. Hydrol., 360, pp: 174–190.

335. White D. 1988. Grid-based Application of Runoff Curve number, Journal of Water Resources Planning and Management, *ASCE* 114(6), pp: 601-612.

336. Wilby RL, 2005. Uncertainty in water resource model parameters used for climate change impact assessment. Hydrol. Process. 19 (16), pp: 3201–3219.

337. Wilby RL, Harris I. 2006. A framework for assessing uncertainties in climate change impacts: low-flow scenarios for the River Thames, UK. Water Resour. Res. 42, W02419. doi:10.1029/2005WR004065.

338. Wilby RL, Hay LE, Leavesley GH. 1999. A comparison of downscaled and raw GCM output: Implications for climate change scenarios in the San Juan River basin, Colorado. Journal of Hydrology 225, pp: 67-91.

339. Wilby RL, Wigley TML, Conway D, Jones PD, Hewitson BC, Main J, Wilks DS. 1998. Statistical downscaling of general circulation model output: A comparison of methods. Water Resources Research, 34(11), pp: 2995-3008.

340. Wilby RL, Wigley TML. 1997. Downscaling general circulation model output: a review of methods and limitations. Prog. Phys. Geogr. 21, pp: 530–548.

341. Wilby RL. 2008. Water, Hydropower and Climate Change. Water Management 2008: Climate Change Impacts on Hydroelectric Water Resource Management, CEATI, Montreal, Canada, October, pp: 8–9.

342. Wilby, R.L., S.P. Charles, E. Zorita, B. Timbal, P. Whetton, and L.O. Mearns. 2004. Guidelines for use of climate scenarios developed from statistical downscaling methods. Available from the DDC of IPCC TGCIA, 27 pp.

343. Williams JR, Dyke, PT, Jones CA. 1983. EPIC: a model for assessing the effects of erosion on soil productivity. In. Laurenroth WK et al (eds) Analysis ecological systems. State-of-the-Art in ecological modelling, pp: 553-572, Amsterdam.

344. Williams JR, Laseur WV. 1976. Water yield model using SCS curve numbers. J. Hydraulics Division, ASCE, 102, (HY9), Proc. Paper 12377, pp: 1241-1253.

345. Williams JR. 1975. Sediment routing for agricultural watersheds, Water Resources Bulletin, 11(5), pp: 965-974.

346. Willmott CJ. 1981. On the validation of models. Physical Geography. 2, pp: 184-194.

347. Willmott CJ. 1984. On the evaluation of model performance in physical geography. In G. L. Gaile and C. J. Willmott (eds.). Spatial Statistics and Models, Dordrecht, Holland: D. Reidel, pp: 443-460.

348. Witten IH, Frank E. 2000. Data mining, Morgan Kaufmann, San Francisco.

349. Wright JL. 1982. New evapotranspiration crop coefficients. J. Irrig. and Drain. Div., 108(IR1), pp: 57-74.

350. Wright, J.L., Jensen, M.E., 1972. Peak water requirements of crops in Southen Idaho. J. Irrig. Drain. Div. ASCE 98 (IR1), pp: 193–201.

351. Wu W, Lynch AM. 2000. Response of the seasonal carbon cycle in high latitudes to climate anomalies. Journal of Geophysical Research, 105, D18, pp: 22,897-22,908.

352. Wypych A. 2010. Twentieth century variability of surface humidity as the climate change indicator in Kraków (Southern Poland). Theor Appl Climatol 101(3), pp: 475–482. doi:10.1007/s00704-009-0221-y

353. Xu 1999. From GCMs to river flow: a review of downscaling methods and hydrologic modeling approaches. Progress in Phys. Geogr. 23, 2, pp: 229-249.

354. Xu CY, Gong L, Jiang T, Chen D, Singh VP. 2006. Analysis of spatial distribution and temporal trend of reference evapotranspiration and pan evaporation in Changjiang (Yangtze River) catchment. J. of Hydrol. 327, pp: 81-93.

355. Xu CY, Singh VP. 2000. Evaluation and Generalization of Radiation-based Methods for Calculating Evaporation, Hydrolog. Processes, 14, pp: 339–349.

356. Xu CY, Singh VP. 2001. Evaluation and Generalization of Radiation-based Methods for Calculating Evaporation. Hydrolog. Processes. 15, pp: 305–319.

357. Xu CY, Singh VP. 2002. Cross comparison of empirical equations for calculating potential evapotranspiration with data from Switzerland. Water Resour. Manage.16 (3), pp: 197–219.

358. Xu ZX, Li JY, Liu CM. 2007. Long-term trend analysis for major climate variables in the Yellow River basin. Hydrol. Process. 21, pp: 1935–1948.

359. Yano T, Aydin M, Haraguchi T. 2007. Impact of climate change on irrigation demand and crop growth in a Mediterranean environment of Turkey. Sensors 7, pp: 2297–2315.

360. Young RA, Onstad CA, Bosch DD, Anderson WP. 1989. AGNPS: a nonpoint source pollution model for evaluating agricultural watersheds. J. Soil and Water Conserv. 44(2), pp: 168-173.

361. Yu B, Neil DT. 1993. Long-term variations in regional rainfall in the south-west of Western Australia and the difference between average and high intensity rainfalls. Int. J. Climatol. 13, pp: 77-88.

362. Yu B. 1998. Theoretical justification of SCS-CN method for runoff estimation. J. Irrig. Drain. Division, ASCE, 124(6), pp: 306–310.

363. Yu PS, Yang TC, Chou CC. 2002. Effects of climate on evapotranspiration from paddy fields in southern Taiwan. Climate Change, 54(1-2), pp: 165-179.

364. Yu XY, Liong SY. 2007. Forecasting of Hydrologic Time Series with Ridge Regression in Feature Space," Journal of Hydrology, Vol 332, pp: 290 - 302.

365. Yuan Y, Mitchell JK, Hirschi MC, Cooke RA. 2001. Modified SCS Curve Number Method for predicting subsurface drainage flow, Trans. ASAE, 44 (6), pp: 1673–1682.

366. Yue S, Hashino M. 2003. Long term trends of annual and monthly precipitation in Japan. J. American Water Resour. Assoc. 39(3), pp: 587–596.

367. Yue S, Pilon P, Phinney B, Cavadias G. 2002. The influence of autocorrelation on the Ability to detect trend in hydrological series. Hydrological Processes 16, pp: 1807-1829.

368. Yue S, Pilon P, Phinney B. 2003. Canadian streamflow trend detection: impacts of serial and cross-correlation. Hydrolo. Sci. J. 48, pp: 51–63.

369. Zhang XC, Nearing MA, Garbrecht JD, Steiner JL. 2004. Downscaling monthly forecasts to simulate impacts of climate change on soil erosion and wheat production. Soil Sci Soc Am J 68, pp: 1376–1385.

370. Zhang Y, Liu C, Tang Y, Yang Y. 2007. Trends in pan evaporation and actual evaporation and reference and actual evapotranspiration across the Tibetan Plateau. J. of Geophysical Research 112; D1210, doi: 10.1029/2006jd008161.

371. Zhao C, Nan Z, Feng Z. 2004. GIS-assisted spatially distributed modeling of the potential evapotranspiration in semi-arid climate of the Chinese Loess Plateau. Journal of Arid Environments, 58, pp: 387–403.

372. Zhi-Hua Shi, Li-Ding Chenb, Nu-Fang Fang, De-Fu Qinc, Chong-Fa Cai. 2009. Research on the SCS-CN initial abstraction ratio using rainfall-runoff event analysis in the Three Gorges Area, China, Catena 77, pp: 1–7.

373. Zorita E, von Storch H. 1999. The analog method as a simple statistical downscaling technique: comparison with more complicated methods. J. Clim., 12, pp: 2474–2489.

ANNEXURES

ANNEXURE A

Table A1 Performance Evaluation Statistics for Evapotranspiration

S.No.	Parameters		MLR		ANN (RBF)		ANN (MLP)		M5P		LS-SVM	
			Cal.	Val.	Cal.	Val.	Cal.	Val.	Cal.	Val.	Cal.	Val.
1.	**Bilaspur**	RMSE	18.34	11.73	29.58	18.55	13.02	7.97	9.20	5.91	5.91	4.03
		NMSE	7.11	2.97	18.49	7.42	3.58	1.37	1.79	0.75	0.74	0.35
		NSE	0.85	0.82	0.61	0.56	0.92	0.92	0.96	0.96	0.98	0.98
		MAE	0.62	0.57	0.32	0.25	0.74	0.73	0.85	0.83	0.92	0.92
		CC	0.92	0.91	0.78	0.75	0.97	0.97	0.98	0.98	0.99	0.99
2.	**Damtari**	RMSE	16.84	10.60	41.97	25.32	12.85	8.10	8.16	5.85	4.58	1.68
		NMSE	6.48	2.61	40.28	14.87	3.78	1.52	1.52	0.80	0.48	0.07
		NSE	0.85	0.83	0.08	0.05	0.91	0.90	0.97	0.95	0.99	1.00
		MAE	0.64	0.64	0.07	0.07	0.74	0.74	0.88	0.86	0.94	0.95
		CC	0.92	0.91	0.28	0.23	0.96	0.96	0.98	0.98	0.99	1.00
3.	**Durg**	RMSE	18.79	11.81	44.26	26.81	14.29	8.78	9.14	6.48	5.75	2.51
		NMSE	7.59	3.03	42.12	15.60	4.39	1.67	1.80	0.91	0.71	0.14
		NSE	0.84	0.82	0.09	0.07	0.91	0.90	0.96	0.95	0.98	0.99
		MAE	0.63	0.63	0.08	0.08	0.73	0.74	0.87	0.85	0.93	0.94
		CC	0.91	0.91	0.30	0.27	0.96	0.96	0.98	0.97	0.99	1.00
4.	**Kanker**	RMSE	17.21	10.80	41.79	25.36	13.05	8.05	8.41	6.02	4.78	2.60
		NMSE	6.76	2.68	39.85	14.77	3.89	1.49	1.62	0.83	0.52	0.16
		NSE	0.85	0.83	0.09	0.07	0.91	0.91	0.96	0.95	0.99	0.99
		MAE	0.64	0.64	0.08	0.08	0.74	0.74	0.88	0.85	0.94	0.94
		CC	0.92	0.91	0.30	0.26	0.96	0.96	0.98	0.97	0.99	1.00
5.	**Kawardha**	RMSE	19.74	12.43	45.31	27.66	14.27	8.80	9.51	6.59	7.37	1.95
		NMSE	8.09	3.22	42.65	15.94	4.23	1.62	1.88	0.90	1.13	0.08
		NSE	0.83	0.82	0.11	0.09	0.91	0.91	0.96	0.95	0.98	1.00
		MAE	0.62	0.62	0.09	0.08	0.75	0.75	0.87	0.86	0.93	0.95
		CC	0.91	0.91	0.33	0.30	0.96	0.96	0.98	0.97	0.99	1.00
6.	**Korba**	RMSE	18.64	11.81	43.70	26.60	15.03	9.81	9.11	6.38	5.79	2.81
		NMSE	7.40	3.00	40.70	15.19	4.81	2.07	1.77	0.88	0.71	0.17
		NSE	0.99	0.82	0.92	0.10	0.99	0.88	1.00	0.95	1.00	0.99
		MAE	0.66	0.62	0.17	0.09	0.76	0.72	0.88	0.86	0.94	0.94
		CC	0.92	0.91	0.36	0.32	0.96	0.95	0.98	0.97	0.99	1.00
7.	**Raipur**	RMSE	17.65	10.98	42.43	25.47	13.54	8.403	9.09	6.31	5.62	3.58
		NMSE	6.98	2.76	40.32	14.86	4.11	1.616	1.85	0.91	0.71	0.29
		NSE	0.92	0.83	0.53	0.07	0.95	0.898	0.98	0.94	0.99	0.98
		MAE	0.66	0.67	0.15	0.18	0.75	0.759	0.87	0.86	0.93	0.94
		CC	0.92	0.91	0.30	0.26	0.96	0.955	0.98	0.97	0.99	0.99
8.	**Rajnandgaon**	RMSE	19.62513	12.32	45.06	27.36	14.52	8.94	9.43	6.65	5.58	2.46
		NMSE	8.066385	3.20	42.52	15.79	4.41	1.69	1.86	0.93	0.65	0.13
		NSE	0.830589	0.81	0.11	0.08	0.91	0.90	0.96	0.95	0.99	0.99
		MAE	0.895909	0.62	0.75	0.08	0.93	0.74	0.97	0.85	0.98	0.95
		CC	0.911387	0.90	0.33	0.29	0.96	0.96	0.98	0.97	0.99	1.00

Table A2 Performance Evaluation Statistics for Rainfall

S.No.	Parameters		MLR		ANN (RBF)		ANN (MLP)		M5P		LS-SVM	
			Cal.	Val.	Cal.	Val.	Cal.	Val.	Cal.	Val.	Cal.	Val.
1.	Bilaspur	RMSE	85.10	54.65	118.97	62.12	84.39	54.48	68.34	53.02	32.74	20.68
		NMSE	49.30	25.68	96.35	33.17	48.48	25.51	31.79	24.16	7.30	3.68
		NSE	0.66	0.39	0.34	0.22	0.66	0.40	0.78	0.43	0.95	0.91
		MAE	0.52	0.27	0.33	0.14	0.54	0.27	0.73	0.51	0.87	0.85
		CC	0.82	0.68	0.59	0.53	0.84	0.72	0.89	0.74	0.97	0.96
2.	Damtari	RMSE	100.46	66.55	105.37	76.22	105.8	66.18	86.19	55.07	45.78	23.77
		NMSE	79.04	29.40	86.96	38.57	87.67	29.08	58.18	20.13	16.41	3.75
		NSE	0.37	0.46	0.32	0.30	0.31	0.47	0.54	0.63	0.87	0.93
		MAE	0.28	0.37	0.31	0.29	0.21	0.35	0.57	0.63	0.80	0.84
		CC	0.62	0.70	0.56	0.55	0.66	0.79	0.74	0.85	0.93	0.97
3.	Durg	RMSE	86.67	34.51	106.11	53.71	86.36	36.35	75.34	29.07	38.01	12.34
		NMSE	58.11	10.47	87.09	25.35	57.70	11.61	43.91	7.43	11.18	1.34
		NSE	0.54	0.74	0.32	0.39	0.55	0.72	0.66	0.82	0.91	0.97
		MAE	0.47	0.55	0.32	0.34	0.46	0.48	0.67	0.75	0.84	0.89
		CC	0.74	0.86	0.57	0.62	0.78	0.90	0.82	0.91	0.96	0.98
4.	Kanker	RMSE	74.03	33.10	104.82	51.31	71.71	30.45	63.59	23.59	25.59	13.91
		NMSE	42.57	10.46	85.35	25.14	39.95	8.86	31.41	5.32	5.09	1.85
		NSE	0.66	0.72	0.34	0.34	0.68	0.77	0.76	0.86	0.96	0.95
		MAE	0.53	0.51	0.33	0.33	0.57	0.61	0.71	0.77	0.88	0.88
		CC	0.81	0.85	0.58	0.60	0.84	0.88	0.87	0.93	0.98	0.98
5.	Kawardha	RMSE	79.24	32.69	104.53	50.59	83.99	33.93	69.26	23.69	32.40	15.24
		NMSE	51.20	10.11	89.10	24.21	57.52	10.89	39.11	5.31	8.56	2.20
		NSE	0.58	0.73	0.27	0.37	0.53	0.72	0.68	0.86	0.93	0.94
		MAE	0.46	0.54	0.23	0.29	0.43	0.55	0.64	0.77	0.83	0.87
		CC	0.76	0.85	0.52	0.62	0.77	0.87	0.83	0.93	0.96	0.97
6.	Korba	RMSE	80.66	36.46	107.30	53.25	76.39	35.93	66.92	29.92	32.88	12.19
		NMSE	49.97	12.34	88.44	26.32	44.82	11.98	34.40	8.31	8.30	1.38
		NSE	0.73	0.684	0.52	0.33	0.75	0.69	0.81	0.79	0.96	0.96
		MAE	0.41	0.519	0.16	0.33	0.48	0.57	0.66	0.75	0.84	0.89
		CC	0.78	0.832	0.56	0.58	0.83	0.85	0.86	0.89	0.97	0.98
7.	Raipur	RMSE	75.57	36.62	112.12	59.97	81.28	38.85	67.45	25.58	32.19	14.16
		NMSE	40.16	10.34	88.41	27.74	46.46	11.64	32.00	5.05	7.29	1.55
		NSE	0.80	0.780	0.56	0.41	0.77	0.75	0.84	0.89	0.96	0.97
		MAE	0.48	0.535	0.24	0.27	0.50	0.52	0.67	0.78	0.86	0.87
		CC	0.84	0.885	0.61	0.64	0.86	0.91	0.88	0.95	0.97	0.98
8.	Rajnandgaon	RMSE	121.90	68.13	126.19	71.04	140.3	81.92	106.4	60.53	42.18	34.66
		NMSE	99.14	35.12	106.23	38.17	131.4	50.77	75.53	27.72	11.87	9.09
		NSE	0.33	0.269	0.29	0.21	0.12	-0.06	0.494	0.42	0.92	0.81
		MAE	0.12	0.260	0.12	0.24	0.054	0.07	0.456	0.52	0.80	0.71
		CC	0.58	0.526	0.54	0.47	0.62	0.62	0.717	0.68	0.96	0.90

Table A3 Performance Evaluation Statistics for Relative Humidity

S.No.	Parameters		MLR		ANN (RBF)		ANN (MLP)		M5P		LS-SVM	
			Cal.	Val.	Cal.	Val.	Cal.	Val.	Cal.	Val.	Cal.	Val.
1.	Bilaspur	RMSE	5.97	3.90	11.50	7.35	4.34	2.48	3.04	1.97	1.63	0.85
		NMSE	3.06	1.25	11.37	4.45	1.62	0.51	0.79	0.32	0.23	0.06
		NSE	0.74	0.72	0.02	-0.01	0.86	0.88	0.93	0.93	0.98	0.99
		MAE	0.52	0.48	0.01	0.00	0.66	0.68	0.81	0.80	0.90	0.91
		CC	0.86	0.86	0.15	0.04	0.94	0.95	0.97	0.96	0.99	0.99
2.	Damtari	RMSE	6.14	3.87	17.40	10.08	4.82	2.66	3.36	1.95	1.75	1.41
		NMSE	2.07	0.84	16.60	5.71	1.27	0.40	0.62	0.21	0.17	0.11
		NSE	0.89	0.87	0.09	0.12	0.93	0.94	0.97	0.97	0.99	0.98
		MAE	0.68	0.67	0.01	0.03	0.76	0.78	0.90	0.88	0.94	0.93
		CC	0.94	0.93	0.30	0.34	0.97	0.97	0.98	0.98	1.00	0.99
3.	Durg	RMSE	7.55	4.71	19.25	11.24	4.95	3.00	4.05	2.30	2.26	1.31
		NMSE	2.87	1.14	18.66	6.52	1.23	0.47	0.82	0.27	0.26	0.09
		NSE	0.86	0.84	0.06	0.08	0.94	0.93	0.96	0.96	0.99	0.99
		MAE	0.65	0.64	-0.01	0.00	0.80	0.79	0.89	0.88	0.95	0.94
		CC	0.92	0.92	0.24	0.28	0.97	0.97	0.98	0.98	0.99	0.99
4.	Kanker	RMSE	6.79	4.14	17.23	10.04	4.45	2.50	3.69	2.01	1.80	1.42
		NMSE	2.58	0.99	16.66	5.82	1.11	0.36	0.76	0.23	0.18	0.12
		NSE	0.85	0.84	0.06	0.08	0.94	0.94	0.96	0.96	0.99	0.98
		MAE	0.65	0.65	-0.01	0.01	0.79	0.80	0.89	0.88	0.94	0.94
		CC	0.92	0.92	0.25	0.28	0.97	0.97	0.98	0.98	0.99	0.99
5.	Kawardha	RMSE	8.12	5.06	20.75	12.17	5.36	3.21	4.31	2.39	1.87	1.33
		NMSE	3.09	1.22	20.14	7.06	1.34	0.49	0.87	0.27	0.16	0.08
		NSE	0.86	0.84	0.05	0.07	0.94	0.94	0.96	0.96	0.99	0.99
		MAE	0.65	0.63	-0.02	0.00	0.80	0.79	0.89	0.89	0.95	0.95
		CC	0.92	0.92	0.23	0.27	0.97	0.97	0.98	0.98	1.00	0.99
6.	Korba	RMSE	6.32	4.14	18.40	17.93	4.63	2.76	3.28	2.09	1.95	1.06
		NMSE	2.08	0.91	17.60	17.05	1.12	0.40	0.56	0.23	0.20	0.06
		NSE	0.99	0.87	0.91	-1.48	0.99	0.94	1.00	0.97	1.00	0.99
		MAE	0.68	0.64	0.00	-0.72	0.78	0.79	0.89	0.88	0.94	0.94
		CC	0.94	0.93	0.28	-0.23	0.97	0.97	0.99	0.98	0.99	1.00
7.	Raipur	RMSE	6.59	3.99	17.4	16.83	5.18	2.97	4.24	2.49	2.28	1.41
		NMSE	2.35	0.89	16.5	15.92	1.46	0.50	0.97	0.35	0.28	0.11
		NSE	0.87	0.86	0.1	-1.46	0.92	0.92	0.95	0.95	0.99	0.98
		MAE	0.67	0.65	0.0	-0.62	0.75	0.74	0.84	0.83	0.92	0.92
		CC	0.93	0.93	0.3	-0.22	0.96	0.96	0.97	0.97	0.99	0.99
8.	Rajnandgaon	RMSE	8.66	5.28	19.92	3.06	5.24	3.06	4.54	2.52	2.07	0.53
		NMSE	3.68	1.41	19.52	0.47	1.35	0.47	1.01	0.32	0.21	0.01
		NSE	0.82	0.81	0.04	0.93	0.93	0.93	0.95	0.96	0.99	1.00
		MAE	0.88	0.61	0.69	0.80	0.94	0.80	0.97	0.89	0.98	0.96
		CC	0.90	0.90	0.19	0.97	0.97	0.97	0.97	0.98	0.99	1.00

Table A4 Performance Evaluation Statistics for Maximum Temperature (Tmax)

S.No.	Parameters		MLR		ANN (RBF)		ANN (MLP)		M5P		LS-SVM	
			Cal.	Val.	Cal.	Val.	Cal.	Val.	Cal.	Val.	Cal.	Val.
1.	Bilaspur	RMSE	2.32	1.34	3.33	2.01	2.20	1.28	1.21	0.77	0.64	0.39
		NMSE	0.81	0.28	1.65	0.63	0.72	0.26	0.22	0.09	0.06	0.02
		NSE	0.88	0.88	0.75	0.73	0.89	0.89	0.97	0.96	0.99	0.99
		MAE	0.68	0.69	0.51	0.47	0.69	0.69	0.86	0.86	0.94	0.93
		CC	0.94	0.94	0.87	0.86	0.97	0.97	0.98	0.98	1.00	1.00
2.	Damtari	RMSE	1.81	1.10	3.92	2.32	1.48	0.83	1.06	0.67	0.63	0.28
		NMSE	0.77	0.30	3.63	1.32	0.52	0.17	0.27	0.11	0.09	0.02
		NSE	0.82	0.80	0.14	0.11	0.88	0.89	0.94	0.93	0.98	0.99
		MAE	0.59	0.58	0.06	0.07	0.67	0.73	0.81	0.80	0.90	0.92
		CC	0.90	0.90	0.38	0.33	0.94	0.94	0.97	0.96	0.99	0.99
3.	Durg	RMSE	1.93	1.19	4.10	2.46	1.52	0.91	1.14	0.73	0.58	0.42
		NMSE	0.82	0.32	3.72	1.37	0.51	0.19	0.29	0.12	0.07	0.04
		NSE	0.82	0.80	0.18	0.14	0.89	0.88	0.94	0.92	0.98	0.98
		MAE	0.59	0.58	0.07	0.09	0.69	0.71	0.81	0.80	0.91	0.90
		CC	0.90	0.89	0.42	0.38	0.94	0.94	0.97	0.96	0.99	0.99
4.	Kanker	RMSE	1.79	1.10	3.94	2.37	1.46	0.83	1.06	0.67	0.56	0.45
		NMSE	0.75	0.29	3.65	1.35	0.50	0.16	0.26	0.11	0.07	0.05
		NSE	0.82	0.81	0.14	0.11	0.88	0.89	0.94	0.93	0.98	0.97
		MAE	0.60	0.59	0.05	0.07	0.69	0.73	0.81	0.81	0.90	0.88
		CC	0.91	0.90	0.38	0.34	0.94	0.95	0.97	0.96	0.99	0.98
5.	Kawardha	RMSE	2.02	1.23	4.13	2.51	1.53	0.95	1.19	0.73	0.62	0.39
		NMSE	0.88	0.33	3.66	1.37	0.50	0.20	0.30	0.11	0.08	0.03
		NSE	0.81	0.80	0.22	0.18	0.89	0.88	0.93	0.93	0.98	0.98
		MAE	0.58	0.58	0.08	0.10	0.70	0.70	0.80	0.81	0.91	0.90
		CC	0.90	0.90	0.46	0.43	0.95	0.95	0.97	0.97	0.99	0.99
6.	Korba	RMSE	2.03	1.23	4.07	2.46	1.53	0.89	1.20	0.72	0.60	0.41
		NMSE	0.87	0.32	3.50	1.30	0.49	0.17	0.30	0.11	0.08	0.04
		NSE	1.00	0.81	0.98	0.23	1.00	0.90	1.00	0.93	1.00	0.98
		MAE	0.69	0.58	0.33	0.11	0.78	0.72	0.85	0.81	0.93	0.90
		CC	0.90	0.90	0.51	0.48	0.95	0.95	0.97	0.97	0.99	0.99
7.	Raipur	RMSE	1.85	1.14	3.95	2.34	1.49	0.84	1.10	0.66	0.51	0.42
		NMSE	0.79	0.31	3.57	1.31	0.51	0.17	0.28	0.11	0.06	0.04
		NSE	0.91	0.80	0.58	0.14	0.94	0.89	0.97	0.93	0.99	0.97
		MAE	0.67	0.68	0.25	0.30	0.74	0.79	0.85	0.86	0.93	0.92
		CC	0.90	0.89	0.42	0.38	0.94	0.95	0.97	0.97	0.99	0.99
8.	Rajnandgaon	RMSE	1.93	1.19	4.12	2.48	1.51	0.91	0.78	0.73	0.62	0.31
		NMSE	0.82	0.32	3.75	1.39	0.50	0.19	0.15	0.12	0.08	0.02
		NSE	0.82	0.80	0.17	0.14	0.89	0.88	0.90	0.93	0.98	0.99
		MAE	0.95	0.59	0.89	0.08	0.96	0.71	0.82	0.80	0.99	0.92
		CC	0.90	0.90	0.41	0.38	0.95	0.94	0.95	0.96	0.99	0.99

Table A5 Performance Evaluation Statistics for Minimum Temperature (Tmin)

S.No.	Parameters		MLR		ANN (RBF)		ANN (MLP)		M5P		LS-SVM	
			Cal.	Val.	Cal.	Val.	Cal.	Val.	Cal.	Val.	Cal.	Val.
1.	Bilaspur	RMSE	1.73	0.98	2.80	1.66	1.69	1.01	1.14	0.65	0.69	0.33
		NMSE	0.39	0.13	1.02	0.37	0.37	0.14	0.17	0.06	0.06	0.01
		NSE	0.95	0.95	0.87	0.87	0.95	0.95	0.98	0.98	0.99	0.99
		MAE	0.80	0.80	0.67	0.67	0.80	0.80	0.89	0.90	0.94	0.94
		CC	0.97	0.98	0.93	0.93	0.98	0.98	0.99	0.99	1.00	1.00
2.	Damtari	RMSE	1.58	0.97	2.40	1.48	1.41	0.79	0.98	0.59	0.56	0.34
		NMSE	0.53	0.21	1.23	0.48	0.43	0.14	0.21	0.08	0.07	0.03
		NSE	0.89	0.88	0.74	0.71	0.91	0.92	0.96	0.95	0.99	0.98
		MAE	0.69	0.67	0.50	0.52	0.73	0.75	0.85	0.84	0.91	0.91
		CC	0.94	0.94	0.86	0.85	0.96	0.96	0.98	0.98	0.99	0.99
3.	Durg	RMSE	1.65	1.02	2.51	1.57	1.47	0.84	1.03	0.65	0.62	0.31
		NMSE	0.55	0.21	1.27	0.50	0.44	0.14	0.21	0.09	0.08	0.02
		NSE	0.89	0.88	0.74	0.72	0.91	0.92	0.96	0.95	0.98	0.99
		MAE	0.69	0.68	0.50	0.52	0.73	0.75	0.85	0.84	0.91	0.93
		CC	0.94	0.94	0.86	0.85	0.96	0.96	0.98	0.98	0.99	0.99
4.	Kanker	RMSE	1.55	0.96	2.39	1.50	1.39	0.77	0.99	0.60	0.54	0.25
		NMSE	0.52	0.20	1.24	0.49	0.42	0.13	0.21	0.08	0.06	0.01
		NSE	0.89	0.88	0.73	0.71	0.91	0.92	0.95	0.95	0.99	0.99
		MAE	0.69	0.68	0.49	0.51	0.73	0.76	0.84	0.84	0.91	0.93
		CC	0.94	0.94	0.86	0.84	0.96	0.96	0.98	0.98	0.99	1.00
5.	Kawardha	RMSE	1.67	1.01	2.49	1.57	1.46	0.83	1.53	0.90	0.62	0.33
		NMSE	0.54	0.20	1.21	0.48	0.41	0.13	0.46	0.16	0.07	0.02
		NSE	0.89	0.89	0.76	0.74	0.92	0.93	0.91	0.91	0.99	0.99
		MAE	0.70	0.70	0.53	0.54	0.75	0.77	0.75	0.76	0.91	0.92
		CC	0.95	0.95	0.87	0.86	0.96	0.97	0.96	0.96	0.99	0.99
6.	Korba	RMSE	1.65	0.99	2.47	1.55	1.39	0.83	1.03	0.62	0.60	0.37
		NMSE	0.53	0.19	1.18	0.47	0.37	0.13	0.20	0.07	0.07	0.03
		NSE	0.99	0.90	0.99	0.75	1.00	0.93	1.00	0.96	1.00	0.99
		MAE	0.82	0.71	0.73	0.55	0.86	0.77	0.91	0.86	0.95	0.92
		CC	0.95	0.95	0.88	0.87	0.96	0.97	0.98	0.98	0.99	0.99
7.	Raipur	RMSE	1.61	0.98	2.44	1.50	1.45	0.81	0.99	0.58	0.57	0.28
		NMSE	0.54	0.21	1.24	0.48	0.44	0.14	0.20	0.07	0.07	0.02
		NSE	0.96	0.88	0.92	0.72	0.97	0.92	0.99	0.96	1.00	0.99
		MAE	0.82	0.82	0.72	0.74	0.84	0.86	0.92	0.92	0.95	0.96
		CC	0.94	0.94	0.86	0.85	0.96	0.96	0.98	0.98	0.99	1.00
8.	Rajnandgaon	RMSE	1.64	1.00	2.50	1.57	1.45	0.82	1.04	0.65	0.64	0.25
		NMSE	0.54	0.21	1.26	0.50	0.43	0.14	0.22	0.09	0.08	0.01
		NSE	0.89	0.89	0.74	0.72	0.91	0.92	0.96	0.95	0.98	0.99
		MAE	0.94	0.69	0.90	0.52	0.95	0.76	0.97	0.84	0.98	0.93
		CC	0.94	0.94	0.86	0.85	0.96	0.96	0.98	0.98	0.99	1.00

Table A6 Performance Evaluation Statistics for Mean Temperature (Tmean)

S.No.	Parameters		MLR		ANN (RBF)		ANN (MLP)		M5P		LS-SVM	
			Cal.	Val.	Cal.	Val.	Cal.	Val.	Cal.	Val.	Cal.	Val.
1.	Bilaspur	RMSE	1.94	1.12	2.84	1.72	1.83	1.07	1.10	0.69	0.70	0.27
		NMSE	0.53	0.18	1.14	0.43	0.48	0.17	0.17	0.07	0.07	0.01
		NSE	0.92	0.93	0.84	0.83	0.93	0.93	0.98	0.97	0.99	1.00
		MAE	0.76	0.76	0.64	0.61	0.76	0.77	0.88	0.89	0.94	0.95
		CC	0.96	0.96	0.92	0.91	0.98	0.98	0.99	0.99	1.00	1.00
2.	Damtari	RMSE	1.64	1.02	3.02	1.82	1.45	0.81	0.99	0.61	0.60	0.35
		NMSE	0.65	0.26	2.20	0.83	0.51	0.16	0.24	0.09	0.09	0.03
		NSE	0.84	0.82	0.47	0.42	0.88	0.89	0.94	0.94	0.98	0.98
		MAE	0.59	0.57	0.17	0.21	0.64	0.69	0.80	0.80	0.89	0.89
		CC	0.92	0.91	0.68	0.66	0.95	0.94	0.97	0.97	0.99	0.99
3.	Durg	RMSE	1.74	1.08	3.17	1.94	1.49	0.87	1.04	0.66	0.58	0.30
		NMSE	0.69	0.27	2.27	0.87	0.50	0.17	0.25	0.10	0.08	0.02
		NSE	0.84	0.83	0.48	0.45	0.89	0.89	0.94	0.94	0.98	0.99
		MAE	0.59	0.58	0.19	0.23	0.66	0.69	0.81	0.80	0.89	0.91
		CC	0.92	0.91	0.70	0.67	0.95	0.95	0.97	0.97	0.99	0.99
4.	Kanker	RMSE	1.62	1.01	3.03	1.86	1.44	0.80	1.00	0.62	0.62	0.29
		NMSE	0.64	0.25	2.24	0.86	0.51	0.16	0.24	0.09	0.09	0.02
		NSE	0.84	0.83	0.45	0.42	0.88	0.89	0.94	0.94	0.98	0.99
		MAE	0.59	0.59	0.17	0.21	0.64	0.70	0.80	0.80	0.88	0.90
		CC	0.92	0.91	0.67	0.65	0.95	0.95	0.97	0.97	0.99	0.99
5.	Kawardha	RMSE	1.79	1.10	3.17	1.97	1.47	0.88	1.07	0.67	0.59	0.27
		NMSE	0.70	0.26	2.19	0.85	0.47	0.17	0.25	0.10	0.07	0.02
		NSE	0.85	0.84	0.52	0.49	0.90	0.90	0.95	0.94	0.98	0.99
		MAE	0.60	0.60	0.22	0.25	0.68	0.70	0.81	0.81	0.89	0.92
		CC	0.92	0.92	0.72	0.70	0.95	0.95	0.97	0.97	0.99	1.00
6.	Korba	RMSE	1.77	1.90	3.12	1.66	1.44	1.78	1.04	1.84	0.58	1.95
		NMSE	0.67	0.78	2.08	0.59	0.44	0.69	0.23	0.73	0.07	0.82
		NSE	1.00	0.54	0.99	0.65	1.00	0.59	1.00	0.57	1.00	0.51
		MAE	0.61	0.29	0.25	0.37	0.70	0.35	0.82	0.32	0.90	0.28
		CC	0.93	0.75	0.74	0.81	0.95	0.80	0.98	0.78	0.99	0.75
7.	Raipur	RMSE	1.68	1.75	3.05	1.56	1.44	1.63	1.00	1.70	0.59	1.79
		NMSE	0.66	0.74	2.17	0.59	0.49	0.64	0.23	0.69	0.08	0.77
		NSE	0.84	0.51	0.49	0.61	0.89	0.58	0.95	0.54	0.98	0.49
		MAE	0.59	0.27	0.19	0.33	0.65	0.32	0.81	0.29	0.90	0.24
		CC	0.92	0.74	0.70	0.79	0.95	0.79	0.97	0.77	0.99	0.74
8.	Rajnandgaon	RMSE	2.27	1.36	3.54	2.15	2.18	1.34	1.27	0.79	0.80	0.34
		NMSE	0.98	0.36	2.39	0.89	0.91	0.35	0.31	0.12	0.12	0.02
		NSE	0.81	0.81	0.54	0.52	0.83	0.82	0.94	0.94	0.98	0.99
		MAE	0.94	0.58	0.89	0.31	0.94	0.59	0.97	0.81	0.98	0.92
		CC	0.90	0.90	0.74	0.73	0.92	0.92	0.97	0.97	0.99	0.99

ANNEXURE B

Table B1 Probable predictors for Tmax, Tmin, Rainfall, RH and WS and their correlation

Stations	Rainfall		Minimum Temperature (Tmin)		Maximum Temperature (Tmax)		Relative Humidity		Wind Speed	
	Selected Predictors	R^2	Selected Predictors	R^2	Selected Predictors	R^2	Selected Predictors	R^2	Selected Predictors	R^2
Korba	Prw	0.80	Ta200	0.80	Ta700	0.85	Ta925	0.88	Ua925	0.87
	Ua200	0.76	Ta500	0.82						
	Ua925	0.85	Ta700	0.87	Zg925	-0.94				
	Va200	0.84	Ta925	0.92			Tasur	0.82		
	Va925	0.89	Zg200	0.86	Ua925	0.87				
	Zg200	0.67	Zg500	0.89						
	Zg500	0.89	Zg925	-0.84	Va925	0.88	LH	0.87	Va925	0.90
	Zg925	0.82	Ua200	0.67						
	Ta200	0.88	Ua925	-0.92	Prw	0.81				
	Hus850	0.81	Va925	0.72			Hus925	0.83		
	Hus925	0.83	Prw	0.81	LH	0.80				
	Ps	0.86	LH	0.75						
Rajnandgaon	Prw	0.81	Ta200	0.82	Ta700	0.81	Ta925	0.92	Ua925	0.88
	Ua200	0.84	Ta500	0.83						
	Ua925	0.84	Ta700	0.82	Ta925	0.83				
	Va200	0.82	Ta925	0.87			Tasur	0.76		
	Va925	0.88	Zg200	0.89	Zg925	-0.86				
	Zg200	0.71	Zg500	0.91						
	Zg500	0.82	Zg925	-0.86			LH	0.78	Va925	0.87
	Zg925	0.62	Ua200	0.71	Ua925	0.88				
	Ta200	0.84	Ua925	-0.89						
	Ta925	0.86	Va925	0.77	Va925	0.81	Hus925	0.89		
	Hus925	0.89	Prw	0.80	Prw	0.83				
	Ps	0.85	LH	0.76	LH	0.85				
Raipur	Prw	0.85	Ta200	0.79	Ta700	0.86	Ta925	0.82	Ua925	0.82
	Ua200	0.86	Ta500	0.80						
	Ua925	0.87	Ta700	0.86			Tasur	0.85		
	Va200	0.85	Ta925	0.85	Zg925	-0.87				
	Va925	0.82	Zg500	0.83						
	Zg200	0.81	Zg925	-0.85			LH	0.75	Va925	0.85
	Zg500	0.80	Ua200	0.85	Ua925	0.82				
	Zg925	0.88	Ua925	-0.79						
	Ta200	0.87	Va925	0.82	Va925	0.86	Hus925	0.80		
	Ta925	0.80	Prw	0.72	Prw	0.85				
	Hus850	0.86								
	Hus925	0.89								
	Ps	0.81								
Damtari	Prw	0.82	Ta500	0.89	Ta700	0.86	Ta925	0.89	Ua925	0.86
	Ua200	0.84	Ta700	0.82						
	Ua925	0.83	Ta925	0.85						
	Va200	0.85	Zg200	0.85	Zg925	-0.85	Tasur	0.83		
	Va925	0.80	Zg925	-0.84						
	Zg200	0.87	Ua200	0.87					Va925	0.87
	Zg500	0.82	Ua925	-0.89	Ua925	0.87	LH	0.78		
	Zg925	0.86	Va925	0.83	Va925	0.88				
	Ta200	0.81	Prw	0.85	Prw	0.87	Hus925	0.89		
	Ta500	0.87	LH	0.81	LH	0.89				
	Ta925	0.84								
	Hus850	0.80								
	Hus925	0.84								
	Ps	0.84								
Kawardha	Prw	0.89	Ta200	0.78	Ta700	0.91	Ta925	0.90	Ua925	0.82

	Ua200	0.83	Ta500	0.83						
	Ua925	0.85	Ta700	0.86	Ta925	0.86				
	Va200	0.86	Ta925	0.88	Zg925	-0.88	Tasur	0.75		
	Va925	0.87	Zg200	0.87						
	Zg500	0.88	Zg500	0.86						
	Zg925	0.84	Zg925	-0.82			LH	0.84	Va925	0.89
	Ta500	0.89	Ua200	0.84	Ua925	0.87				
	Ta925	0.82	Ua925	-0.86						
	Hus850	0.89	Va925	0.80	Va925	0.85	Hus925	0.89		
	Hus925	0.85	Prw	0.85	Prw	0.86				
	Ps	0.88	LH	0.78	LH	0.89				
Durg	Prw	0.89	Ta200	0.86	Ta700	0.86	Ta925	0.89	Ua925	0.89
	Ua200	0.85	Ta500	0.83						
	Ua925	0.81	Ta700	0.84						
	Va200	0.84	Ta925	0.82	Ta925	0.88	Tasur	0.81		
	Va925	0.85	Zg200	0.85	Zg925	-0.87			Va925	0.87
	Zg500	0.83	Zg500	0.89						
	Zg925	0.87	Zg925	-0.86						
	Ta500	0.84	Ua200	0.86	Ua925	0.85	LH	0.89		
	Ta925	0.83	Ua925	-0.86						
	Hus850	0.82	Va925	0.87	Va925	0.85	Hus925	0.87		
	Hus925	0.81	Prw	0.90	Prw	0.89				
Bilaspur	Prw	0.83	Ta200	0.81	Ta700	0.85	Ta925	0.88	Ua925	0.80
	Ua200	0.81	Ta500	0.86						
	Ua925	0.84	Ta700	0.87						
	Va200	0.85	Ta925	0.88	Ta925	0.89				
	Va925	0.81	Zg200	0.87	Zg925	-0.85	Tasur	0.87		
	Zg925	0.88	Zg500	0.88					Va925	0.85
	Ta500	0.89	Zg925	-0.86						
	Ta925	0.85	Ua200	0.81	Ua925	0.89	LH	0.85		
	Hus850	0.83	Ua925	-0.89						
	Hus925	0.81	Va925	0.84	Va925	0.84	Hus925	0.82		
	Ps	0.86	Prw	0.89	Prw	0.88				
Champa	Prw	0.87	Ta200	0.84	Ta700	0.89	Ta925	0.88	Ua925	0.88
	Ua925	0.88	Ta500	0.85						
	Va925	0.87	Ta700	0.88						
	Zg200	0.83	Ta925	0.89	Ta925	0.86				
	Zg500	083	Zg200	0.85	Zg925	-0.75	Tasur	0.78		
	Zg925	0.82	Zg500	0.84					Va925	0.89
	Ta200	0.85	Zg925	-0.85						
	Ta500	0.81	Ua925	-0.80	Ua925	0.85	LH	0.89		
	Ta925	0.91	Va925	0.86	Va925	0.87				
	Hus925	0.80	Prw	0.83	Prw	0.88	Hus925	0.91		
	Ps	0.89	LH	0.86	LH	0.85				

ANNEXURE C

Figure C1 Station-wise downscaling results of meteorological variables

Evapotranspiration

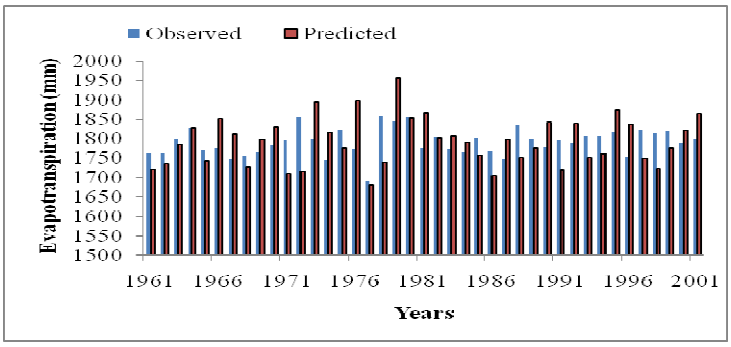

SSE	39520.86
MSE	109.7802
RMSE	10.48
NMSE	2.51
NSE	0.84
MAE	0.78
CC	0.92

Raipur

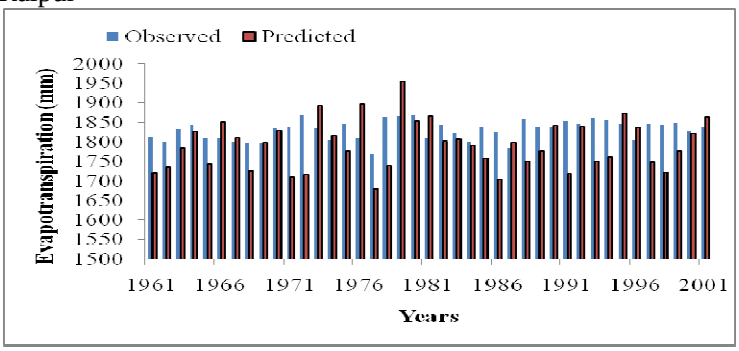

SSE	31196.53
MSE	86.65703
RMSE	9.31
NMSE	1.99
NSE	0.87
MAE	0.77
CC	0.94

Kanker

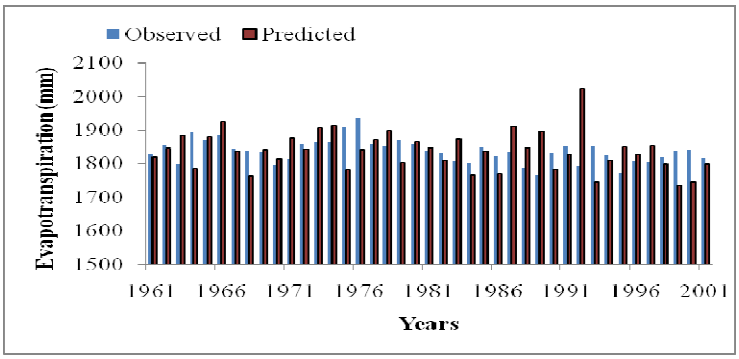

SSE	39469.45
MSE	109.6374
RMSE	10.47
NMSE	2.36
NSE	0.86
MAE	0.74
CC	0.93

Bilaspur

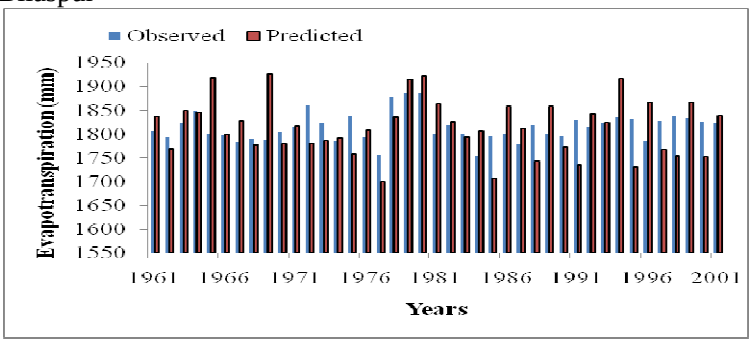

SSE	43200.52
MSE	120.0014
RMSE	10.95
NMSE	2.50
NSE	0.86
MAE	0.77
CC	0.93

Kawardha

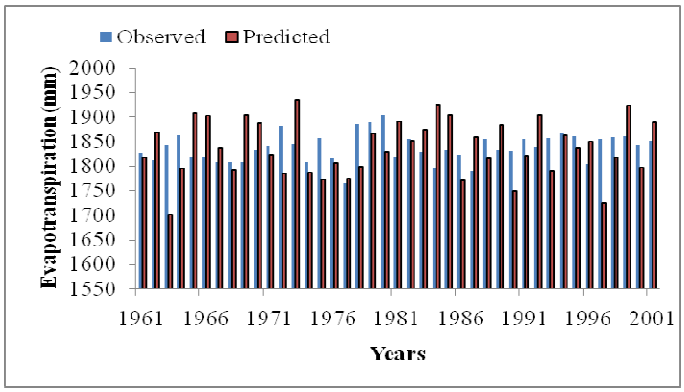

SSE	36099.5
MSE	100.2764
RMSE	10.01
NMSE	2.18
NSE	0.87
MAE	0.79
CC	0.93

Durg

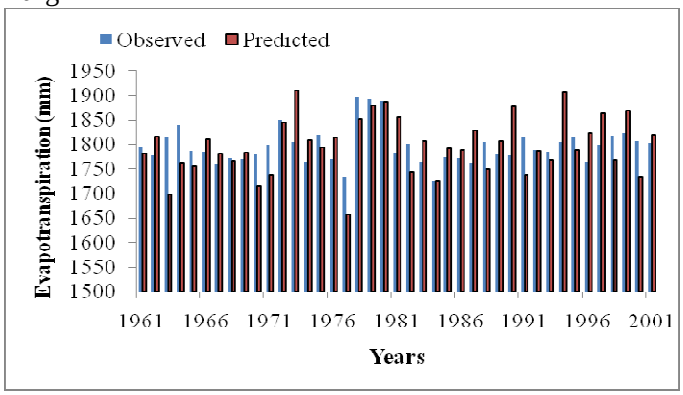

SSE	33348.41
MSE	92.63446
RMSE	9.62
NMSE	1.99
NSE	0.88
MAE	0.79
CC	0.94

Korba

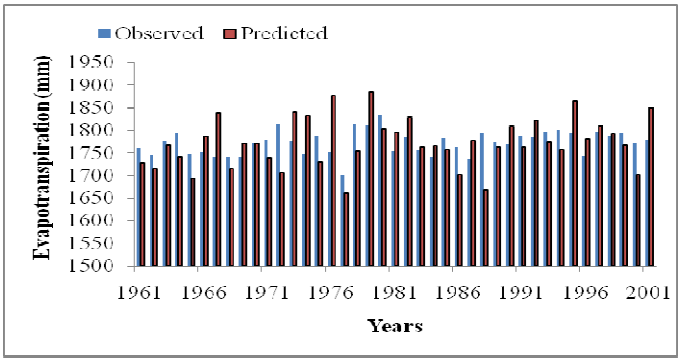

SSE	35575.76
MSE	98.82157
RMSE	9.94
NMSE	2.29
NSE	0.85
MAE	0.76
CC	0.92

Damtari

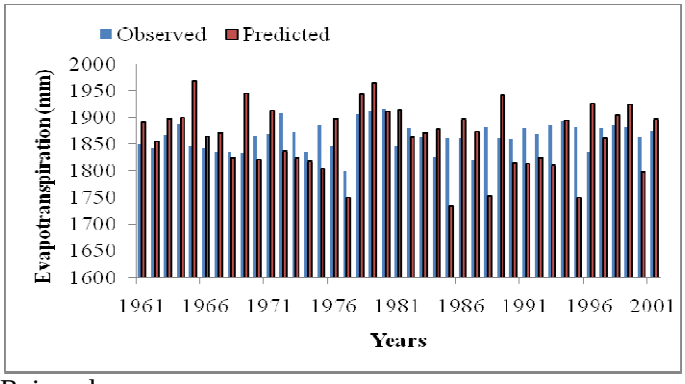

SSE	45659.38
MSE	126.8316
RMSE	11.26
NMSE	2.68
NSE	0.84
MAE	0.75
CC	0.92

Rajnandgaon

Relative Humidity

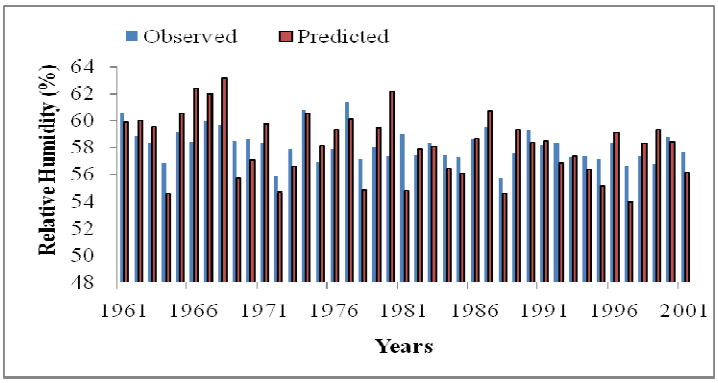

SSE	4411.241
MSE	12.25345
RMSE	3.50
NMSE	0.69
NSE	0.89
MAE	0.75
CC	0.95

Raipur

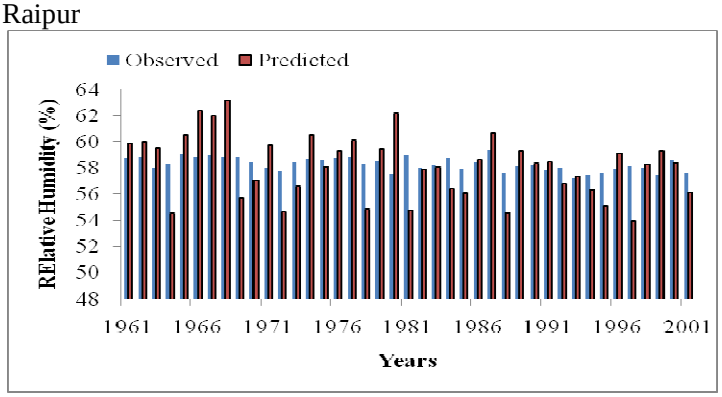

SSE	6599.151
MSE	18.33097
RMSE	4.28
NMSE	1.06
NSE	0.83
MAE	0.72
CC	0.91

Kanker

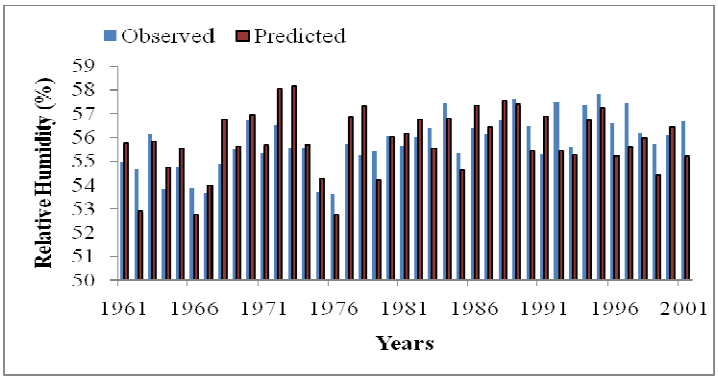

SSE	2547.278
MSE	7.075773
RMSE	2.66
NMSE	0.58
NSE	0.87
MAE	0.71
CC	0.93

Bilaspur

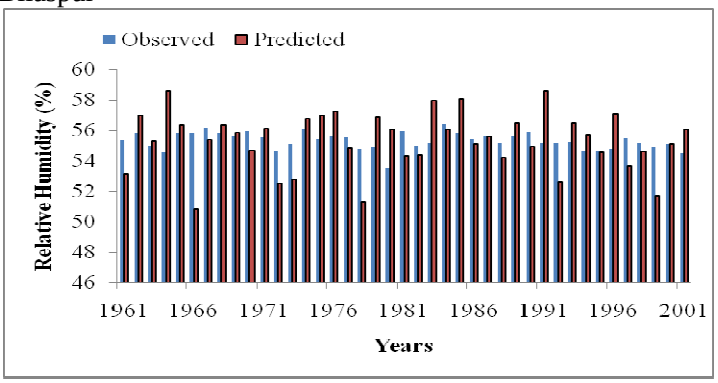

SSE	9517.243
MSE	26.43679
RMSE	5.14
NMSE	1.26
NSE	0.83
MAE	0.73
CC	0.91

Kawardha

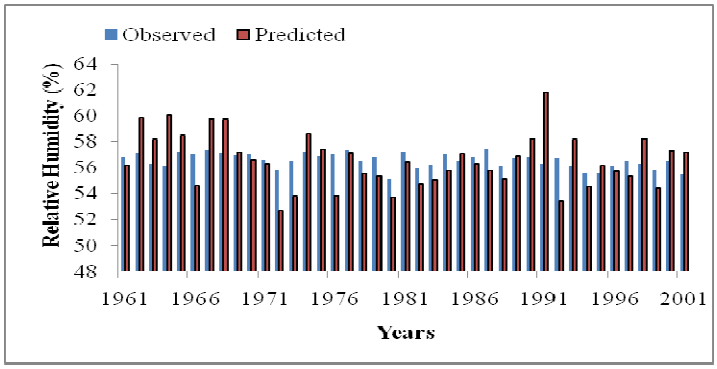

SSE	7026.234
MSE	19.51732
RMSE	4.42
NMSE	1.01
NSE	0.86
MAE	0.75
CC	0.93

Durg

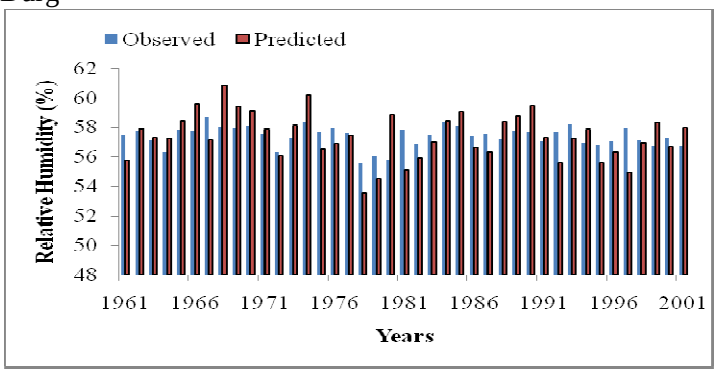

SSE	6837.8
MSE	18.99389
RMSE	4.36
NMSE	1.01
NSE	0.85
MAE	0.73
CC	0.92

Korba

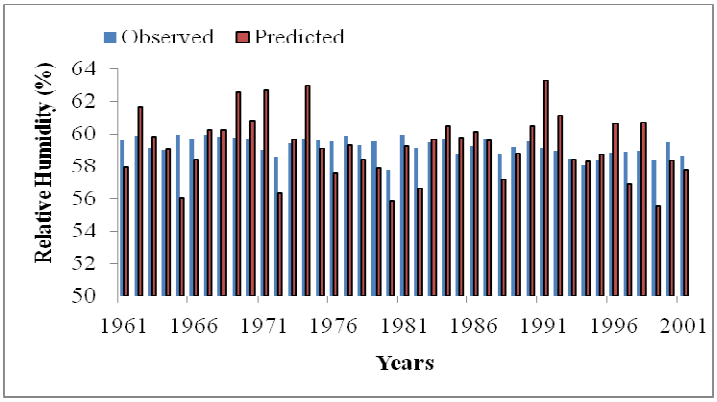

SSE	5242.17
MSE	14.56158
RMSE	3.82
NMSE	0.82
NSE	0.87
MAE	0.75
CC	0.93

Damtari

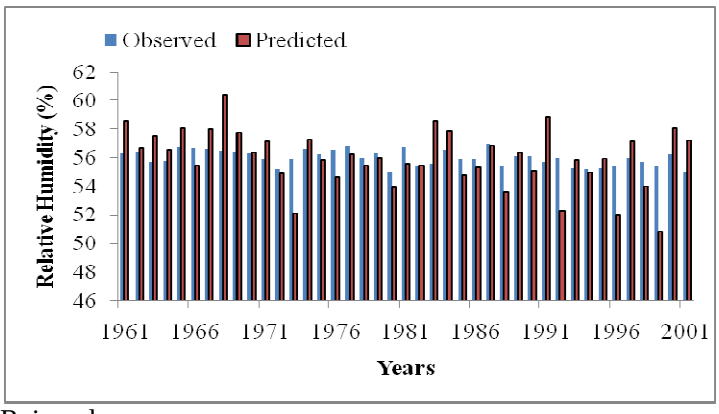

SSE	9549.518
MSE	26.52644
RMSE	5.15
NMSE	1.34
NSE	0.82
MAE	0.72
CC	0.90

Rajnandgaon

Maximum Temperature (Tmax)

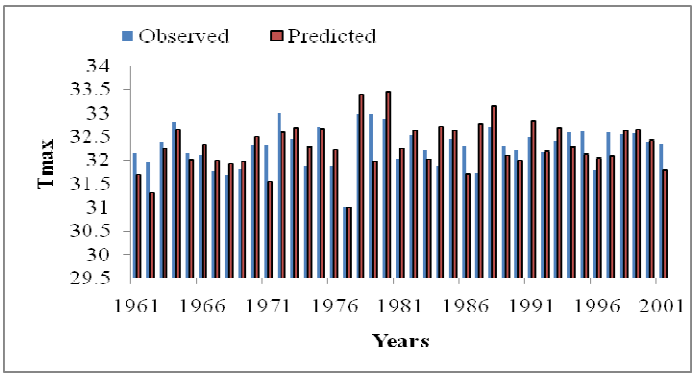

SSE	462.2329
MSE	1.28398
RMSE	1.13
NMSE	0.31
NSE	0.80
MAE	0.77
CC	0.89

Raipur

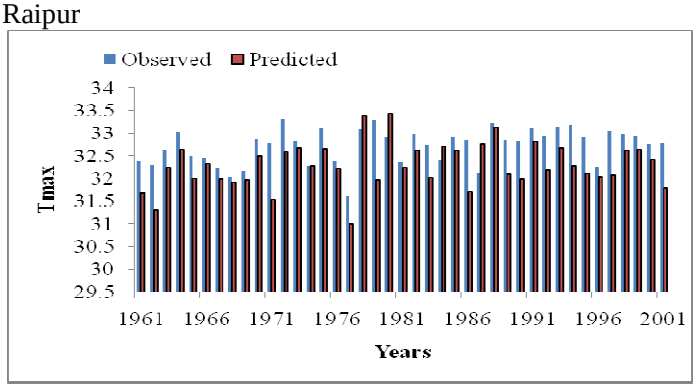

SSE	302.8336
MSE	0.841204
RMSE	0.92
NMSE	0.20
NSE	0.87
MAE	0.73
CC	0.93

Kanker

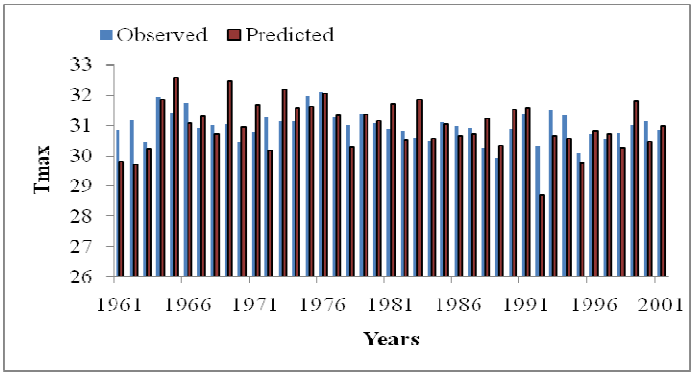

SSE	786.84
MSE	2.185667
RMSE	1.48
NMSE	0.34
NSE	0.86
MAE	0.73
CC	0.93

Bilaspur

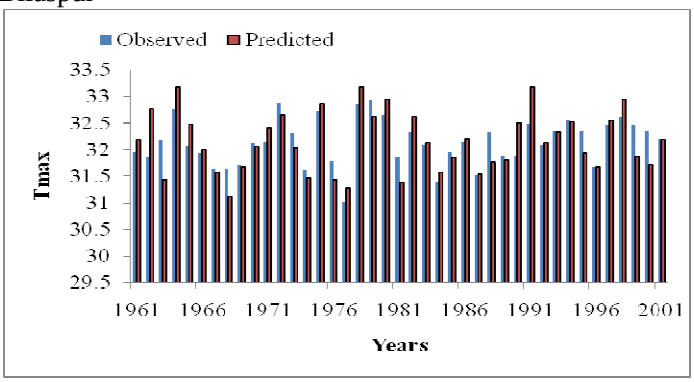

SSE	406.6659
MSE	1.129627
RMSE	1.06
NMSE	0.25
NSE	0.85
MAE	0.70
CC	0.92

Kawardha

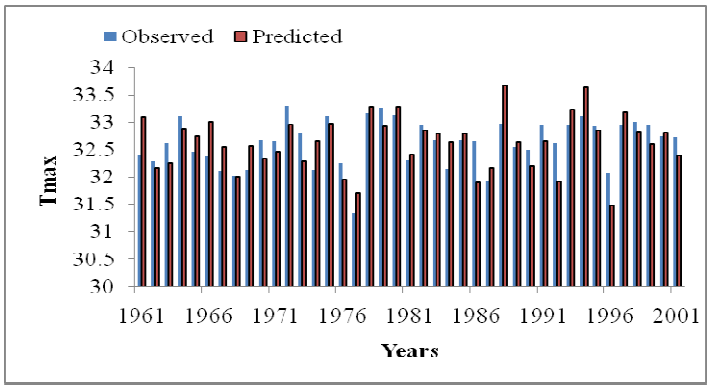

SSE	439.3679
MSE	1.220466
RMSE	1.10
NMSE	0.28
NSE	0.83
MAE	0.69
CC	0.91

Durg

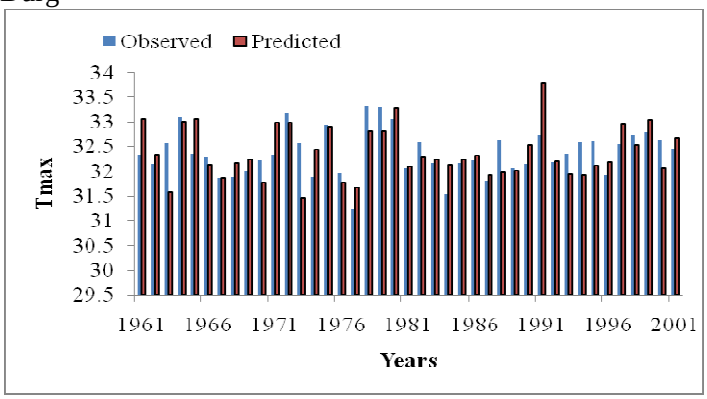

SSE	413.65
MSE	1.149028
RMSE	1.07
NMSE	0.25
NSE	0.85
MAE	0.70
CC	0.92

Korba

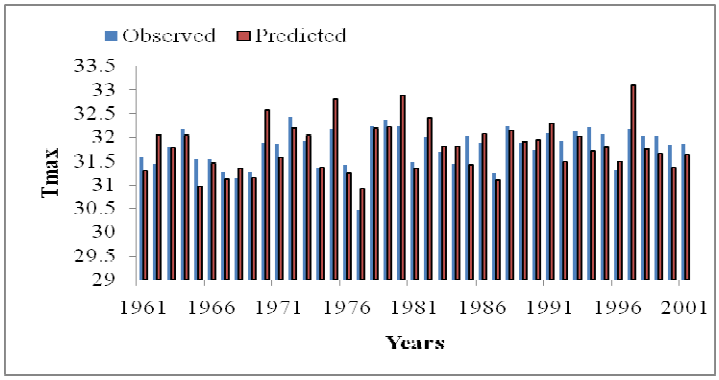

SSE	305.9662
MSE	0.849906
RMSE	0.92
NMSE	0.21
NSE	0.86
MAE	0.73
CC	0.93

Damtari

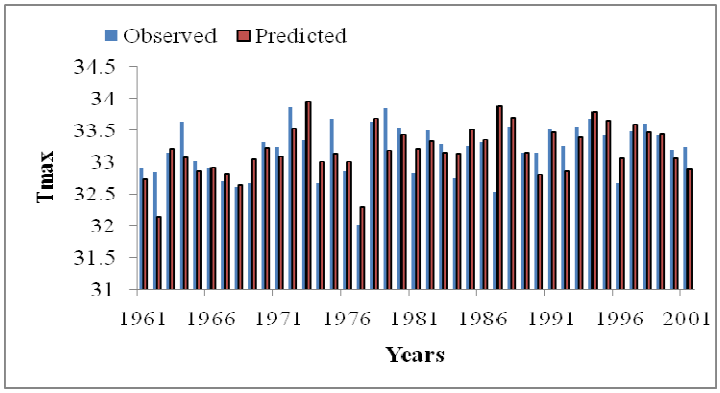

SSE	541.0691
MSE	1.50297
RMSE	1.23
NMSE	0.34
NSE	0.79
MAE	0.69
CC	0.89

Rajnandgaon

Minimum Temperature (Tmin)

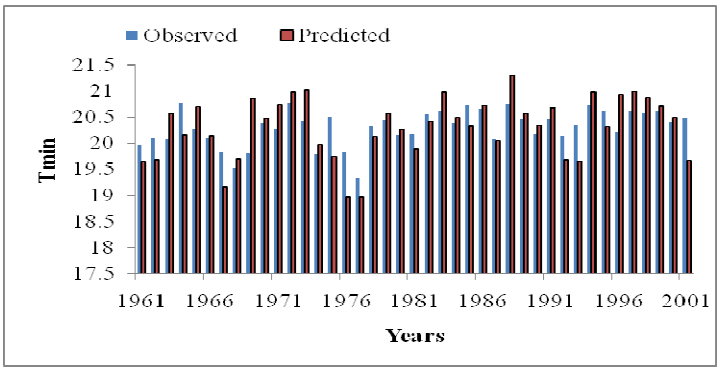

SSE	261.5543
MSE	0.72654
RMSE	0.85
NMSE	0.15
NSE	0.91
MAE	0.88
CC	0.95

Raipur

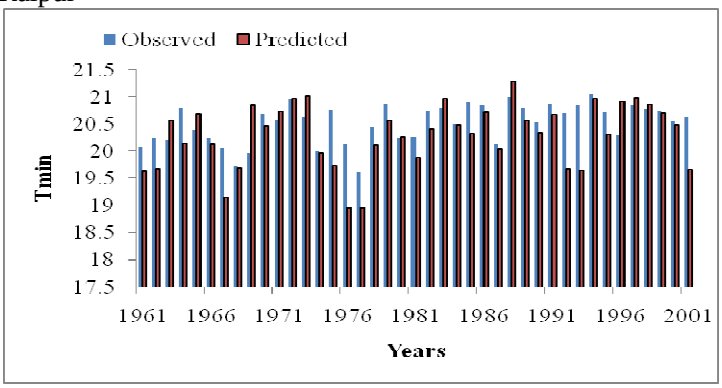

SSE	496.4111
MSE	1.37892
RMSE	1.17
NMSE	0.30
NSE	0.82
MAE	0.71
CC	0.91

Kanker

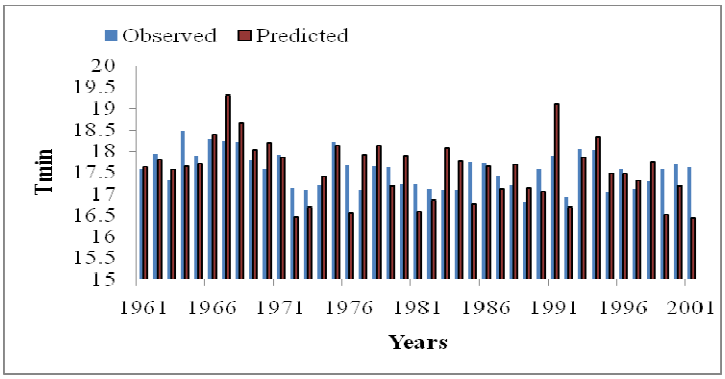

SSE	642.5947
MSE	1.784985
RMSE	1.34
NMSE	0.24
NSE	0.91
MAE	0.79
CC	0.96

Bilaspur

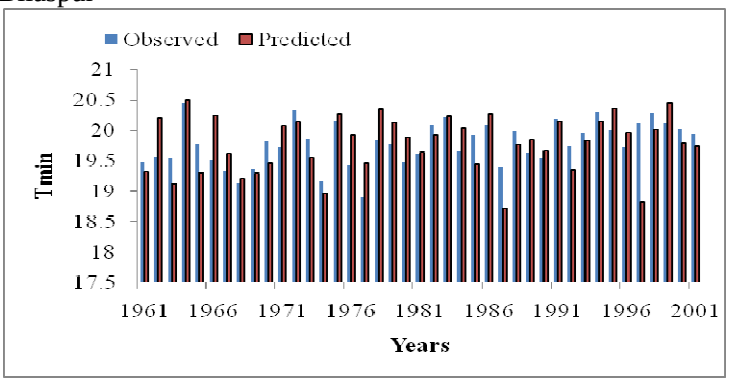

SSE	426.5849
MSE	1.184958
RMSE	1.09
NMSE	0.23
NSE	0.87
MAE	0.75
CC	0.94

Kawardha

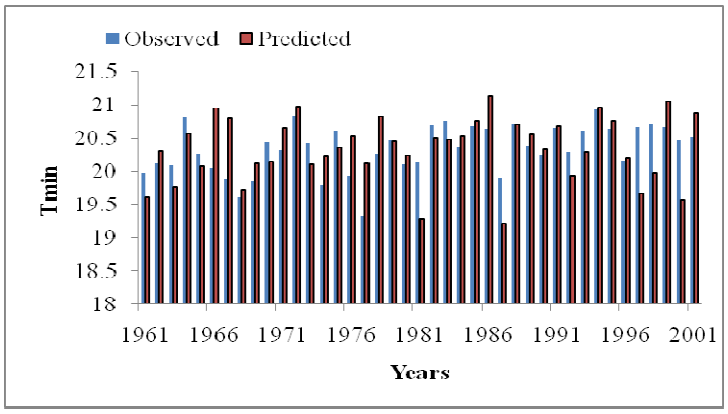

SSE	533.2298
MSE	1.481194
RMSE	1.22
NMSE	0.30
NSE	0.83
MAE	0.71
CC	0.91

Durg

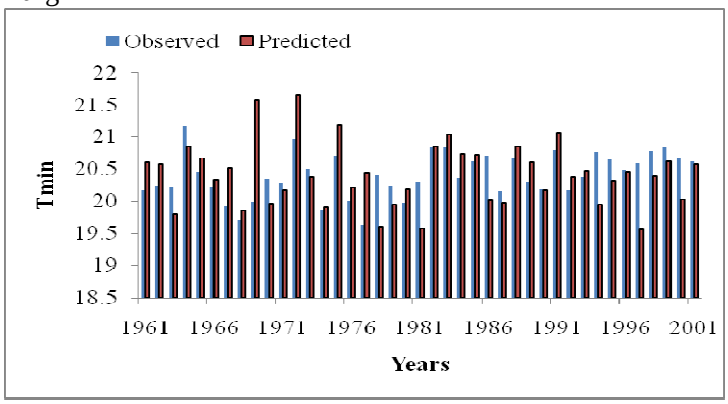

SSE	492.8465
MSE	1.369018
RMSE	1.17
NMSE	0.27
NSE	0.86
MAE	0.76
CC	0.93

Korba

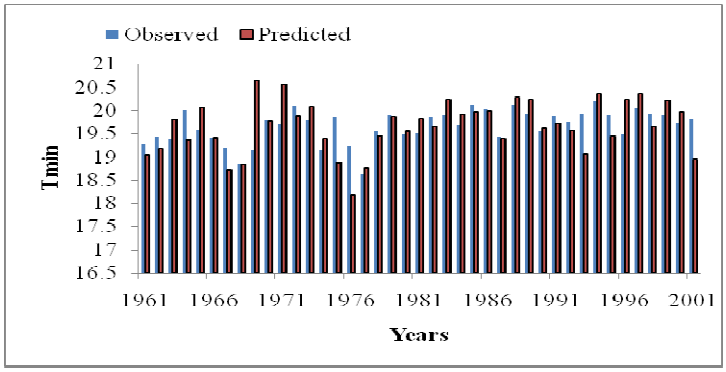

SSE	273.0318
MSE	0.758422
RMSE	0.87
NMSE	0.17
NSE	0.90
MAE	0.77
CC	0.95

Damtari

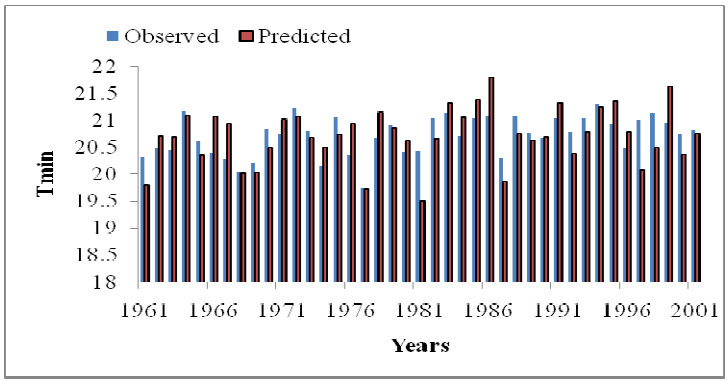

SSE	593.3856
MSE	1.648293
RMSE	1.28
NMSE	0.34
NSE	0.81
MAE	0.71
CC	0.90

Rajnandgaon

Mean Temperature (Tmean)

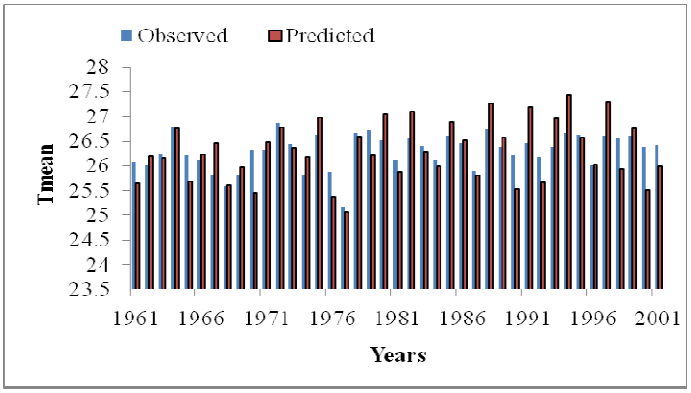

SSE	396.571
MSE	0.712697
RMSE	2.17
NMSE	1.02
NSE	0.80
MAE	0.22
CC	0.88

Raipur

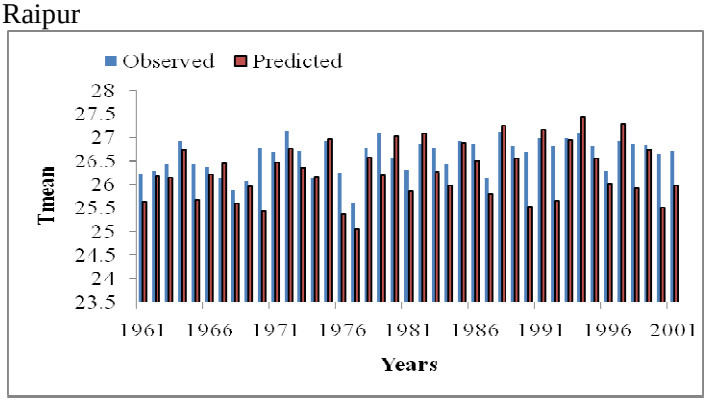

SSE	284.1201
MSE	0.789223
RMSE	0.89
NMSE	0.19
NSE	0.87
MAE	0.69
CC	0.93

Kanker

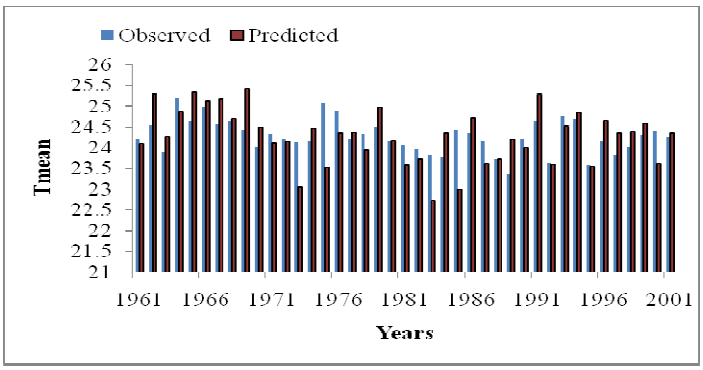

SSE	967.8613
MSE	2.688504
RMSE	1.64
NMSE	0.39
NSE	0.84
MAE	0.72
CC	0.92

Bilaspur

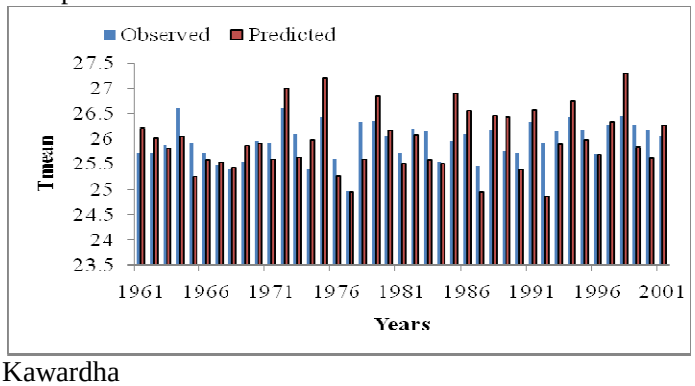

SSE	574.5484
MSE	1.595968
RMSE	1.26
NMSE	0.35
NSE	0.89
MAE	0.64
CC	0.90

Kawardha

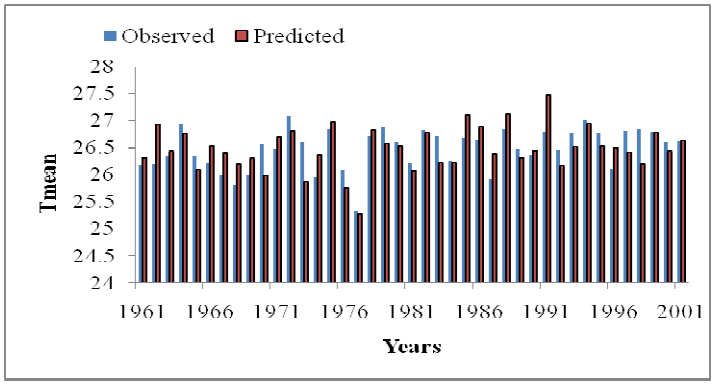

SSE	322.9416
MSE	0.89706
RMSE	0.95
NMSE	0.21
NSE	0.87
MAE	0.70
CC	0.93

Durg

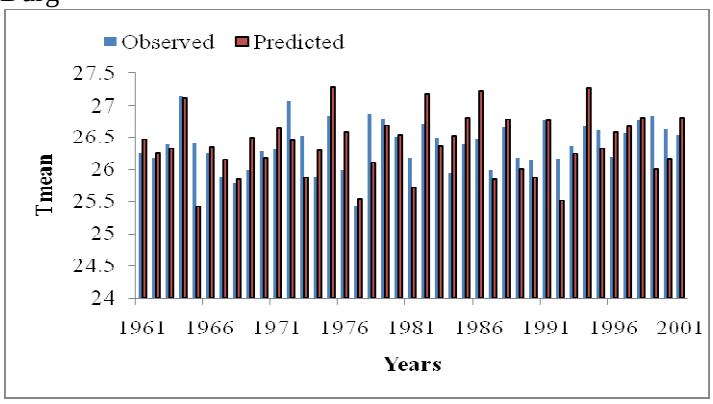

SSE	361.0099
MSE	1.002805
RMSE	1.00
NMSE	0.19
NSE	0.90
MAE	0.75
CC	0.95

Korba

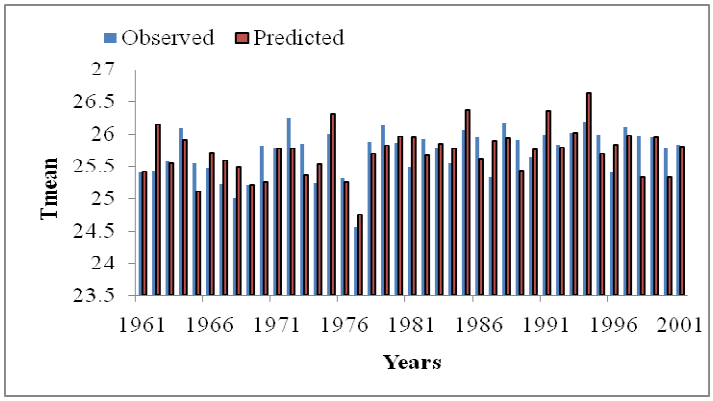

SSE	281.0114
MSE	0.780587
RMSE	0.88
NMSE	0.20
NSE	0.86
MAE	0.69
CC	0.93

Damtari

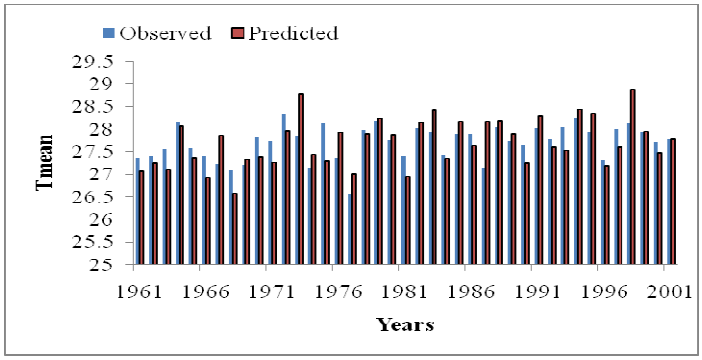

SSE	1704.335
MSE	4.734263
RMSE	2.18
NMSE	1.14
NSE	0.84
MAE	0.12
CC	0.86

Rajnandgaon

Rainfall

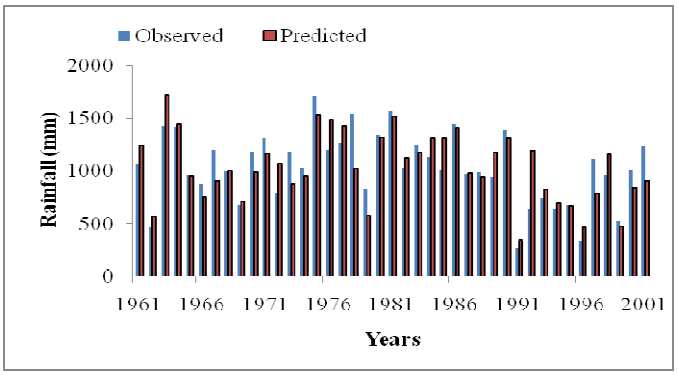

SSE	449680.2
MSE	1249.112
RMSE	35.34
NMSE	10.74
NSE	0.75
MAE	0.69
CC	0.86

Ambagarh Chowki

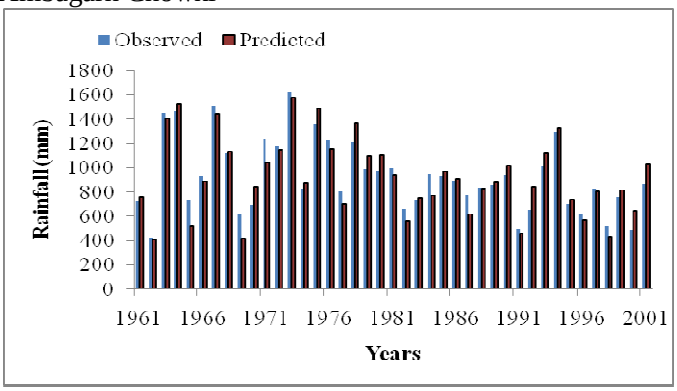

SSE	131041.6
MSE	364.0045
RMSE	19.08
NMSE	3.48
NSE	0.91
MAE	0.81
CC	0.95

Balod Bazar

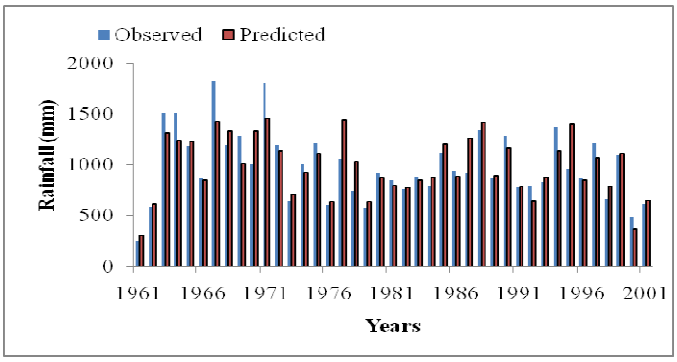

SSE	179074.5
MSE	497.4291
RMSE	22.30
NMSE	4.62
NSE	0.88
MAE	0.78
CC	0.94

Bodala

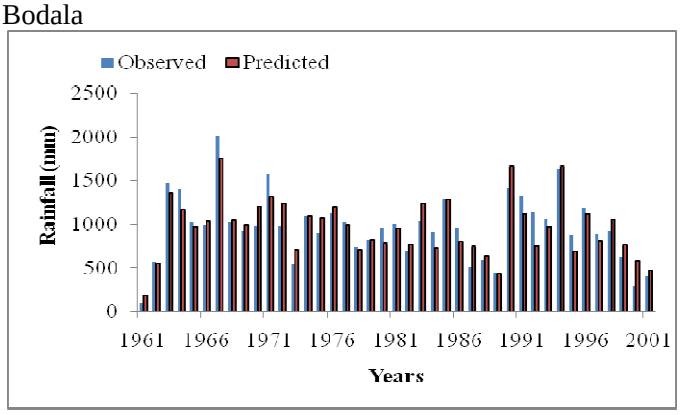

SSE	404465.4
MSE	1123.515
RMSE	33.52
NMSE	7.83
NSE	0.85
MAE	0.75
CC	0.92

Chhatti

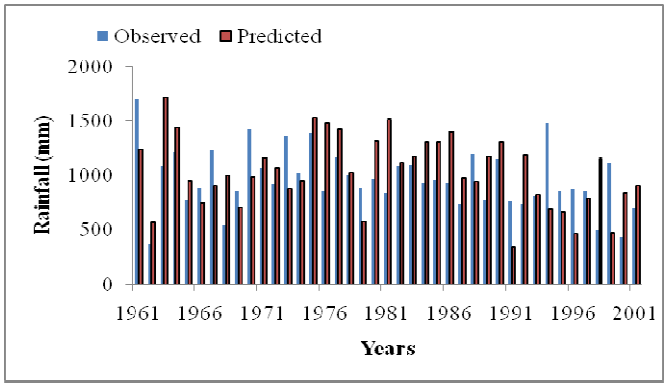

SSE	296517.3
MSE	823.6591
RMSE	28.70
NMSE	7.63
NSE	0.81
MAE	0.74
CC	0.90

Chuikhaddan

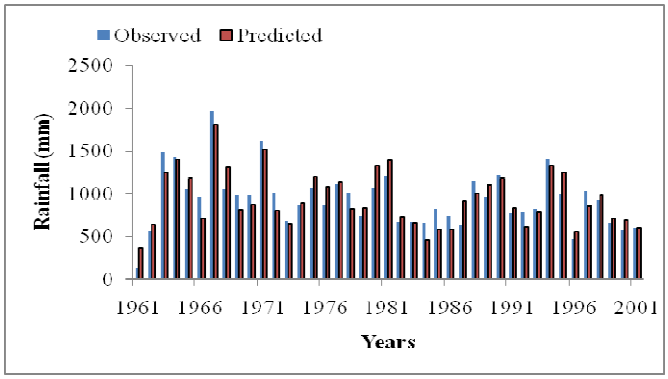

SSE	135932.2
MSE	377.5895
RMSE	19.43
NMSE	3.90
NSE	0.89
MAE	0.76
CC	0.94

Chirapani

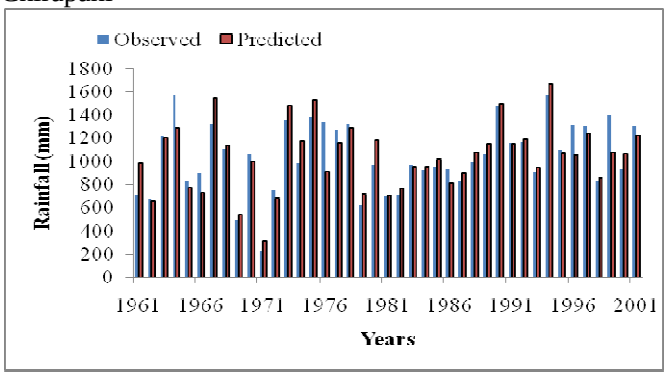

SSE	350308.9
MSE	973.0802
RMSE	31.19
NMSE	6.46
NSE	0.88
MAE	0.78
CC	0.94

Damtari

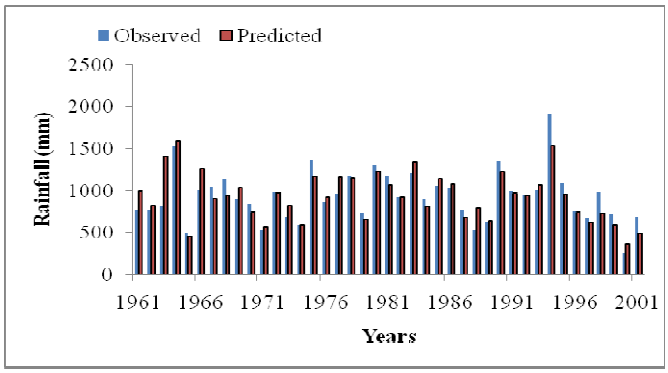

SSE	558454.7
MSE	1551.263
RMSE	39.39
NMSE	11.25
NSE	0.78
MAE	0.70
CC	0.90

Doundi Lohara

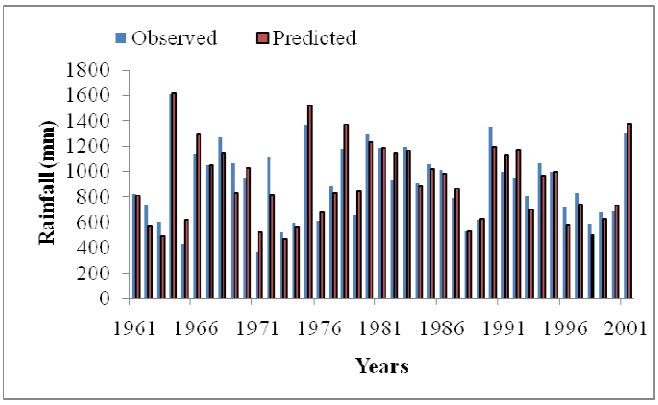

SSE	206214.6
MSE	572.8183
RMSE	23.93
NMSE	5.03
NSE	0.88
MAE	0.73
CC	0.94

Durg

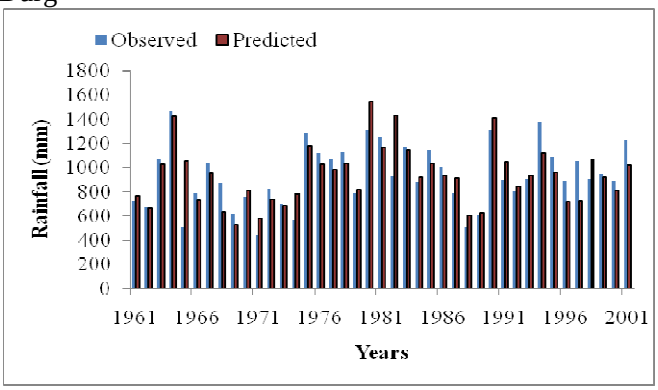

SSE	289668.6
MSE	804.635
RMSE	28.36609
NMSE	6.27363
NSE	0.865578
MAE	0.777622
CC	0.936529

Dongargaon

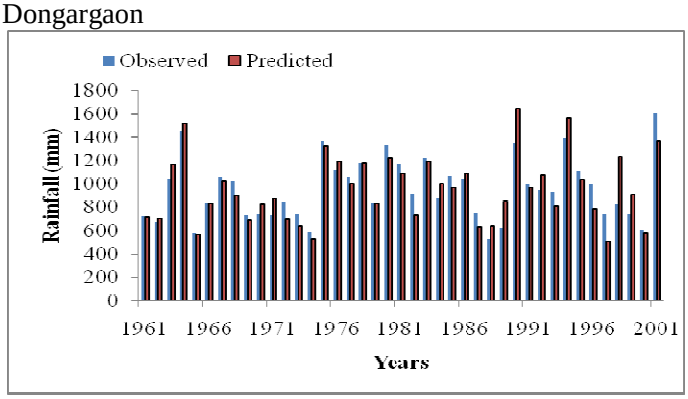

SSE	423171.8
MSE	1175.477
RMSE	34.29
NMSE	8.32
NSE	0.84
MAE	0.66
CC	0.92

Doundi

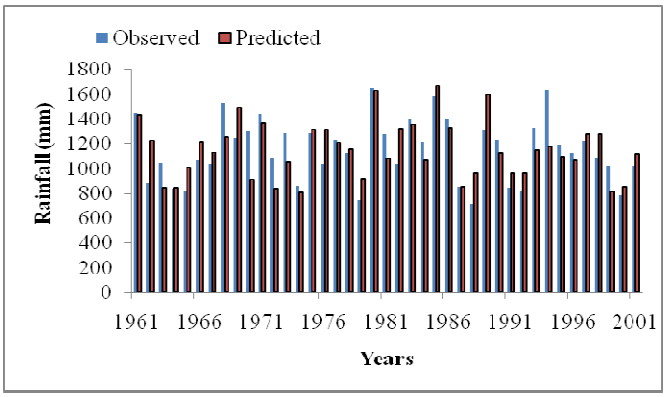

SSE	401248.8
MSE	1114.58
RMSE	33.39
NMSE	8.60
NSE	0.82
MAE	0.68
CC	0.90

Raipur

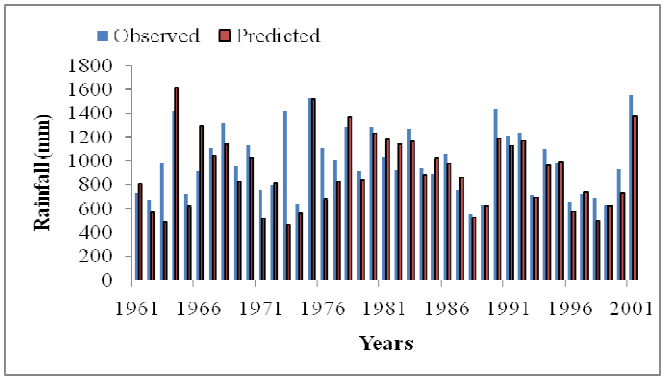

SSE	382330.9
MSE	1062.03
RMSE	32.59
NMSE	8.01
NSE	0.83
MAE	0.72
CC	0.91

Admabad

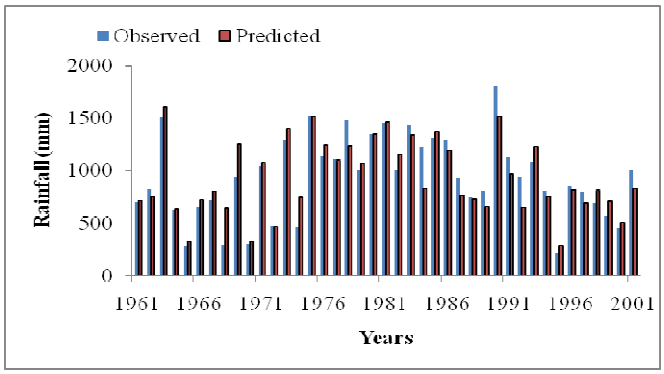

SSE	230144.8
MSE	639.2911
RMSE	25.28
NMSE	5.41
NSE	0.87
MAE	0.77
CC	0.94

Balod

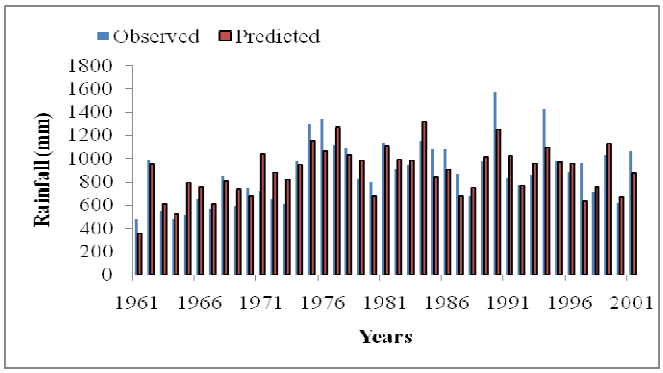

SSE	477302.8
MSE	1325.841
RMSE	36.41
NMSE	11.86
NSE	0.71
MAE	0.66
CC	0.84

Mohala

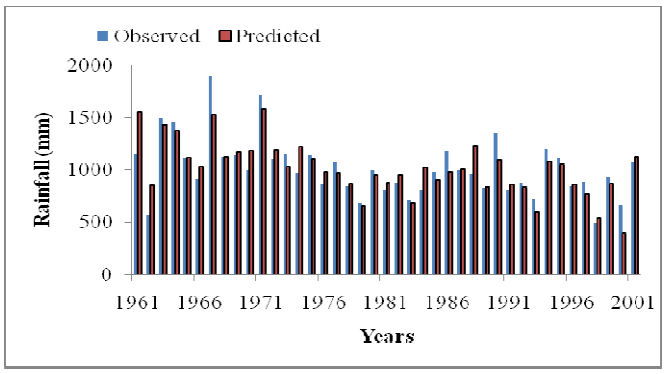

SSE	149710.4
MSE	415.8621
RMSE	20.39
NMSE	3.93
NSE	0.90
MAE	0.80
CC	0.95

Kawardha

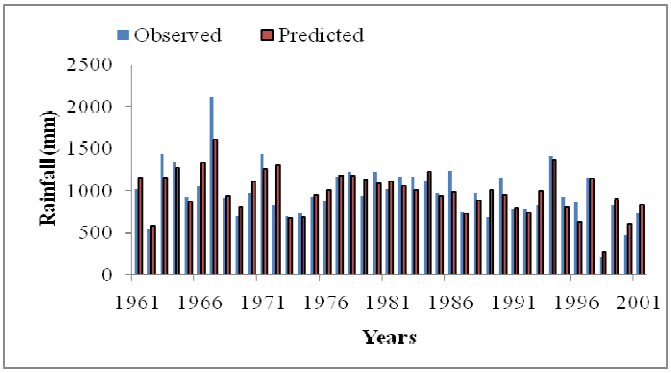

SSE	180922.8
MSE	502.5633
RMSE	22.42
NMSE	4.71
NSE	0.88
MAE	0.78
CC	0.94

Gandai

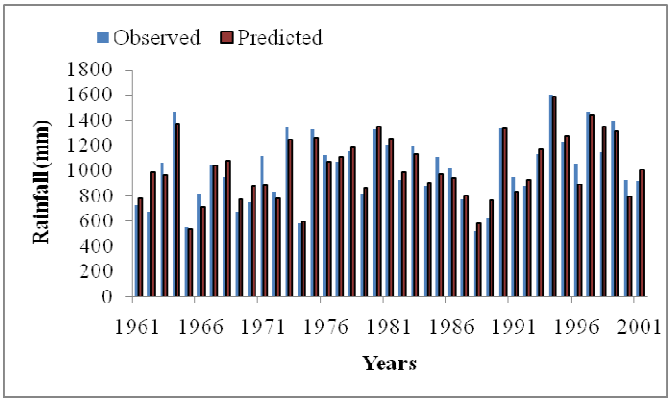

SSE	207761.2
MSE	577.1145
RMSE	24.02321
NMSE	3.791326
NSE	0.931553
MAE	0.8068
CC	0.966501

Patan

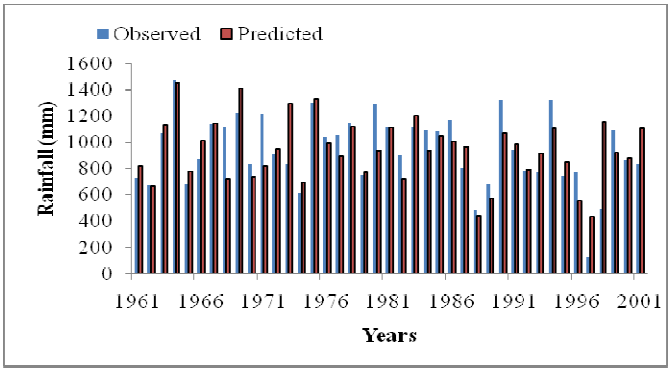

SSE	379961.8
MSE	1055.449
RMSE	32.49
NMSE	8.48
NSE	0.81
MAE	0.71
CC	0.90

Gudhiyari

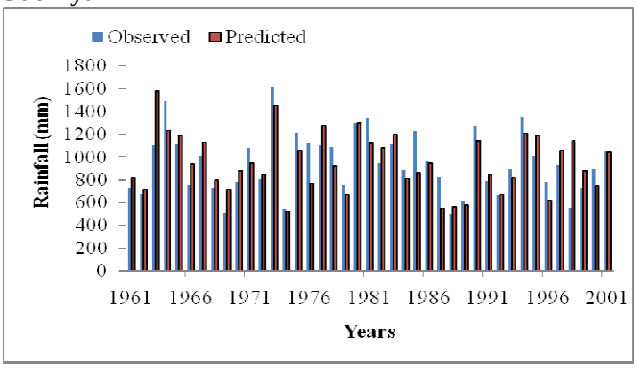

SSE	403680.4
MSE	1121.334
RMSE	33.49
NMSE	9.11
NSE	0.80
MAE	0.71
CC	0.89

Gondly

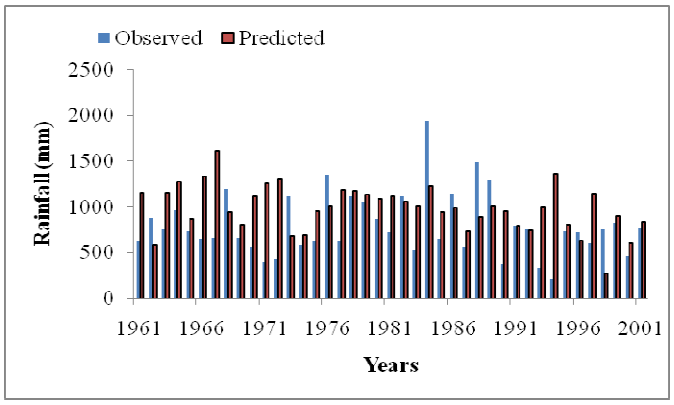

SSE	647581.8
MSE	1798.838
RMSE	42.41
NMSE	15.03
NSE	0.65
MAE	0.68
CC	0.84

Gurur

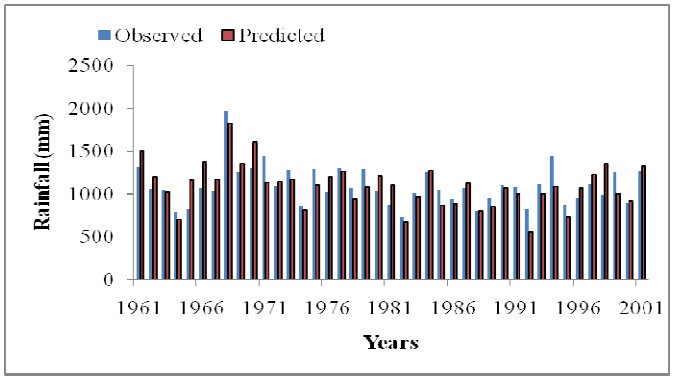

SSE	375376.8
MSE	1042.713
RMSE	32.29
NMSE	7.13
NSE	0.87
MAE	0.74
CC	0.93

Simga

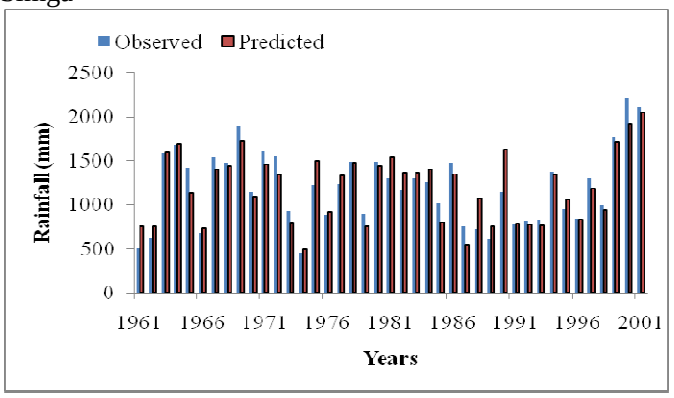

SSE	237673.2
MSE	660.2033
RMSE	25.69
NMSE	4.99
NSE	0.90
MAE	0.76
CC	0.95

Rajnandgaon

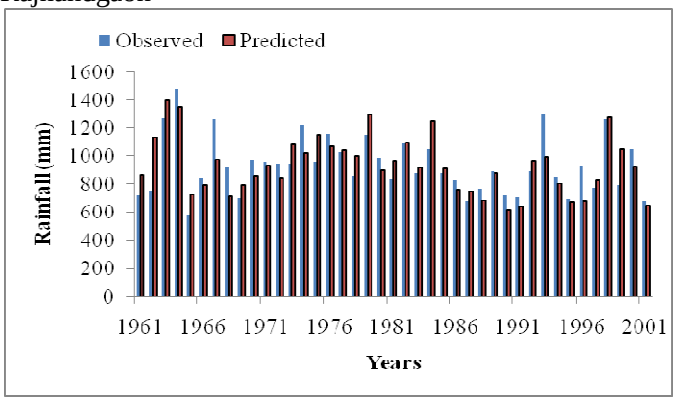

SSE	284793
MSE	791.0915
RMSE	28.13
NMSE	6.22
NSE	0.87
MAE	0.78
CC	0.93

Gunderdehi

ANNEXURE D

Figure D1 Boxplots for monthly growing season (a) rainfall, (b) Tmax (c) Relative Humidity and (d) wind speed

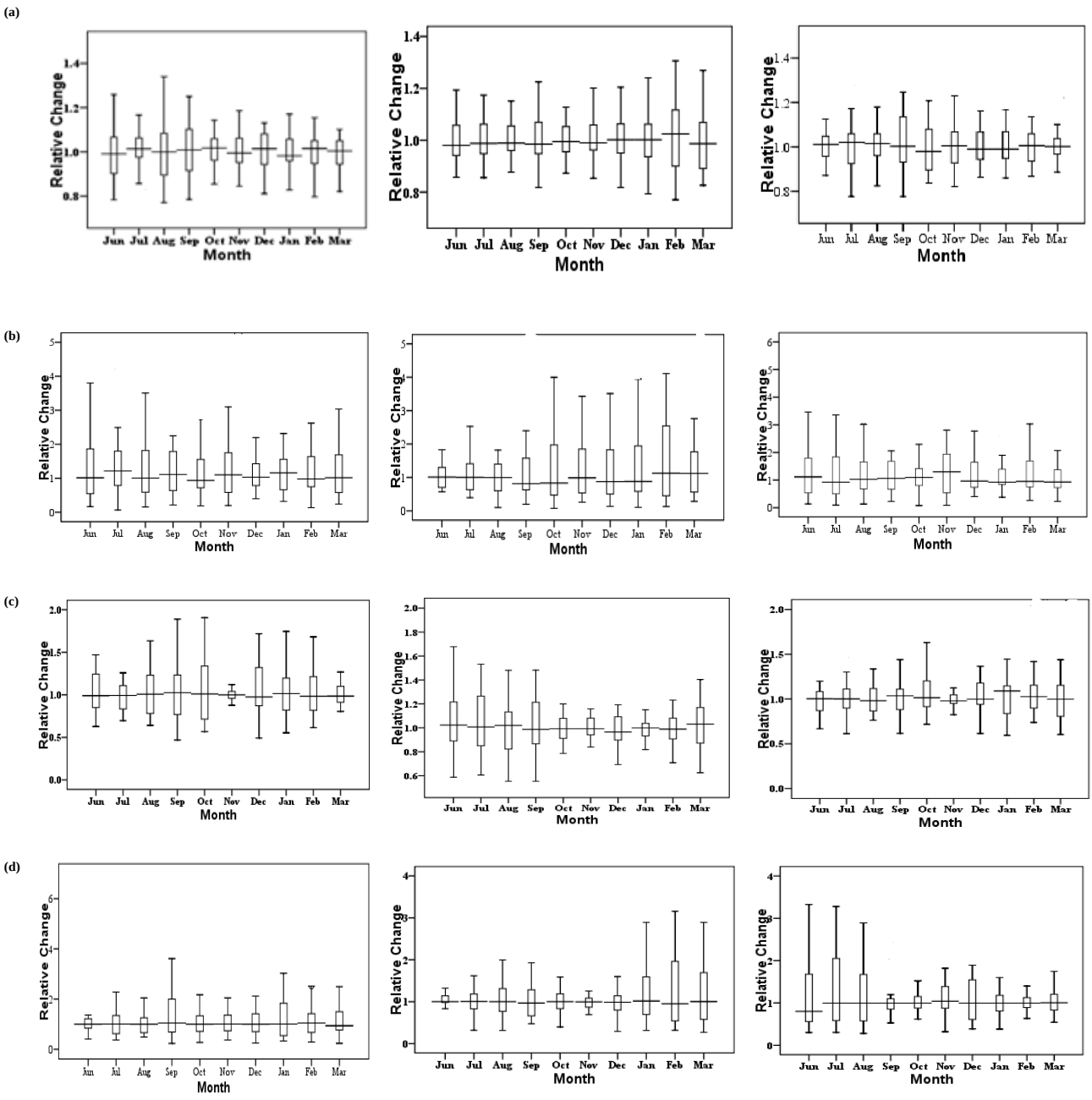

LIST OF PUBLICATIONS

1) Shiulee Chakraborty, S.K. Mishra, R.P. Pandey and U.C. Chaube. 2013. Long-term Changes of Irrigation Water Requirement in the Context of Climatic Variability. ISH Journal of Hydraulic Engineering, pp: 257-266.

2) Shiulee Chakraborty, R. P. Pandey, U.C Chaube and S.K. Mishra. 2013. Trend and variability analysis of rainfall series at Seonath River Basin, Chhattisgarh (India). Int. Journal of Applied Sciences and Engineering Research, 2(4), pp: 425-434.

3) Shiulee Chakraborty, U.C Chaube, R. P. Pandey and S. K Mishra. 2013. International Journal of Advances in Engineering Science and Technology, 2(2), pp: 144-152.

4) S. K. Mishra, S. S. Rawat, R. P. Pandey, Shiulee Chakraborty, M. K. Jain, and U. C. Chaube. 2014. Relationship between Runoff Curve Number and PET. Journal of Hydrologic Engineering, 19, pp: 355-365.

Papers Communicated:

1) Shiulee Chakraborty, U.C. Chaube, R.P. Pandey, S.K. Mishra. Assessment of Region Specific Crop Coefficient for Realistic Estimation of Crop Water Requirement. Submitted to Arabian Journal for Sciences and Engineering.

2) Shiulee Chakraborty, R.P. Pandey, S.K. Mishra, U.C. Chaube. Realtionship between Runoff Curve Number and Irrigation Water Requirement. Submitted to Agricultural Research. Tentatively accepted submitted revised manuscript to the Journal.